HOLOCENE PALAEOCLIMATE RECONSTRUCTION FROM NEW ZEALAND PEATLANDS

by

ZOË JENNIFER HAZELL

A thesis submitted to the University of Plymouth (United Kingdom)
and to the University of Waikato (New Zealand)
in partial fulfilment for the degree of

DOCTOR OF PHILOSOPHY

School of Geography
Faculty of Social Science and Business (Plymouth)

School of Earth Sciences
Faculty of Science (Waikato)

November 2004

Zoë Jennifer Hazell

Holocene Palaeoclimate Reconstruction from New Zealand Peatlands

ABSTRACT

A selection of palaeoecological proxies were tested on two raised, ombrotrophic, restiad peat bog sites from the North Island of New Zealand. With varying degrees of success, peat humification, testate amoebae, plant macrofossil and charcoal analyses contributed to determining the palaeomoisture records from three cores on each site. Climatic inferences have successfully been made for the Waikato region, mid North Island, over the period between the Tuhua (6,130±30 ^{14}C years BP; 6,800-7,150 cal. years BP) and Taupo (1,850±10 ^{14}C years BP; 1,650-1,800 cal. years BP) tephras. 47 AMS radiocarbon ages contributed to the production of age-depth models.

The peat humification records have a resolution of 20-30 years and are the first replicated records for this region. Whilst peat humification and charcoal were the most successful analyses, the limited plant macrofossil work has also shown potential. Testate amoebae analysis, however, was not appropriate for these particular sites due to extremely low fossil test abundances.

From the peat humification record, the main palaeomoisture trend identified in all cores is a shift towards wetter conditions *c.*5,000-4,000 cal. years BP. This is thought to have resulted from stronger westerly circulation, driven by increasing temperature and pressure gradients across the Southern Ocean from equatorial to polar latitudes. This in turn is likely to have been due to an increasing differential between insolation received at these latitudes, ultimately forced by the precessional cycle.

The 'Mid-Holocene Transition' to wet conditions appears to contradict previous work from New Zealand that infers a *drier* late Holocene. This apparent contradiction can, however, be reconciled by increasing seasonality that would also explain the rise in charcoal abundance following the Mid-Holocene Transition. Colder, wetter winters resulted from decreasing winter (June) insolation and stronger rain-bearing westerlies, causing a decrease in peat humification. Warmer, drier summers resulted from an increase in summer (December) insolation and caused increased regional burning. An intensifying ENSO signal at the mid-Holocene is also thought to be responsible for increased drought occurrence and weather extremes.

CONTENTS

LIST OF FIGURES, TABLES AND PLATES

Page number

Figures

Tables

Plates

ACKNOWLEDGEMENTS

Many thanks to my supervisors Dr. Rewi Newnham (Plymouth), Prof. Dan Charman (Plymouth) and Assoc. Prof. David Lowe (Waikato) for all their help and support. Also to Dr. Marcus Vandergoes (Plymouth), Dr. Hiroshi Moriwaki (Kagoshima) and Phil Hodge (Waikato) for help on fieldwork, together with Chris Hendy (Waikato) and Malcolm McLeod (Landcare, Hamilton). And to Dr. Janet Wilmshurst (Landcare, Christchurch), Bev Clarkson (Landcare, Hamilton) and Dr. Peter de Lange (Auckland) for plant advice and help. Thanks too to the Department of Conservation (Hamilton) for permission to sample the sites, and to those at Wallace Farm (Moanatuatua) for permission to core their pasture and gain access to the reserve.

The radiocarbon dating was facilitated by NERC for the AMS dates (Grant number 948.1201) and the Waikato Radiocarbon Laboratory (D. Lowe) for the bulk peat dates. Thank you to the staff at NERC Radiocarbon Laboratory (East Kilbride) especially Dr. Charlotte Bryant and Dr. Mark Garnett, and Margaret and Maureen.

Thanks too to Owen Hazell, Adam Cherrett and Matt Jones for their inspiration and mathematical help. An enormous thank you to the technical staff at the School of Geography (Plymouth) especially A. Kelly, K. Solman and P. Bloomfield, and to Annette, Alison, Laurence and Steve at the Department of Earth Sciences (Waikato). Also, to P. Framingham and D. Antwis for computing support, and to T. Absalom and J. Quinn for the production of maps/diagrams. Without them, none of this would have been possible.

And on a more personal note, thank you to Elaine Norton for looking after me and making me feel so welcome whilst in New Zealand. Thank you to Matt, Marcus, Miranda & Mathias and the rest of the Geography/Geology bunch, for making the tough times not so bad, and to Becky and Dave for putting me up so welcomingly on my visits back to Plymouth. And thank you especially to Alastair – for being there for me and making me laugh, not forgetting the numerous stimulating peat conversations... and of course to Mum and Dad for all their support and encouragement over the years and for pestering me to "just get the damn thing finished!".

AUTHOR'S DECLARATION

At no time during the registration for the degree of Doctor of Philosophy has the author been registered for any other University award.

This study was financed with a studentship from the University of Plymouth (UK), together with grants for radiocarbon ages from the Natural Environmental Research Council (UK) and the University of Waikato (NZ). The NERC Radiocarbon Laboratory in East Kilbride was visited for consultation purposes.

Relevant scientific seminars and conferences were attended at which work was presented:

BGRG Postgraduate Meeting, Windsor, December 2000 (oral presentation)
QRA Postgraduate Symposium, St Andrew's, September 2001 (oral presentation)
QRA Postgraduate Symposium, Amsterdam, September 2002 (oral presentation)
BES Annual Meeting, Manchester, September, 2003 (poster presentation)
AGU Chapman Conference, Honolulu, February 2005 (oral presentation)

Seminars were also presented to:

The Department of Geography, University of Plymouth (May 2001, October 2003)
The Department of Earth Sciences, University of Waikato (May, 2002)

Signed: Z. J. Hazell
Date: 16 - 5. 05 .

CHAPTER ONE – INTRODUCTION

1.1 Project background and rationale

Raised ombrotrophic bogs are ideal study sites for palaeoclimatic reconstructions as their hydrology is controlled by 'effective precipitation' – the balance between water input (precipitation) and water loss (evaporation) – which is in turn controlled by the prevailing climate. Various palaeoecological techniques are regularly employed in palaeoclimatic studies to reconstruct palaeomoisture records, including analysis of testate amoebae, plant macrofossils, charcoal and peat humification. Extensive work of this kind has been carried out in Europe, particularly in the British Isles (e.g. Barber *et al.*, 1998, 1999; Hughes *et al.*, 2000; Langdon *et al.*, 2003) but much less has so far been attempted in the Southern Hemisphere (McGlone and Wilmshurst, 1999b; Wilmshurst *et al.*, 2003).

New Zealand, however, offers excellent opportunities for Holocene palaeoclimate reconstruction from peatlands for the following reasons. First, as a relatively small landmass located within the expanse of the Southern Ocean, New Zealand is ideally situated to respond sensitively to climatic fluctuations. Its weather, characterised by highly variable precipitation regimes, is dominated by rain-bearing westerly oceanic winds driven by regional atmospheric circulation patterns (Newnham *et al.*, 1999). Second, the widespread presence in New Zealand of peatland sites of a similar form to those in the Northern Hemisphere facilitates comparable Holocene palaeoecological studies and enables inter-hemispheric comparisons of palaeoclimatic reconstructions. Third, the relatively short period of human occupation and landscape disturbance is estimated at only the last 600-700 years (McGlone and Wilmshurst, 1999a). This means that coherent hydrological changes reconstructed from peatland sites can be attributed to natural, rather than anthropogenic factors. In the majority of Holocene peat records (those from areas with a long population history) these factors are often difficult to distinguish. Finally, the rapidly accumulating New Zealand peatlands contain a suite of tephras (volcanic ash layers) preserved within the stratigraphy (Lowe, 1988a, 1988b; Lowe and Newnham, 1999). Because the particular combination of chemical constituents are unique to specific eruptions, tephra layers are invaluable as chronologic reference points to enable the derivation of well constrained age-depth models and for correlating between separate peat profiles.

A combination of non-peatland based palaeoclimate reconstructions suggest that the late Holocene was drier and more variable than preceding conditions. Evidence from increased charcoal and *Agathis australis* (kauri) pollen abundances (Newnham *et al.*, 1989) and a decline in *Ascarina* pollen (McGlone and Moar, 1977) also suggest an increase in climate variability, thought to relate to strengthening ENSO signals (McGlone *et al.*, 1992).

1.2 Project aims and objectives

The main aims of this project, therefore, are:

- To test the applicability of palaeoecological techniques developed for Northern Hemisphere peatlands, on raised bogs of New Zealand.
- To reconstruct mid-to-late Holocene moisture regimes at two hydrologically-separate raised ombrotrophic peatlands in the North Island of New Zealand using a multi-proxy palaeoecological approach, and to investigate the intra- and inter-site replication of these records.
- To infer past climate, in particular precipitation and atmospheric circulation, from the reconstructed palaeomoisture records, for the period covered by these records.
- To test the inference of a drier, more variable late Holocene climate, as inferred by (Newnham *et al.*, 1989).
- To examine the relationship between the New Zealand palaeoclimate record and broader-scale regional and global precipitation and atmospheric circulation changes, identifying possible climate-forcing mechanisms.

The two raised peat bogs selected as sites suitable for analysis are Kopouatai and Moanatuatua, both from the centre of New Zealand's North Island (*Figure 3.1*) and therefore within the same regional climate regime. They are dominated by the restiad (herbaceous rushes) plant species *Empodisma minus* and *Sporadanthus ferrugineus*, and, crucially, the sites are hydrologically separate. The palaeoecological techniques employed are all proxy indicators of past moisture levels that are routinely used in Northern Hemisphere peatland research: testate amoebae, peat humification, plant macrofossils and charcoal fragment abundance. Relatively little research has been carried out into the potential and success of these palaeoecological techniques in peatland studies from New Zealand, particularly that of testate amoebae. The first testate amoebae study was that of Charman (1997) who derived a training set for the reconstruction of palaeomoisture values. In terms of reconstructing past moisture records, McGlone and Wilmshurst (1999b) have demonstrated that the combination of methods listed above gave complementary climate

signals, therefore implying their potential to provide coherent records of climate change. This project will also add to the understanding of work by Wilmshurst *et al.* (2003) who produced the first Southern Hemisphere testate amoebae- and peat humification-based Holocene palaeomoisture reconstruction from New Zealand.

Climatic implications tested will include the assertion that climates in northern New Zealand became drier and more variable in the late-Holocene (as inferred from pollen records) (Newnham *et al.*, 1989; McGlone, 1988), perhaps associated with the intensification of El Niño Southern Oscillation (ENSO) cycles (McGlone *et al.*, 1992; Fowler *et al.*, 2000). Records will also be examined for the presence of possible global events that have already been identified in other peatland records, for example, the development of wetter conditions in Europe from *c.*4,400 cal. years BP onwards (Barber *et al.*, 2003), or the climatic deterioration 2,700 ^{14}C years BP in Europe and Chile (van Geel *et al.*, 1996; van Geel *et al.* 2000). Ultimately, the work will contribute to the critical debate concerning inter-hemispheric symmetry of climate change (e.g. Stocker, 2002) and the mechanisms responsible for teleconnections in global climates.

The time period of study covers the mid to late Holocene and uses two tephra layers as chronological boundaries (section 4.1.2). These are the Taupo and Tuhua tephras, dated to 1,850±10 ^{14}C years BP and 6,130±30 ^{14}C years BP, respectively. In addition to tephrochronology, radiocarbon dating is used to derive more detailed age-depth models.

1.3 Organisation of this document

The following chapter of this thesis (Chapter 2) discusses the main literature concerning global patterns of climate change during the Holocene, particularly as reconstructed from peatland sites, and the possible forcing mechanisms. The current weather and oceanographic setting of New Zealand is also described, thereby outlining its climatic context. The field sites (Chapter 3) and the methodologies (Chapter 4) are then described fully. The results within this thesis are divided into three chapters. The first covers all aspects of the testate amoebae findings (Chapter 5). This is presented separately from the palaeoecological records due to the self-contained nature of the testate amoebae investigations. The remaining results from Kopouatai and Moanatuatua are also presented in separate chapters (Chapters 6 and 7 respectively), and then compared to each other in the subsequent discursive chapter (Chapter 8). Conclusions are then drawn in the final chapter (Chapter 9).

CHAPTER TWO – BACKGROUND AND CONTEXT

2.1 Introduction

The majority of this chapter reviews the main literature on peatlands, with particular focus on those of New Zealand and Europe, their use in climate reconstruction studies, and the applications of methods used in palaeomoisture reconstructions (detailed methodology is covered in Chapter 4). The current climate of New Zealand is also described (section 2.4) together with the main synoptic weather features.

2.2 Peatlands and climate change

This section first covers raised peatland formation, focusing on the development and characteristics of the Southern Hemisphere raised bogs that are to be studied in this project. Peatlands are important archives of numerous ecological remains and chemical and physical characteristics that respond to and record climate changes. The use of such proxy indicators in palaeoclimatic studies is explored here, covering in particular the techniques used to reconstruct past moisture conditions. Examples from both hemispheres are used, because most such peatland work has so far been carried out in the Northern Hemisphere.

2.2.1 Peatland development and formation

Raised peatlands form where water input (precipitation) exceeds that of output (evapotranspiration) (*Figure 2.1*). The resulting anaerobic (oxygen-depleted) conditions inhibit the decay of vegetative matter and result in the gradual vertical build-up of organic matter (Barber, 1981). Such raised bog sites are termed 'ombrotrophic', meaning that their only source of water is from precipitation. This results in a raised 'lens' water table that is elevated above the regional groundwater table.

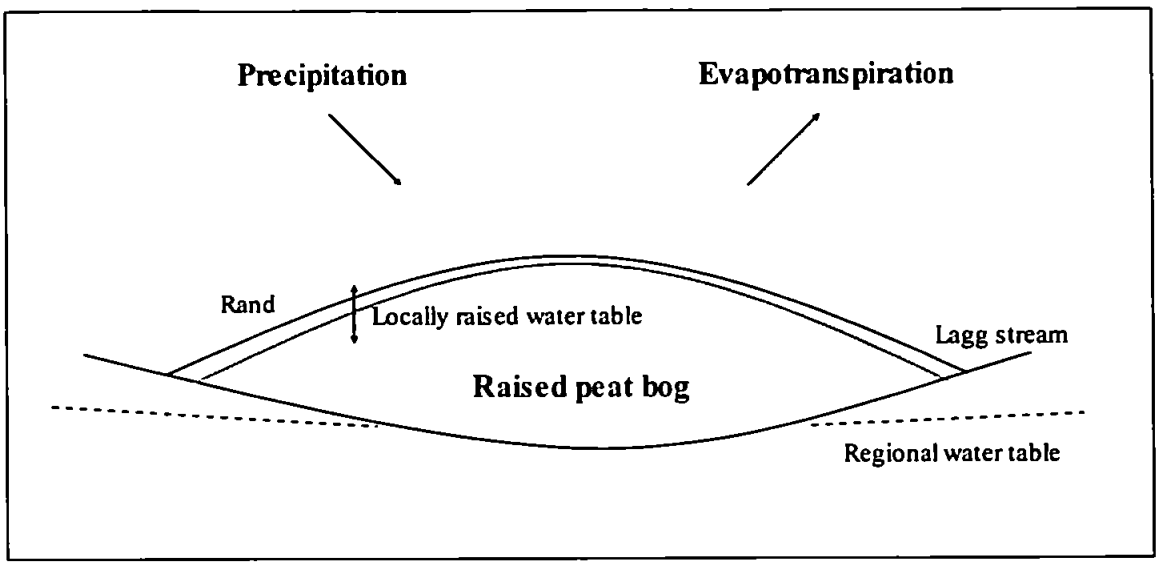

Figure 2.1 Conceptual cross-section through a raised peat bog. Hydrology is controlled by 'effective precipitation', which is a function of climate; input by precipitation, minus output by evapotranspiration.

New Zealand peatlands

Of particular importance when carrying out inter-hemispheric comparative palaeoclimatic studies, is the presence in the Southern Hemisphere of peatlands of similar raised form to those found in the Northern Hemisphere. Of the four main types of peatland in New Zealand identified by Campbell (1975) (forest, sedge, moss and restiad) the two most common are *Sphagnum*- and herbaceous restiad-dominated types. The latter type, as used in this project, are now rare in New Zealand but are particularly sensitive to both natural and human-induced influences. Clarkson (2002) considers these vascular restiad raised bogs to be the southern equivalent to the Northern Hemisphere non-vascular *Sphagnum* raised bogs. Kuder *et al.* (1998), however, state that there can be no direct Southern Hemisphere analogues to Northern Hemisphere bogs, including *Sphagnum* bogs, since the climatic conditions under which they develop and perpetuate are very different. The North Island of New Zealand experiences a warmer and more humid climate than typical Northern Hemisphere bog locations that tend to be generally colder and more boreal. Nevertheless, there is no evidence to suggest that the manner in which organisms within restiad-dominated bogs respond to climatic changes is different to that of Northern Hemisphere *Sphagnum* bogs i.e. changes in moisture variability of the restiad bogs are, too, recorded in the degree of peat humification and in the types of plant remains. This will therefore enable the comparison of inferred climate signals between hemispheres.

The formation of such raised bogs requires specific conditions: a) a high water table sourced from rainfall, b) impeded drainage and c) the presence of highly water-retentive

vegetation to keep the water table elevated. These factors combine to inhibit decay and lead to peat accumulation (Campbell, 1975). As peat accumulates there are fewer nutrients available, therefore limiting microbial activity, as water input increasingly comes from precipitation (Shearer, 1997). Peatlands form for a variety of reasons, mainly initiated by climatic variations resulting in wetter conditions. Under favourable climatic conditions, other influences can contribute to their formation. Kopouatai and Moanatuatua, the peat bogs studied in this project, formed on the former flood plains of the ancestral Waikato River during the last deglaciation, when the previously migrating channel assumed its present position (Green and Lowe, 1985).

Over time, raised bogs develop certain characteristic features (*Figure 2.1*). Typical restiad raised peat bogs have a convex surface (the dome) surrounded by a moat (the lagg stream) reached by a steep slope downwards (the rand). The lagg drains not only the bog itself, but also the surrounding area, and is therefore higher in nutrients, and able to sustain higher nutrient demanding plants, such as scrub or swamp forest (Campbell, 1975, 1971).

These raised restiad bogs react sensitively to climate (and drainage) changes, just as their Northern Hemisphere raised bog counterparts do. For this reason they are valuable archives of past climatic changes, particularly hydrological shifts, since they contain a variety of different palaeoecological indicators that act as proxies for these variables. These rare ecosystems are extremely fragile and are likely to be just as sensitive to future climatological changes.

Restiad peatlands

As mentioned earlier, the moderate rainfall and high summer temperatures of the North Island of New Zealand are not climatic conditions usually conducive to raised peatland development (Kuder *et al.*, 1998) especially when moisture deficits are common during the summer in the Waikato region investigated here. However, bog formation is facilitated by the extensive root and rhizome systems of two vascular restiads (Restionaceae) that have extremely low evapotranspiration rates (see below). These are 1) *Empodisma minus* ((lesser) wire rush) (previously grouped with *Calorophus minor* (Hook.f.) found in Tasmania (Connor and Edgar, 1987)) and 2) *Sporadanthus ferrugineus* (greater wire rush or cane rush) (previously categorised with *Sporadanthus traversii* ((F.Muell.) Kirk)) from the Chatham Islands) (de Lange *et al.*, 1999). Together, these two are the dominant vegetation and the main peat constituents on raised bogs in the region, and are found only

between 37-38°S (Clarkson *et al.*, 2004). *S. ferrugineus* is endemic to northern New Zealand (de Lange *et al.*, 1999) whereas *E. minus* is found throughout New Zealand as well as in eastern Australia (Campbell, 1975). *S. ferrugineus* is often a successional climax plant species growing in clumps of 200-300 stems (Thompson *et al.*, 1999; Clarkson, 2002). Its rigid, jointed stems are 0.2-1.5 cm in diameter and can grow up to 2 m tall, with its dense rhizomes forming a kind of floating platform. *E. minus* also thrives in acidic conditions. Its 1-3 mm diameter stems (Thompson *et al.*, 1999) straggle to heights of 0.6 m but can reach 1.2 m where it competes amongst *S. ferrugineus* clumps (Wardle, 1991). These restiad clumps develop into characteristic peatland hummock and hollow topography by increasing plant matter accumulation in certain locations (Agnew *et al.*, 1993).

As already mentioned briefly, the physiology of *E. minus* and *S. ferrugineus* is very important in the formation of peat bogs for the following reasons:

a) The compact root mat of *E. minus*, a white-pinkish colour, absorbs and holds a large volume of water. It has an extremely high water holding capacity (Agnew *et al.*, 1993), capable of retaining 15 times its dry weight of water (Campbell, 1964). Its very dense canopy and litter layer, mostly composed of dead stem material, limits transpiration moisture loss, reduces evaporation and restricts competitors from the bog surface by preventing virtually all sunlight from reaching the surface (Campbell and Williamson, 1997). *S. ferrugineus* evaporation rates were compared between Kopouatai and Moanatuatua by Thompson *et al.* (1999) and it was found that there was little variation between the evaporation rates of *S. ferrugineus* between the two sites considering their very different hydrological regimes. At Kopouatai rates were 3.01 mm/day and at Moanatuatua 2.74 mm/day. Even though *S. ferrugineus* has evaporation rates twice as high as *E. minus*, compared to other vegetation and wetland types these two plant species result in substantially lower evaporation rates (Campbell and Williamson, 1997).
b) *E. minus* focuses rain water down its stem, and has twice the capture efficiency of this water source as *S. ferrugineus* (Agnew *et al.*, 1993). As a result, approximately 30% of total water input to the bog is via restiad plant stem flow.
c) Its leaves have developed into small, scale-like sheaths in order to reduce evapotranspiration rates (Clarkson *et al.*, 2004).

d) In addition to these factors, both *S. ferrugineus* and *E. minus* have high phenolic acid and tannin contents that aid their resistance to decay (Given and Dickinson, 1975) thus encouraging peat accumulation.
e) Kuder *et al.* (1998) suggest that *Empodisma* has allelopathic properties, releasing chemicals that negatively affect other plants in order to reduce competition.

Field site vegetation composition

In addition to the restiads, Kopouatai and Moanatuatua are also home to additional plant species, many of which are rare and protected. The main plant species that compose the sites are listed in *Table 2.1*, with the authorities and families following Clarkson *et al.* (2004) and Connor and Edgar (1987).

There are two main wetland systems of significance to the two sites: bog and fen. The main peat formers on the central bog zone are the restiads of which *Sporadanthus* is currently classed as 'nationally vulnerable' (Wetlands International, 2005). The current successional vegetation consists of an upper storey of intertwined *Empodisma* and *Sporadanthus*, together with the shrubs *Epacris*, *Leptospermum* and *Dracophyllum* (although the latter is not present at Moanatuatua), with an intermediate level of the *Baumea* spp. and *Schoenus* sedges. The ground-level vegetation consists of mostly mosses (*Sphagnum* and *Campylopus acuminatus* var. *kirkii* (rare)), liverworts (*Goebelobryum* and *Riccardia*), lycopods (*Lycopodiella serpentinum* (vulnerable)), bladderworts (*Utricularia*), orchids (e.g. *Anzybas* (formerly *Corybas*) *carsei*) and sundews (*Drosera*) (Clarkson, 2002). The fen group surrounds the raised bog of Kopouatai (Clarkson, 2002); now common around Kopouatai's margins are swathes of the introduced willow (*Salix*) spp. that are forcing out the native species raupo (*Typha orientalis*), the leafy sedge *Carex*, club-palm (*Cordyline*) spp. and flax (*Phormium tenax*) (Wetlands International, 2005). The southwest of the site is also home to a protected ecologically-important remnant of *Dacrycarpus dacrydioides* (kahikatea) forest, of which only 2% of the North Island's original cover remains.

Latin binomial	Family	Common name	Authority
Baumea arthrophylla	Cyperaceae	-	(Nees) Boeck.
Baumea rubiginosa	Cyperaceae	Twig rush	(Sprengel) Boeck.
Baumea teretifolia	Cyperaceae	Pakihi rush	(R.Br.) Palla
Campylopus acuminatus var. *kirkii*	Dicranaceae	-	(Mitt.) Frahm
Coprosma tenuicaulis	Rubiaceae	Hukihuki; swamp coprosma	Hook.f.
Anzybas carsei	Orchidaceae	Swamp helmet orchid	(Cheeseman) Jones & Clem.
Dracophyllum lessonianum	Epacridaceae	-	A.Rich.
Dracophyllum scoparium	Epacridaceae	Swamp heath	Hook.f.
Drosera binata	Droseraceae	Forked sundew	Labill.
Empodisma minus	Restionaceae	(Lesser) wire rush	(Hook.f.) L.Johnson & D.Cutler
Epacris pauciflora	Epacridaceae	Bog epacris; tumingi heather	A.Rich.
Gleichenia dicarpa	Gleicheniaceae	Swamp/umbrella/tangle fern; waewae kotuku	R.Br.
Goebelobryum unguiculatum	Southbyaceae	-	(Hook.f. & Taylor) Grolle
Leptospermum scoparium	Myrtaceae	Manuka; tea tree	J.Forst. & G.Forst.
Lycopodiella lateralis	Lycopodiaceae	Club moss	(R.Br.) B.Ollg.
Lycopodium serpentinum (Lycopodiella serpentina)	Lycopodiaceae	Bog club moss	Kunze
Phormium tenax	Agavaceae	New Zealand flax; harakeke	J.Forst. & G.Forst.
Riccardia crassa	Aneuraceae		(Schwaegr.) C.Massal.
Salix cinerea	Salicaceae	Grey willow; sallow	L.
Salix fragilis	Salicaceae	Crack willow	L.
Schoenus brevifolius	Cyperaceae	Short-leaf bog rush	R.Br.
Sphagnum cristatum	Sphagnaceae	Moss	Hampe
Sporadanthus ferrugineus	Restionaceae	Greater wire rush; cane rush	de Lange Heenan & B.D.Clarkson
Utricularia laterifolia	Lentibulariaceae	Bladderwort	R.Br.

Table 2.1 Major vegetation species of Waikato restiad peatlands.

Initial bog development is through a predominantly sedge phase (*Carex* spp. and *Baumea* spp.) with *Leptospermum* and *Gleichenia*. This stage varies in duration depending on disturbance events, the local hydrology and nutrient status, and lasts between 100s to 1,000s of years (Clarkson *et al.*, 2004). This is followed by the restiad phase, firstly dominated by *Empodisma* and then *Sporadanthus*. *Empodisma* is required before *Sporadanthus* will colonise (Clarkson *et al.*, 2004), lagging by at least 1,100 years (de

Lange, 1989). Hence Whangamarino has yet to be colonised by *Sporadanthus* due to the relatively young age of the bog complex (approximately 1,800 years old) compared to Kopouatai and Moanatuatua (Clarkson *et al.*, 2004).

The vegetation succession is paralleled by a progression in nutrient status from mesotrophic to oligotrophic conditions, with nutrient levels varying as the sources change. This is manifest as a change from *Leptospermum-Baumea* vegetation (mesotrophic), through *Baumea-Leptospermum*, and then *Empodisma-Leptospermum* and finally to *Empodisma-Sporadanthus* (oligotrophic) (*Figure 2.2*). The plants associated with the different stages of succession have different environmental tolerances (Clarkson *et al.*, 2004); the early sedges and *Gleichenia* have wide environmental ranges, as does the subsequent *Empodisma* stage, and these are therefore able to colonise minerotrophic sites and survive in ombrotrophic conditions. In contrast, *Sporadanthus* and *Epacris* have narrow environmental ranges (Clarkson *et al.*, 2004).

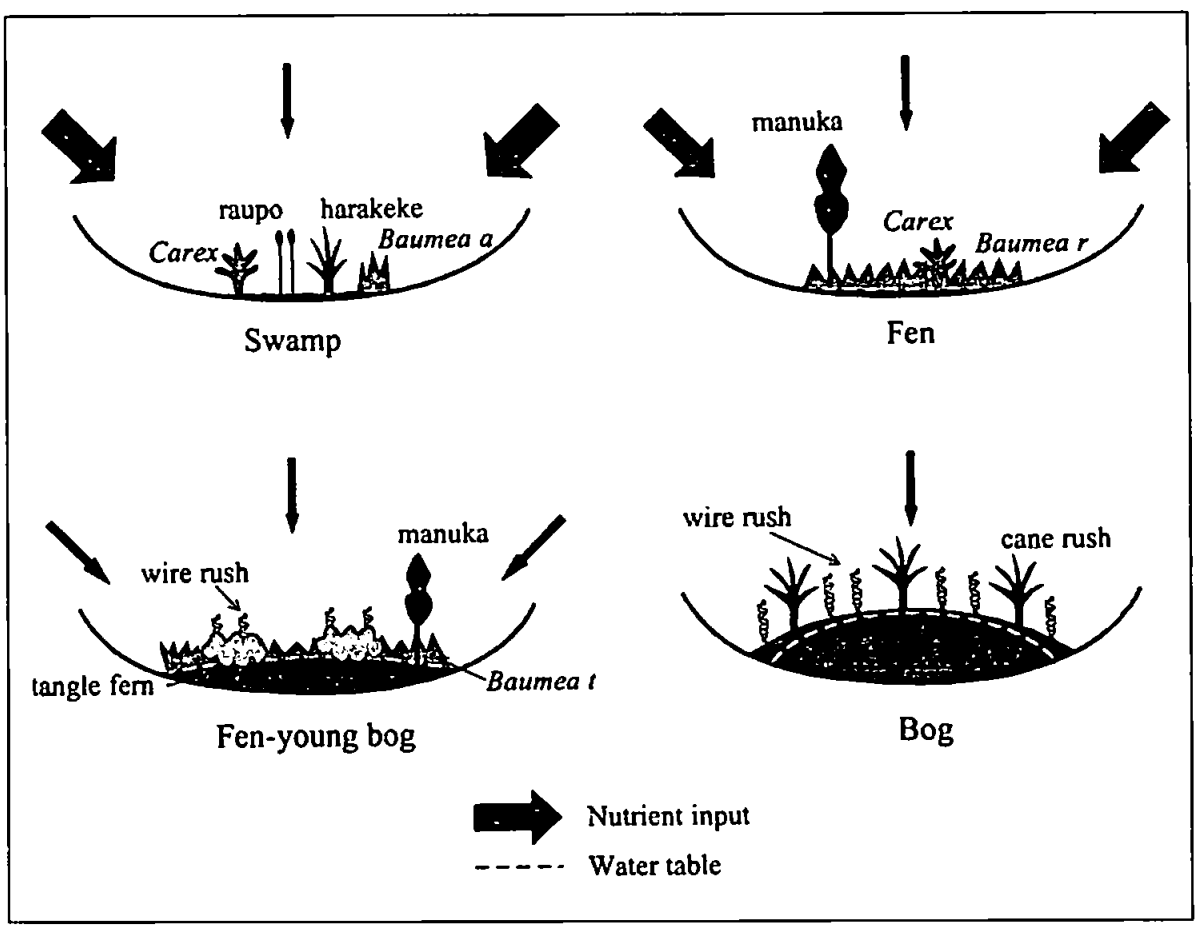

Figure 2.2 Bog development and its associated plant succession (from Clarkson 2002). Arrow width is proportional to nutrient input. Raupo = Typha latifolia, harakeke = Phormium tenax, manuka = Leptospermum scoparium, wire rush = Empodisma minus, cane rush = Sporadanthus ferrugineus, tangle fern = Gleichenia, Baumea a = Baumea arthrophylla, Baumea r = Baumea rubiginosa and Baumea t = Baumea teretifolia.

Varying proportions of each plant assemblage are associated with different ages of a peat bog (*Figure 2.3*). These different vegetation assemblages are found in different areas of the bog. The former two assemblages are mostly at the bog margins where nutrient status is higher, but the latter two are more often found in central bog areas (Shearer, 1997).

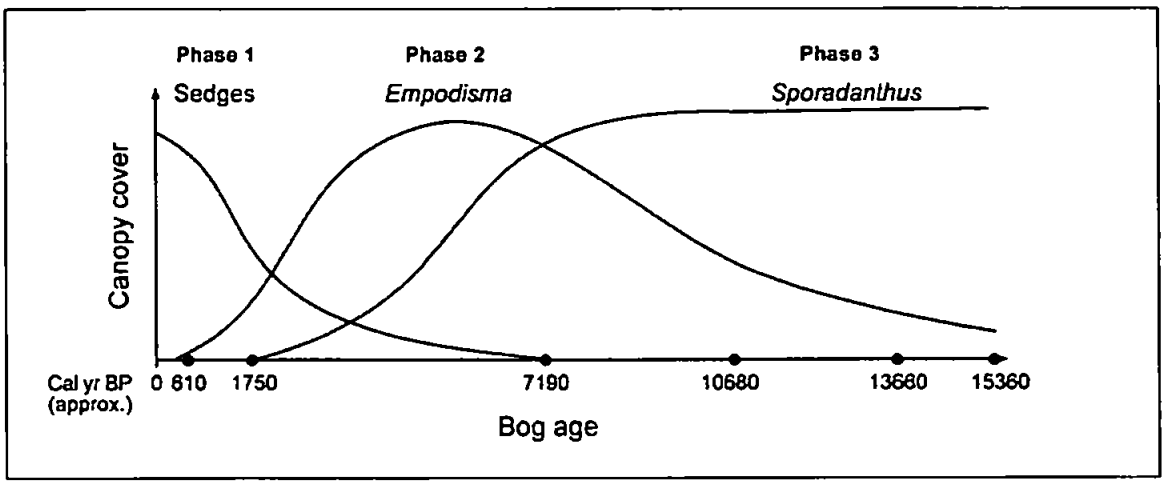

Figure 2.3 Changes in species dominance over time (from Clarkson et al., 2004).

The remaining (non-restiad) plants found on these peatbogs contribute very little to peat formation (Campbell, 1975). The creation of infertile, waterlogged conditions discourages the growth of woody plants such as *Leptospermum* and *Gleichenia*, although the former can adapt to a certain degree (Cook *et al.*, 1980). However, these are typically found growing on raised, drier hummocks within the bog, and on the drier bog margins. Whilst *Sphagnum* also grows at these sites, it only occurs in discrete clumps across the bog where conditions are sufficiently damp (such as in hollows) and where light levels are adequate. These moisture affinities among the principle bog plants will be used to interpret the plant macrofossil results in this investigation, and are discussed later in this chapter (section 2.2.2).

The bog development information outlined above is synthesised in *Table 2.2*.

Location	Stage	Dominant species	Nutrient level	Age sequence
Woody vegetation of modified bogs; bog margins	1	*S. cinerea*	High	Young
	2	*L. scoparium*		
Young bogs and margins of older bogs	3	*B. rubiginosa – G. dicarpa*		
	4	*B. teretifolia*		
	5	*B. teretifolia – E. minus*	Medium	
	6	*E. minus*		
Central areas of old 'unmodified' bogs	7	*E. pauciflora – E. minus*		
	8	*S. ferrugineus*	Low	Old

Table 2.2 Bog vegetation succession through time and space of typical restiad bog development in the Waikato region (compiled from Clarkson et al. (2004)).

Vegetation history

In terms of previous plant macrofossil investigations at the sites, very little has so far been carried out. At Kopouatai, most notable are the limited studies of de Lange (1989) and Newnham *et al.* (1995). This work identified the abundance of plant species based on a simple category system: abundant, frequent, occasional and rare, to reconstruct the site's plant history and nutrient status development; from oligotrophic, to mesotrophic and back to oligotrophic. At Moanatuatua, the main palaeoecological study is the limited description of the stratigraphy by Cranwell (1953) describing the level of peat decomposition whilst noting the presence of readily identifiable plant remains, such as *Leptospermum*, *Gleichenia* and *Schoenus*. Results from these palaeo-investigations presenting the vegetation development history of the bogs seem to match the vegetation differences seen in young and old bogs supporting the proposed succession patterns (Clarkson *et al.*, 2004).

Shearer (1997) compared the development of Kopouatai Bog, a relatively untouched site, with two other significantly altered sites, Moanatuatua and Whangamarino bogs. The latter two (excluding the area of scientific reserve at Moanatuatua) have been greatly altered by fire, fertiliser and weeds, and their hydrology has been significantly affected by drainage ditches. The type of peat varies between the three sites, but they all showed vertical trends in decomposition – older peats, lower down, were more degraded due to longer exposure to microbial decay. However, some cores from Moanatuatua and Whangamarino showed a return to more humified peat up-core, unlike Kopouatai that showed a consistent upwards trend towards less humified peat. Present climate cannot explain these differences observed

between sites, since they are all close together, within 60 km of each other, and therefore experiencing similar climate/weather conditions. Instead, Shearer (1997) suggested the differences in decomposition were probably linked to hydrology. Moanatuatua could have experienced greater water table variations than Kopouatai whose water table has been kept relatively stable by close proximity to sea level. However, even though there is the possibility that sea level might have had an influence on northern Kopouatai during the earlier part of the Holocene (Newnham *et al.*, 1995), this is thought to be minor, since no major vegetation changes that would be associated with more minerotrophic conditions have occurred. Instead, restiad vegetation dominates throughout the profile. In fact, it is more likely that the sea's influence on Kopouatai is manifest by moderating the microclimates of the area. Newnham *et al.* (1995) inferred the return to oligotrophic (mineral poor) conditions from 6,130±30 ^{14}C years BP onwards (i.e. the time period of this study) following the mid-Holocene sea-level incursion into the northern parts of the bog, with areas in the south west and the east remaining above the influence of the regional water table.

Tephras are used to calculate the sedimentation rates of peat bogs. Work on high altitude bogs in the North Island (Froggatt and Rogers, 1990) calculated low but uniform accumulation rates since their formation 6,000 ^{14}C years ago, ranging from 0.25 to 0.4 mm/year, implying that biomass productivity and decomposition were more-or-less constant over time. Peat accumulation was also seen to decline with increased altitude, presumably as vegetational productivity decreased in colder environments.

2.2.2 Palaeoclimate studies from peatland archives

Since founding work was carried out in northern England by Aaby (1976) and Barber (1981), various methods are now routinely used in the reconstruction of peatland palaeomoisture records, from which palaeoclimate can be inferred. This section outlines the theories behind the palaeoecological techniques employed in this project, describing and discussing their merits and applications with examples.

Proxy methods for palaeomoisture variation

The proxy techniques widely used to reconstruct palaeomoisture records are peat humification, the identification of plant macrofossil remains and, more recently, testate amoebae analysis (e.g. in England: Hendon *et al.*, 2001; Langdon *et al.*, 2003; and in New Zealand: Wilmshurst *et al.*, 2003). These are often used in conjunction with each other to

obtain multi-proxy records of surface wetness, which tend to show a good general degree of agreement with each other (Charman *et al.*, 1999).

Peat humification (and carbon analysis)

Peat humification is a measure of the degree of peat decomposition, controlled by the moisture content of the peat itself (which is closely related to the height of the water table). The most widely used method for determining the degree of peat decomposition is that of humic acid extraction using the alkali sodium hydroxide (NaOH) (Blackford and Chambers, 1993) through which colorimetric measurements (as a light transmission reading) are taken using a spectrophotometer. An alternative method devised by Caseldine *et al.* (2000) uses luminescence spectroscopy to chemically analyse humified peats, determining the chemical composition of the extract. Even though Caseldine *et al.* (2000) consider the colorimetric method to produce results that are too general and reflect only major climatic shifts, as well as criticising the use of NaOH as an extractant (by altering the organic matter and mixing all the decay products), they agree that it still remains a good proxy indicator of relative changes in the degree of peat humification.

Using the peat humification method of Blackford and Chambers (1993), high light transmission readings imply low peat humification values. In ombrotrophic conditions, this is thought to result from a high water table created by wetter conditions from which increased precipitation (and/or reduced evapotranspiration) can be inferred. Anaerobic conditions resulting from water logged conditions inhibit microbial decay and lead to good fossil preservation and reduced humic acid production and therefore increased light transmission. Conversely, high humification values imply a lower water table as a result of drier conditions, allowing availability of oxygen for decomposition processes and production of more humic acid, limiting light transmission through the sample.

It is essential in palaeoclimate studies to be able to distinguish between a climatically induced change in peat humification and changes caused by the differential decay of different plant species. Some species are more susceptible to decay than others, as Johnson *et al.* (1990) found when comparing the decay rates of different *Sphagnum* species. If more-humified conditions are observed independently from any changes in vegetation, then a climate-driven forcing can be inferred. Peat humification responds very rapidly to changing forcing variables and might therefore be preferable to plant macrofossils for

example, which experience slower vegetational species reaction and succession times (Blackford, 1993).

The peat humification technique does, however, have its limitations:

a) It is only a qualitative technique – it is not possible to reconstruct a moisture value from the light transmission reading. It is only possible to infer a relative measure of moisture content e.g. wetter, drier. In contrast, plant macrofossils and testate amoebae analysis can facilitate quantitative inferences of past ecological conditions and therefore are useful complementary techniques.
b) Once the peat has reached saturation point, it cannot get any wetter, even though rainfall might have been increasing.
c) As stated above, the decay of peat can be related to vegetation composition, thus necessitating comparison with plant macrofossil data to determine this. At these New Zealand restiad sites, however, there is very little variation in species composition down-core; samples tend to be dominated throughout by root matter of the restiads *Empodisma* and *Sporadanthus*.
d) Secondary peat decay can occur if the water table later falls, allowing peat that was formed under wet conditions to decompose and erroneously suggest dry conditions.
e) Humic acids are complex compounds, the characteristics of which are not fully understood. It is not clear how different components can vary between samples and affect light transmission values, nor exactly how NaOH might alter them during processing.

The mineral content of samples is often obtained in conjunction with peat humification analysis in order to be able to correct for mineral contamination affecting the light transmission of peat samples. This can either be measured as traditional loss on ignition, or as the amount of carbon in the sample (Total Organic Carbon (TOC)). In New Zealand, tephra layers are a particularly important source of mineral input as both macro- and microscopic deposits. Tephra shards deposited on the bog surface are then incorporated into the peat.

The only humification-based palaeomoisture reconstructions from New Zealand so far are those of McGlone and Wilmshurst (1999b) and Wilmshurst *et al.* (2003), demonstrating the need for more such studies from this region. These authors worked on sites from

southern New Zealand. Prior to this investigation, no such investigations have been undertaken of the tephric peats of northern New Zealand.

Plant macrofossils

Fossil plant remains extracted at depth from a peat bog can reveal much about the past hydrological conditions of the site. By identifying the plants' modern preferred growing conditions, it is possible to infer that those same conditions prevailed at the time at which the plant was growing. For example, Barber *et al.* (1999) used macrofossils of aquatic bog moss species to infer the previous existence of open water pools on the peatland surface at Fallohogy, Ulster. Reconstructions of moisture levels of Bolton Fell Moss, Cumbria (Barber *et al.*, 1994) for the latter half of the Holocene were also derived using plant macrofossils. Spectral analysis of that record identified a periodicity of *c.*800 years for wetness variations. Hughes *et al.* (2000) subsequently used plant macrofossils to reconstruct plant succession communities in the development of the nearby Walton Moss, and wet shifts identified here agreed well with the previous work in the area. However, the degree of plant response is controlled by both the size of climatic change and the preceding bog conditions (Blackford, 1993). For example, if the bog was previously very dry then even a small increase in wetness can have a large effect on species, and vice versa.

In New Zealand fewer investigations of plant macrofossils preserved in peat have been undertaken. Comparisons of three different palaeoecological methods for palaeobotanical reconstructions were carried out on North Island bogs by Clarkson *et al.* (1995). Methods used were pollen, plant litter and wood. Plant macrofossils were shown to represent more reliably the local *in situ* vegetation, whereas pollen records gave more regional signals. However, between the sites that are 20 km apart, there were actually more similarities between the litter and wood records than there were for the pollen, reflecting the varying source areas for the latter. Another benefit of plant macrofossils is that even though they are often not as abundant as pollen, they are often identifiable to a higher taxonomic resolution i.e. species level, thereby serving as better palaeoclimate proxies.

From the few studies undertaken, it is possible to rank the principal plant species of this study along a moisture gradient, based on observed plant-moisture relationships in the modern vegetation. For example, work by Campbell *et al.* (1973) on plant fragments from the North Island peatlands identified alternating dry and wet periods – with *Leptospermum* and *Gleichenia* indicating dry phases and *Sporadanthus* and *Empodisma* indicating wetter

periods. Building on this work, Clarkson (2002, pers. comm.) has suggested a more detailed hydrological gradient for ombrotrophic peatlands in New Zealand (*Figure 2.4*).

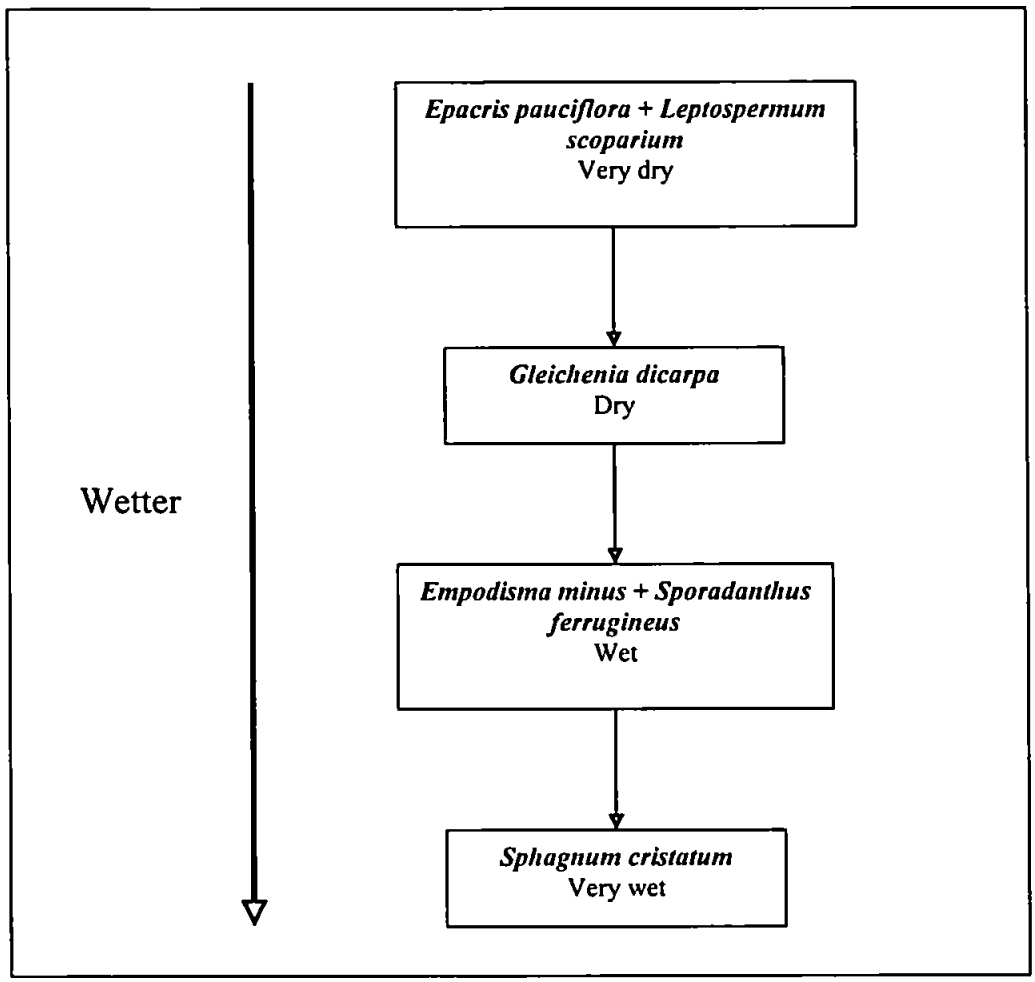

Figure 2.4 The main moisture indicator plant species from Kopouatai and Moanatuatua (after work by Campbell et al., 1973; Clarkson, 2002, pers. comm.).

At Kopouatai some limited plant macrofossil work has been carried out (Newnham *et al.*, 1995) the results of which, when combined with palynological findings, contributed to the reconstruction of the bog's history and development over the Holocene.

However, the use of plant macrofossils has certain limitations. First, it is generally assumed that all plant macrofossils are remains of plants that were once growing *in situ*. However, small plant fragments, such as seeds, can also be wind dispersed far from their source. Second, above-ground plant fragments are more reliable for palaeostudies than root remains, as many of the roots that penetrate to depth are actually derived from plants currently living on the bog's surface. Finally, it is possible that plants could have changed their ecological affinities throughout the Holocene, and the limited spatial range of different species may complicate between-site comparisons. Neither of these factors are

considered to be problematic in this investigation which concerns the mid-to-late Holocene at two sites of similar vegetation composition.

Charcoal

Charcoal fragments found within cores are an indicator of past fire occurrence. Both microscopic and macroscopic pieces can be counted, representing different source areas of fires. Microscopic charcoal can be carried further on the wind and is therefore thought to be indicative of distant regional burning (which can also be climate related). Macroscopic charcoal, however, indicates nearby, local, possibly *in situ* burning. It is often difficult, but vitally important to distinguish the causes of fire i.e. whether they are natural or anthropogenic, as discussed later in section 2.4.3. However, if human factors can be excluded, as is the case in this investigation, then charcoal gives good indications of past bog moisture conditions. For example, McGlone and Wilmshurst (1999b) use charcoal to identify ENSO-driven wet and dry climatic phases in New Zealand, shown by higher charcoal fragment concentration indicative of increased burning during dry periods.

Fire can also be initiated by the deposition of hot tephra fall directly onto vegetation, the effects of which Giles (1999) investigated. Giles concluded that the effects on vegetation by altering species composition can last for *c.*100 years, but in these cases the causal mechanism of burning is clearly identified by the presence of substantial macro-tephras.

Testate amoebae

Recently-renewed interest in the use of testate amoebae has led to the successful reconstruction of past hydrological and moisture conditions, particularly of peatland and other mire habitats, with founding work carried out in Germany, Sweden, Finland and the Netherlands (e.g. Hoogenraad, 1935; Tolonen, 1966; Tolonen *et al.*, 1992, Tolonen *et al.*, 1994; Grospietsch, 1954), and more recently in the UK and North America (e.g. Charman and Warner, 1992; Hendon *et al.*, 2001).

Testate amoebae (Protozoa: Rhizopoda) are microscopic single-celled fauna, usually between 20 and 200 μm in diameter, consisting of an inner, living cytoplasm surrounded and protected by a resistant shell. Their diagnostic external tests, each with at least one aperture, are either a) xenosomic (produced from material taken up from the local environment such as mineral grains, diatom frustules), b) idiosomic (made from self-produced materials, in the form of either siliceous/calcareous plates or organic secretions)

or c) a mix of the two (Charman, 2001). Testate amoebae feed on bacteria, fungi, algae and other amoebae, and reproduce at fast rates, usually by asexual division.

Testate amoebae can be used as palaeoecological indicators because their tests are resistant to decay and therefore are well preserved and abundant as fossils in sediments (especially in *Sphagnum* peats). However, in certain conditions, fossilisation processes can detrimentally affect test preservation, as they can be subject to dissolution and breakage, inhibiting counts and identifications.

Much work has been done on the taxonomy of testate amoebae and many tests are identifiable to a low taxonomic level relatively easily, enabling accurate reconstructions of past conditions, assuming adequate knowledge of their modern habitats. Their short life cycle, together with rapid reproduction rates, means that they react very quickly to environmental changes, which makes them preferable in some cases to alternative microfossil analyses, such as pollen, that have longer reaction/adaptation times (McCarthy *et al.*, 1995).

Testate amoebae require water to live, to protect their exposed pseudopodia that are used for movement and feeding, and so inhabit the films of water around soil particles and plant roots. However, they can survive extreme conditions, by 'encysting' (closing up) during dry periods to prevent drying out (Sleigh, 1973).

Testate amoebae are found in a range of aquatic environments, ranging from freshwater to marine, such as peatlands, lakes and salt marshes (Charman, 2001). Recent, widespread work has established that many species, but not all are cosmopolitan (Warner, 1991). However, caution is required when inferring past environmental conditions, particularly when comparing sites on different continents, and even within hemispheres. For example, Tolonen (1986) found different ecological preferences of the species *Difflugia oviformis* between England and Finland, and Charman and Warner (1997) found different taxa in Newfoundland sites than on the North American mainland, possibly due to the more oceanic climate of the former location.

It has long been recognised that the main environmental variable influencing species distribution of testate amoebae taxa is water availability (e.g. Tolonen *et al.*, 1994), proxies for which are percentage moisture and water table depth. However, nutrient status and pH

are also thought to be important. Ordination of testate assemblages in relation to measured environmental variables in Newfoundland, Canada (Charman and Warner, 1997) shows water table depth and soil moisture explaining 41.3% of variance, and pH explaining 24.8%. Tolonen *et al.* (1994) also identified trophic status, C/N ratio of peat, depth of the testate amoebae sample and dissolved organic carbon levels of the water as important variables influencing distribution, demonstrating that a combination of variables rather than one single factor influences assemblages.

Many other factors can play a role in influencing testate amoebae distributions, affecting the reliability of environmental parameter reconstructions. For example, Woodland *et al.* (1998) inferred that variance between measured and reconstructed values could be due to water chemistry and nutrients, the presence of unexpected vegetation types, or microtopography e.g. a high hummock of unusual dryness. Obvious outliers should therefore be excluded from models.

Modern relationships between testate amoebae assemblages and measured environmental variables can be used to derive models known as 'transfer functions' to reconstruct quantitatively depth to water table from fossil data. The first testate amoebae transfer function was developed by Warner and Charman (1994) for a site in Ontario, Canada. Since then, it has been found that palaeowater tables can successfully be reconstructed to within ±3.5 cm and palaeomoisture to ±4% (Woodland, 1996) i.e. with small errors. Woodland *et al.* (1998) derived a UK transfer function for both water table and percentage moisture. This was then used to reconstruct the hydrological history of Bolton Fell Moss, Cumbria. In the Southern Hemisphere, Wilmshurst *et al.* (2003) added samples to the training set of Charman (1997) and attempted to reconstruct the first Holocene palaeomoisture values for the Southern Hemisphere. However, there was little overlap between the fossil and modern testate assemblages, inhibiting reliable palaeomoisture reconstructions.

As demonstrated, much work has been carried out using testate amoebae as a microfossil technique on peatland areas, in both the British Isles (e.g. Hendon *et al.*, 2001) and Canada (e.g. Warner, 1991). From reconstructed variables, inferences can be made about palaeoclimatic conditions prevailing at that time. It is possible to determine the degree of regionality of the records by comparing two hydrologically separate sites. If there is good agreement between the reconstructions, then it can be inferred that such changes are

climate-driven, rather than a result of internal bog characteristics such as microtopography, aerial expansion and vegetation changes. At Coom Rigg Moss, Northumberland, records 10 m apart showed a high degree of similarity, best for the last 1,000 years (Charman *et al.*, 1999).

Work in peatlands of the British Isles (Charman and Hendon, 2000) used testate amoebae to relate reconstructed moisture levels with instrumental i.e. directly measured, and ice accumulation records of moisture budgets of the North Atlantic. Comparing moisture reconstructions with Lamb's climate records (a summer wetness and winter severity index) it was seen that the period of increased bog surface wetness at the time of the Little Ice Age (LIA) coincided with wet summers and severe winters causing a high water table. Former atmospheric circulation can be inferred, such as movements of weather pressure centres over the North Atlantic, as well as inferences on past influencing oceanic conditions.

The uncertainty surrounding the interplay between precipitation and evapotranspiration, and determining which most influences peatland moisture regimes, was investigated by Charman *et al.* (2004). Reconstructed water tables from northern England and from Estonia were compared with instrumental records from those regions, and inferred as showing that the strongest control on water table depth was summer precipitation, with summer temperature an additional factor in continental locations.

Other climate proxy techniques

In addition to the main palaeoecological techniques outlined previously and employed here, alternative methods related to peatland research that can be used in the reconstruction of palaeoclimate indicators include Coleoptera, opal phytoliths, tree rings and leaf stomata size (that relates to atmospheric carbon dioxide levels (Beerling and Chaloner, 1993)) and stomata density. Unlike the methods adopted here, which can generate near-continuous high-resolution records, these alternative methods are limited to a greater extent by more spasmodic recovery of targets in the peat profile.

Speleothems i.e. stalactites and stalagmites, in caves below areas of peatland may yield similar palaeoclimatic records from luminescence emission wavelength measurements, as the local surface peat humification records above. This record results from the overlying peat decaying and creating a proxy-climate signal in the bog water that subsequently drips

through into the caves to form the speleothems (Charman *et al.*, 2001). This approach was applied in New Zealand by Hellstrom *et al.* (1998) who found that the carbon isotopic variations in speleothems closely matched the CO_2 records (indicative of forest productivity) from the soil above the cave, while the oxygen isotopes reflected the source of precipitation. They concluded that heavier isotopic values are associated with an equator-ward shift of the Subtropical Front, and increasing strength of the westerlies across the South Island.

Recently renewed interest has developed in using carbon isotopes from vegetative remains from peatlands that relate to atmospheric carbon dioxide (White *et al.*, 1994). Examples are studies by Ménot and Burns (2001) and Pancost *et al.* (2003). Work by Turney *et al.* (2002) touched on the potential of such palaeoclimatic reconstructions in New Zealand, by analysing $\delta^{13}C$ values from Late Otiran fossil leaf material.

2.3 Palaeomoisture and palaeoclimatic reconstructions in New Zealand

The following section describes New Zealand's main climatic changes since the late Tertiary based primarily on palynology, supplemented with alternative techniques such as glacial and isotopic evidence. The emphasis here is on Holocene climate, in keeping with the scope of this project. For a more extensive account of techniques used to reconstruct the Quaternary history of New Zealand, and their principal results, the reader is referred to Newnham *et al.* (1999).

2.3.1 Longterm variations

The late Tertiary of New Zealand was an arid period and was followed by climatic fluctuations leading to an overall deterioration during the Pliocene. The climate of the North Island was more stable than that of the South Island, where more-open vegetation developed. Into the Pleistocene, *Nothofagus brassii*-type forest declined, eventually to extinction, and grasses increased as conditions cooled once again. Throughout the Pleistocene, various other plant species became extinct, such as *Eucalyptus* and *Acacia*, resulting in New Zealand vegetation types and assemblages that are very different to those of its nearest neighbouring landmasses, such as Australia (Kershaw, 1988).

Throughout the Quaternary, New Zealand experienced numerous glacial/interglacial cycles, evidence for which is best preserved in the landscape for the most recent glaciated period, the Otiran, which lasted from approximately 100,000 to 10,000 years BP

(Newnham *et al.*, 1999). Most of this glacial activity was centred on the higher altitude Southern Alps of the South Island, with the North Island affected by mostly periglacial conditions. During the Last Glacial Maximum (LGM) at 22-14,000 ^{14}C years BP, grass and shrubland dominated and levels of sediment erosion were high, indicating a cold, dry and windy climate associated with the lower mean annual temperatures. However, a range of evidence suggests that at the LGM temperatures were only 5°C lower than today, which is insufficient to have been responsible for the extensive scarcity of forest cover across most of New Zealand. Other factors such as fire, drought, frost and wind are thought to have contributed (McGlone, 1988).

Subsequently, numerous lakes formed throughout the Waikato region. Many became established *c.*17-15,000 ^{14}C years BP during the last aggradations of the Hinuera Formation (McCraw, 1967) by ponding behind valley-blocking deposits. These sites therefore have a long undisturbed, well-preserved stratigraphy. Pollen work by Newnham *et al.* (1989) has shown that throughout this region Lateglacial and Postglacial vegetation changes recorded in lakes across the Waikato region were broadly synchronous. Following the largely unforested LGM, the tree taxa *Prumnopitys* and subsequently *Dacrydium cupressinum* increased rapidly at 14,500 ^{14}C years BP, immediately after the Rerewhakaaitu Ash was deposited (Newnham *et al.*, 2003). In these early postglacial times, 11,000-9,000 ^{14}C years BP, conditions were at their warmest and wettest.

From 14-10,000 ^{14}C years BP, most of New Zealand underwent re-afforestation. From 13,000 ^{14}C years BP onwards, landscape stability, implying also climatic stability, had become widely established (McGlone, 1995). By *c.*12,000 ^{14}C years BP, some 90% of land below the modern treeline was covered with forest (McGlone *et al.*, 1993) and as conditions became warmer and wetter, forests spread southwards rapidly.

2.3.2 Holocene variations

The Holocene (locally known in New Zealand as the Aranuian) was warmer and wetter than the preceding Lateglacial climatic conditions, resulting in a further spread in forest extent. The vegetation mostly comprised podocarps (Southern Hemisphere conifers) with some restricted *Nothofagus* (McGlone *et al.*, 1993), reaching maximum coverage 10-7,000 ^{14}C years BP (Ogden *et al.* 1998). At 7,000 ^{14}C years BP numerous lakes and bogs formed in the east, as winters there became wetter (McGlone *et al.*, 1993).

Newnham *et al.* (1989), Newnham (1999) and McGlone (1988) all suggest that New Zealand's climate became drier and more variable as the Holocene progressed. Shulmeister (1999) identified a drier, more frost prone mid-Holocene climate between 7,000 and 3,000 ^{14}C years BP. This agrees with pollen work by McGlone and Moar (1977) and Newnham *et al.* (1989, 1995) who found *Ascarina lucida*, a plant species indicative of an absence of frost and drought, dominating pollen assemblages until its rapid decline after 5,000 ^{14}C years BP. Newnham *et al.* (1989) also identified a large increase in the amount of macroscopic charcoal at 5,500 ^{14}C years BP from their sites on the North Island, again inferring drier conditions. Glacier evidence of Gellatly *et al.* (1988) suggests a similarly timed climatic change, by an increase in glacier activity after 5,000 ^{14}C years BP following a period of standstill, controlled by an increase in the strength of westerly airflows. This glacial advance however implies either cooler and/or moister conditions (controlled by stronger westerlies) which is not consistent with drier conditions in the north.

The cooling identified at 5,000 ^{14}C years BP is also supported by Hodell *et al.* (2001) who identified a sudden cooling in the Antarctic surface waters of the southern Atlantic Ocean at 5,000 cal. years BP. A rapid increase in ice-rafted debris is found in this study area, similar to the North Atlantic events of *c.*1,500 year periodicity (Bond *et al.*, 1997). At a similar time (6,000 cal. years BP) a cooling is inferred from the Taylor Dome ice core from the Ross shelf in the Antarctica, as seen by oxygen isotope records (Steig *et al.*, 1998).

From Waitomo speleothems (western North Island, New Zealand) Williams *et al.* (2003) found that δ^{18}O relates positively with temperature and negatively with rainfall, and that δ^{13}C is mostly controlled by rainfall. They derived Holocene isotope records and found there to be strong agreement with the pollen records of Newnham *et al.* (1989) and McGlone *et al.* (1993), and with glacier moraine evidence of Gellatly *et al.* (1988). Williams *et al.* (2003) reconstructed a postglacial climatic optimum at 10,800 ^{14}C years BP (earlier by 2,000 years than that of the Northern Hemisphere), a cold period at 3,000 ^{14}C years BP and a warm peak 750 years ago coinciding with the Medieval Warm Period in Europe.

2.3.3 Possible forcing mechanisms

There is much debate concerning the possible mechanisms that are responsible for driving global climate change. The main contention surrounds the respective roles of orbital and solar forcing, the effects of which are enhanced by various, complex feed-backs.

The principle behind the theory of orbital forcing is that climate change is driven primarily by variations in solar insolation input to the Earth, caused by patterns in planetary orbits (i.e. changes in the Earth's orbit around the Sun) (Rind, 2002). Long-term Milankovitch-scale orbital forcing operates on timescales of 10^3 to 10^5 years, the three main periodicities of which are approximately 22,000, 41,000 and 100,000 years for the precessional, obliquity and eccentricity cycles respectively, all of which act simultaneously.

There is some evidence linking Holocene climate change in New Zealand to orbital forcing. In a recent review of the Australasian region, Shulmeister *et al.* (2004) identify a possible pattern in changes in the strength of the circum-Antarctic westerlies throughout Australasia since the last glacial, and suggest that this was forced by the precessional cycle. Westerlies are thought to have peaked in strength at the LGM, been at a minimum at 11,000 ^{14}C years BP and experienced a second maximum during the Late Holocene, although evidence for the latter is less conclusive.

The strength of westerlies is thought to be strongly linked to precipitation variations in New Zealand in particular (see section 2.4.1). Shulmeister (1999) concludes that after an initial decline in the early Holocene, Walker cell circulation strength subsequently increased from 5,000 ^{14}C years BP onwards. He suggests this is the most important climatic shift during the Holocene period for New Zealand. It is thought to have been initiated by an increased temperature, and therefore pressure, gradient between the equator and poles, resulting from increased seasonality caused by the precessional cycle. This then prompted increased Southern Hemisphere atmospheric circulation of the mid-latitude westerlies and trade winds, similar to the orbital forcing mechanisms identified from westerly intensity dust particle-size records by Janecek and Rea (1984) as operating in the Northern Hemisphere.

It has also been proposed that shorter-term variations in Earth's climate (10^1 to 10^2 years) are caused by variations in the Sun's output, referred to here as solar variation (discussed by Chambers *et al.*, 1999). The Earth system is thought to amplify changes in solar output through various mechanisms. During solar minima (e.g. the Maunder Minimum, an event of enhanced sunspot activity) solar winds are less efficient at dispersing cosmic rays, allowing more to reach the Earth's atmosphere. This is thought to cause a cooler and wetter climate (van Geel *et al.*, 1999) possibly via the creation of increasingly cloudy conditions.

Blackford and Chambers (1995) demonstrate the coincidence of a wetter/cooler climate (as inferred from a peat bog record) with reduced solar activity. The link between solar activity and cloud formation was first proposed by Svensmark and Friis-Christensen (1997); an increase in cosmic rays is thought to result in an increase of charged particles acting as cloud condensation nuclei leading to increased cloud cover during periods of low solar activity. Increased cloudiness then inhibits incoming solar radiation and thus lowers temperatures (see also Carslaw *et al.*, 2002; Baker, 1997). These processes are at present, however, little understood, resulting in difficulties with modelling possible climatic scenarios. Past changes in the strength of solar radiation can be inferred from ^{14}C measurements because the amount of atmospheric ^{14}C created is affected by solar activity (Magny, 1993, 1995). During reduced sunspot activity more atmospheric ^{14}C is created.

An 11 (or 22) year cycle has also been identified in palaeoclimatic studies, and this is thought to relate to variations in the solar cycle itself; the solar magnetic field switches direction every 11 years, resulting in the 22 year Hale cycle. However, this mechanism is debated, since it is questioned how so 'small' a change can have such major climatic repercussions. Van Geel *et al.* (1999) argue that even a minor variation in solar input can have a significant climatic effect, via various atmospheric feed-backs involving the propagation of energy from the troposphere into the stratosphere (Rind, 2002).

There is some evidence of solar linkages in peat records. Early work by Aaby (1976) found a 260-year long climate cycle acting over the last 5,500 years. Blackford and Chambers (1995) related a 1,000 year old peat humification record of a west Ireland bog to such solar influences. Periods of reduced peat decomposition seemed to coincide with periods of reduced sunspot activity, for example the Maunder Minimum, which occurred at about the time of the coldest period of the Little Ice Age, from AD 1645-1715. Subsequent work by Chambers *et al.* (1997) found an approximately 210-year cycle in a peat humification record from Scotland spanning 5,500 ^{14}C years BP, that probably results from the solar 'Suess' ('de Vries') cycle (Rind, 2002) of that periodicity. In addition, Chambers and Blackford (2001) have since found a (tentatively ascribed) similarly-timed periodicity in peat humification records from blanket peat bogs situated though the British Isles (as well as a possible 80-year Gleissberg cycle).

2.3.4 Inter-annual and inter-decadal climate oscillations

There is currently much interest in the distal effects of ENSO weather regimes throughout the globe, as it is considered to be the most dominant signal of interannual climatic variation (Gordon, 1985). Rasmusson *et al.* (1990) identified two ENSO time cycles in operation: a two-year cycle and four/five-year cycle, the former of which is more certain to exist. The ENSO climatic phenomenon, centred on the tropical Pacific Ocean, is well documented as a change in atmospheric circulation, driven by sea surface temperature contrasts, and pressure within the Walker Circulation cell. During El Niño phases, a reversal of the normal (La Niña) conditions, trade winds weaken and ocean upwelling off the coast of south west South America decreases. The locus of convection-driven precipitation moves eastwards across the central Pacific Ocean, resulting in heavy rainfall in South America.

Variations in the Southern Oscillation Index (SOI) (the normalised pressure difference between Tahiti and Darwin) displace the South Pacific Convergence Zone (SPCZ) (a branch of the Inter Tropical Convergence Zone (ITCZ)), to the north during El Niño and south during La Niña. El Niño periods are associated with low SOI values, and La Niña with high values.

New Zealand is of particular interest regarding sensitivity to ENSO signals. Hay *et al.* (1993) identified that zones *between* central pivotal regions of ENSO influences are more sensitive to changing ENSO conditions than the core regions themselves. Such pivotal regions are *always* affected by the SPCZ and therefore show minimal variation between El Niño and La Niña conditions. New Zealand is located between two such centres of relatively enhanced activity, one located to the east and one to the west. During the equator-ward excursion of the SPCZ throughout El Niño conditions, New Zealand experiences stronger and more frequent westerly airflows in summer, resulting in enhanced rainfall in the west and drought in the east (NIWA, 2004). During winter, winds are more southerly and therefore colder. During La Niña, poleward displacement of the SPCZ results in increased northerly and northeasterly wind regimes, resulting in wetter conditions in the north east of the North Island and drier in the south of the South Island (NIWA, 2004). ENSO illustrates well the atmospheric teleconnections between the tropics and mid-latitudes. The effects of ENSO phases on New Zealand climate are discussed further in section 2.4.1.

Dendrochronological work on tree rings has identified what are thought to be ENSO climate signals in North America e.g. (Cook *et al.*, 2000). This method is well suited to detecting decadal and sub-decadal signals due to the absolute, annual dating capability and monthly, seasonal and annual climatic reconstructions are possible (Cook, 1992). In New Zealand, Fowler *et al.* (2000) have found a significant relationship between *Agathis australis* (kauri) tree-ring growth and ENSO's climatic influences, expressed as the SOI. In the Southern Hemisphere, an ENSO event occurs within one growing season (the strength of an event's influence is greatest in New Zealand between September and November), rather than crossing over two separate growth periods, as is the case in the Northern Hemisphere. This simplifies the issue of correlating climatic events with seasonal growth in New Zealand. Kauri growth and the SOI index of the two preceding years are significantly positively correlated (Fowler *et al.*, 2000) who conclude that cool, dry El Niño conditions in northern New Zealand cause negative temperature and precipitation anomalies, resulting in enhanced kauri growth, with the reverse occurring during La Niña events.

From work using pollen and charcoal, McGlone *et al.* (1992) suggest that either the onset or intensification of ENSO conditions began during the mid-Holocene. Also over this time period, Markgraf *et al.* (1992) inferred an increase in the strength of ENSO activity, causing an increase in precipitation variability. Pollen, plant macrofossils, testate amoebae and peat humification records have been used by McGlone and Wilmshurst (1999b) in a small montane bog in east Otago to investigate Holocene vegetation change. The spread of *Nothofagus menziesii* and increased fire incidence commencing 5,000 ^{14}C years BP were linked to changes in atmospheric circulation, namely ENSO, causing irregular rainfall and severe droughts during the resulting cooler, wetter winters and variable, drier summers of the mid-late Holocene.

New Zealand is also thought to respond to what was identified and termed by Hare in 1996 as the Pacific Decadal Oscillation, which occurs over a timescale of 20-30 years (Mantua *et al.*, 1997). Due to its relatively recent discovery, little is known about this phenomenon, in particular its driving force. Most work has concentrated on its manifestation in the northern Pacific, and over North America, and it is thought to cause changes in sea temperatures which then affect storm occurrences. However, limited work in Australia has found links with rainfall patterns there (Power *et al.*, 1998).

Another climatic cycle in the Southern Hemisphere is the High Latitude Mode (Kidson, 1988), also known as the Antarctic Oscillation (AAO) (Thompson and Wallace, 2000). It is a fluctuation in atmospheric mass between mid and high latitudes (Carleton, 2003) that is thought to have more recently developed into a more positive index phase, manifest at mid latitudes as an increase in westerly winds (IPCC, 2001).

2.3.5 Inter-hemispheric patterns of climate change

The issue of whether Northern and Southern Hemisphere climate changes are and have been similar and/or synchronous is of considerable interest. This is because the patterns of climate change around the world have important implications for identifying the mechanisms by which energy is transferred.

For example, research has been carried out on the climatic reversal of the 'Younger Dryas' that occurred during the start of the post-glacial warming trend and that has been well established in the Northern Hemisphere. The conflicting evidence in New Zealand for such an event is of great interest. Work by Hellstrom *et al.* (1998) shows an inferred temperature drop deduced from speleothem oxygen isotopes on Mount Arthur, at the time of the Younger Dryas, which is supported by Ivy-Ochs *et al.* (1999) who inferred a synchronous advance of glaciers in the European Alps (11,860±210 ^{14}C years BP) and the New Zealand Southern Alps (11,720±320 ^{14}C years BP) from ^{10}Be mass spectrometry. Hendy and Denton (1994) dated the Waiho Loop terminal moraine advance of the Franz Josef Glacier, South Island to 11,050 cal. years BP, synchronous with the Younger Dryas in the North Atlantic. This implies that the two hemispheres were responding synchronously to climatic forcing. However, McGlone (1995) saw no pollen trends indicating such a cold period and Singer *et al.* (1998) conclude that pollen evidence from a kettle-hole north-west of Nelson infers no temperature drop, as postglacial afforestation was continuing throughout that period. Any glacial advances (e.g. of Franz Josef Glacier) at that time (11-10,000 ^{14}C years BP) were thought to be due to increased snow/ice accumulation from increased precipitation, due to enhanced airflow from the west and reduced summer ablation (i.e. melt) due to increased cloud cover. Turney *et al.* (2003) reinforce the idea of inter-hemispheric heterogeneity from their work on sites throughout New Zealand that suggests a *warming* at the time of the Northern Hemisphere Younger Dryas cooling due to shifts in the thermohaline circulation of the region. Interestingly, Newnham and Lowe (2000) had also found evidence of the lateglacial cooling, but

occurring 600 ^{14}C years *before* that seen in the Northern Hemisphere, suggesting a possible Southern Hemisphere lead in this event.

With regards to Holocene variations in particular, van Geel *et al.* (1996) and van Geel and Renssen (1998) identified a period of enhanced atmospheric ^{14}C from 2,750-2,450 ^{14}C years BP (*c.*850-760 cal. years BC) from a site in The Netherlands, synchronous with a sudden deterioration in climatic conditions, identified from a population migration out of marginal sites. Van Geels *et al.*'s (1999) proposed forcing mechanism is that of solar variation. More recently, a similarly timed event has been identified in Chile (van Geel *et al.*, 2000), manifest as cooler and wetter conditions. Contemporaneous changes were also identified throughout the rest of Europe e.g. Barber (1982), and more importantly in New Zealand, from McGlone and Moar's (1977) observed decline in the frost sensitive *Ascarina lucida* approximately 2,600 ^{14}C years BP and an expansion of Southern Alps glaciers at numerous times, including 2,700-2,200 ^{14}C years BP (Gellatly *et al.*, 1988).

However, conclusions should not be made too readily regarding the synchronicity of events. Early work has suggested that the Southern Hemisphere was actually *leading* the Northern Hemisphere in climatic changes, supporting Hays' (1977) theory that Southern Hemisphere sea surface temperatures led northern ones into and out of glaciations (possibly due to the more rapid response of the Antarctic ice sheet to climate changes than the Arctic's reaction time (Salinger, 1984)). A Southern Hemisphere lead was reinforced by Williams *et al.*'s (2003) isotope record from North Island speleothems suggesting that New Zealand's postglacial temperature optimum preceded that of the Northern Hemisphere by 2,000 years. However, through the Holocene, time lags may have reduced, as the Medieval Warm Period and Little Ice Age events between hemispheres seem to have coincided (Williams *et al.*, 2003). Climatic synchronicity is complex even within hemispheres. Dodson (1998) states that the climatic shifts experienced in Australia and New Zealand were similarly timed prior to the Holocene, but that New Zealand subsequently led changes throughout the Holocene. Therefore, comparing between different hemispheres is likely to be even more problematic.

Other climatic events that have been well recognised in the Northern Hemisphere, such as the Medieval Warm Period (Lamb, 1965) and Little Ice Age (LIA) (Lamb, 1977) are of particular interest in the Southern Hemisphere. Were these events experienced in New Zealand, and if so, what was the degree of inter-hemispheric synchronicity? Unfortunately,

these specific events are beyond the timeframe of this project. Concerning the LIA, Shulmeister *et al.* (2004) suggest that it was evident in southern New Zealand as a strengthening in south westerly circulation resulting in a spell of renewed glaciation (which followed a weakening in circumpolar atmospheric circulation during the early Holocene).

2.3.6 Summary

The various issues discussed in this section illustrate the need for additional Southern Hemisphere climate studies and show that this work could help advance understanding of inter-hemispheric climate patterns, to identify the similarity of climate records between hemispheres, as well as identifying their possible causes and mechanisms.

The orbital forcing model and concept of late Holocene enhancement of ENSO patterns would suggest that results from this study should show a change from a warm, moist, relatively stable climate from the early-to-mid Holocene, to one of more variable climate in the late Holocene. Unfortunately, the sampling resolution adopted in this study is too coarse to allow the investigation of inter-annual (ENSO) and probably inter-decadal (solar forcing) cycles. However, the manifestation of ENSO might be indirectly identifiable from the palaeomoisture records produced, from greater record variability during the late Holocene.

2.4 New Zealand

This section begins by describing the geography and climate of New Zealand. This is followed by a description of its geological development, outlining its tectonic and volcanic activity and discussing in detail resultant volcanic deposits used in this project for dating.

2.4.1 Geographical setting and location

New Zealand is located between 34 and 47°S in the mid-latitudes of the Southern Hemisphere (*Figure 2.5*), just north of the Subtropical Convergence where the Southern Ocean and the more northerly subtropical waters meet (*Figure 2.6*). It is ideally located in the midst of the Southern Ocean, in the path of westerly flowing circumpolar currents, to respond sensitively to changes in the strength of these flows, particularly the dominant rain-bearing westerly winds.

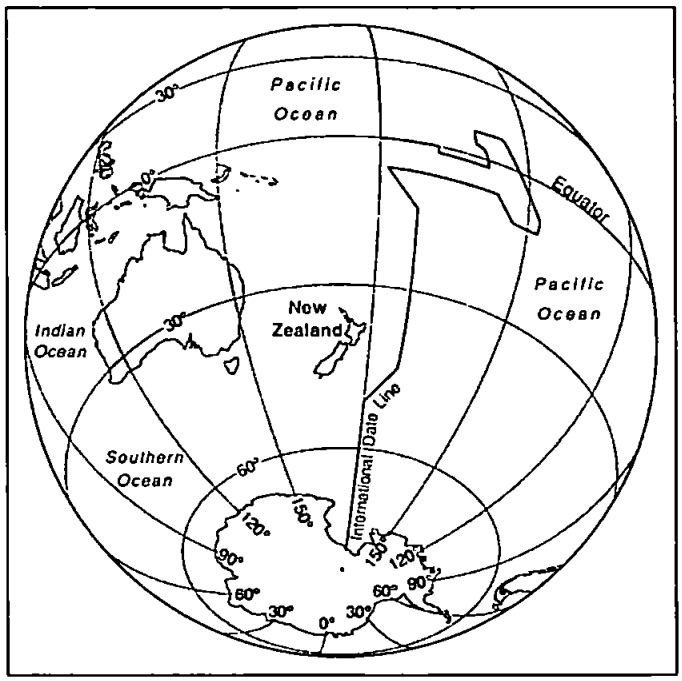

Figure 2.5 Location of New Zealand.

Current climate

New Zealand's modern air circulation patterns and climate are thought to have formed by 2,500 years BP (Salinger and McGlone, 1990). New Zealand's relatively small size in a mid-latitude oceanic location results in a warm-to-cool temperate climate moderated by maritime influences. Its synoptic weather is currently dominated by water-laden circumpolar westerly airflows (Newnham *et al.*, 1999). This is manifest as a series of alternating, irregularly paced, eastward moving high pressure anticyclones, associated with fine weather in the north of the country, and low pressure depressions across the south bringing rain (MetService, 2001). These cycles last for approximately one week (Sturman *et al.*, 1999) and their characteristics vary greatly from each other in size, intensity and speed of travel (Robertson, 1959). Most commonly they cross the North Island, following more northerly paths in Spring (September to November), and more southerly ones in Autumn (March to May) and Winter (June to August) (Robertson, 1959).

Overall, winds dominate from the west, but vary locally, especially as they pass over the Southern Alps mountain range of the South Island, changing from north-east moving on the west coast to south-east on the eastern coast (Robertson, 1959). In the North Island, winds decrease during the summer and early autumn months, compared to the South Island, where they are at a minimum in the winter (MetService, 2001). In general they decline in strength northwards. The barrier of the Southern Alps also causes a pronounced

rainshadow effect and the development of dry, warm föhn winds on the eastern lee side (MetService, 2001).

Average annual temperatures are 15.5°C in northern North Island and 10°C in southern South Island (McGlone, 1988) and there is also a warming gradient from west to east. The warmest months are January and February, and the coldest is July (MetService, 2001). In the North Island, winters tend to be mild, except in the central plateau region (Robertson, 1959).

New Zealand precipitation levels are generally high, but vary on average between 600-1500 mm, although some regions are much wetter (MetService, 2001). The amount of seasonal precipitation does not vary significantly from year to year and throughout most of the country, rain does not fall with any great seasonality. However, in the North Island, which on average has 130 days of at least 1 mm of rain per year, twice as much rain falls in winter. This effect declines southwards, where southern South Island summer experiences most precipitation (MetService, 2001). There is a strongly decreasing precipitation gradient from west to east, as a result of the orographic effect of the Southern Alps and of similarly trending mountain ranges on the North Island. Values fall from 11,000 mm in the west of central South Island, to only 800 mm in the east (Griffiths and McSaveney, 1983). As a result, the eastern regions of the South Island frequently experience droughts in the summer months (MetService, 2001).

Locally, frost occurrences can vary greatly. Less elevated areas can collect sinking cold air, and inland areas, such as Otago, are especially prone to frosts at anytime of year (Robertson, 1959). The North Island has a permanent snowfield above 2500 m on the central plateau, but otherwise snow is rare, even in winter (MetService, 2001). The Southern Alps however, have permanent snowfields and glaciers.

The number of sunshine hours is high throughout the country (averaging at least 2,000 hours per year) but is less in westerly regions (around 1,800 hours) due to higher cloud levels (MetService, 2001). Numbers are evenly spread throughout the year, with little seasonal variation.

New Zealand is also affected by the ENSO. Under normal (La Niña) conditions, atmospheric circulation across the low latitude Pacific Ocean is from east to west, as air

sinks over the coast of South America and rises over Australasia, bringing with it the relatively warm north easterly 'Trade' winds to New Zealand. El Niño events, a reversal in this circulation, are associated with increased occurrences of winds from the south west, bringing colder temperatures than normal (Brenstrum, 1998). In terms of precipitation in northern parts of New Zealand where this investigation takes place, El Niño phases are associated with below average rainfall, whereas La Niña periods bring unusually high amounts of rain due to the increased incidence of north easterly winds (Brenstrum, 1998).

Oceanic setting

New Zealand's oceanic situation has a major moderating influence on its climate. It is surrounded by five major water masses separated from each other by 'oceanic fronts' (*Figure 2.6*). Each ocean mass has its individual characteristics of temperature and salinity. Surface water temperatures (during February) range from 25°C in the north to 10°C in the south of the country, with maximum values during February and minima in August (Heath, 1985).

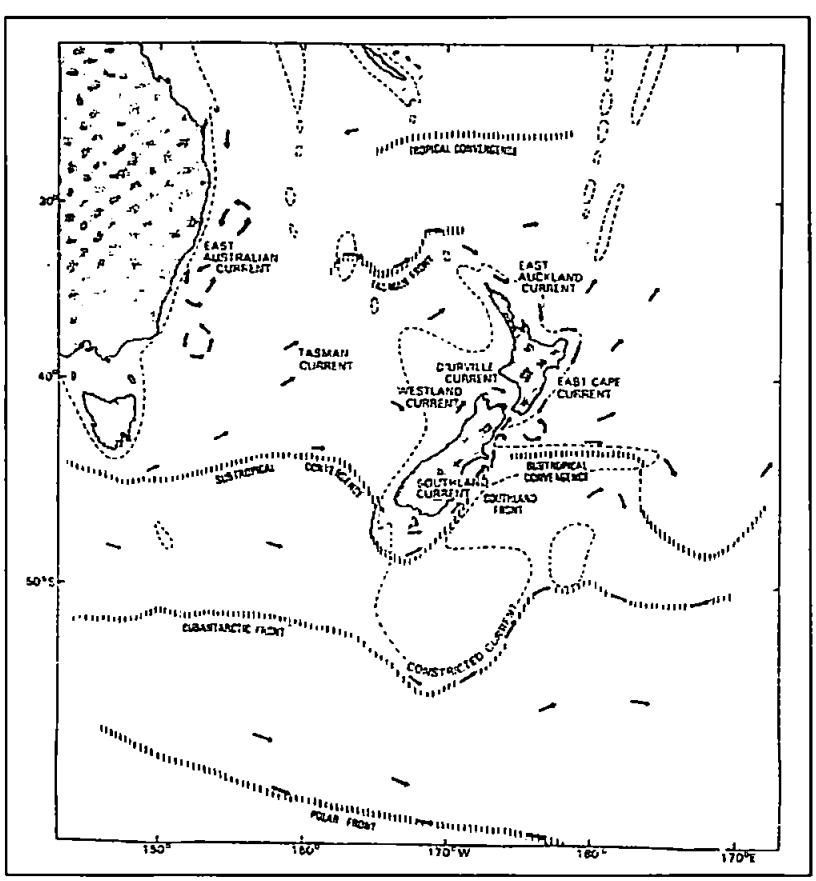

Figure 2.6 The main ocean water masses surrounding New Zealand (from Heath, 1985). The Subtropical Convergence approximately follows the 15°C surface isotherm in summer and that of 10°C in winter.

Current vegetation distribution

There are currently three main forest types present in New Zealand: *Nothofagus* (beech) forest in southern and mountain areas, *Agathis australis* (kauri) forest in the north of the North Island, and podocarp-angiosperm forest occupying much of the remaining areas. Of these, *Nothofagus*-dominated forest is the most common indigenous forest (McGlone *et al.*, 1993). Higher altitude, montane areas are covered with shrub and grassland vegetation (McGlone, 1988). Much of the natural vegetation on the low-lying land on the east of the South Island and central North Island has been cleared since European colonisation and converted into pasture land for dairy farming (*Figure 2.7*) where associated plant species, such as *Trifolium repens* (white clover) and *Ulex europaeus* (gorse) have colonised (Wardle, 1991).

Relationships between vegetation distribution and rainfall are stronger and more evident than those with temperature, but other environmental factors also play a role, such as wind strength (Norton *et al.*, 1986). Species favouring wetter climates include *Dacrydium cupressinum* (rimu), *Metrosideros* and *Weinmannia*, and those preferring dry environments include *Podocarpus* and *Prumnopitys* (in lowland areas) and *Nothofagus solandri* (beech) and *Phyllocladus-Podocarpus hallii* (upland areas) (McGlone *et al.*, 1993).

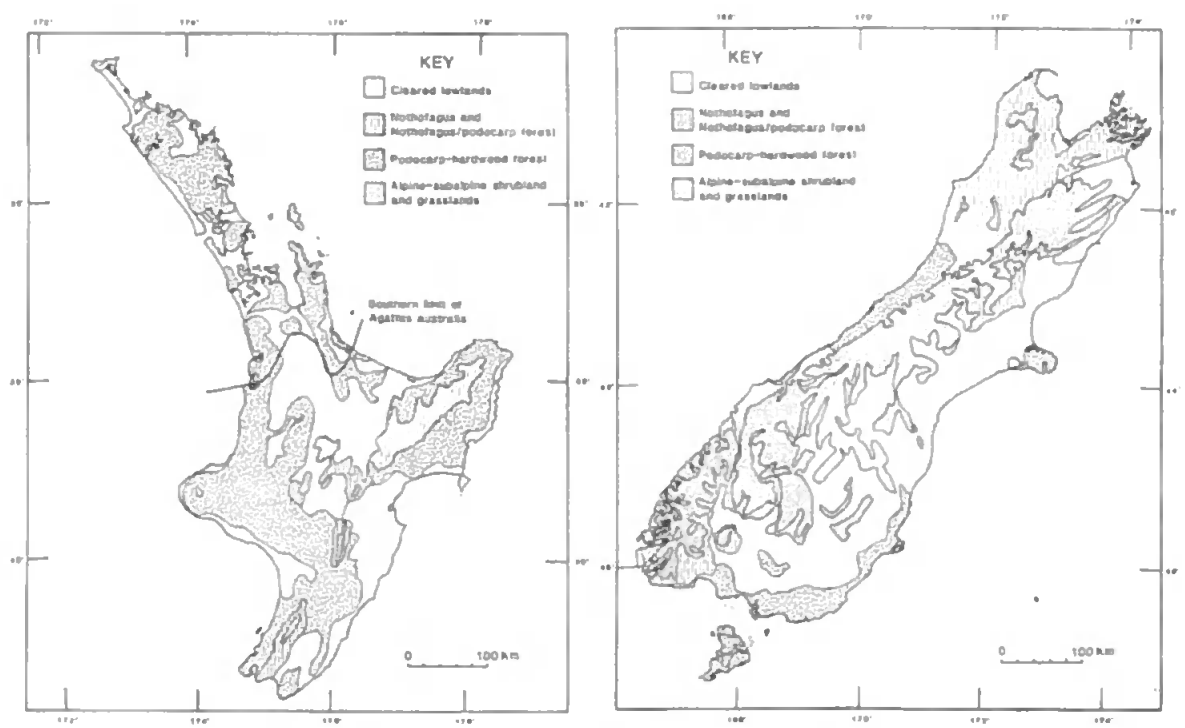

Figure 2.7 Maps of New Zealand's current vegetation cover (McGlone, 1988).

Waikato region vegetation

The Waikato Ecological Region is a band of land reaching between Port Waikato and Taumarunui, and connecting the Tasman Sea to the Bay of Plenty. Before human land-clearance the vegetation was predominantly podocarp (coniferous)-hardwood (broadleaf) forest (hardwoods include all non-*Nothofagus* angiosperm trees (McGlone *et al.*, 1993)). This forest-type now covers only 11% (approximately 100,000 ha) of the Waikato and is concentrated in a few tracts, the largest of which is on Mt Pirongia (Burns and Smale, 2002). It is assumed that Polynesian settlement was responsible for the subsequent clearance to manuka scrub and bracken fern vegetation (Newnham *et al.*, 1989), but now the region is mainly drained, farmland pasture (McGlone, 1988) begun by the early European settlers. Across the region there is a north to south pattern of lowland forest types, with *Agathis australis* (kauri) and *Beilschmiedia tarairi* (taraire) to the north and *Dacrydium cupressinum* (rimu) and *Beilschmiedia tawa* (tawa) to the south (Burns and Smale, 2002). The Waikato is also noted for being dissected by the southern limit of kauri, that trends east-west across the region.

Amongst the region are located relatively extensive remains of previously abundant wetland systems, including Kopouatai and Moanatuatua. At the time of Kopouatai's formation, the region was originally swamp forest vegetated by the podocarps *Dacrydium cupressinum* (rimu), *Dacrycarpus dacrydioides* (kahikatea) and *Lagarostrobos colensoi* (silver pine) (Newnham *et al.*, 1995).

2.4.2 Geological setting

Geological development

The area of Earth's crust that now comprises New Zealand was once attached to the ancient landmass of Gondwanaland and at times submerged. The first main landmass was formed during the Rangitata Orogeny period, mainly in the late Jurassic and early Cretaceous (140-120 million years ago (Ma)) (Stevens, 1985) and since at least the Carboniferous (360 Ma) New Zealand has been on an active plate boundary, experiencing frequent tectonic and volcanic activity. Since then, plates have shifted location on top of the Earth's mantle, resulting in New Zealand separating from Gondwanaland 100-80 Ma (Riddolls, 1987).

Most of New Zealand's features are geologically young, being less than two million years old (Pillans *et al.*, 1992). Modern surface characteristics were mostly formed since the

mid-Pleistocene (see *Table 2.3* for the most recent New Zealand stage names and their Northern Hemisphere European equivalents), but have been particularly modified more recently by Holocene depositional and erosional processes. Some remnants of late Cretaceous and Tertiary surfaces remain in Otago and Northland, but even these have been greatly altered by subsequent volcanic or tectonic activity.

Northern hemisphere stage names		New Zealand stage names	Stage type	Marine oxygen isotope stage
N. Europe	B. Isles			
Holocene	Flandrian*	Aranuian	Interglacial	1
Weichselian	Devensian	Otiran	Glacial	2-5d
Eemian	Ipswichian	Kaihinuan	Interglacial	5e
Warthe	Wolstonian	Waimean	Glacial	6
Saale/Drenthe		Karoroian	Interglacial	7

*Table 2.3 New Zealand stage names with their Northern Hemisphere equivalents (in part from Lowe and Walker, 1997). * recent works from the British Isles have now adopted the term 'Holocene' (rather than Flandrian) as standard.*

Pleistocene glaciation has played a major role in landscape formation of the South Island, but has had little effect on the North Island, where only the very highest mountains sustained any substantial amounts of permanent ice (Pillans *et al.*, 1992). Sea-level variations have changed the coastal configuration and land surface area of the country greatly over time, the most recent being the Holocene sea-level rise of approximately 120 m.

Tectonic and volcanic activity

The volcanic arc of New Zealand is presently located on the obliquely converging active plate boundary of the Indian-Australian Plate and the subducting Pacific Plate (*Figure 2.8*). Only a small proportion of the extensive New Zealand subcontinent, composed of continental crust, emerges above sea level (Kamp, 1992).

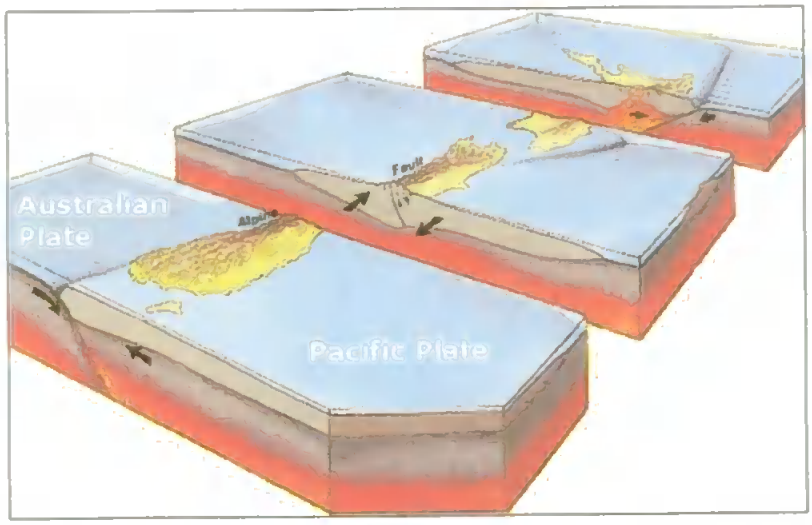

Figure 2.8 A cross-section of New Zealand showing the plate boundaries, their direction of movement and the central North Island tectonic region (Taupo Volcanic Zone) (Cox (1999) taken from 'New Zealand tectonics' website).

Situated offshore are extensive fault networks, basins and trenches (*Figure 2.9*). To the north of New Zealand is the Tonga-Kermadec System subduction zone, and to the south is the more complex Macquarie system, where vertical plate motion is reversed, with the edge of the Pacific Plate pushed *above* the Indian-Australian Plate. These two fault systems merge on land as the Alpine Fault, uplifting the Southern Alps mountain range to altitudes of 3 km and dissecting the South Island in two. Uplift rates for parts of the Southern Alps are currently 15-20 mm/year (McGlone, 1988).

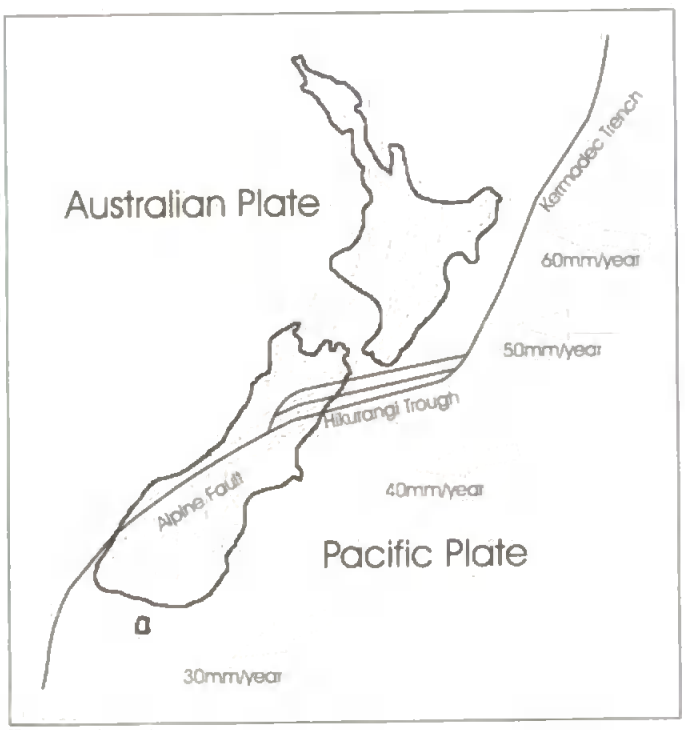

Figure 2.9 Tectonic fault systems of New Zealand and rates of plate movement (after diagrams on 'New Zealand tectonics (part 2a)' website).

Friction along the plate boundaries often results in earthquakes and tectonic activity throughout the country. Of particular relevance to this project is the fault system (notably the Kerepehi Fault) surrounding Kopouatai Bog (de Lange and Lowe, 1990) (section 3.2.4).

The North Island of New Zealand is also volcanically active, the main region of which is the Taupo Volcanic Zone (TVZ) comprising a line of six major active volcanic systems trending from south west to north east (*Figure 2.10*). These are the Okataina, Taupo, Maroa, Tuhua (Mayor Island), Tongariro and Egmont systems. The TVZ is the largest and most frequently active rhyolitic magmatic system on Earth (Houghton *et al.*, 1995). As well as its constant thermal activity, the TVZ has experienced numerous major eruptions during the Holocene (Froggatt, 1981). The most recent significant volcanic eruption was that of Mount Ruapehu in 1995-1996.

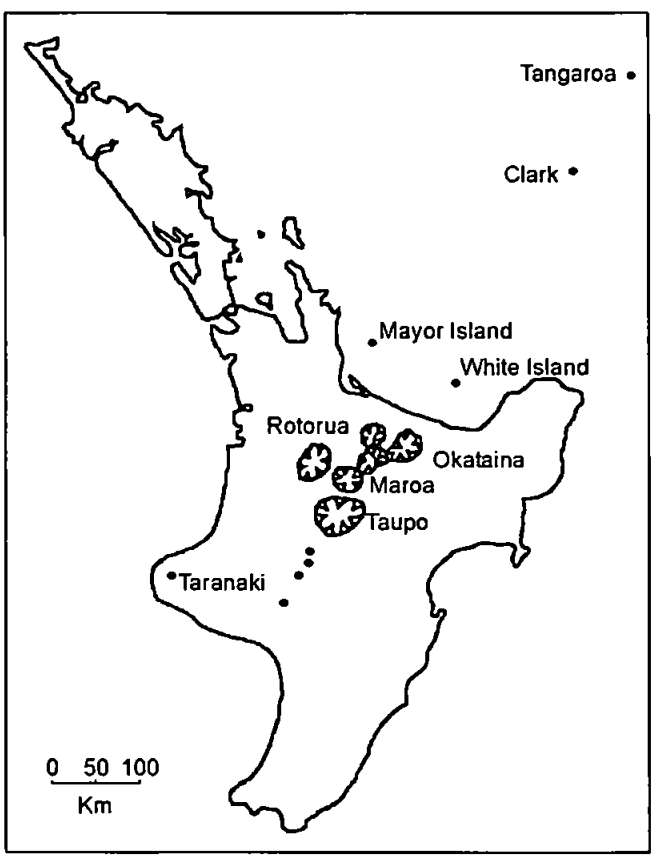

Figure 2.10 The North Island volcanic regions; relevant to this project are the Taupo and Mayor Island volcanic centres, the sources of the Taupo and Tuhua Tephras respectively (GNS, 2004).

Major Holocene eruptions

The main eruptions during the Holocene have been identified by the tephra layers (see explanation below) that they have deposited. Work in eastern North Island (Lowe *et al.*,

1999) has identified 16 such layers, the main ones of which are shown in *Table 2.4* (together with the Whakaipo dated by Froggatt and Lowe (1990)).

Tephra	Age (^{14}C years BP)	Volcanic source
Kaharoa*	655±15	Okataina
Taupo*	1,850±10	Taupo
Whakaipo*	2,685±20	Taupo
Waimihia	3,230±20	Taupo
Whakatane	4,830±20	Okataina
Tuhua*	6,130±30	Tuhua
Mamaku*	7,250±20	Taupo
Rotoma	8,530±10	Okataina
Opepe	9,050±40	Taupo
Konini	10,150±50	Egmont
Waiohau	11,850±60	Taupo

*Table 2.4 An outline of the main North Island Holocene volcanic eruptions and tephra layers (from Lowe et al. (1999)) with * indicating those of particular relevance to this project.*

Tephras

The volcanic activity arising from New Zealand's location on an active plate boundary, has resulted in the deposition of numerous, extensive tephra layers. The term 'tephra' encompasses all volcanic material ejected during a volcanic eruption (Froggatt and Lowe, 1990) ranging from fine ash to unconsolidated pyroclastic flows (Lowe and Hunt, 2001). The tephra-fall constituent, of which the tephra layers in this project consist, comprises: microscopic glass shards, fine ash (<0.06 mm), coarse ash (0.06-2 mm) and lapilli (2-64 mm) as categorised by Lowe and Hunt (2001).

The TVZ is the source of numerous tephra layers, most of which originated from the Taupo and Okataina volcanic systems (Lowe, 1981). Eruptions from this system are also very explosive; Walker (1980) concluded that the Taupo pumice (1,850±10 ^{14}C years BP) was the most widely dispersed New Zealand tephra found so far, and it has since been found to extend even further, into the Waikato and Hauraki lowland regions (Newnham *et al.*, 1995).

Tephras are best studied in areas distant from their source, since nearby site records can be destroyed by subsequent eruptions (Lowe and Newnham, 1999). They are well preserved in lakes and bogs; the Waikato lakes, especially Rotomanuka and Maratoto, have some of the longest, most complete tephra sequences of the North Island (of which rhyolitic tephras predominate) (Lowe, 1988a). They are preserved as compact, macroscopic layers 2-110 mm thick, with smooth contacts with the surrounding sediment, although Lowe (1988b) found them to be thinner deposits than their land equivalents due to compaction.

Tephrochronology

Because tephra layers can be deposited virtually instantaneously across a region, their main use is for dating and correlation between stratigraphic sequences. A range of techniques has been used for dating these layers, including Potassium-Argon, Argon-Argon, fission track and palaeomagnetic methods (Lowe and Newnham, 1999). However, Holocene tephras are typically dated by ^{14}C-dating very thin slices of sediment or macrofossils from directly above and below the tephra layer. Individual dates are then determined from a pool of multiple ages. Dates can be double-checked by cross-referencing with results obtained for the same tephra at different sites (Lowe, 1988a). For example, Lowe *et al.* (1998) used cluster analysis of 22 separate dates to obtain the age of the Kaharoa Tephra (665±15 ^{14}C years BP) and then calibrated it using the Northern Hemisphere tree ring data, with a 27 year deduction for Southern Hemisphere offset (McCormac *et al.*, 1997, 1998) to 600 calendar years BP (AD 1350). More recently, however, this date has been revised to AD 1314±12 by wiggle matching the ^{14}C dates (Hogg *et al.*, 2003).

Identification

Each tephra deposit is not only characteristic of its source volcano, but also of its specific eruption. Various techniques are used to identify tephra layers, including mineralogy, chemical composition, stratigraphical relations, ^{14}C chronology (e.g. Lowe, 1998a) and physical characteristics e.g. thickness, lithology, bedding characteristics. Work in north west Europe is showing further potential of microscopic techniques in recognising the glass tephra shards deposited in the British Isles (e.g. Hall and Pilcher, 2002); methods which can be readily applied to New Zealand.

Extensive work by Lowe (1988a, b) and Lowe *et al.* (1999) investigated the relationship between eruptives from the six main North Island volcanic centres. The tephras were identified using heavy and light mineral fractions and glass chemistry 'finger-printing',

using electron microprobe analysis to identify the major elements. Different tephras have different diagnostic constituents. For example, rhyolitic Taupo eruptions are identifiable by high levels of hypersthene and small amounts of augite (Lowe, 1988a) and Okataina eruptives contain high levels of the very distinctive cummingtonite (Froggatt and Rogers, 1990). The statistical 'discriminant function analysis' method was used by Stokes *et al.* (1992) to distinguish tephras less than 22,000 ^{14}C years old from each other. This method, using a series of two mathematical models to separate out tephras, is advantageous as it is an objective technique.

Distribution

The presence or absence of tephras in distal sediments is controlled by the strength and explosiveness of the eruptions and the strength and direction of the prevailing wind conditions. For example, Taupo-derived tephras have been deposited extensively across the south west Pacific Ocean (Carter *et al.*, 1995) whilst Lowe (1988b) explains the absence of Kaharoa and Waimihia Tephras from parts of Waikato by strong winds. Changes in wind direction during an eruption can alter a tephra's final depositional patterns too; the Waimihia Tephra was initially blown east, but then shifted to east south east (Walker, 1981) reaching up to 500 km offshore as a result.

After tephras have been released into the atmosphere, they settle out onto subaerial surfaces under the forces of gravity or aided by rainfall. Generally, tephra layer thickness decreases exponentially with increased distance from the source (Fisher and Schmincke, 1984). Cas and Wright (1987) noticed a secondary thickening of deposits due to premature fallout because of particle aggregation or scavenging. This was also seen by Carter *et al.* (1995) for the Taupo tephra, 660km away from the source, and is accounted for by a possible drop in wind speed. Typically, the 1 mm isopach (i.e. 1 mm tephra thickness layer) is 200-350 km away from the sources of Taupo and Okataina (Lowe, 1988b) but most tephras in the Waikato lakes are certain to occur beyond this region (Lowe, 1988a). *Figures 2.11* and *2.12* show isopach maps for the Taupo and Tuhua Tephras throughout the Waikato region.

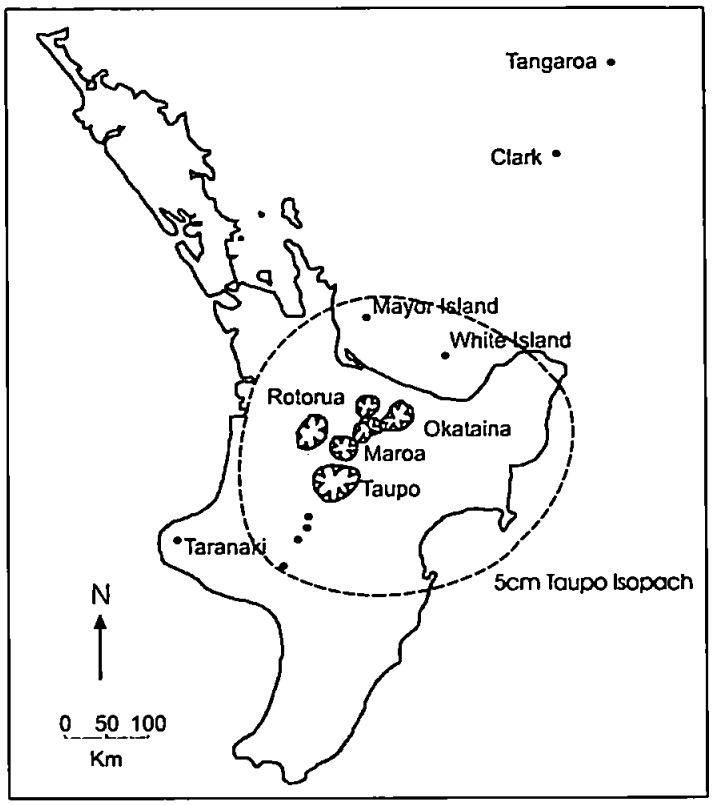

Figure 2.11 Isopach map of the Taupo Tephra (after Pullar et al., 1977).

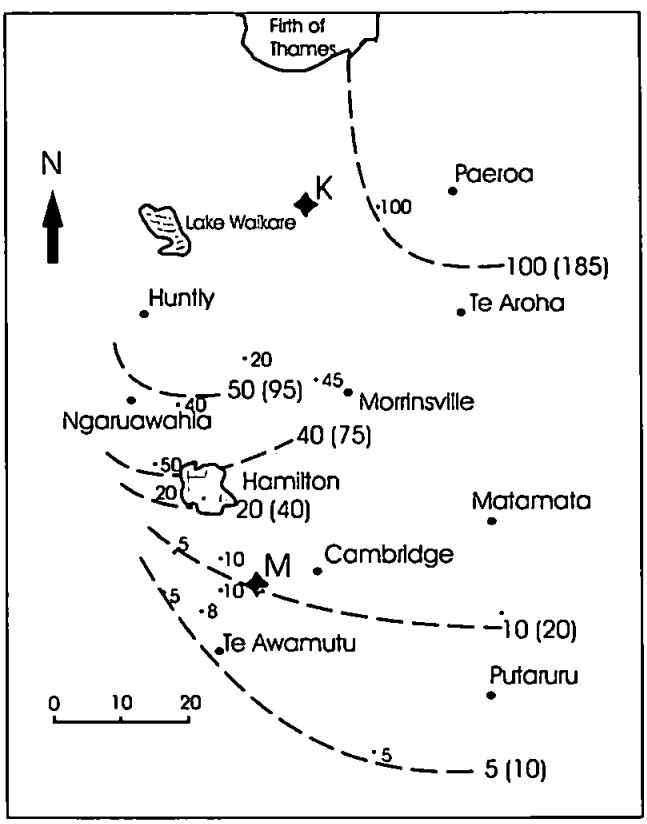

Figure 2.12 Isopach map of the Tuhua Tephra (from Lowe (1988b)) in the region of Moanatuatua (M) and Kopouatai (K). Layer thicknesses are in mm, with uncompacted 'dry-land' values in brackets.

Isopach mapping of areas with equal thickness tephra deposits permits the calculation of volumes of material emitted from eruptions. Carter *et al.* (1995) used marine as well as terrestrial deposits to improve the accuracy of volume calculations; total airfall estimates are: Taupo – 50 km^3, Waimihia – 22 km^3, Rerewhakaaitu – 14 km^3 and Kawakawa – 400 km^3.

Environmental effects

Volcanic eruptions can cause fires both directly, as hot acidic ash lands onto leaves, and indirectly, by causing convectional lightning storms that trigger fires (Ogden *et al.*, 1998). The degree of direct damage, ranging from minor disturbance to complete destruction, depends on the scale of the initial disturbance and the type of substrate. Clarkson (1990) found that plant recovery on volcanic substrates varied greatly in terms of the sequence of species and the rate of recolonisation, with no single volcanic succession existing. New Zealand plants particularly sensitive to ash deposition include *Halocarpus*, *Dacrydium* and *Metrosideros* (Giles, 1999). Giles (1999) also concluded from pollen analysis that local site factors such as drainage and degree of shelter were often more important than the thickness of the deposited tephra layer. Generally the vegetation and catchment revert to pre-eruption status within *c.*100 years after the event.

Work by McGlone (1981) identified greater forest destruction at sites proximal to the Taupo and Kaharoa tephra sources than at sites close to the Tongariro volcanic region. This was inferred from an increase of *Pteridium esculentum* (bracken) spores and a decline in *Dacrydium cupressinum* (rimu) pollen grains. Widespread burning events at distal sites were also evident from the abundance of charcoal fragments. Vegetation damaged by ashfall became more prone to burning, particularly as bracken, which grows in the clearings created by fire, is itself highly flammable. The effects of the most recent major eruption of Mount Tarawera in AD 1886 were directly observed. Trees were seen to survive tephra layer deposition of up to 600 mm. However, smaller plants and shrubs that were completely obliterated, regrew after four years, suggesting that tephra effects are only temporary (McGlone, 1981).

Limitations

The identification and use of tephra layers as chronostratigraphical markers has certain limitations that must be acknowledged:

a) Bioturbation, the mixing of the sediment by organisms such as worms and insect larvae, is always a potential risk in palaeoenvironmental reconstructions, but is usually visible in the stratigraphy. Lowe (1988b) considered that it was not a serious problem in the Waikato area, where tephra layers were intact, with clearly visible smooth contacts. Reworking in high altitude bogs of the North Island by wind or surface water flow is also a problem, identified from the presence of more tephra layers than there have been known eruptions (Froggatt and Rogers, 1990).
b) Some of the constituents of the tephras, in particular ferromagnesian minerals from certain rhyolitic tephras in the North Island can be dissolved over time altering their diagnostic characteristics (Hodder *et al.*, 1991). For example, biotite, a key constituent of the Kaharoa Tephra, is absent in Kopouatai Bog when in other sites it is abundant. From the dissolution features of remaining tephra shards, it is thought that the process responsible was chemical solution, occurring in highly acidic conditions (pH < 4) where silica levels are also low. Thus, used on its own, this identifying minerogenic characteristic is insufficient for tephra identification.
c) The characteristic elements of tephras can also differ between separate studies, possibly due to fractionation during initial eruptions or plagioclase microlites affecting the microprobe analysis (Lowe *et al.*, 1999). Whatever the cause, this leads to complications when trying to identify and compare these tephra identifications between sites.
d) Unfortunately, not all tephra layers occur in one core, or even in one site. This therefore has limitations for deriving detailed chronologies and correlating cores.

2.4.3 Human settlement

Recent work is clarifying the contentious subject of the timing and impact of initial human settlement of New Zealand by Polynesians (Maoris). The main arguments are for either a 'long' (since AD 1-500) (Anderson, 1991), 'intermediate' (since AD 750-950) (Davidson, 1984) or 'short' (since AD 1150-1300) (Sutton, 1987) duration of settlement. From erosional evidence, such as silt layers inwashed into organic dominated lake sediments, and large declines in tree pollen, McGlone and Wilmshurst (1999a) support a 'short' prehistory over the last 600-700 years.

The use of datable tephra layers is a particularly useful method in resolving this timing issue. In 8 out of 11 sites studied by Newnham *et al.* (1998a) in northern New Zealand, the first detectable human impact was at about the time, within 100 ^{14}C years maximum, of the

rhyolitic Kaharoa Tephra (665±15 BP i.e. 600 cal. years BP) (Lowe *et al.*, 1998). As yet, no archaeological remains have been found below it within the stratigraphy. Kopouatai Bog (Newnham *et al.*, 1995) showed synchronous timing between the Kaharoa Tephra and human presence indicated by a dramatic, persistent increase in *Pteridium* (bracken) spores in the pollen record, due to forest clearance. Pollen analysis of a North Island lake, by Newnham *et al.* (1998b), identified a possible lull in human activity (manifest as a decline in bracken) at the time of the Little Ice Age maximum, from the late AD 1600s to the early AD 1800s.

It is vitally important to be able to distinguish vegetation changes as either naturally or anthropogenically induced. In addition to the use of pollen records, other indicators such as fire incidence and erosion could be used. Ogden *et al.* (1998) identified a definite fire frequency increase due to humans at approximately 700 ^{14}C years BP. These anthropogenic fires were characterised by sustained charcoal peaks as human clearance required repeated burning to keep the vegetation open, together with increases in bracken and other early colonisers, and decreases in tree pollen. Together, these are very different signals to natural fires. Polynesians could well have taken advantage of this subsequent ease of burning after the Kaharoa tephra eruption to clear land for their own use (McGlone, 1981).

The fire history of Kopouatai has previously been reported by Newnham *et al.* (1995) suggesting the possibility of bog vegetation burning throughout the Holocene as inferred from abundant microscopic charcoal. However, because the charcoal frequency is increasing up-core since well before times of human settlement, it is not clear how much of the most recent (post-settlement) burning was caused by anthropogenic versus natural factors.

Certain plant communities such as those dominated by grass, shrub and heathland are more susceptible than others to fire. Natural fires were less frequent than human ones, and because New Zealand plants are not adapted to burning, when Polynesian settlers arrived, the original plant assemblages never fully recovered (Ogden *et al.*, 1998). The more recent settlement of the islands by Europeans is well documented. Together with certain weeds and other exotics, they brought cultivars, such as *Juglans* (walnut) (Newnham and Lowe, 1991) and cleared massive tracts of land for farming and artificial pine tree plantations.

Beneficial to this project is that human impact can be excluded as the causal mechanism of any environmental changes, since the timeframe from 6,130±30 ^{14}C years BP to 1,850±10 ^{14}C years BP predates human settlement in New Zealand.

2.5 Summary

New Zealand's geographic setting in relation to regional oceanic and atmospheric circulation is of prime importance in creating the country's moist, but variable, climate. The volcanically active nature of the New Zealand landscape and the resulting presence of tephras in sediments make this part of the world ideal for establishing reliable chronologies. The presence of the raised, ombrotrophic restiad peat bogs Kopouatai and Moanatuatua, together with their climatically-responsive, abundantly preserved micro- and macrofossils (e.g. plant macrofossils, charcoal, testate amoebae) facilitates the reconstruction of former environmental conditions and changes, both natural and anthropogenic. Hence, there is great potential for palaeoecological and palaeoclimatological studies in New Zealand, and due to the short settlement history the changes observed are inferred not to be anthropogenically-driven. The overall lack of Southern Hemisphere studies compared to the Northern Hemisphere highlights the need for such research. This study will complement and extend existing knowledge of New Zealand's climatic history, based on palaeomoisture records, to enable inter-hemispheric comparisons to be drawn.

Having set the context and background for peatland palaeoclimatic work in New Zealand, the next chapter describes the field sites that have been chosen on which to carry out this work.

CHAPTER THREE – FIELD SITES

3.1 Introduction

This chapter explains the rationale behind site selection, and describes in detail the locations and pertinent features of the sites used in this study.

Peatland work in the Northern Hemisphere has investigated the similarity of replicated records in order to determine how representative a single-core might be of a climate record. For example, Hendon *et al.* (2001) compared records from eight cores from three sites in northern England and found there to be generally good replication of reconstructed watertable records within sites, and of major climate shifts between sites over the last 2,000 years in particular. Examining multi-core records adds significant confidence in the identification of climate shifts – if a similarly-timed event is replicated in multiple cores from more than one site, then that signal is likely to be real rather than peculiar to a single core. Hence, two field sites were selected for analysis. In order to be able to carry out between-site comparisons of palaeomoisture records, as well as allowing the testing of within-site core replicability, three cores were studied from each site.

The fieldsites were chosen from the Waikato region for the following reasons:

a) the presence of hydrologically-separate but otherwise similar ombrogenous peatlands,
b) previous work in the region, and more specifically at Kopouatai and Moanatuatua, would help inform this study,
c) the presence of common tephras would help guide field sampling and, more importantly, provide precise tie points between sequences and provide a coarse chronological framework,
d) the only other New Zealand Holocene studies of this kind have been undertaken in southern New Zealand on different peat-forming systems, with only limited success,
e) the project's supervisory team was familiar with the region,
f) excellent scientific input and logistical support (for the field and laboratory work) was available from staff at the nearby University of Waikato, particularly from Assoc. Prof. David Lowe.

3.2 Field sites

3.2.1 Site selection

This project focuses on the climatic history derived from the two peatlands of Kopouatai and Moanatuatua from the North Island of New Zealand. To facilitate the comparison of the reconstructed records, the chosen sites had to be close enough together to be within the same regional climatic regime, but distant enough to be hydrologically separate. They also had to be of the same form and vegetational composition (i.e. ombrotrophic, raised restiad peat bogs) to minimise non-climate variability between sites. The sites also had to be of approximately the same age, with peat profiles covering the same Holocene time period of interest. The ombrogenous nature of these chosen New Zealand sites also meant that the palaeoecological techniques used on such sites in the Northern Hemisphere could also be applied and tested here. Their palaeomoisture records could also be used for inter-hemispheric climate record comparisons, by directly comparing Southern Hemisphere records with their Northern Hemisphere (*Sphagnum*) counterparts.

Numerous appropriate peatlands are found on New Zealand's North Island, where modern vegetation and hydrological surveys have been carried out and potential for palaeoclimatic work is good. However, many sites have been affected by human disturbance, mainly through agriculture and its associated drainage. Ideally, the selected sites were to have experienced minimal damage from such activities.

Originally, three sites from the North Island were sampled: Kopouatai, Moanatuatua and Whangamarino. However, only cores from Kopouatai and Moanatuatua were used in this research. This was due to a combination of factors, namely a) core retrieval from Whangamarino was often poor due to the very wet and fibrous nature of the substrate, and this was exacerbated during transit, b) due to the wet nature of the peat, tephra layers/grains were frequently washed down and smeared through sections, and c) as a younger bog (less than 2,000 years old) its record did not extend far enough back through the Holocene to cover the same tephra-constrained period of study as Kopouatai and Moanatuatua.

3.2.2 Site locations

The two selected sites used in this study are the protected raised bogs of Kopouatai and Moanatuatua, 60 km apart in the Waikato region in the north west of the North Island (*Figure 3.1*).

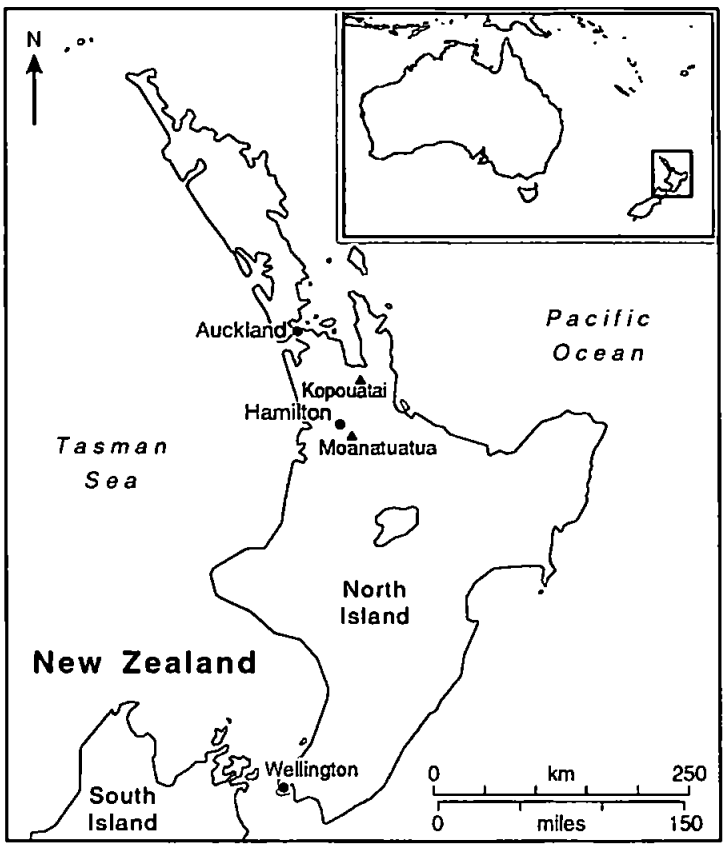

Figure 3.1 Location map of field sites Kopouatai and Moanatuatua.

3.2.3 Time interval chosen for this investigation

In order to be able to directly compare core records, all records had to cover the same time period. The most effective way to achieve this from field observations was by using the presence of large tephra layers (here, the Taupo and the Tuhua Tephras) as upper and lower boundaries respectively of each retrieved core. In practice, core retrieval above the Taupo was variable and by no means comprehensive, and would have resulted in undesirable gaps in the record. Further detail concerning the period of investigation is described in section 4.1.2.

3.2.4 Site description, history and development

Kopouatai and Moanatuatua are both raised restiad peat bogs (as described in section 2.2.1) with a relatively low plant biodiversity. There are only 10-15 common species, including *Sporadanthus ferrugineus* (greater wire rush or cane rush), *Empodisma minus* (lesser wire rush), *Leptospermum scoparium* (manuka), *Gleichenia dicarpa* (swamp umbrella/tangle fern), *Dracophyllum scoparium* (swamp heath), *Epacris pauciflora* (tumingi heather), *Schoenus pauciflorus* (bog-rush), *Schoenus brevifolius* (sedge), *Baumea teretifolia* (pakihi rush), *Drosera* (sundew), *Baumea rubiginosa* (twig rush) and *Sphagnum cristatum* (moss), as well as the extremely rare *Lycopodiella lateralis* (clubmoss) and

Anzybas/Corybas carsei (swamp helmet orchid) (Stephenson, 1986). *Plate 3.1* shows the main plant species. The two rushes, in particular *Empodisma minus*, are the main peat formers, due to their dense rhizome and root networks (Irving *et al.*, 1984). As well as representing rare vegetation types, both peat bogs are also home to many rare birds and are therefore of high conservation value.

Plate 3.1 Typical vegetation from Moanatuatua showing the light green Empodisma minus (a) composing the bulk of the vegetative matter, (b) the red headed Sporadanthus ferrugineus, (c) the bright green Gleichenia dicarpa and tall shrubs of Epacris pauciflora (d).

Importantly, Kopouatai and Moanatuatua are hydrologically separate. As a result, reconstructed moisture patterns found to be similar across such a broad study region strongly implicate non-local forcing factors, in particular climate (e.g. Barber *et al.*, 2000) rather than, for example, local hydrology. The sites are also ombrotrophic, which means that their water input is solely from rainfall. Thus their water balance is a function of climate, with increased water content during wet periods and vice versa.

The sites both formed approximately 12,000 ^{14}C years BP on top of the impermeable volcaniclastic alluvium of the Hinuera Formation, deposited during the last glacial by the ancestral Waikato River and other fluvial systems draining the central North Island volcanic plateau (*Figure 3.2*). Accumulation rates at the sites increased 12-10,000 ^{14}C years BP due to increased rainfall and a resulting rise in water levels (Green and Lowe, 1985). The peat at Kopouatai is interbedded with blue-grey muds and sands and clays of fluvial and estuarine origin (de Lange and Lowe, 1990) known as the Tauranga Group (Maggs, 1997).

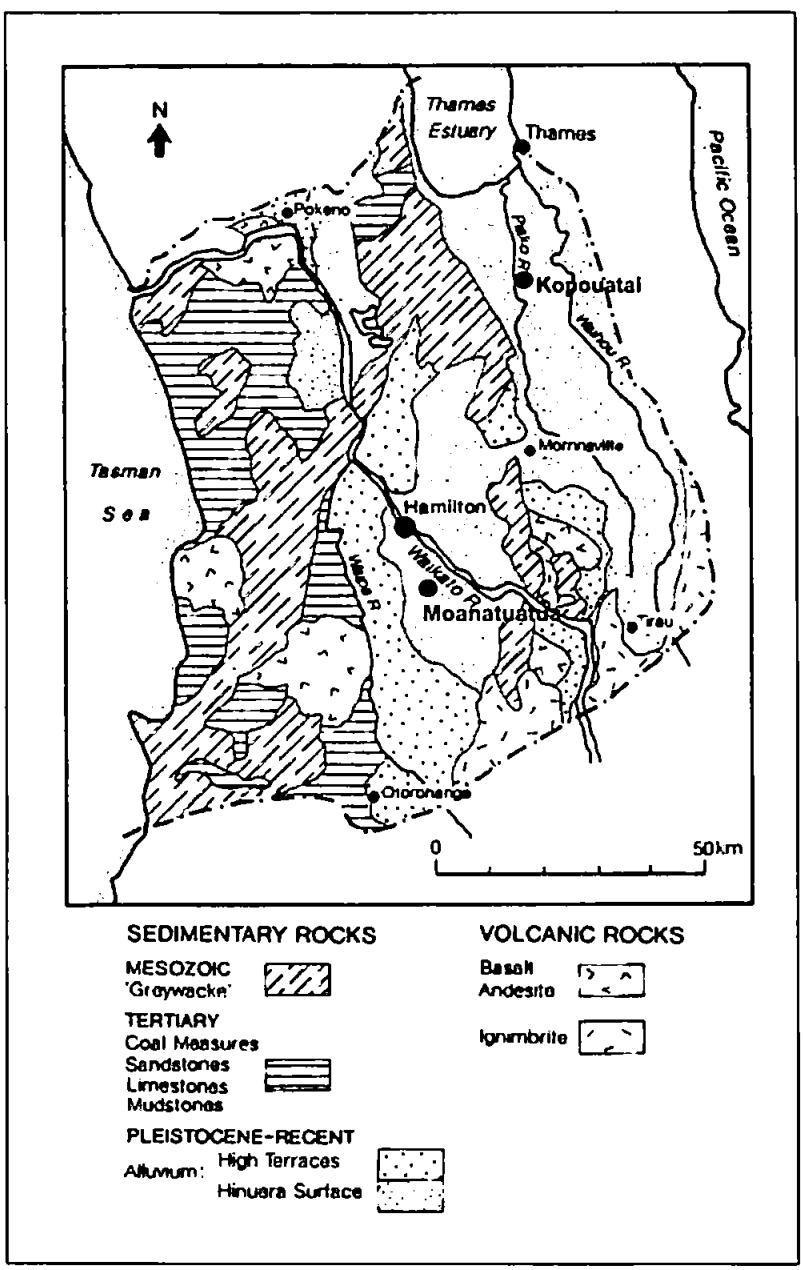

Figure 3.2 Geology of the Waikato region, New Zealand (from McCraw, 2002).

Kopouatai

Kopouatai bog is located in central North Island (37°26'S, 175°34'E) 30 km NE of Hamilton City (*Figure 3.1*), and is the largest remaining natural-state peat bog in New Zealand; it is a maximum of 18 km long and 10 km wide (Maggs, 1997). It is an internationally-recognised wetland site: Ramsar site number 444. Over time, it has progressively been reduced in area from its margins inwards by drainage (Thompson *et al.*, 1999). It is surrounded by an extensive network of wide ditches, canals (*Plate 3.2*) and farmland. The two restiad rushes *Empodisma* and *Sporadanthus* have dominated since 6,100 ^{14}C years BP. However, *Sporadanthus* has been in decline since 700 ^{14}C years BP (Shearer, 1997).

Plate 3.2 A marginal drainage ditch at Kopouatai.

Long term mean annual rainfall in the locality is 1150 mm (Jones and Maggs, 1990) and this is spread evenly throughout the year. The mean annual temperature is 13°C, with means of 18°C in January and 8°C in July (Shearer, 1997) and there are between 70 and 80 frost days per year (Newnham *et al.*, 1989).

Kopouatai is situated 2 to 6.5 m above sea level in the Hauraki Depression, an east to west trending rift 20-30 km wide, in the Hauraki lowlands. The area is bounded by a series of faults, namely the Hauraki and Kerepehi Faults (*Figure 3.3*).

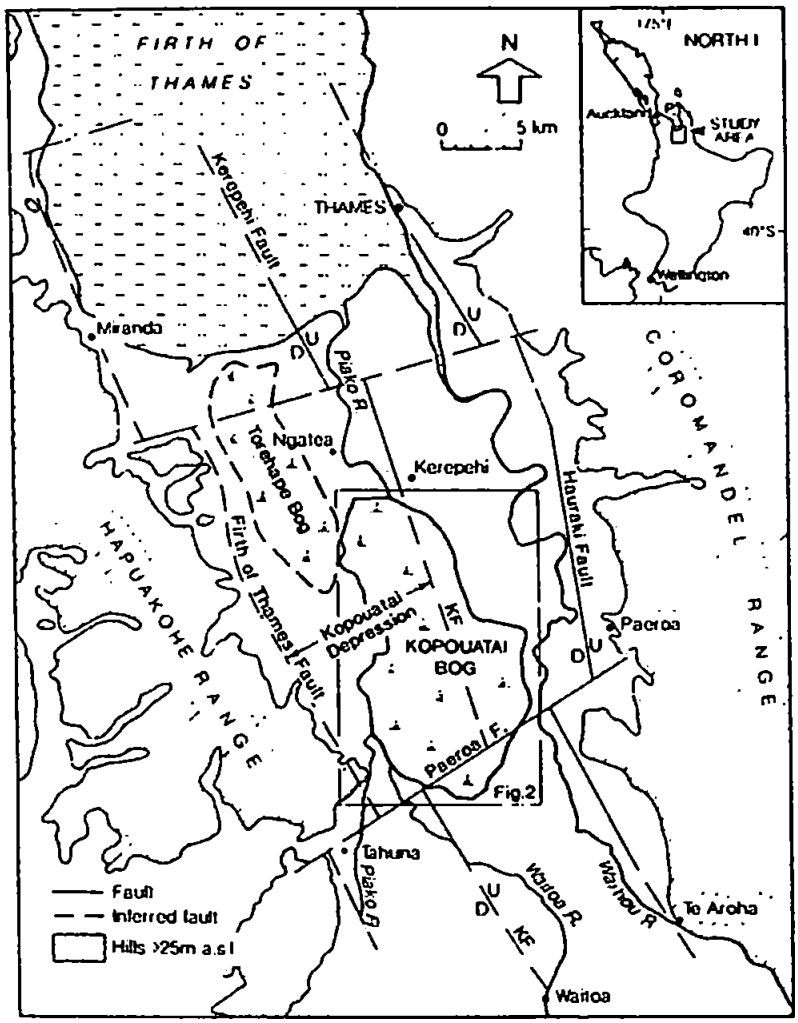

Figure 3.3 Map showing the fault locations surrounding Kopouatai Bog (from Newnham et al. (1995)).

Along the northern section of Kopouatai the Kerepehi Fault is the only major active fault in the South Auckland-Waikato region (de Lange and Lowe, 1990). It passes through the east of Kopouatai Bog itself, and is seen at the bog surface by a subtle change in vegetation from tall shrubs on the elevated eastern block, to low rushes in the west (de Lange, 1989). Movement is thought to have been occurring since 10,700 ^{14}C years BP, at an average rate of approximately 0.13 mm/year, but with major earthquake events occurring on average every 2,500 years. The latest event is thought to have occurred just after the deposition of the Kaharoa Tephra around 655±15 ^{14}C years BP.

Since peat development began 12,000 ^{14}C years BP, accumulation rates have varied both temporally and spatially, but have averaged 0.9 mm/yr during the Holocene (Newnham *et al.*, 1995). However, after a large area of the northern part of the bog was flooded around 6,000 ^{14}C years BP by a marine transgression depositing deltaic muds, average peat accumulation rates have increased to 1.7 mm/yr (Newnham *et al.*, 1995).

The peat bog is comprised of three main peat domes: a larger one in the south, and two smaller ones in the north. Its raised centre is 3 m above the surrounding edges and the maxium peat depth is 12 m in central areas (Davoren, 1978). The acrotelm at this relatively unmodified site is thought to be relatively shallow, at 15 to 20 cm (Clarkson *et al.*, 1999) and the mean pH is 3.2 (Hodder *et al.*, 1991).

The centre of the bog is ombrotrophic, resulting in nutrient poor, oligotrophic, conditions because the water input here is solely from precipitation. Kopouatai is, however, also bordered by the Piako and Waitoa rivers in the west, and the Waihou river in the east, contributing to contrasting nutrient conditions at the bog's edges. The margins therefore receive some input from nutrient-rich groundwater as well as runoff from the surroundings, resulting in eutrophic and mesotrophic nutrient status, in turn creating a more diverse vegetation assemblage. In addition, at periods of high tide the water level in the drainage ditches surrounding the peat bog will rise visibly and tidal variation on the south west margin of the bog was recorded as 1.5 m (Maggs, 1997).

A three-year hydrological monitoring study from 1991-1994 by Maggs (1997) found that maximum water through-flow occurred at the bog margins. Hydraulic conductivity of the peat, which controls infiltration rates (Rycroft *et al.*, 1975), showed a stronger horizontal than vertical pattern, with lower conductivity in more decomposed peat layers. Hydraulic conductivity was also lower in the western regions of the site. Most water movement is within the top 1.5 m layer of less decomposed surface peat, preferentially flowing through naturally occurring water pipes (Maggs, 1997). The water table was seen to fluctuate between 0 and 12 cm below the surface (Shearer, 1997) and its form follows the surface peat topography. Groundwater levels at the bog margins fluctuated seasonally, between high levels in July through to September, and lower levels from February to April, and seasonal differences were seen to be greater in the east than the west (Maggs, 1997). Most runoff occurred from June to November i.e. winter to spring, when the peat has less

capacity to hold water, and some small surface streams stopped flowing completely in summer and autumn.

Within the peat stratigraphy at this site 17 macroscopic tephras have been identified (Newnham *et al.*, 1995) providing a well-established chronology. These include the Kaharoa (655±15 ^{14}C years BP), Taupo (1,850±10), Tuhua (6,130±30), Mamaku (7,250±20), Rotoma (8,530±10) and Opepe (9,050±40). The presence and identification of some of these layers is crucial in dating and correlating the cores taken for this research.

Moanatuatua

Moanatuatua (37°58'S, 175°72'E) is 20 km SSE of Hamilton and 60 km SSW of Kopouatai (*Figure 3.1*). Although the two sites are of a similar from, much less work has been carried out on Moanatuatua. It is the same age, and was once the same size as Kopouatai but has been greatly reduced in area to only 1.1 km^2 (Thompson *et al.*, 1999). Like Kopouatai, Moanatuatua formed when the Waikato River ceased migrating and began downcutting in its present position (Kuder *et al.*, 1998). It is 60 m above sea level, with a peat dome 1-2 m above the surrounding farmland and peat depths reaching 12 m.

Its current climate is very similar to that of Kopouatai: a mean annual rainfall of 1252 mm with a peak in winter, a mean annual temperature of 13.6°C and an average of 28.8 frost days a year (New Zealand Meteorological Service, 1973).

Moanatuatua is home to the same plant species as Kopouatai; the dominant plants are the restiads *S. ferrugineus* and *E. minus*, although a study by Cranwell (1953) identified a decline in *S. ferrugineus* in the surface 50 cm, similar to that seen at Kopouatai. Within the *S. ferrugineus* and *E. minus* communities can be found *Campylopus acuminatus* var. *kirkii*, liverworts, *Sphagnum* in pools and occasionally *Lycopodiella lateralis*. Around this vegetation zone lays a lower *Schoenus* and *Empodisma* assemblage, with *Baumea* and *Empodisma* on wetter ground. A zone of *Baumea* and *Gleichenia* occupies drier locations at the margins, surrounded in turn by dense, tall *Leptospermum* (Wardle, 1991).

Farming practices have removed the top 1-2 m of sediment from the edges of the peatland, as demonstrated by the comparison of tephra layer depths from within and outside the reserve (Shearer, 1997). Despite the interference with bog growth by agriculture, levels of peat humification, total nitrogen and total potassium are not as high as other more

anthropogenically disturbed sites, suggesting that Moanatuatua might not be as negatively affected as once thought (Clarkson *et al.*, 1999). However, Moanatuatua does have higher total phosphorous levels than Kopouatai (Clarkson *et al.*, 1999) and phosphorous is an element that is thought to limit the late vegetation succession of peatlands (Verhoeven *et al.*, 1996). Work on the response to fire activity showed that Moanatuatua has a very slow recovery period, slower than that of Whangamarino bog to the north. In the four years following extensive burning, only 30% of the vascular plant cover had returned, compared to 60% at Whangamarino (Clarkson *et al.*, 1999).

Throughout its development, Moanatuatua has experienced larger fluctuations in water table than Kopouatai. Like Kopouatai, this site is surrounded by ditches 2-3 m deep and the effects of these are thought to be felt up to 350 m away (Shearer, 1997). Water tables are artificially lowered from 20-40 cm at the bog's centre to 80 cm at the margins (Kuder *et al.*, 1998). However, the ditches vary in the degree of maintenance and the eastern ditch is gradually filling in due to lack of clearance. The presence of such ditches results in increased peat decay rates, as demonstrated by petrography, fungal analysis and analytical pyrolysis (Kuder *et al.*, 1998). However, from records derived from these three analyses, it is thought that Moanatuatua has always had a high level of peat degradation, long before artificial drainage began. In contrast, peat from Kopouatai is relatively less decomposed, and this is thought to result from a generally higher water table (Kuder *et al.*, 1998). The acrotelm at Moanatuatua is deeper (at 70 cm) than at the less altered site of Kopouatai, due to greater variation in the level of the water table.

3.3 Summary

As detailed above, Kopouatai and Moanatuatua are peatlands of very similar age and form (*Table 3.1*). The sites are raised restiad-dominated, ombrotrophic peat bogs, that experience very similar climatic conditions. Hence, they are ideal for a comparative palaeomoisture study – if both sites yield similar results, then climate, rather than local hydrological factors, can be inferred as the driving force of these changes. The two bogs have similar tephrostratigraphies and, as a consequence, the same tephra layers were able to be used to precisely synchronise the start and end points for all six core sequences investigated here. Despite the recent (19^{th}-20^{th} century) substantial anthropogenic interference at the two sites, the target period of study is well before the time of human colonisation and their actions.

	Kopouatai	Moanatuatua
Location	37°26'S 175°34'E	37°58'S 175°72'E
Approximate age (years)	12,000	12,000
Elevation above sea level (m)	2-6.5	60
Area (km^2)	96	1.1
Maximum peat depth (m)	12	12
Rainfall (mean annual)	1150	1252
Temperature (mean annual)	13.0	13.6
Water table depth (cm)	0-12	20-40 (site centre)
Principal vegetation	*Empodisma minus* *Sporadanthus ferrugineus*	*Empodisma minus* *Sporadanthus ferrugineus*

Table 3.1 A summary of the main characteristics of Kopouatai and Moanatuatua.

The following chapter details the methods used in this project to reconstruct the palaeomoisture records of these two chosen sites.

CHAPTER FOUR – METHODOLOGY

Having described the field sites and the rationale for their selection in the previous chapter, the following sections describe the various field and laboratory methods used throughout this project.

4.1 Fieldwork

The first stage of fieldwork was carried out in the late austral summer of March 2001 and the second field season in the autumn of May 2002; long cores, short cores and modern vegetation samples were collected. The methods used and sampling locations are described below.

4.1.1 Coring

Coring methods

During the two trips, a total of 13 long cores were taken. All cores were extracted using a 'wide' Russian corer with a 10 cm diameter and 30 cm long barrel (*Plate 4.1*), except cores Z0102 and Z0203/Z0205 which were taken using a 'narrow' 5 cm diameter, 49 cm long barrel Russian corer (*Plate 4.2*) and another (WR3) taken with a piston corer. Only the seven best-extracted and preserved cores were sampled (core retrieval was poor from very wet peat and some sections incurred damage from slumping during transit to the UK); three from Kopouatai (Z0106, Z0108 and Z0204) and four from Moanatuatua (Z0102 (plus Z0203/Z0205 if supplementary plant macrofossils were required), Z0103 and Z0206).

Due to the extremely tough and fibrous nature of the surface biomass, it was necessary to first remove it to allow the corer to penetrate the surface (these sections were sliced and kept for analysis (section 4.1.3)). For each core, two holes approximately 1 m apart were used, and each 30 cm section was extracted from them alternately. This was to avoid disturbance of the adjacent, lower-lying sediment by the pointed nose of the corer.

Cores were labelled with a year reference (01 or 02) and then numbered consecutively. For example, Z0102 was taken in 2001 (i.e. 01) and was the second core to be retrieved (i.e. 02). (A site reference would also have been beneficial). For grid references see *Table 4.1*.

Plate 4.1 Short barrelled wide Russian corer. (Note the arrowed white pumiceous Kaharoa tephra (655±15 ^{14}C years BP (Lowe et al., 1999)) (AD 1314±12 (Hogg et al., 2003) which is outside the time frame of this project).

Plate 4.2 Long barrelled narrow Russian corer.

Core locations and selection

Due to the dense nature of the vegetation, access across the bogs was difficult. Core locations were taken far enough in from the bog margins to sample peat that was fully ombrotrophic (avoiding any mineral input usually associated with bog margins), and sufficiently distant from the marginal drainage ditches, to minimise their effect on the hydrology (although, as drainage has only been occurring since the 20th century, these

features are unlikely to have had an effect on the peat pre-dating this era). At Kopouatai, coring sites needed to be sufficiently south, beyond the reach of the marine transgression that flooded the northern section of bog and deposited a thick clay layer *c.*6,000 ^{14}C years BP (Newnham *et al.*, 1995).

All three cores from Kopouatai (Z0106, Z0108, Z0204) were taken from within the reserve (indicated on *Figure 4.1* by the shaded area) within approximately 300 m from each other.

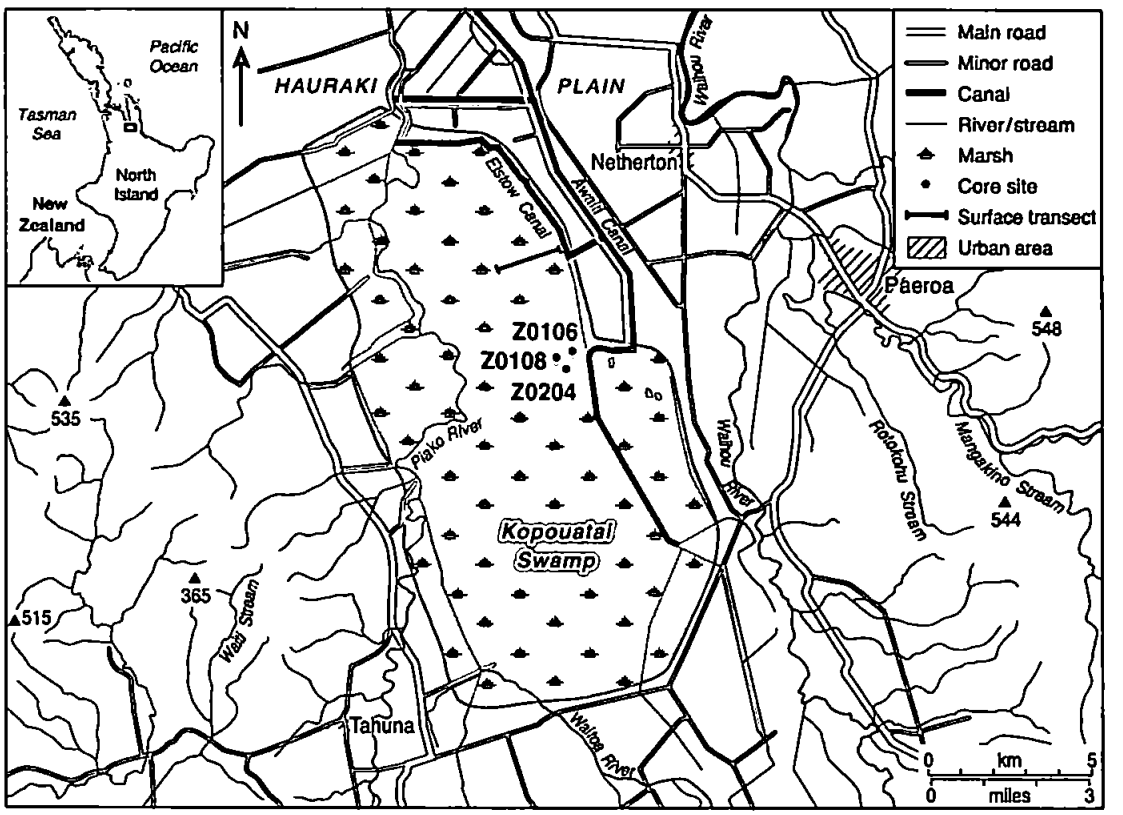

Figure 4.1 Core locations from Kopouatai. The shaded area indicates the protected reserve.

However, only two Moanatuatua cores (Z0103, Z0206) were from the reserve. The others (Z0102, Z0203/Z0205) were from the marginal drained pasture farmland within 500 m of each other (*Figure 4.2*).

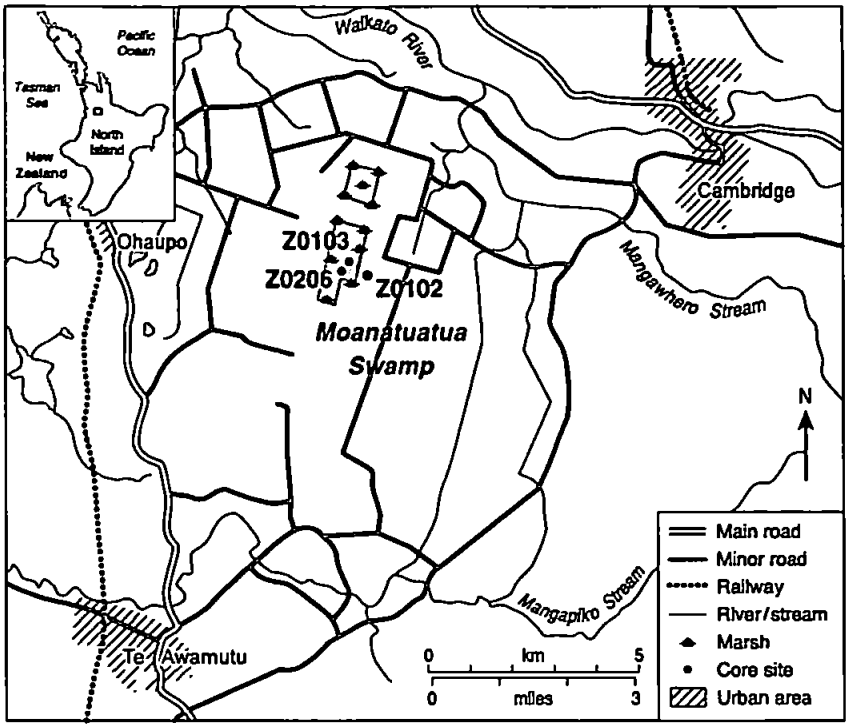

Figure 4.2 Core locations from Moanatuatua. (Z0203/Z0205 were sampled as close to Z0102 as possible). The shaded area indicates the protected reserve.

Information on all the cores is summarised in *Table 4.1*.

Site	Core reference	Grid reference	Core location	Core size	Date
Kopouatai	Z0105	-	Reserve	Wide	7/3/01
	Z0106*	73383 64193	Reserve	Wide	7/3/01
	Z0108*	73381 64191	Reserve	Wide	9/3/01
	Z0204*	73382 64189	Reserve	Wide	21/5/02
Moanatuatua	Z0102*	27192 63618	Pastureland	Narrow	2/3/01
	Z0103*	27186 63612	Reserve	Wide	6/3/01
	Z0104	-	Reserve	Wide	6/3/01
	Z0202	-	Reserve	Wide	15/5/02
	Z0203* Z0205*	27192 63617	Pastureland	Narrow	16/5/02 22/5/02
	Z0206*	27186 63611	Reserve	Wide	23/5/02
	WR3	-	Pastureland	Piston	9/3/01
Whangamarino	Z0109	-	Reserve	Wide	21/3/01
	Z0110	-	Reserve	Wide	21/3/01

*Table 4.1 The type of cores, their locations and years extracted from Kopouatai, Moanatuatua and Whangamarino. Cores used in this project are indicated by *. Core Z0205 is a deeper continuation of Z0203; both were taken from the same hole.*

Core storage

The cores were wrapped in non-PVC cling-film and refrigerated at 4°C later the same day in order to inhibit microbial decay. The surface samples were stored in sealed plastic bags and kept at the same temperature. All cores and samples were subsequently air freighted back to the UK where they have since been refrigerated at the University of Plymouth at 4°C.

4.1.2 Time interval chosen for this study

Originally, it was hoped to sample as close to the present as was practicable, but also, as far as possible, to use common tephra layers to constrain precisely the start and end points of each core. In practice, core sections in the upper *c.*1 m of peat at Kopouatai were too fluid and unconsolidated to be sampled effectively at the volume required, whilst, at Moanatuatua the most recent sediments were thought to have been affected by drainage of the bog, certainly in the pastureland. In light of these developments, the decision was taken at the end of the first field season to use the Taupo and Tuhua Tephras to constrain the timeframe of this investigation; these two tephras were present in all cores.

4.1.3 Testate amoebae surface and short-core sampling

The surface 0 to 30 cm sections of each coring location were collected, and additional short cores, also of the surface peat (from the surface to between 15 to 30 cm depth) were taken. This was in order to a) investigate the preferred environmental conditions of the testate amoebae taxa, b) to identify the zone of living tests and c) to determine at what depth test abundances start to decline, in order to be able to suggest possible reasons for the extremely low test abundances that were discovered during preliminary fossil sample counts carried out whilst in New Zealand (see further details in Chapter 5).

Method

The top 0 to 30 cm section of each core was dug out as a solid block using a spade, then cut up into 1 cm slices with a bread knife and bagged individually. The additional short cores were cut out using a bread knife.

Locations

The same supplementary short cores were sampled from areas in the vicinity of the long cores dominated by different vegetation types, for example, by *Gleichenia* or by *Sphagnum*. Because of this requirement, these locations were not chosen in a systematic

manner i.e. they were scattered across the nearby area within a radius of approximately 200 m from the cored site. The number of short cores retrieved was 30 in 2001 (10 of which were from Whangamarino) and 46 in 2002.

Vegetation survey

At each long and short core sampling location, the vegetation types within a 1-2 m radius were recorded by simply listing them in order of dominance. On reflection, the species should have been quantified, perhaps using percentage abundance in a quadrat.

Field measurements

During the first fieldwork season, water table depth was measured using a tape measure at every long and short core sampling location at Kopouatai. However, this was not possible for the surface samples at Moanatuatua, where, in late summer, the water table was too deep to reach without digging with a spade. During the second stage of fieldwork, water table depth, pH (degree of acidity) and conductivity (a measure of nutrient status) were all measured for each sampling location; the former in the field, and the latter two in the laboratory the following day. pH was measured using a Mettler Toledo MP220 instrument, and conductivity on a GP383 Series 3 by EDT Instruments.

Contemporary samples for plant macrofossil identifications

To aid in the identification of fossil plant fragments in the laboratory, a reference collection was produced using modern plant specimens collected from the field and from the University of Waikato greenhouse. Because these were for long term storage they were preserved in FAA, a solution comprised of 10 parts formaldehyde (of 37-45%), 70 parts ethanol (of 95%), 15 parts water and 5 parts acetic acid.

High power magnification images (x100 and x400) were taken of thin slices and leaf parts of the fresh plants at the University of Plymouth and the University of Waikato, to aid in identifications. Dried specimens from the University of Waikato's Herbarium were also examined.

4.2 Chronology

A combination of tephra layers and radiocarbon dates were used to derive chronologies for the cores, in order to develop age-depth models and correlate cores within and between sites.

4.2.1 Tephrochronology

The macroscopic tephra layers, i.e. those visible to the naked eye, formed the basis of the chronology in all cores. Microscopic tephra layers were not used directly due to the time consuming nature of the locating and identifying processes, and also because very fine tephra layers were more likely to have been subjected to reworking than thick layers, either *in situ* or during coring. It was observed with the visible Kaharoa Tephra layer that its grains had been 'washed down' the extracted core section where the substrate was saturated, presumably by the coring process. Ballinger (2003) examined the presence of microscopic tephra deposits in some of the cores, results of which will be used later in the interpretation of the Total Organic Carbon records (in Chapters 6 and 7).

Most of the tephras were readily identifiable in the field, for example, the orangey-brown pumiceous Taupo Tephra at both sites (*Plate 4.3*), and the distinctive double layered, reverse bedded Tuhua Tephra at Kopouatai (*Plate 4.4*). Some less obvious tephras that were not seen in the field were discovered during the core logging and subsampling process. Such unidentifiable tephras required microprobe analysis (overseen by Assoc. Prof. David Lowe at the University of Waikato) to try and determine their identity.

Plate 4.3 Taupo tephra (arrowed) at Moanatuatua (the top of the core section is to the left). Note the highlighted thick charcoal-rich band directly above the tephra layer.

Plate 4.4 Tuhua tephra from Kopouatai (the top of the core section is to the left). The dashed red line indicates the boundary between the lower (fine) and upper (coarse) deposits.

4.2.2 ^{14}C dating

Radiocarbon dating was also used to support and supplement the tephrochronologies. By improving the chronologies it was possible to date each core individually and to link chronologies between cores more accurately. A combination of bulk peat dates and AMS dates on individual plant macrofossils was used. All radiocarbon data quoted in this thesis are given as radiocarbon years BP (^{14}C years BP) or calibrated years BP (cal. years BP).

Radiocarbon dating is subject to certain constraints and potential problems including the following that are relevant to this project:

a) All ^{14}C ages have errors associated with them, expressed as an age range, and radiocarbon years do not equal calendar years because atmospheric ^{14}C levels have varied over time. Therefore radiocarbon dates must be calibrated with an absolute dating technique, such as tree rings. All dates were calibrated using the programme CALIB 4.4.2 (Stuiver and Reimer, 1993).

b) Samples can be contaminated by ^{14}C of a different age in a variety of ways, both *in situ* and in the laboratory, and this can vary in nature and degree between bulk and AMS dates. A peat 'reservoir effect' is thought to exist where samples are not in equilibrium with the atmospheric ^{14}C levels. Kilian *et al.* (1995) established that peat bog-derived radiocarbon dates from a site in the Netherlands on *Sphagnum* samples containing minute, young Ericaceae roots were, surprisingly, 100-200 years too old. They

suggested that plants or their associated fungi can fix old CO_2 that is being released from depth, leading to dates that are older than expected. However, work by Blaauw *et al.* (2004) suggests that there is in fact no evidence for such a reservoir effect on bulk dates. More common is contamination by the downward growth of roots from younger plants further up in the stratigraphy resulting in ages that are younger than expected. Other forms of contamination can occur in the laboratory, for example from an unclean working environment. Experimental work by Wohlfarth *et al.* (1998) found that Swedish varved clay samples stored in de-ionised water for prolonged periods of time (even refrigerated) led to erroneously 'young' dates.

c) Of particular relevance to this project, is the offset in atmospheric ^{14}C levels between hemispheres, with the Southern Hemisphere containing less due to the different land-sea ratios in each hemisphere (Pilcher, 2003). This varies the amount of vertical mixing of old carbon (from deep water) with the atmosphere (de Vries, 1958). A study by McCormac *et al.* (2002) comparing dates back to AD950 from Irish and New Zealand wood found the offset to have varied between 20-80 years over time. Here, the Southern Hemisphere dataset in CALIB 4.4.2 was used.

Bulk peat ages (using conventional dating)

The standard dating technique, measuring the amount of remaining radioactivity, requires a considerable amount of carbon for dating (between 10 mg to 20 g of sample carbon per date depending on the accuracy and size of sample). This is even more in terms of actual material, since plant remains are not pure carbon.

This method uses a large amount of 'bulk' sample i.e. a complete section of material extracted from the substrate. This is a mix of above- and below-ground matter, as well as humic/humin/fulvic acids (which also provide different ages (Shore *et al.*, 1995)), and can lead to sample contamination by small rootlets of younger plants (and therefore younger carbon) and/or younger humic acids from above mixing with older peat below. The date obtained is therefore only an average of these constituents (Pilcher, 2003).

In this study bulk peat ages were obtained first as a preliminary check to confirm the identification of the visible tephras. A total of seven bulk peat ages were obtained at the University of Waikato Radiocarbon Laboratory (*Table 4.2*).

Site	Core	Depth (m)
Moanatuatua	Z0203	3.47-3.50
	Z0205	5.32-5.35
	Z0206	5.42-5.43
Kopouatai	Z0204	7.76-7.78
		8.26-8.28
		8.44-8.46
		9.28-9.30

Table 4.2 Depths of samples for bulk dating.

AMS ages

AMS dating works by using different masses to separate out and count the remaining ^{14}C atoms. An advantage of this method over that of bulk peat dating, is that it only requires a minimum of 0.2 mg of carbon and can therefore be carried out on individual above ground plant macrofossils e.g. seeds and leaves. This was of great importance for this project, when sample volume was limited. However, it does mean that contamination of even minute amounts of carbon on such a small sample can result in large dating errors (Shore *et al*, 1995; Wohlfarth *et al*, 1998). Therefore, as much sample as possible is used to minimise any contamination effects.

AMS dating of individual plant remains is also preferable to that of conventional bulk ages because it avoids any issue of carbon contamination from roots growing down from above. Although individual plant fragments are more reliable for dating purposes than bulk samples, Nilsson *et al.* (2001) concluded that *Sphagnum* plant fragments are the most reliable, as *Sphagnum* does not assimilate 'old' ^{14}C through the roots (due to absence of root systems). Unfortunately, this was not feasible in the New Zealand sites of this study, where *Sphagnum* is rare.

A selection of plant remains from different species was used, depending on availability. These were mainly *Leptospermum* and *Epacris* leaves, but where they were absent or present in only low numbers, *Epacris* and (what are most likely to be) *Empodisma* seeds, and *Gleichenia* fronds (some of which were burnt) were used.

Sampling strategy

A total of 47 AMS age estimates on above-ground plant macrofossils were obtained from the NERC Radiocarbon Laboratory (East Kilbride). The eight ages per core (except core Z0102 which only has seven) were evenly spaced between the Taupo and the Tuhua tephras (*Table 4.3*).

Depth of samples for AMS dating (m)					
Kopouatai			Moanatuatua		
Z0106	Z0108	Z0204	Z0102	Z0103	Z0206
3.36-3.37	3.80-3.81	4.17-4.18	0.79-0.80**	1.975-1.985	1.96-1.97
3.89-3.90	4.25-4.26	4.62-4.63	1.08-1.10*	2.325-2.335	2.34-2.35
4.45-4.46	4.69-4.70	5.06-5.07	1.38-1.39	2.595-2.605	2.71-2.72
4.99-5.00	5.14-5.15	5.51-5.52	1.63-1.65*	3.015-3.025	3.08-3.09
5.54-5.55	5.58-5.59	5.95-5.96	1.92-1.93	3.35-3.37*	3.46-3.47
6.09-6.10	6.03-6.05*	6.40-6.41	2.21-2.22	3.70-3.71	3.83-3.84
6.63-6.65*	6.47-6.49*	6.84-6.85	2.48-2.49	4.045-4.055	4.21-4.23*
7.37-7.38	6.86-6.88*	7.29-7.31*	2.77-2.78	4.395-4.405	4.58-4.59

*Table 4.3 Depths of samples for AMS dating. * indicates samples where a depth of 2 cm was used due to a lack of suitable material in 1 cm. ** indicates the sample that was not processed successfully in time for this project write-up.*

All plant macrofossils for AMS dating were picked from samples that had been sieved through a 180 μm sieve and washed and stored in distilled water. Only above-ground remains were used, and care was taken to detach any fine rootlets adhered to the samples that could have been a contamination source. Samples were then pretreated as standard at the NERC Radiocarbon Laboratory with 1M HCl (at 80°C for eight hours) and then washed with distilled water. Where sample weight was low, samples were burnt on their glass filter papers to minimise loss.

The ^{14}C ages were calibrated to calendar ages using CALIB v.4.4.2 (Stuiver and Reimer, 1993) accessed via the website http://radiocarbon.pa.qub.ac.uk/calib using the Southern Hemisphere calibration curve (shcal02.14c), with an offset (deduction) of 41 years (McCormac *et al.*, 2002).

4.2.3 Age-depth modelling

Modelling age-depth relationships is a complicated procedure that often requires trade-offs between accuracy, precision and simplicity. Telford *et al.* (2004a) highlight the fact that no age-depth model is perfect, as each has its associated errors. It is therefore a question of choosing the model that is the most appropriate in terms of the site and its record. Because of this it would be wise to derive a selection of age-depth models and compare differences in the age reconstructions derived. Even so, it is generally acknowledged (e.g. Birks and Heegaard, 2003) that age-depth models need much work to improve their reliability.

Birks and Heegaard (2003) recommend using 'generalised additive models' (GAMs) which allow weighting more-reliable ages (e.g. tephra layers) more-heavily. Alternatively, Bayesian techniques take into consideration the ages of other samples (including tephras) within the chronology when calibrating each individual age. In New Zealand, this has been used successfully in the dating of the Kaharoa tephra (Buck *et al.*, 2003), although this was on a single horizon, rather than a complete core chronology.

The age-depth models derived are described in sections 6.2.3 and 7.2.3.

4.3 Laboratory methods

Here, the subsampling strategy is outlined, together with the various laboratory methods employed in this project.

4.3.1 Subsampling strategy

Sub-samples were initially taken at a relatively coarse resolution of 8 cm intervals, subsequently increased to 4 cm for all cores and then 2 cm for cores Z0204 (Kopouatai) and Z0206 (Moanatuatua). The time period studied is that between two tephra layers – the Taupo Tephra (1,850±10 ^{14}C years BP) and the Tuhua Tephra (6,130±30 ^{14}C years BP) – as this core section was retrieved in all cores, facilitating the direct comparison of palaeomoisture reconstructions of the same time period between cores. The first subsample was taken from the 1 cm section immediately below the Taupo ash layer, with subsequent samples extracted down-core at the regular intervals specified above. Each sub-sample was 1 cm deep because the fibrous nature of the peat in places made finer subsampling difficult. This subsampling strategy of 1 cm-deep samples aimed to yield results of approximately 20-40 years.

Depth correction

Due to the compression of the peat that occurred during transit within a few core sections from cores Z0103, Z0106 and Z0108, a depth correction had to be made to account for this, based on the depth within the peat that any measurements had been taken and the amount of compression that had occurred:

$$\text{Corrected depth} = \left(\frac{d_{sample} \times t_{core}}{t_{actual}} \right) + d_{top}$$

where: d_{sample} = depth of the sample from the top of peat profile,

t_{core} = thickness of peat that should be in the core section (0.30 m),

t_{actual} = thickness of peat that is actually in the core section,

and d_{top} = depth of the top of the core section.

For every sample (including those for radiocarbon dating), the upper and lower depths were both corrected after sampling, and then the midpoint of this range was calculated and used for plotting.

4.3.2 Core description

Each core was described systematically in terms of constituents and colour using Troels-Smith (1955) and Munsell soil colour. Troels-Smith (1955) uses a four degree scale to describe the organic and mineral content of the sediment. Despite having been criticised for its subjectivity, it is a useful scheme to detect relative changes, as long as care is taken to be consistent between cores. This work was done within a week of core retrieval, the delay being due to time constraints, when only relatively little oxidation should have occurred. Ideally, this should be carried out as soon as possible after extraction, as sediments can change colour when exposed to air. In this case, the peat oxidised from a red-brown to black colour, thus concealing subtle changes in decomposition and normally readily visible dark charcoal layers. Cores were also re-logged on their return to the UK.

4.3.3 Moisture content

A known weight of wet sample (measured to four decimal places) was dried in a drying cupboard overnight at approximately 40°C and then reweighed. This moderate temperature was used so as to ensure that no sample was burnt off during drying. The amount of water content was calculated as a percentage of the total wet weight:

$$\%\ \text{moisture content} = \frac{\text{wet weight} - \text{dry weight}}{\text{wet weight}} \times 100$$

4.3.4 Peat humification

Palaeomoisture inferences

Peat humification (the amount of peat decomposition) is regularly used as a moisture proxy in palaeoclimatic studies of peatlands. The standard method by Blackford and Chambers (1993) is based on light transmittance of an alkali extract at a specified wavelength (usually 550 nm). The amount of light that passes through the sample depends on the degree of peat decomposition; the more light that passes through the extract the less decomposed the peat is as anaerobic conditions have inhibited microbial decay. This in turn implies wetter conditions at the time of peat formation. Conversely, lower light transmission implies more peat decay as a result of drier conditions.

Method

Peat decomposition was determined following the standard light transmission method outlined by Blackford and Chambers (1993). The samples were dried at 40°C in a drying cupboard overnight, and ground to a powder in a Specamill machine for approximately 10 minutes, depending on the sample composition, but also with concern for consistent treatment of samples. This machine, composed of an agate cylinder containing the sample and three small agate spheres, was preferable to the laborious pestle and mortar. Samples were removed using a tiny spatula rather than a brush (which can attract fine grains to its bristles and result in cross-contamination) and care was taken to thoroughly wash and dry the chamber between samples. Samples were then kept in a desiccator until use, to keep them dry and prevent re-absorption of water from the atmosphere.

200 mg of dried sample was weighed into a 250 ml glass beaker and 100 ml of freshly-made 8% sodium hydroxide (NaOH) was added to extract the humic acids. The time of mixing was recorded, as each sample had to be measured the *exact* same length of time after the initial mixing with the NaOH (four hours as advised in Blackford and Chambers (1993)). Each beaker was placed on a hot plate, covered with a watchglass to minimise evaporation and brought to the boil. As soon as boiling point was reached, the temperature was lowered to allow samples to simmer for an hour.

After cooling, samples were diluted with 100 ml of distilled water, mixed thoroughly and filtered through Whatman Qualitative 1 filter paper. 50 ml of the filtrate was mixed well with 50 ml of distilled water, and the light transmission was measured at 550 nm wavelength, using a Zeiss Specord M500 spectrophotometer and the programme 'Aspect Plus' version 1.31. Each sample was placed in a clear glass cuvette, with two polished sides and two opaque sides, and measured against a clear standard of distilled water. The 500 nm wavelength was used because it gave the greatest difference in readings between samples of differently humified peat (*Figure 4.3*).

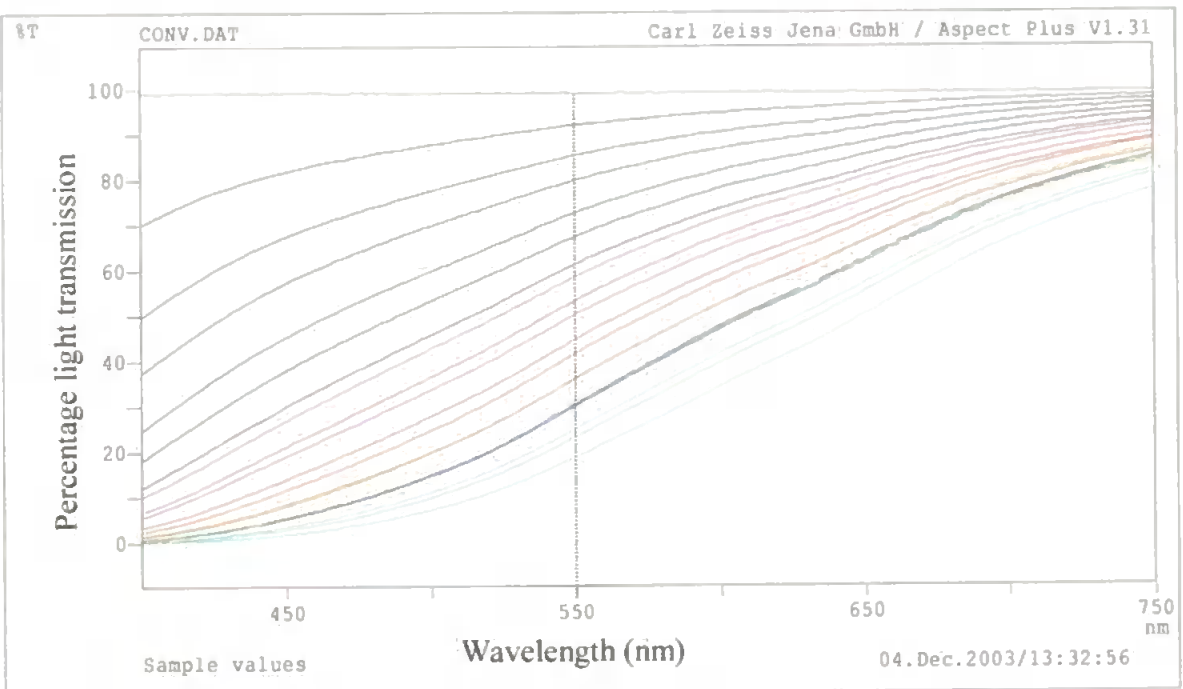

Figure 4.3 Light transmission of peat samples with varying mineral content, between 400 and 750 nm. This demonstrates the maximum difference between samples at 550 nm.

Various factors can affect the accuracy of the reading, mainly by reducing light transmission, so various checks were made before taking any measurements. The internal workings were thoroughly dusted, as dust particles can deflect the light beam away from its usual straight line path through the sample to the sensor. Only the opaque sides of the cuvette were held (to avoid fingerprints) and care was taken to load it into the machine with the polished sides facing the direction of the light beam, and to keep the edges of the cuvette as vertical as possible. Any air bubbles were left to settle out of the subsample before making any measurements, as their presence could also have affected results, and to avoid contamination between samples, the cuvette was washed thoroughly with distilled water.

Three repeats were measured for each sample, and the average was calculated.

Identification of wet and dry shifts

Shifts were identified (sections 6.3 and 7.3) where reversals in the direction of the immediately preceding light transmission record occurred. They were dated using the age of the first excursion point from the background level. Hence, all start points were identified consistently.

To ensure that only real climate signals were interpreted i.e. excluding any increases in light transmission that were due to an increase in mineral content, a series of steps were followed (*Figure 4.4*).

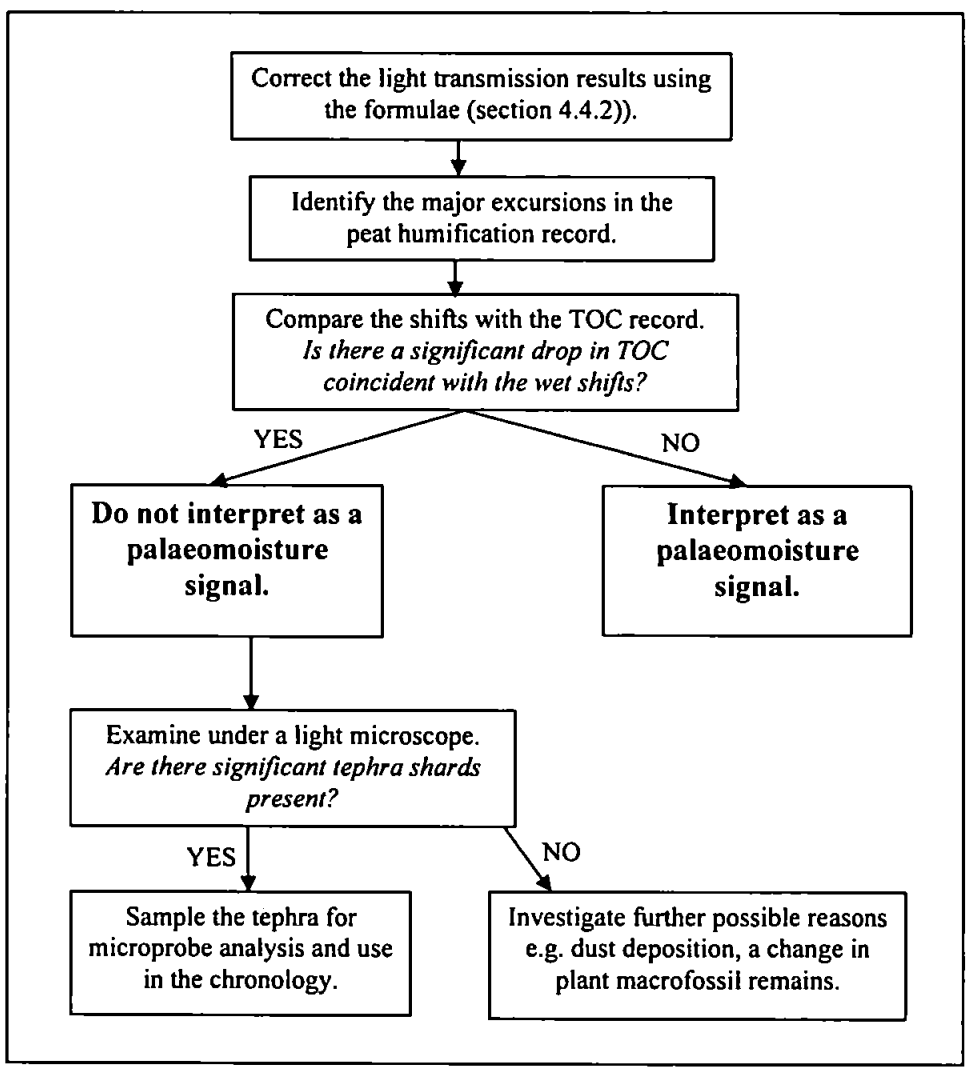

Figure 4.4 Diagram illustrating the process in separating 'real' palaeomoisture signals from mineral-driven light transmission shifts.

4.3.5 Carbon analysis

The amount of Total Organic Carbon (TOC) (i.e. the amount of carbon in the organics) was measured instead of the standard loss-on-ignition (LOI) furnace technique, because it uses much less sample and is potentially more accurate. However, it was a more time-consuming process than LOI, as running each sample took approximately five minutes. Samples were first dried in a drying cupboard at 40°C overnight and powdered finely using a Specamill grinder. They were then placed in a desiccator ready for analysis.

Method

10-20 mg (to two decimal places) was measured out into a ceramic 'boat' and covered completely with a small amount of quartz wool to prevent the sample burning prematurely in the carbon analyser's furnace. Each sample was processed individually using a Shimadzu TOC-5000 Total Organic Carbon Analyser, with the SSM (Solid Sample Module) -5000A furnace at 900°C. This machine measures the amount of CO_2 released from the sample during combustion, which is proportional to the amount of its organic carbon. Care was taken not to leave the port open too long whilst loading and unloading the sample boat to avoid large quantities of atmospheric CO_2 entering the machine and affecting results. At least two runs were carried out for each level and their similarity assessed. This was sufficient if the Coefficient of Variation (CV) errors were low (less than five). If errors were larger, then repeats were carried out as checks. Errors less than five are considered good, however it is not always possible to achieve this, since using only 20 mg of sample might not be representative. In fact, replicated results were often very similar to each other with CV errors even less than one. This confirmed that multiple measurements of an individual sample did not vary greatly from each other.

Since none of the samples had any 'shoulders' (a tailing off) indicative of inorganic carbon, it is inferred that all the carbon present is organic carbon. Therefore the results are expressed as Total Organic Carbon.

The machine was regularly checked and calibrated by K. Solman (School of Geography) by running test samples of known carbon content (*Table 4.4*).

Date	Reference	Measured TOC (%)	Pass/Fail
19/01/2001	Mess 1	2.901	P
12/03/2001	Mess 1	3.012	P
22/03/2001	Mess 1	2.987	P
24/05/2001	Mess 1	2.988	P
08/08/2001	Mess 1	2.897	P
20/09/2001	Mess 1	3.012	P
16/10/2001	Mess 1	2.889	P
23/10/2001	AQC	39.87	P
17/01/2002	Mess 1	2.879	P
18/01/2002	Mess 1	2.976	P
23/04/2002	Mess 1	2.997	P
10/06/2002	AQC	39.96	P
21/06/2002	AQC	39.94	P
09/10/2002	AQC	39.95	P
12/12/2002	AQC	39.99	P
20/01/2003	AQC	39.95	P
21/01/2003	Mess 1	3.002	P
04/03/2003	AQC	39.97	P
16/05/2003	AQC	39.98	P
06/06/2003	AQC	39.94	P
20/06/2003	AQC	39.92	P
08/10/2003	Mess 1	3.015	P
08/10/2003	LGC6137	4.563	P
30/10/2003	LGC6137	4.661	P
31/10/2003	LGC6137	4.352	P
14/11/2003	LGC6137	4.796	P
9/1/2004	LGC6137	4.701	P
9/1/2004	GBW07412	1.06	P
20/02/04	GBW07412	1.35	P*
27/02/04	GBW07412	1.16	P
28/02/04	GBW07412	1.05	P

*Table 4.4 Carbon analyser standard measurements and errors are: Mess 1 = 2.9±0.09%, AQC = 39.93±0.5%, LGC6137 = 4-5% and GBW07412 = 1.136±0.2%. * indicates that even though the measurement on 20/02/04 was just outside the error range, it was passed due to its proximity.*

However, as samples were processed, it became evident that there was offset between sample runs despite standards running within the acceptable error margin and extensive checks on the machine identifying no mechanical errors. Possibly, the machine was running more precisely at lower carbon contents. Due to this offset, a correction had to be made for each run. In order to give each data point the same weighting, particularly important where different runs on the same core had a different number of measurements, the results were corrected so that each run had the same average as the overall average of the whole dataset:

$$\text{Corrected value} = \text{uncorrected}_1 + (\text{uncorrected average}_1 - \text{uncorrected average}_2)$$

where: uncorrected_1 = uncorrected value,

$\text{uncorrected average}_1$ = average of the uncorrected complete dataset,

and $\text{uncorrected average}_2$ = average of the uncorrected run.

Data points used in the corrections were only from the sections of core that had been sampled at the highest resolution, from the Taupo to below the Tuhua Tephra layers (often, sampling at lower resolution had extended unnecessarily to further depths).

As an example, the correction for core Z0103 is shown below (*Figure 4.5*).

In addition, samples that clearly showed drops in carbon content relative to their neighbouring samples were examined to determine if volcanic glass shards (tephra) were responsible for the drop in carbon. Samples were sieved through 15 μm and 300 μm meshes and then viewed under a high power light microscope. No systematic tephra shard counts were made as part of this project – abundances were qualitatively estimated by comparing samples to each other.

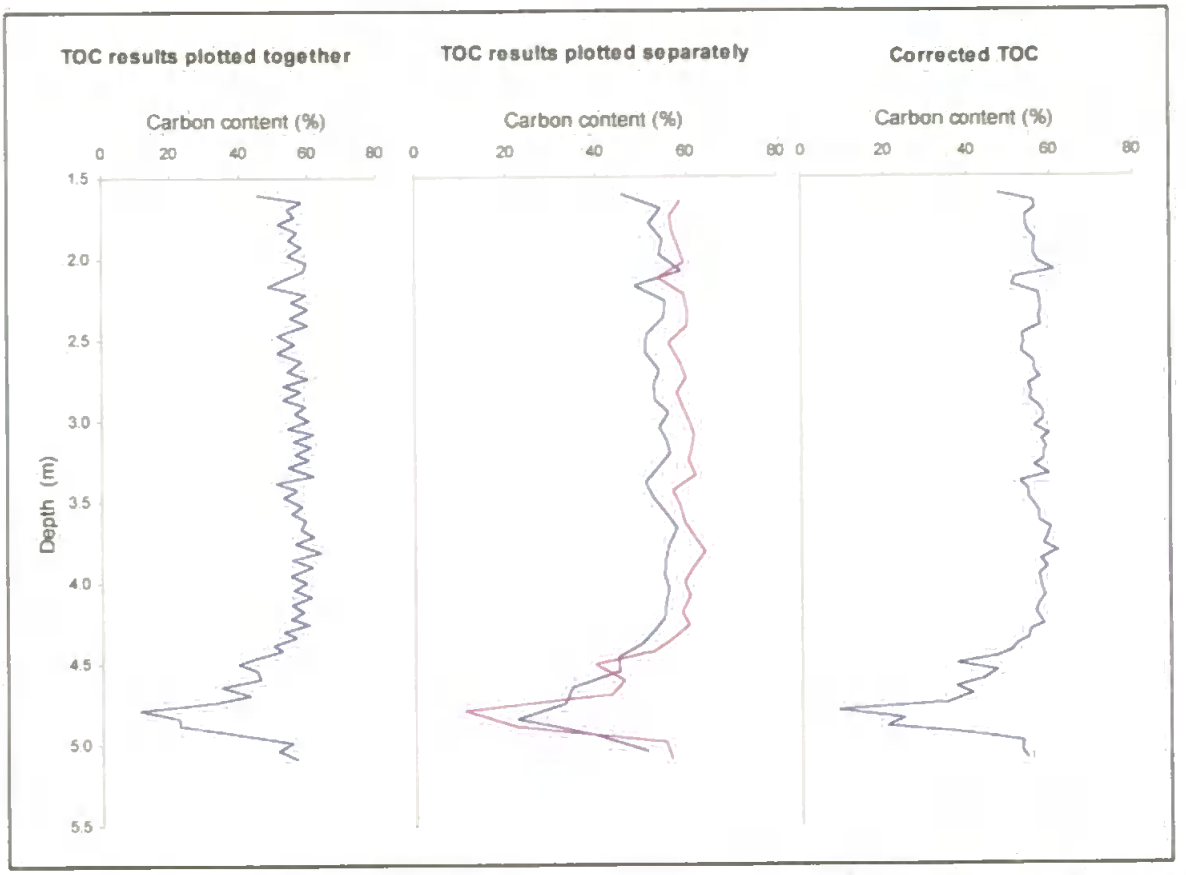

Figure 4.5 Showing the carbon correction procedure for Z0103. The middle panel indicates a systematic offset between sample runs (when using alternative depths) that is not apparent when the two runs are plotted together (left panel). See text for the correction procedure used to obtain a corrected TOC value (right panel).

4.3.6 Plant macrofossils

Analysis of the plant subfossils was carried out on only one core from each site due to time constraints. The two cores selected for analysis were the same cores as those that had been sliced and bagged before transit, thus ensuring that the cores were vertically coherent. These two cores were also those that had been analysed at the highest resolution for peat humification and carbon analysis.

Palaeomoisture inferences

The plant remains preserved in the peat were identified and used to make palaeomoisture inferences, based on their modern affinities to water availability and on the assumption that their preferences have not changed over time. At these sites certain indicator species lie along a moisture gradient (*Figure 2.4* (section 2.2.2)).

Method

Due to the future use of specific, but at that time unknown, plant remains for AMS dating, fragments were picked and stored in distilled water to avoid any carbon contamination. The method used followed that of McGlone and Wilshurst (1999b) based on Barber *et al.* (1994); carefully washing 5 ml of sample through a 125 μm sieve with distilled water, and then examining it under x10 to x100 magnification in a petri dish. Because the majority of the peat was so highly decomposed, it was very hard to identify small, degraded fragments of plant, particularly pieces of root and stem[1]. Exceptions were that of the restiad stems, which had very distinctive fibrous celery-like stems, and the root systems of *Gleichenia* that were black and wiry. For parts such as these, that could not be counted as 'wholes', an abundance scale was used (McGlone and Wilmshurst, 1999b) (*Table 4.5*). Emphasis was instead placed on absolute counts where whole, complete plant fragments (tending to be above-ground remains e.g. leaves, seeds, seed cases, sporangia) could be readily identified. This also avoided including in counts the root systems of plants that would have been growing at the surface.

% abundance	Group name	Abbreviation	Scale
50-75	Abundant	(a)	5
26-50	Common	(c)	4
11-25	Frequent	(f)	3
5-10	Occasional	(o)	2
<5	Rare	(r)	1

Table 4.5 Abundance groups used for plant macrofossil remains that could not be counted as wholes (McGlone and Wilmshurst, 1999b).

Because plant macrofossils were later to be used for radiocarbon dating, they had to be as well constrained vertically as possible. Therefore samples of 1 cm depths were extracted.

Higher magnification work helped identify plant fragments that were incomplete or partially decomposed. Cell configuration, shape and structure could also be used for

[1] It is possible to distinguish *Sporadanthus* and *Empodisma* roots from each other using two criteria. *Empodisma* roots are covered in very fine root hairs (Clarkson, 2001, pers. comm.) (however these are poorly preserved in fossil sediments). From work on Australian restiads (Meney and Pate, 1999) it was found that *Empodisma minus* roots contain starch, which is stained black using iodine. However, attempts using this staining technique proved unsuccessful for this study.

identification (Campbell, 1975). Diagnostic cross sections of stems and leaves were cut as thinly as possible using a scalpel, stained to enhance the visibility of the cell structure and then washed in distilled water. The biological stain contained 100 ml distilled water, 150 ml glycerol, 50 ml Alcian Blue (0.5% ethanol), 30 ml Safranin (1% in distilled water) and 5 ml Glacial acetic acid. These slices were then mounted on a slide in glycerol jelly and covered with a coverslip for observation under a high magnification microscope at x100 to x400. High magnification images were taken using the analySIS® imaging software via a Leica DC100 camera on a high power Olympus BX50 and a low power Nikon SMZ-U microscope.

The task of identifying plant remains was simplified by the limited number of different plant species on the sites (approximately fifteen). Plant pieces were identified using specimens from the University of Waikato Herbarium, aided by B. Clarkson (Landcare, Hamilton), identification guides such as Poole and Adams (1994) and Johnson and Brooke (1998), and from comparisons with modern vegetation specimens taken during fieldwork. Some samples were also sent to Dr Peter de Lange (University of Auckland) for identification.

Results were plotted using Tilia and Tilia Graph (versions 2.0.b.4) (Grimm, 1993) and TGView (version 1.6.1) (Grimm, 2004).

4.3.7 Charcoal analysis

Method

Macro-charcoal fragments were counted in conjunction with the plant macrofossil analysis, hence only pieces larger than the 125 μm sieve size were retained. The method, following that of McGlone and Wilmshurst (1999b), involved estimating by eye the percentage abundance in fifteen fields of view, and then averaging them (Barber *et al.*, 1994). Fragments were divided into two size groups (<1 mm and >1 mm) based on the length of longest axis. The larger size of charcoal is thought to primarily reflect local burning on the bog itself, as micro-charcoal (<1 mm) can be transported considerable distances by the wind from distant fires (Clark, 1988).

4.3.8 Testate amoebae

Fossil testate amoebae were analysed downcore and found to be sparse. In order to investigate possible reasons for this (e.g. decay, low numbers of living tests) surface tests

were also counted from a series of short cores. Both living and dead tests were counted in order investigate a possible depth-life relationship. See Chapter 5 for more details.

Preparation technique (fossil and surface samples)

The procedure for processing fossil samples followed Charman *et al.* (2000). In order to be able to quantify results and calculate test abundances, two tablets of the exotic spore *Lycopodium clavatum* (12,542±3.3% spores per tablet) (Stockmarr, 1971) were dissolved in 10% hydrochloric acid and then added to 2 cm^3 of sample (measured by displacement of water). This was then boiled in 100 ml of distilled water for ten minutes on a hotplate, stirring occasionally to help disaggregation. It was then sieved through stacked 15 and 300 µm mesh sizes sieves (Hendon and Charman, 1997) to remove the very fine organics/mineral content and the larger pieces of detritus respectively. (Fossil samples from Z0204 were processed using a 180 µm sieve, rather than 300 µm, to reduce the amount of larger organics in the sample). The remaining sample was then stained with two drops of safranine, and washed twice in distilled water, before being mounted on slides using glycerol for counting at x400 magnification on an Olympus BX50 microscope.

Identifications were made using keys such as Charman *et al.* (2000) and various literature e.g. van Oye (1956), Hoogenraad and de Groot (1948) and Corbet (1973). Charman *et al.* (2000) recommend that 150 tests should be representative of the whole assemblage. This recommendation was tested by accumulating incremental counts for several samples from short cores (results from a Moanatuatua core are shown in *Figure 4.6*). The results indicate that the diversity of taxa does not change after approximately 120 tests are counted and this supports Charman *et al.*'s (2000) recommended target of 150 tests per sample.

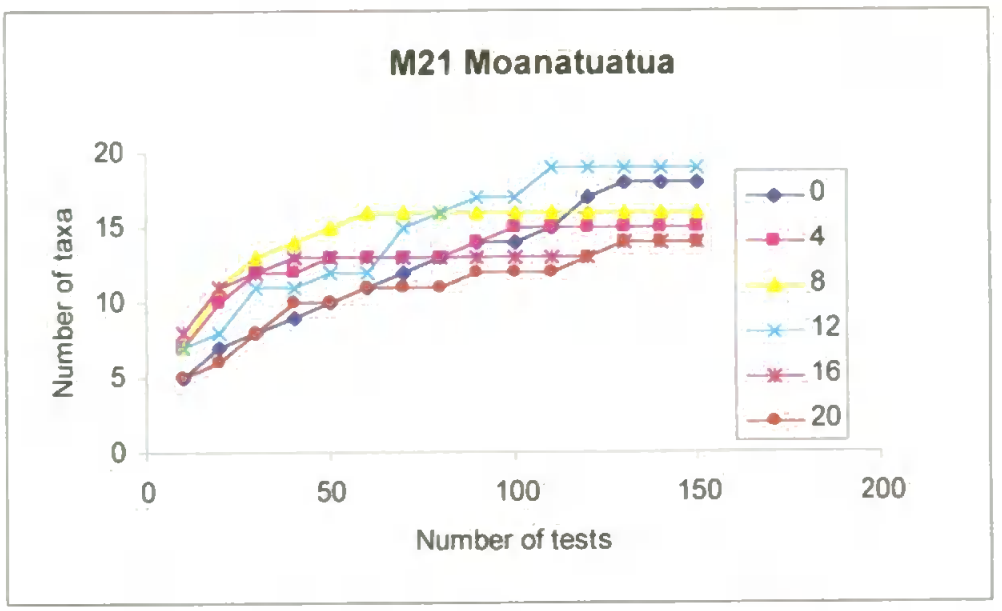

Figure 4.6 Taxa counts compared to test counts for short core M21, showing that the number of new taxa encountered declines as test counts reach 150. Each line represents a sample from a known depth (cm).

Individual taxa counts were represented as a percentage of the total fauna. If test concentrations were low, then counting was stopped when 100 *Lycopodium* spores were reached.

High resolution reference images were taken at x400 magnification using the analySIS® imaging software via a Leica DC100 camera attached to the microscope. This allowed features to be measured, and the measurements superimposed on the image itself. Pictures could then be printed to aid identification.

For the surface samples collected in 2001, 4 ml of sample was used, and two *Lycopodium* spore tablets (each containing 12,542±3.3% spores) were added to facilitate calculation of concentrations. Rose Bengal was added to samples in order to identify the living tests by staining the living tissue. Samples were prepared at 5 cm intervals.

For the surface samples collected in 2002 the sampling resolution was at 4 cm intervals. 2 ml of sample was used with two *Lycopodium* spore tablets and a 180 µm sieve was used to remove larger plant fragments.

To calculate the concentration of tests:

$$\text{Total fossil tests} = \frac{\text{number of tests counted} \times \text{number of exotic spores added}}{\text{number of exotic spores counted}}$$

However, because the surface samples varied so much in their bulk density and they were all subsampled by displacement of water, samples with a low bulk density e.g. *Sphagnum*-rich, appeared to have very low test concentrations. To overcome this problem, 2 cm^3 of each sample was dried and weighed so that test abundance per gram of dry weight could be calculated to enable the direct comparison of samples:

$$\text{Test conc. per dry g} = \frac{\text{number of tests per } 2cm^3}{\text{dried weight of } 2cm^3}$$

Results were plotted using Tilia and Tilia Graph (versions 2.0.b.4) (Grimm, 1993) and TGView (version 1.6.1) (Grimm, 2004).

As discussed in Chapter 5, fossil samples from deeper sections of cores appeared to have low test concentrations. This could be due to a) dissolution under poor preservation conditions, b) high dilution by a large amount of very fine organics that was not removed during the sieving process, or c) a combination of both. As a result, slides were very laborious to count and it was not possible to achieve statistically useful counts. In order to determine whether or not sufficient tests were present, and to facilitate the microscope work, some method of concentrating them was further required. One method explored was density separation. A preliminary investigation into its potential for improving the yield of testate amoebae was undertaken, as detailed below, although there was insufficient time in this project to make a comprehensive study.

Density separation

Lithium hetropolytungstate (LST) is a heavy liquid used to separate out different specific gravity fractions of samples. Most commonly, this is used to float off pollen from mineral substrates. However, preliminary trials were carried out to see if the same principle allowed the separation of testate amoebae from the well-humified peat fragments within which they are preserved.

The specific gravity of testate amoebae must be determined using a range of different density LST. Initial trials were carried out on near-surface samples, where testate amoebae concentrations were higher.

Samples were first prepared in the standard way (up to and including the sieving process) then mixed with a known density of LST, centrifuged for 5 minutes at 3000 rpm, and left to stand for 1 hour. They were then re-centrifuged for 10 minutes at 2000 rpm and left overnight to separate. The following day, the two fractions were separated by pipetting off the floating sample. Each fraction was then washed in distilled water and examined microscopically for testate amoebae.

This process should be repeated until the optimum specific density for separation has been determined, and the method separates out as much of the fine organics as possible. In order to achieve this, the procedure might require a double separation, first floating off all the lighter organics as the tests sink, and then sinking out the heavier organics as the tests float.

Preliminary results proved to be insufficiently encouraging as to justify further time investment in this study (even though it might prove profitable in the future), and as a consequence, the optimum density for testate amoebae was not determined. However, various observations were made that will aid future work:

a) The two fractions of the settled samples were very hard to separate, as much of the very fine organic matter neither settled out nor floated completely. It remained suspended, in 'fluffy'-like conglomerations.
b) It appeared that separations seemed to be species-specific i.e. certain species were consistently separated out from others, suggesting that there is no single density of testate amoebae. This is not be wholly unexpected, as tests are composed of a variety of materials that vary with location.
c) Often, a large amount of fine organic matter remained incorporated in each fraction, which still 'diluted' the samples sufficiently to make counting impractical.
d) The *Lycopodium* spores that are vital for calculating test abundances were often separated out from tests.

More work needs to be carried out in order to determine whether density separation holds any prospects for significantly increasing test concentrations.

4.4 Peat humification correction experiment

As Chambers (1984) and Blackford and Chambers (1993) reported, peat samples containing mineral matter appear to have artificially-high light transmission readings. The presence of mineral matter dilutes the organic component of the peat sample, resulting in less extracted humic acid, and thus leading to an artificially high light transmission value for such samples.

To overcome this problem, Blackford and Chambers (1993) suggested a correction formula for light transmission values on peat samples containing mineral matter. The suggested relationship was linear, i.e. if half the sample was composed of mineral matter, then the light transmission value should have been halved. The formula reported in Blackford and Chambers (1993) is: $t = r/_{LOI}$ (where t = corrected value, r = initial transmission reading and LOI = loss on ignition value as a proportion).

Whilst processing samples for this study, it became evident that enhanced light transmission was occurring as a result of tephra layers in the stratigraphy. An experiment was devised to test the relationship between mineral content and light transmission, and to quantify more accurately the effect of highly minerogenic peats on light transmission readings. A new correction procedure is proposed based on an exponential relationship between light transmission and mineral 'contamination', to enable the calculation of a more accurate light transmission value for such 'contaminated' samples.

As tephra layers are considered to be instantaneous events, peat humification samples taken from within large, visible layers were not meaningful in terms of time elapsed. However, a correction formula was of great use for microtephras (i.e. those not visible with the naked eye) and for correcting for the attenuation of tephra shards directly above and below major tephra layers that affect humification values.

4.4.1 Method

Test samples were made using typical *Empodisma minus*-dominated peat from Kopouatai mixed with fine, dried silica sand (Grade HH). The peat contained a small amount of background mineral content (2.24% from the LOI measurement). The sand was first placed in a furnace at 550°C for four hours to ensure that it contained no organic material. The peat was dried, ground to powder in a Specamill, and thoroughly mixed until

homogeneous. Samples of varying proportions of peat and sand were then made according to weight (*Table 4.6*).

For each sample, three replicates (sampled after the peat-sand mixing) were measured as usual for light transmission, loss on ignition (LOI) and total organic carbon (TOC). LOI was measured as this is the standard technique regularly used for determining the organic content of samples (including the work by Blackford and Chambers (1993) in determining their correction equation). TOC is an alternative technique to LOI, used to derive the amount of carbon in the organics, and was measured for this experiment because it is used regularly in this project (section 4.3.5). Thus, the correction can therefore be applied to either technique.

Sample numbers	Percentage weight sand	Percentage weight peat	Mean light transmission %
1-3	0	100	17.24
4-6	5	95	20.16
7-9	10	90	21.67
10-12	15	85	24.50
13-15	20	80	26.20
16-18	25	75	28.78
19-21	30	70	31.39
22-24	35	65	32.00
24-27	40	60	36.22
28-30	45	55	39.77
31-33	50	50	44.30
34-36	55	45	47.11
37-39	60	40	51.58
40-42	65	35	55.16
43-45	70	30	60.12
46-48	75	25	65.22
49-51	80	20	70.47
52-54	85	15	76.60
55-57	90	10	83.01
58-60	95	5	89.80
61-63	100	0	96.07

Table 4.6 Mineral contamination experiment samples with varying proportions of peat and sand and the average light transmission reading taken from three replicate samples (three readings each).

The methods for determining peat humification (Blackford and Chambers, 1993), LOI and TOC were as detailed in section 4.3.

4.4.2 Results

This section outlines the results of the peat humification experiment.

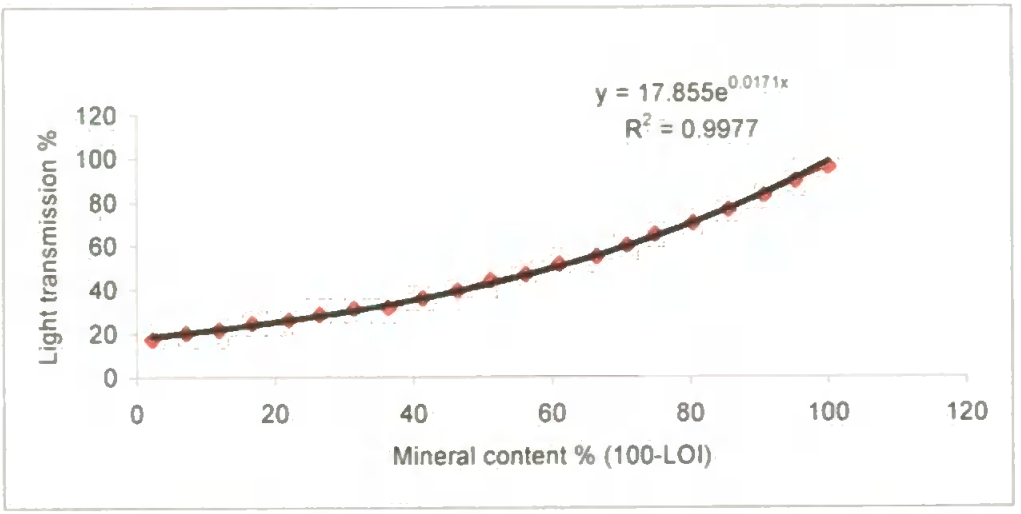

Figure 4.7 Light transmission against mineral content (calculated from LOI). Mineral content does not cross the y-axis due to a background level of mineral content (2.24%) already present in the peat.

As seen in *Figure 4.7*, the relationship between mineral content and light transmission is exponential[2], contrasting with Blackford and Chambers (1993) who suggested from experimental work that it is explained by a linear relationship (*Figure 4.8*). A likely explanation for the curvilinear relationship could be that a more complete extraction of the humic acids occurs on the samples with less organic matter as the ratio of extract to organics increases.

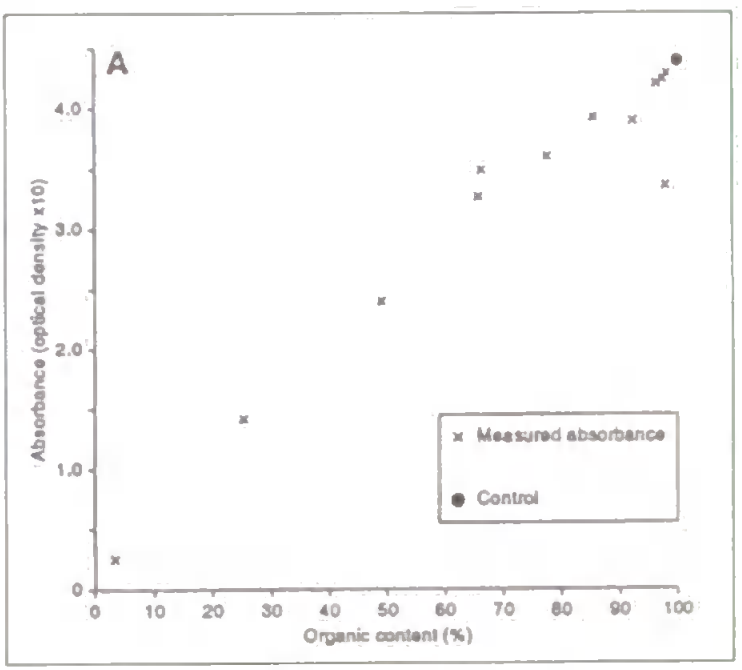

Figure 4.8 The relationship between mineral content and light absorbance as proposed by Blackford and Chambers (1993).

[2] The data also fits a quadratic curve with a slightly higher r^2 value (0.9987), but a quadratic relationship cannot be used due to the infinite number of possible curves that could join two points.

For a 100% mineral sample, a 100% light transmission reading would be expected as it will contain no humic acid. However in this experiment, the 100% mineral samples had a mean light transmission value of 96.07%. Measurement error could be a factor despite best efforts to minimise this; if there is dust in the machine it can diffract light particles away from the sensor, or if the glass cuvette is dirty or not exactly oblique to the light beam not all the light will pass through. The effects of most of these possible instrumental errors, however, should all be accounted for using the standard cell as a comparison. A difference in optical properties between water and NaOH could be excluded (each humification sample is measured and referenced to a blank sample – a second cuvette containing distilled water). This was subsequently tested (*Table 4.7*). The average light transmission of distilled water at 550 nm was 97.83% and that of 2% NaOH (the strength after the two dilutions) was 97.73% before processing and 97.66% after processing.

	% light transmission				
	Reading 1	Reading 2	Reading 3	Reading 4	**Average**
Distilled water	97.72	97.85	97.73	-	**97.83**
2% NaOH unprocessed	97.88	97.81	97.50	-	**97.73**
2% NaOH processed	97.70	97.39	97.85	97.71	**97.66**

Table 4.7 Light transmission results comparing the optical properties of distilled water and NaOH.

The results of the experimental data described the exponential curve:

(1) $$\text{light transmission} = 17.855e^{(0.0171*\text{mineral content})}$$ (*Figure 4.7*)

From this experiment, it was known that for any given sample with a known mineral content (x) and known light transmission (y), an exponential curve could be drawn through the point (x, y) and the point (100, 100(or 96.07)). Hence, for a known sample it was possible to plot an individual curve and calculate y when $x = 0$ i.e. the light transmission of the peat sample with no mineral contamination.

From the exponential relationship ($y = ae^{bx}$) it was then possible to calculate a and b for any given peat sample by solving simultaneous equations:

(2) $$b = \frac{\ln y_0 - \ln y_e}{x_0 - x_e}$$

(3) $$a = \frac{y_0}{\exp(bx_0)}$$

where: x_0 = the mineral content of the 'real' data point,

x_e = 100,

y_0 = the light transmission value of the 'real' data point,

and y_e = 100 (or 96.07).

Correcting for mineral content could then be done on *any* data point - where a is the corrected light transmission for the sample if it contained no mineral matter. When correcting the results of this project, 96.07% was used as the light transmission reading of the 100% mineral sample (rather than the theoretical 100%) since this was the value obtained on this machine for these samples.

Results for TOC also showed an exponential relationship with light transmission (*Figure 4.9*).

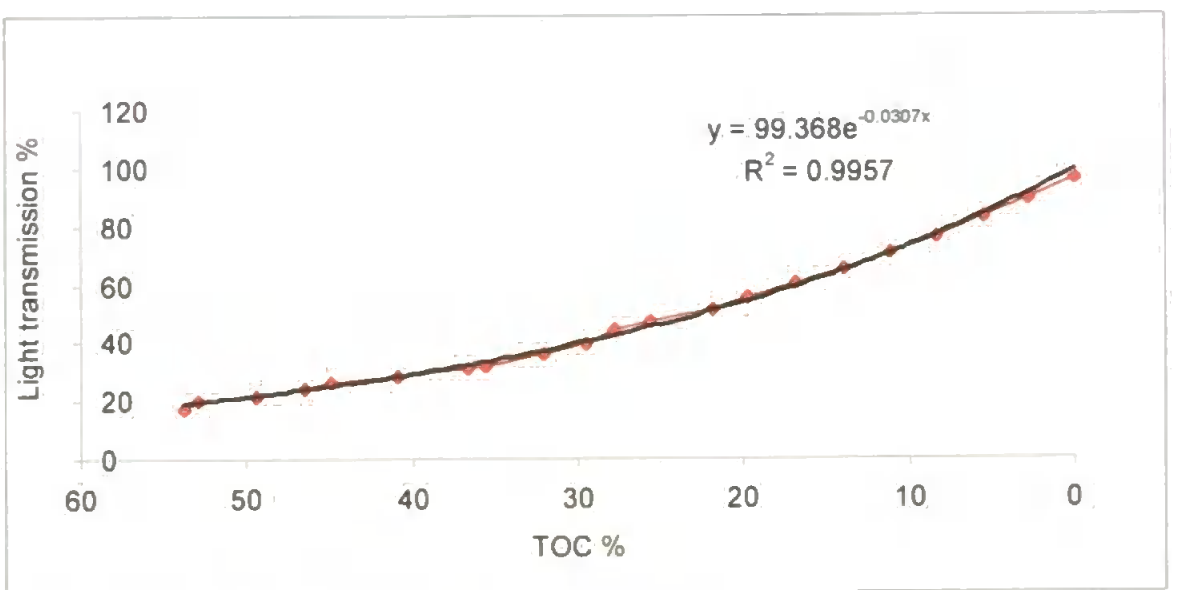

Figure 4.9 Light transmission against TOC (note reversal of x axis).

However, to calculate the corrected light transmission for samples on which TOC, not LOI, had been measured, the LOI values would have to be replaced using the relationship between TOC and LOI (*Figure 4.10*). TOC could not directly be used in the exponential

relationship, because the value of TOC for a sample of 100% organic matter is not 100% (i.e. the percentage mineral content of a sample for which TOC has been measured is not 100% minus the TOC value).

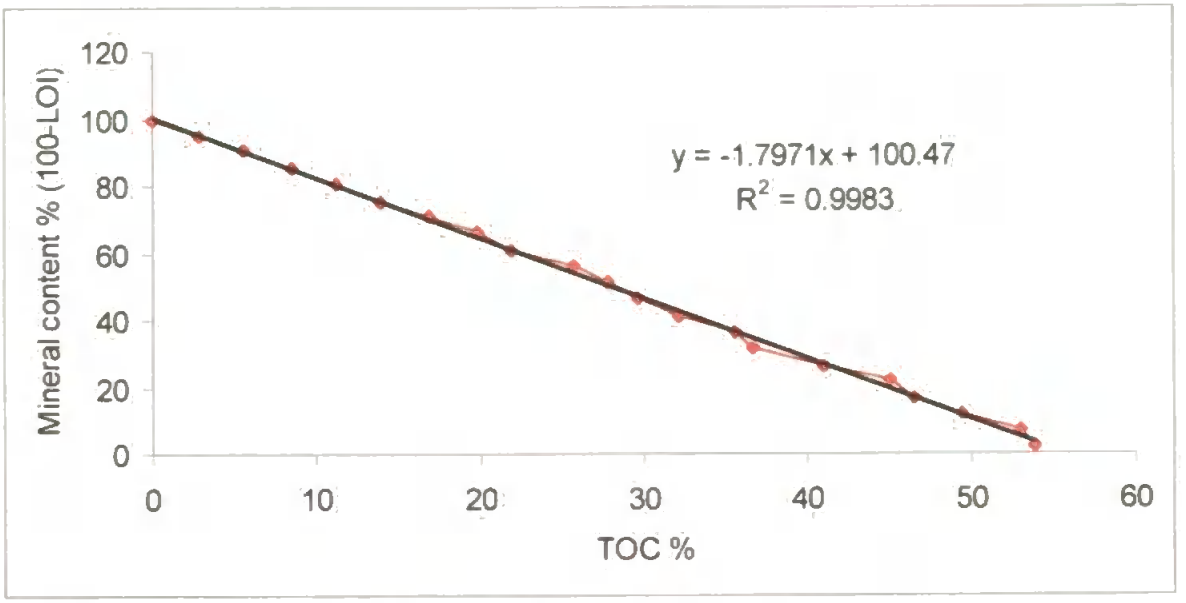

Figure 4.10 The relationship between TOC and mineral content (expressed as 100-LOI).

These two variables, LOI and TOC, were related linearly:

(4) $$\text{mineral content} = 100.47 - 1.7971 \times \text{TOC}$$

with a high r^2 value of 0.9983.

Hence, for a TOC measured sample, x_0 in equations (2) and (3) can be replaced such that:

(5) $$b = \frac{\ln y_0 - \ln y_e}{(100.47 - 1.7971x) - x_e}$$

(6) $$a = \frac{y_0}{\exp(b(100.47 - 1.7971x))}$$

These formulae could then be applied to any peat humification light transmission result of known LOI or TOC. The correction procedure was applied to each core, and the results are presented and interpreted in Chapters 6 and 7.

4.5 Summary

A variety of palaeoecological methods that were used in the reconstruction of peatland palaeomoisture records have been described, together with their palaeoclimatic implications.

In addition, the results of some exploratory work on methods has been reported. A number of associated problems were identified and adjusted for (*Table 4.8*). Preliminary work on concentrating testate amoebae for samples with low test concentrations proved difficult and was not pursued further. Tests on the effects of high mineral (tephra) content on humification measurements resulted in a new correction procedure for these samples.

Problem	Description	Resolution	Section
Core compression.	During transit some core sections became vertically compressed.	Depths were corrected using a formula that assumed that constant compression had occurred throughout the core section.	4.3.1
Offset in TOC between separate runs.	A difference in baseline TOC values (thought to be an instrumental error) was observed between the separate runs measuring alternate samples.	A corrective formula was derived based on calculating middle values between the separate runs.	4.3.5
Poor yield of testate amoebae at depth.	Fossil testate amoebae concentrations were found to be too low for statistically significant counts.	-Short cores from the surface were investigated for testate amoebae, and found to be abundant. -Preliminary density separation work was carried out to assess its potential for improving concentrations.	4.3.8
Non-visible mineral/tephra layers within the peat.	These layers, if undetected, would result in erroneous climatic interpretation, as they substantially raise light transmission values of the peat humification record.	Layers were detected (and omitted from climate interpretation) on the basis of: -a marked decline in TOC, -a marked decline in % moisture, -microtephra analysis (Ballinger, 2003), -microscopic spot checks on light transmission excursions.	6.3 and 7.3
		A non-linear correction for mineral 'contamination' of light transmission was derived from an experiment using artificial samples of varying peat-sand ratios.	4.4.2
Age-decay effect in humification.	Light transmission records gave progressively higher light transmission values towards the surface. This age-factor could be obscuring longterm climate signals.	The light transmission records were corrected by calculating the residuals from the straight line that explained the age-decay relationship.	8.2.1, 8.2.2 and 8.3.1

Table 4.8 The main problems identified with samples/methods and how they were resolved.

The next chapter presents and discusses the results of the testate amoebae studies from both sites and focuses on methodological issues because of difficulties with obtaining adequate data in initial analyses.

CHAPTER FIVE – RESULTS: TESTATE AMOEBAE

At both sites, analyses of testate amoebae assemblages were undertaken down the peat profile and, in order to investigate further the low concentrations found, across a range of surface samples. In this chapter, results of both sets of analyses are presented and related to the surface measurements recorded of pH, conductivity, depth to water table and moisture content. All methods applied in these analyses are described in the previous chapter.

5.1 Testate amoebae taxonomy

Testate amoebae work at these New Zealand sites identified numerous taxonomic issues that required taxa previously unseen or rare in Northern Hemisphere samples to be categorised. The majority of identifications were made using the diagnostic features given in the key from Charman *et al.* (2000) that focused on Northern Hemisphere taxa. The taxonomy of the more unusual taxa is described in Appendix 1.

5.2 Fossil samples

In order to investigate the down-core content of fossil testate amoebae, samples from depth were prepared and counted from both Moanatuatua and Kopouatai. At Moanatuatua, core Z0102 was used as this was the first core to be retrieved and analysis was carried out immediately. From Kopouatai, core Z0204 was used for the reason that it had been sampled at the highest resolution for peat humification analysis. Samples with very low abundances (the majority) were counted until 100 *Lycopodium* spores or the whole slide was counted, whichever was reached first. The results of the preliminary counts are presented below (*Tables 5.1* and *5.2*).

5.2.1 Moanatuatua

Samples were selected systematically every 1 m down-core, starting just below the Taupo tephra layer.

Depth (m)	Number of tests	Number of taxa	Number of *Lycopodium*	Test concentration per cm^3
0.51-0.52	25	5	100	3,136
1.51-1.52	20	6	100	2,508
2.51-2.52	10	5	100	1,254
3.51-3.52	34	6	100	4,264
4.51-4.52*	2	1	99	253
5.51-5.52*	7	4	94	934

Table 5.1 Fossil testate amoebae counts from Moanatuatua (Core Z0102) (indicates where the whole slide was counted). Concentrations near the surface are estimated as 10-30,000/cm^3.*

Counts from the initial study show a dramatic difference between surface and fossil samples, with tests up to ten times more abundant at the surface. There appears to be a more or less constant decline in fossil test concentration with depth, except at 3.51-3.52 m where abundances were actually at their highest, and at 5.51-5.52 m where the declining trend was also reversed, but to a lesser extent.

Confidence ranges of 95% were calculated for each sample (Moore and Webb, 1978) (*Figure 5.1*):

$$95\%\ \text{confidence interval} = \frac{\hat{u} + \left[\frac{(1.96)^2}{2n}\right] \pm (1.96)\sqrt{\left[\hat{u}(1+\hat{u})/n\right] + \left[(1.96)^2/(4n^2)\right]}}{1 - \left[(1.96)^2/n\right]}$$

where: $\hat{u}$ = proportion to marker grains,
x = number of type grains counted,
and n = number of marker grains counted.

$$\hat{u} = \frac{x}{n}$$

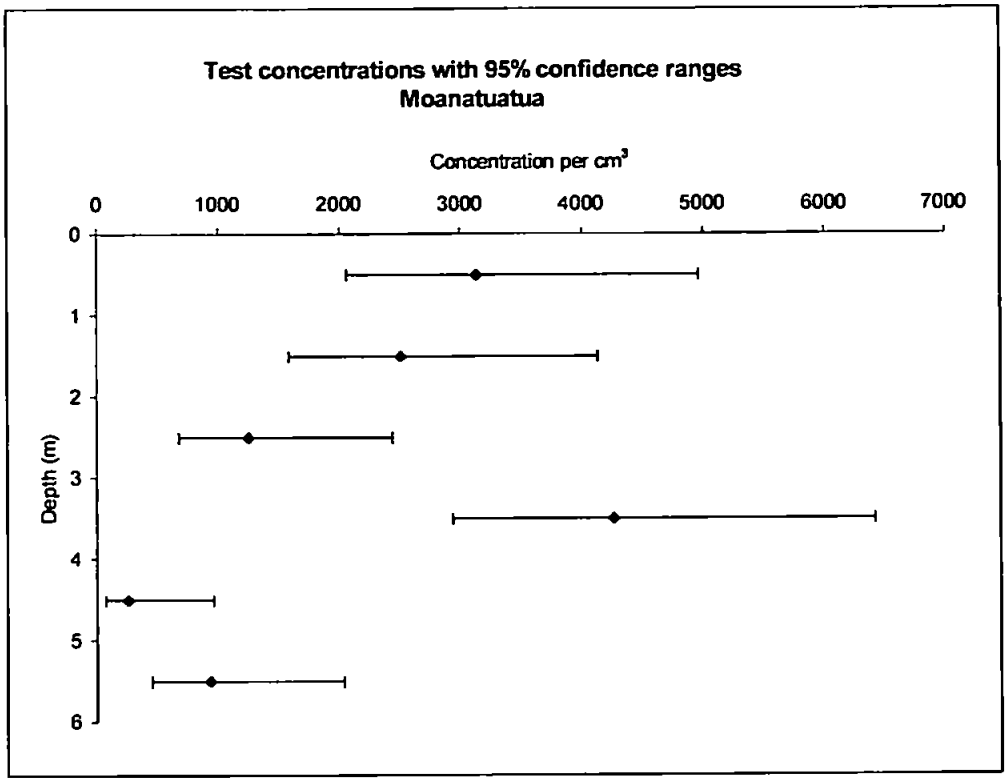

Figure 5.1 Fossil test concentrations, with 95% confidence intervals, for Moanatuatua.

The 95% confidence limits were used to investigate the significance of changes downcore. For 3.51-3.52 m, the results suggest that because its test concentration (4,264) is not within the confidence ranges of its nearest samples, then the reversal in the decline at this depth is statistically significant at this confidence level. However the same does not hold at 5.51-5.52 m, where the test concentration (934) is within the range of the sample above i.e. the increase in concentration for this sample is not significant at 95%.

Taxa diversity is low in all samples, but also tends to decline downcore. The most diversity is in 1.51-1.52 m, where each taxon is an average of 16.5% of the count. The least diverse sample is 4.51-4.52 m where 100% of the sample is the same taxon (although only two tests were counted in total).

Very high levels of extremely fine, highly decomposed organic matter were characteristic of all samples, making counting slow and laborious. Slides were often low in both *Lycopodium* spores and tests, suggesting that samples were being 'diluted' by such organic remains, with this problem most likely compounded by a general paucity of tests. This has serious implications when counting the slides, because large amounts of extraneous matter on slides can hinder counting significantly, even where test numbers are high.

5.2.2 Kopouatai

Similar fossil test analysis was undertaken for comparisons at Kopouatai (Core Z0204), and in addition the possible causal link between peat degradation and test abundance, as discussed by Wilmshurst *et al.* (2003), was investigated. Six pairs of samples were chosen from near-adjacent depths covering varying humification values and these pairs were selected from different depths. The hypothesis that "Samples with high humification levels[1] (i.e. reduced light transmission) contain fewer tests because they were more decayed" was investigated (*Table 5.2*).

When preparing the samples it was observed that, after sieving, the more humified peat samples contained much more sediment. For example, 7.01-7.02 m contained almost twice that of 7.13-7.14 m, so that when counting the smaller sample, it was quicker to count 100 *Lycopodium* spores, over which time not as many tests had been observed. This difference was probably due to the fact that plant fragments were less decomposed and therefore had been removed by the large sieve. Another possible cause could have been that the 2 cm^3 samples had been measured using displacement of water, and the samples had different densities and water contents. To investigate the effect of sediment volume on test concentrations, test concentrations per gram dry weight were calculated as well as concentrations per cm^3 (section 4.3.8) (*Table 5.2*).

First, these results indicate that, in general, fossil test diversity and abundance are greater at Kopouatai than at Moanatuatua. This could be due to the higher water table at Kopouatai giving rise to higher test populations and/or inhibiting decay. Nevertheless, both sites seem to suggest an overall down-core decline in abundances.

[1] These samples were selected prior to the application of the mineral correction, when it was not known whether high light transmission values were due to a real wetness signal (or the possible presence of microtephra). Following corrections based on TOC measurements, it was found that the relationship between pairs of samples remained the same.

Depth (m)	Raw light transmission value	Test count	Number of taxa	Number of *Lycopodium*	Test concentration per	
					cm^3	dry g
4.495	16.19 L	67	7	100	8,403	109,989
4.515	22.58 H	17	8	100	2,132	16,301
4.795	18.66 L	27	6	100	3,386	46,073
4.835	25.67 H	21	4	100	2,634	34,633
5.135*	16.89 L	12	7	100	1,505	24,774
5.115	22.94 H	49	9	100	6,146	91,931
5.815*	11.09 L	11	4	100	1,380	18,556
5.795	20.01 H	38	11	100	4,766	66,332
6.735*	15.35 L	2	2	100	251	3,824
6.695	21.73 H	2	1	100	251	3,260
7.015	14.19	13	4	100	1,630	15,876
7.135	22.70	10	2	100	1,254	17,615

*Table 5.2 Fossil testate amoebae counts from Kopouatai (Core Z0204). Concentrations near the surface are estimated as 11-32,000/cm^3 (130-300,000/dry g) (section 5.3.1). L refers to the samples of low light transmission, and H to those of high light transmission. High light transmission values (>20%) imply reduced humification. * indicates where samples have been reversed within their couplet according to their light transmission value (L or H).*

A limited number of taxa seem to dominate the assemblages, particularly *Difflugia pulex* (large), *Hyalosphenia subflava* and *Assulina muscorum*. Of these three taxa, *D. pulex* shows the most pronounced decline in abundance downcore, with a more fluctuating count demonstrated by *A. muscorum*. The remainder of the counts are composed of only one or two individuals of the other taxa, the most abundant of which are *Amphitrema wrightianum* and *Difflugia pulex* (small). The two types of *D. pulex* (large and small) were seen to be highly decomposed, suggesting that the testate amoebae were subjected to strong decay processes.

As before, 95% confidence intervals were also calculated for these samples, separately for per cm^3 and per dry g (*Figures 5.2* and *5.3*).

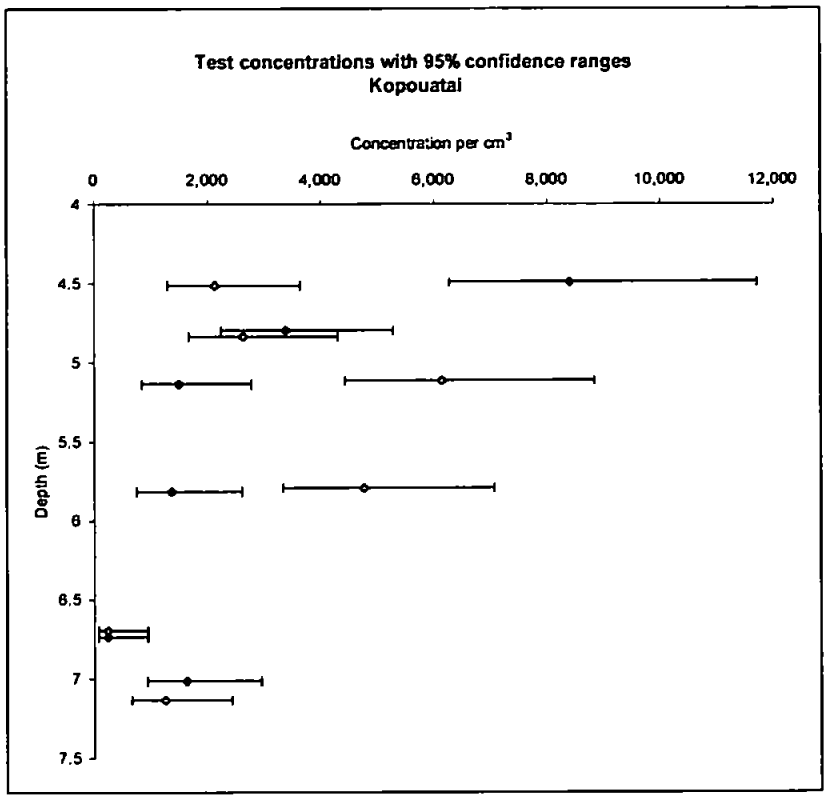

Figure 5.2 Fossil test concentrations per cm^3, with 95% confidence intervals, for Kopouatai. Yellow symbols indicate samples of high light transmission and blue symbols indicate samples of low light transmission.

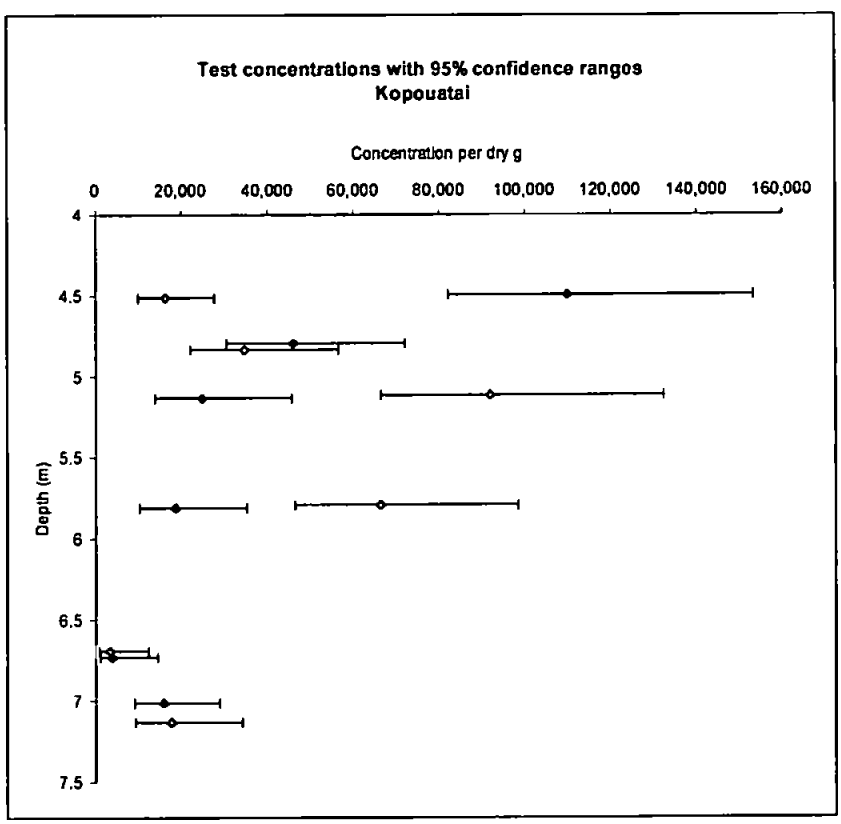

Figure 5.3 Fossil test concentrations per dry g, with 95% confidence intervals, for Kopouatai. Yellow symbols indicate samples of high light transmission and blue symbols indicate samples of low light transmission.

The confidence intervals and trends are similar for concentrations derived per cm^3 and per dry g. The low and high light transmission results will be considered separately. The low light transmission plots suggest that the majority of results are significantly different at the 95% confidence range.

When considered separately from the samples of high light transmission values, the samples with low light transmission have concentrations that decline steadily down-core (apart from the reversal in the lowest sample). However, high light transmission samples show no distinct trend in test concentrations and are highly variable (*Figure 5.4*). However, it should be noted that these are based on a small number of samples.

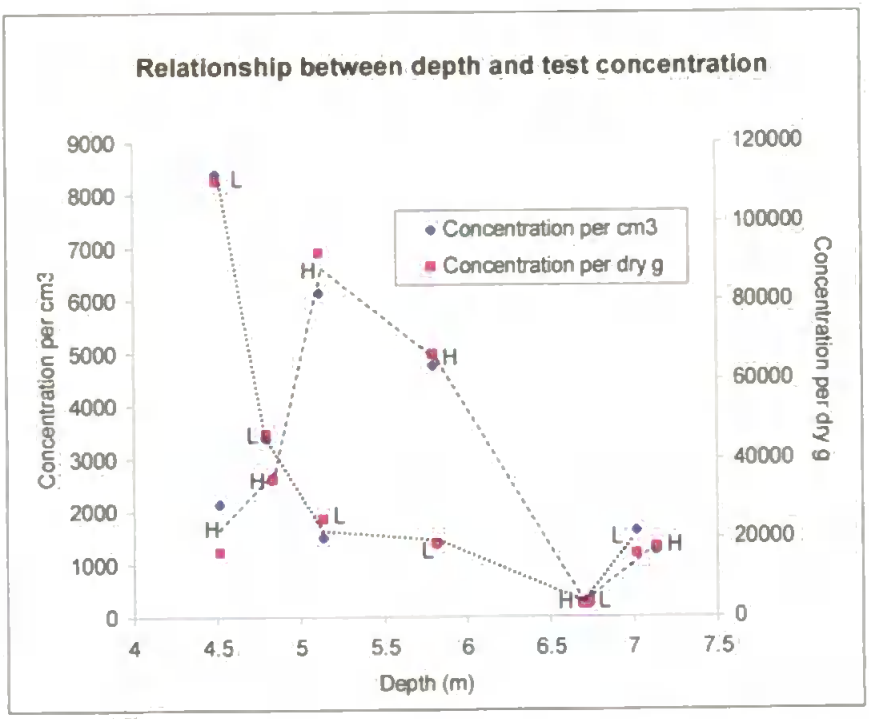

Figure 5.4 Test concentrations from core Z0204 (Kopouatai). H = samples of high light transmission and L = samples of low light transmission.

Comparing concentrations per cm^3 and per dry gram *(Figure 5.4)* shows the same relationships between paired samples (i.e. the low and high light transmissions) except for pair 6.69-6.70/6.73-6.74 m (that had exactly the same concentrations per cm^3, but not per dry gram) and 7.01-7.02/7.13-7.14 m (where the alternative sample had the higher concentration per dry gram). However, these are very small differences when compared to the overall pattern. These results suggest that test concentrations of fossil samples can be directly compared, whichever unit (cm^3 or dry gram) is used for calculating their abundance.

Figure 5.4 confirms the findings above inferred from *Table 5.2*. When high and low light transmission samples are considered separately, there is a generally consistent downcore trend in test concentrations through the humified peat, except for the upper two samples of low light transmission samples. Perhaps these samples had initially low test concentrations, and therefore using only six samples of each light transmission group is insufficient. Again, the overall trends appear to be indicative of downcore decay, but other factors must also be involved, and the number of observations is too few to draw definitive conclusions.

Light transmission results were then correlated with test concentration to investigate statistically their relationship (*Figures 5.5* and *5.6*).

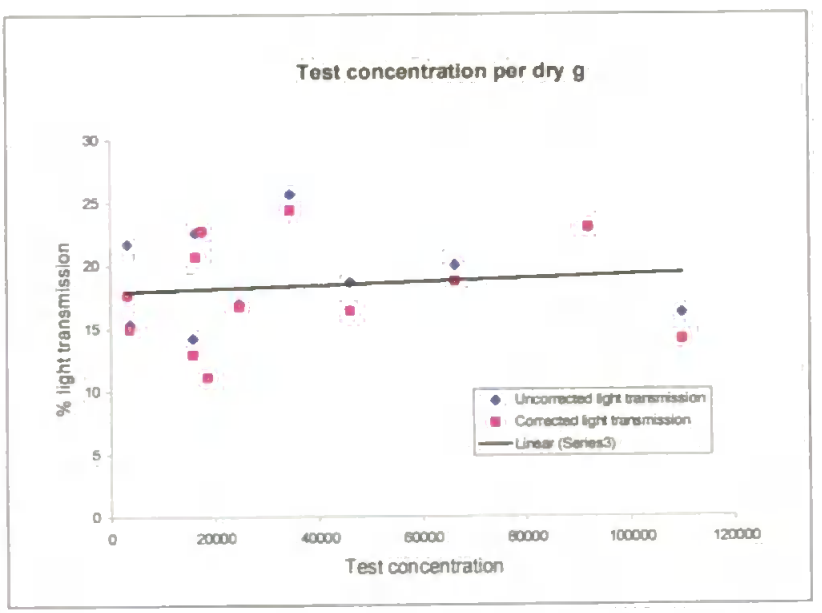

Figure 5.5 Concentrations of tests per dry gram of peat, and its relationship with light transmission values; there is nearly no correlation between the two variables, suggested by the near-horizontal best-fit linear line and very low r values of 0.096 and 0.101 for test concentrations correlated with corrected and uncorrected light transmission values respectively.

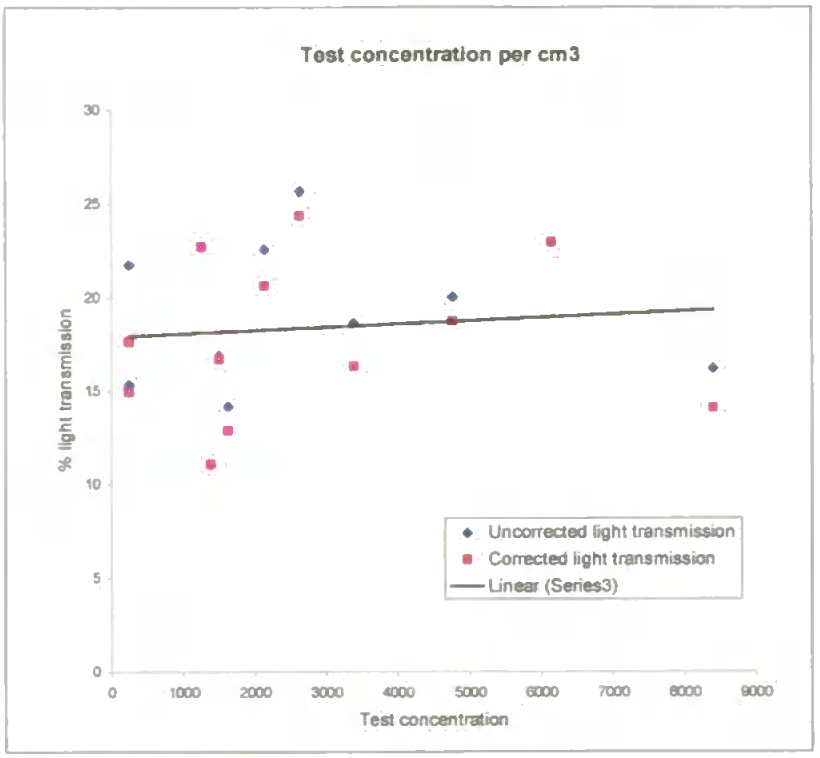

Figure 5.6 Concentrations of tests per cm^3 of peat, and its relationship with light transmission values; there is no correlation between the two variables, suggested by the near-horizontal best-fit linear line and very low r values of 0.122 and 0.108 for test concentrations correlated with corrected and uncorrected light transmission values respectively.

Together with light transmission (the proxy for peat humification), depth could also be a factor affecting test concentration. The relationship between depth and test concentrations is therefore investigated using both Pearson and Spearman's Rank correlations (*Table 5.3*).

		Pearson		Spearman's Rank	
	Concentration	r	p value	r_s	p value
High light transmission	per cm^3	-0.480	0.336	-0.429	0.397
	per dry g	-0.356	0.488	-0.143	0.787
Low light transmission	per cm^3	-0.713	0.112	-0.657	0.156
	dry g	-0.766	0.076	-0.943	0.005

Table 5.3 Correlation coefficients of depth and test concentration.

Results (*Table 5.3*) show that the two variables are negatively correlated i.e. as depth increases test concentration decreases. Both the r and r_s values suggest that there is a clear difference between high and low light transmission samples, but due to the small number of samples, the non-parametric Spearman's correlation is more appropriate. Samples of lower light transmission (more-humified peat) have higher correlation values suggesting

that they are more strongly correlated with depth than samples of high light transmission. The strongest r value is for the Spearman's Rank (r_s) on concentrations per dry g from low light transmission samples. However, when considering the p values, only the Spearman's correlation of the low light transmission sample, with concentrations calculated per dry g, is statistically significant at the 95% level. It is a very strong negative correlation (-0.943). These results confirm that the trends might be indicative, but are not statistically significant due to the low number of samples.

Overall, it appears that test concentrations relate more strongly to the depth factor (i.e. time passed for decay to have occurred) (*Table 5.3*) rather than to light transmission values (*Figures 5.5* and *5.6*) i.e. the degree of peat humification, suggesting that the hypothesis that test concentrations are related to light transmission should be rejected.

Based on observations of the Moanatuatua fossil slides, Wilmshurst (2001, pers. comm.) advised that the time spent counting such samples was not sufficiently productive. So, after careful consideration of all the fossil test data, together with the inconclusive results of the density separation work[2], the method of using fossil testate amoebae as a valid palaeomoisture technique at these sites was abandoned. However, some further investigation into the low test abundances was undertaken, as described below.

5.3 Surface samples – relationships with pH, conductivity and depth to water table

To investigate further the reasons for the paucity of fossil tests, short core samples (including the surface 0-1 cm) were counted to a) determine testate amoebae concentrations at and near the surface, b) to investigate changes with depth in recent time, and c) to identify the depth at which test concentrations decline.

Short cores from both Kopouatai and Moanatuatua were prepared in two batches. In the first run (*Table 5.4*), cores were not selected according to any particular investigative strategy, but purely to identify if any testate amoebae were present.

[2] Due to time constraints, insufficient density separation work for separating out tests from their substrate was carried out, thereby preventing its application in this project.

	Sample name	Depth (cm)	Dominant vegetation of sample location
Kopouatai	Z0106	0-30	*E. minus, S. ferrugineus, Sphagnum*
	Z0108	0-30	*E. minus, S. ferrugineus, G. dicarpa, E. pauciflora*
Moanatuatua	Z0103B	0-25	*E. minus, G. dicarpa, E. pauciflora, S. ferrugineus*
	Z0104#2	0-36	*E. minus, G. dicarpa, S. ferrugineus*

Table 5.4 The first short cores selected for testate amoebae analysis.

In the second batch, short cores were selected according to the water table level and the dominant vegetation types at the sampling point (*Table 5.5*). This sampling strategy aimed to test whether hydrological conditions and host vegetation affected test abundance and preservation. *Gleichenia* is associated with dry conditions, i.e. where the water table is low, the restiads *Empodisma* and *Sporadanthus* are associated with wet conditions (but as these species are dominant throughout the bog, samples were chosen that had a low and a high water table), and *Sphagnum* prefers very wet conditions i.e. a higher water table.

Sample name	Depth (cm)	Water table depth (cm)	Water content (%)	pH	Conductivity (μS)	Dominant vegetation of sample location
Kopouatai						
K2	0-17	18 (M)	96.6	4.16	76	***Sphagnum*** *E. minus* *S. ferrugineus* *G. dicarpa*
Z0204A	0-24	20 (L)	89.7	4.73	455	*E. minus* ***G. dicarpa*** *S. ferrugineus* *L. scoparium* *E. pauciflora*
Moanatuatua						
M5	0-18	70 (L)	83.7	3.87	306	***E. minus*** ***S. ferrugineus***
M21	0-21	78 (L)	81.7	4.02	164	***E. minus*** ***S. ferrugineus***
M22	0-21	74 (L)	90.7	3.87	181	*E. minus* ***G. dicarpa*** *S. ferrugineus*
Z0206A	0-30	59 (H)	89.1	4.08	96	***E. minus*** ***S. ferrugineus***

Table 5.5 The second run of short cores selected for sampling, showing site, dominant vegetation species (in order of dominance) and measured variables. Water table depth is described as high (H), middle (M) or low (L) relative to the range of water tables at that site. Plant species ***in bold*** *indicate those of most importance for short core selection.*

K2 was the only sample where *Sphagnum* was dominant, M5 and M21 were dominated by restiads and had a low water table, Z0206A was dominated by restiads and had a high water table, and at M22 and Z0204A *Gleichenia* was the second most dominant species (at no sample location was it dominant) with a low water table. Z0204A and Z0206A were also the surface section of the long cores used for palaeomoisture reconstructions. In addition, whilst sub-sampling it was observed that M21 contained *Gleichenia* roots throughout and that they were also present lower in K2. M22 and Z0206A also contained *Campylopus* remains throughout and a liverwort was present at the very surface of M22.

All short core counts are shown below, beginning with samples dominant with dry indicator plant species, through to very wet ones. Only the main features are described. Concentrations are shown as tests per cm^3, subsampled by displacement of water. Due to the varying bulk densities of samples (particularly that of the *Sphagnum*), concentration per dry gram was also used in order to make direct comparisons between samples. The percentage of living tests is also presented and discussed

5.3.1 *Gleichenia* second dominant (dry)

Short core M22

The main species present at this site (*Figure 5.7*) are *Assulina muscorum* and the large individuals of the *Heleopera*-type taxon. *Assulina muscorum* fluctuates in abundance, seeming to alternate with *Assulina seminulum* that is more abundant midway through the core. The large *Heleopera*-types decline in overall abundance up-core, with type 2 peaking in presence (almost 40%) at 12 cm. *Euglypha tuberculata* is also present throughout the core, at noticeable percentages of up to nearly 20%, increasing towards the surface. Other noticeable features are the domination of *Cryptodifflugia cf. oviformis* at the surface (70%) and *Difflugia pulex* at the base of the core (approximately 30%). Both of these taxa are only present in these individual samples.

Test abundances overall show a clear decline down core, particularly in the surface 8 cm, where concentrations decline to less than 20% of the surface value. Concentrations remain low throughout the rest of the core. Living tests, stained pink by rose bengal, only comprise approximately 6% of the tests at their greatest (the surface), but they are present throughout the short-core indicating that the living zone of certain species extends to a depth of (at least) 20 cm. Within this zone though, proportions of living tests do decline steadily.

Short core Z0204A

The main taxa present in this core (*Figure 5.8*) are *Assulina muscorum* and *Euglypha tuberculata* both of which increase in abundance up-core. *Assulina muscorum* increases more gradually than *Euglypha tuberculata* which increases most rapidly between 4 to 0 cm. *Cryptodifflugia cf. oviformis* is present throughout the core increasing upwards. This is interesting compared to M22 where it was only present in the surface sample. *Difflugia* C (called type C here, following Wilmshurst (2001, pers. comm.)) dominates at the base of the core with percentages of up to 40%, and a large *Difflugia pristis* dominates samples mid-core. *Hyalosphenia subflava* is present throughout this core, and typically, the *Euglypha* taxa increase up towards the surface, with *E. tuberculata* reaching 30% at 0 cm. The *Nebela* species also seem to increase overall upwards.

The test concentrations trend overall to increasing values down-core, after an initial drop in values between the surface and 4 cm. This short core also contains the sample with the greatest species diversity. The proportion of living tests remains constant, between 5-10% throughout the core, except for a peak at 16 cm where the percentage reaches almost 20%.

5.3.2 *Empodisma* and *Sporadanthus* dominated (wet)

Short core Z0206A

The main dominant taxa throughout this core (*Figure 5.9*) are *Assulina muscorum* and *Difflugia* C. *A. muscorum* declines up-core, from nearly 50% abundance at 28 cm. *Difflugia* C reaches a maximum of over 40% in the middle of the core. Large *Difflugia pulex* peaks mid-core too, at over 30% at 16 cm. Again, *Euglypha* species are most abundant in the upper samples. Large *Heleopera*-types are present throughout the core, more so above 12 cm, and *Pseudodifflugia fulva* peaks at 8 cm.

Overall, there is a slight decline in test concentrations down-core, with a peak in abundances at 8 cm. The living tests are present in low abundances (less than 10%) to 24 cm, declining down-core, with a maximum at 8 cm, coinciding with the peak of test concentrations.

Short core M21

Asssulina muscorum is present throughout the core (*Figure 5.10*), declining slightly mid-core, with concentrations reaching up to 30%. *Centropyxis cassis* is present in the upper part of the core, increasing at the same level as the *Euglypha* taxa. *Difflugia* C is most abundant mid-core. Other *Difflugia* taxa are more dominant at lower parts of the core, particularly the large *Difflugia pulex* that is at 25% at 16 cm. *Nebela militaris* is also more common in upper samples. *Pseudodifflugia fulva* is present at the base of the core.

Overall, test concentrations have a declining trend down-core, except a slight reversal at the lowest sample (20 cm). Somewhat unusual is the lack of living tests in the surface sample. The percentage of living tests increases and then decreases down-core, peaking at over 10% at 12 cm, which coincides with a minimum in the total test concentrations i.e. there are fewer tests, but more of them are living.

Testate amoebae counts Z0204A Kopouatai

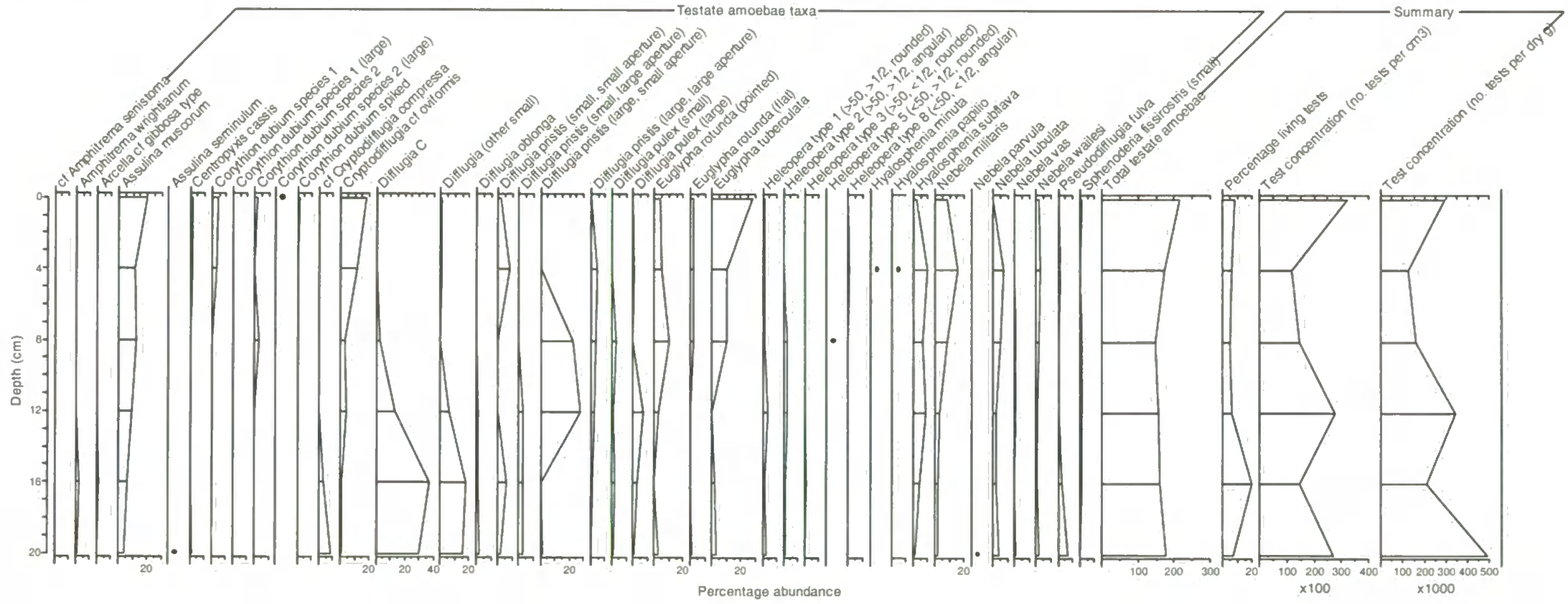

Figure 5.8 Short core testate amoebae counts from Z0204A, Gleichenia second dominant. • indicates values <1%.

Testate amoebae counts M21 Moanatuatua

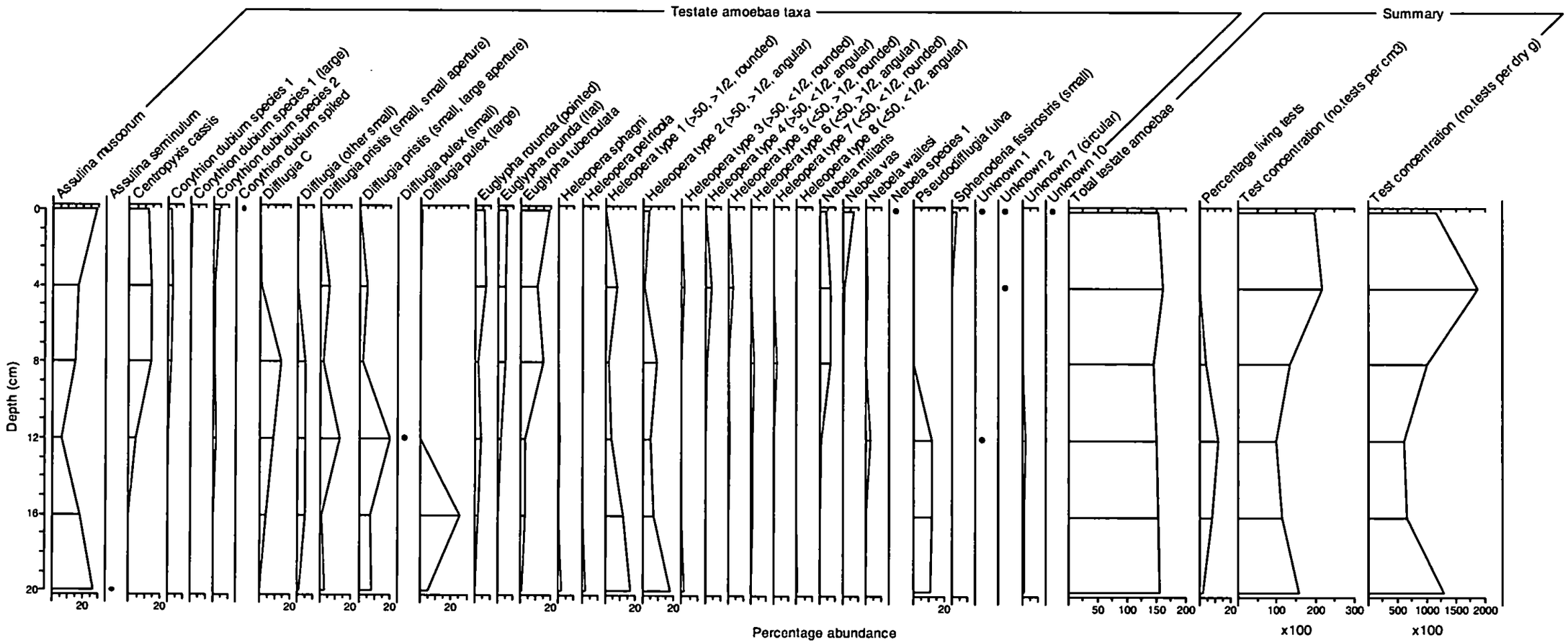

Figure 5.10 Short core testate amoebae counts from M21, Empodisma and Sporadanthus dominated. • indicates values <1%.

Testate amoebae counts Z0206A Moanatuatua

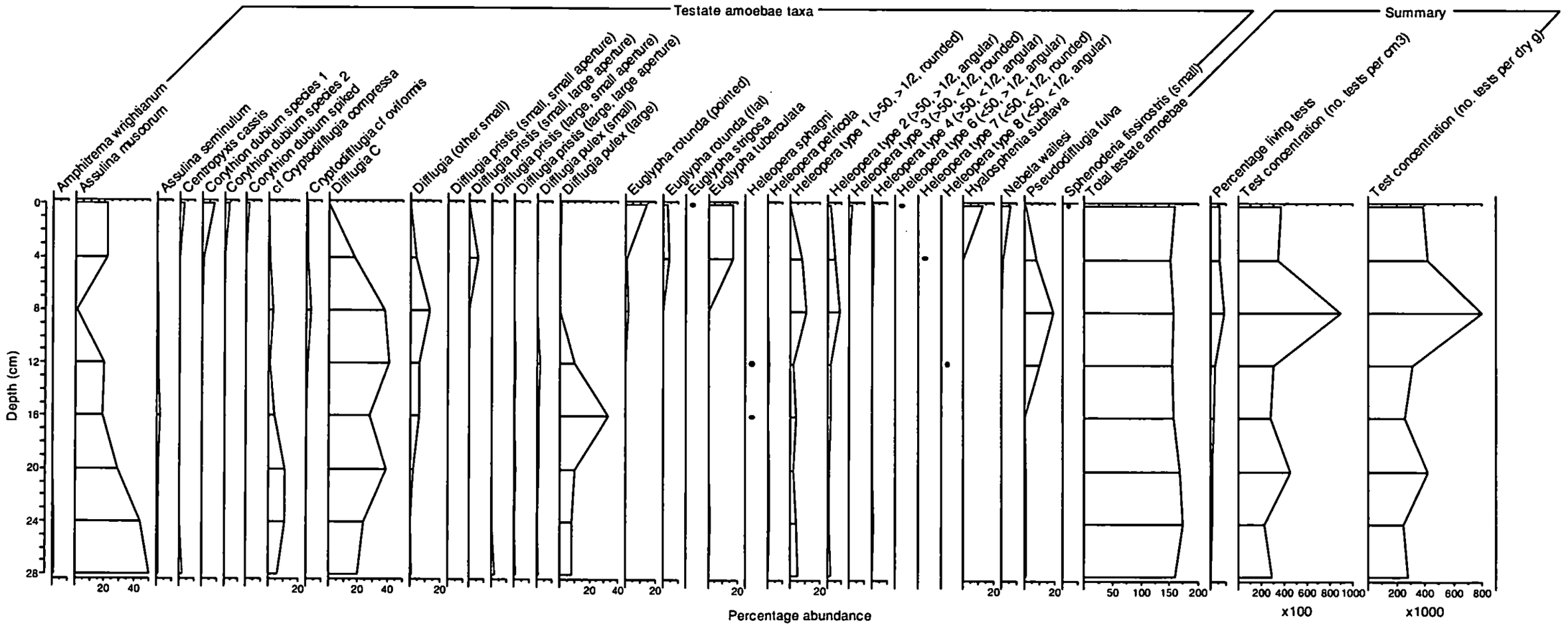

Figure 5.9 Short core testate amoebae counts from Z0206A, Empodisma and Sporadanthus dominated. • indicates values <1%.

Short core M5

The dominant taxon here (*Figure 5.11*) is *Hyalosphenia subflava* that is present throughout the core but dominates in the upper parts, particularly at 4 cm (at over 40%). *Assulina muscorum* is also common, and *Euglypha* taxa more so at the top of the core. *Centropyxis cassis* is present throughout, and *Corythion dubium* is found only in the upper samples. *Difflugia* taxa are only present in the lower parts of the core, dominated by *Difflugia* C at 12 cm. The rare *Trinema lineare*-type is found in this core with highest percentages in the mid-core. Unknown 7 (a circular test) was common at 15% at the base of the core.

Overall, test concentrations decline down-core, with a slight increase in the lower samples, following a peak at 4 cm. The percentage of living tests is more-or-less constant throughout, at low levels of between 5-10%. However there is a minimum at 4 cm.

Testate amoebae counts M5 Moanatuatua

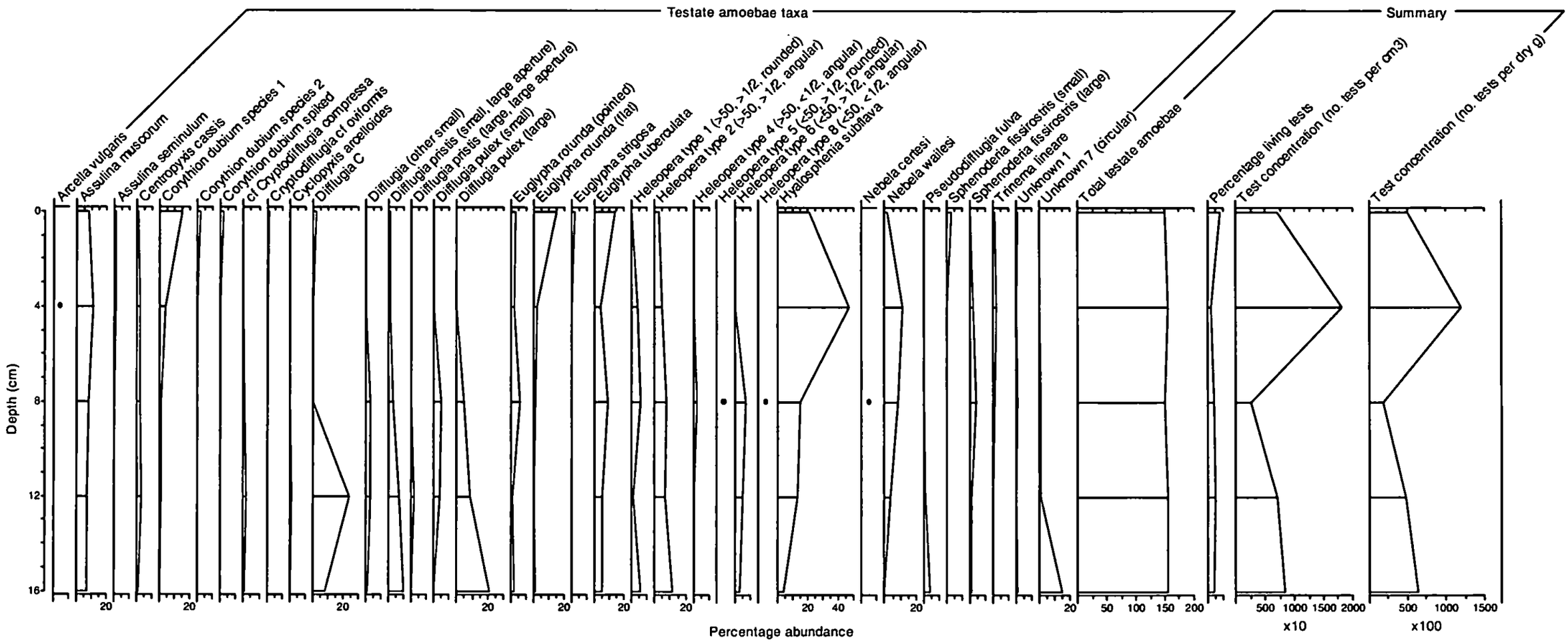

Figure 5.11 Short core testate amoebae counts from M5, Empodisma and Sporadanthus dominated. • indicates values <1%.

5.3.3 *Sphagnum* dominant (very wet)

Short core K2

The dominant taxa (*Figure 5.12*) are *Cryptodifflugia cf. oviformis* and *Difflugia* C, with the former dominating in the upper samples (to nearly 50% at the surface) and the latter dominating further down. *cf. Cryptodifflugia compressa* has a sharp decline from the 16 cm to 12 cm samples. Certain taxa are present throughout the short core, namely *Assulina muscorum* and *Difflugia oblonga*, and *Corythion* and *Euglypha* taxa. *Sphenoderia fissirostris* (large) increases from zero abundance further up near the surface. In terms of test diversity, there are taxa at this core site that are not found elsewhere, for example, Unknowns 8 and 9. Other taxa are more common here than elsewhere e.g. *Euglypha strigosa* and *cf. Cryptodifflugia compressa*. Interestingly, all these had spines attached to them, possibly due to the increased water content associated with *Sphagnum* vegetation cover. Spines are thought to assist the test in remaining in a fixed location in aquatic environments.

Test concentrations actually seem to decline up-core, the opposite trend than expected – both concentrations show the similar trend, but that of tests per dry gram is greater and shows less variation than that of tests per cm^3. Percentages of living tests are quite high throughout (between 20-25%) and unusually increase down-core, suggesting that this short core is well within the living zone of certain taxa.

Testate amoebae counts K2 Kopouatai

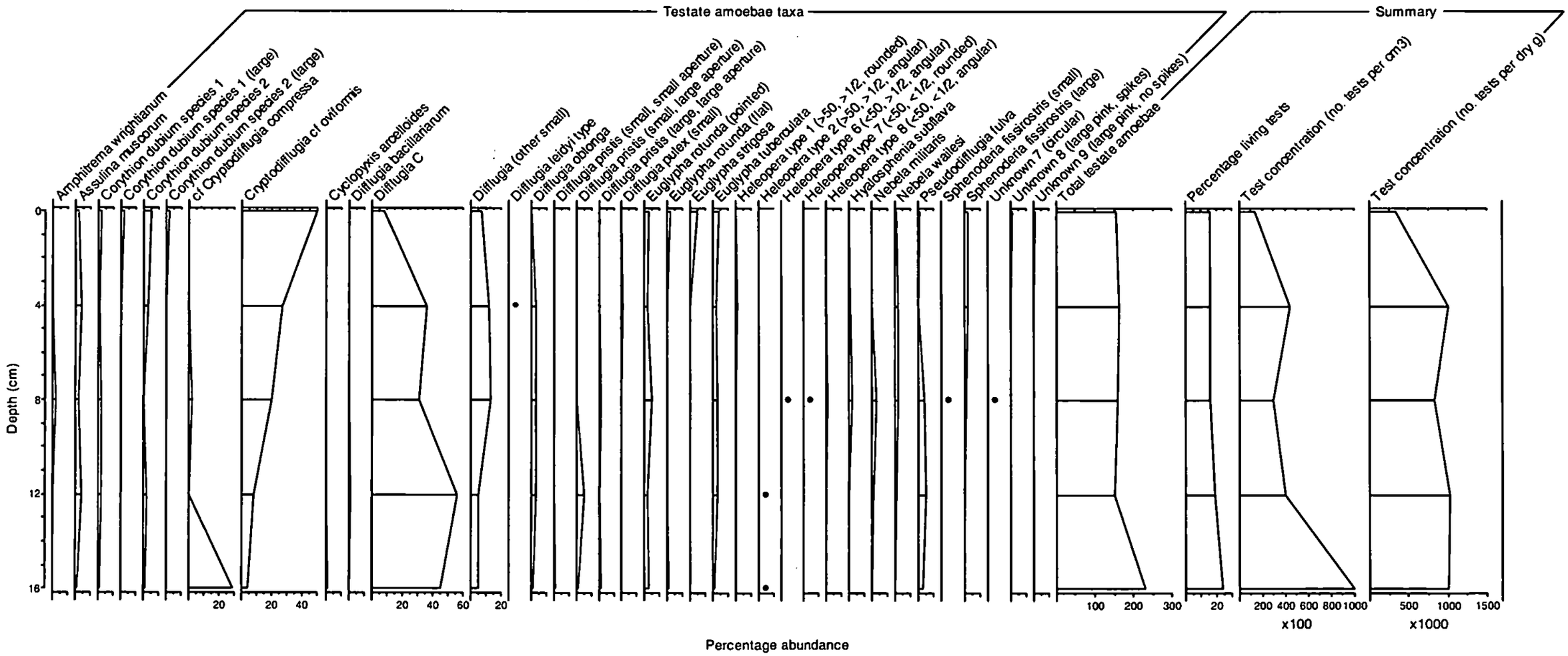

Figure 5.12 Short core testate amoebae counts from K2, Sphagnum dominant. • indicates values <1%.

5.3.4 Additional surface samples

For the following samples, that were processed initially, only concentration per cm^3 was derived, not concentration per dry g.

Short core Z0106 (*Sporadanthus* dominant, with *Sphagnum* nearby)

The main taxa (*Figure 5.13*) that dominate this assemblage are the small *Difflugia* C species and the second small, more rounded species (*Difflugia* (other, small)). The former is highly abundant from 10 cm downwards. *Nebela* taxa (particularly *N. militaris*) are quite common in the upper samples, as are *Euglypha* (mostly *E. tuberculata*) but both taxa decline down-core, within the top 5 to 10 cm. *Hyalosphenia subflava* is present mainly in the top 0-5 cm.

Test concentrations are quite low even in the surface samples, being only 1-2000 per cm^3. Percentages are constant throughout, with a slight maximum at 15 cm depth. Living tests are extremely low in abundance, and are only present to 10 cm depth.

Testate amoebae counts Z0106 Kopouatai

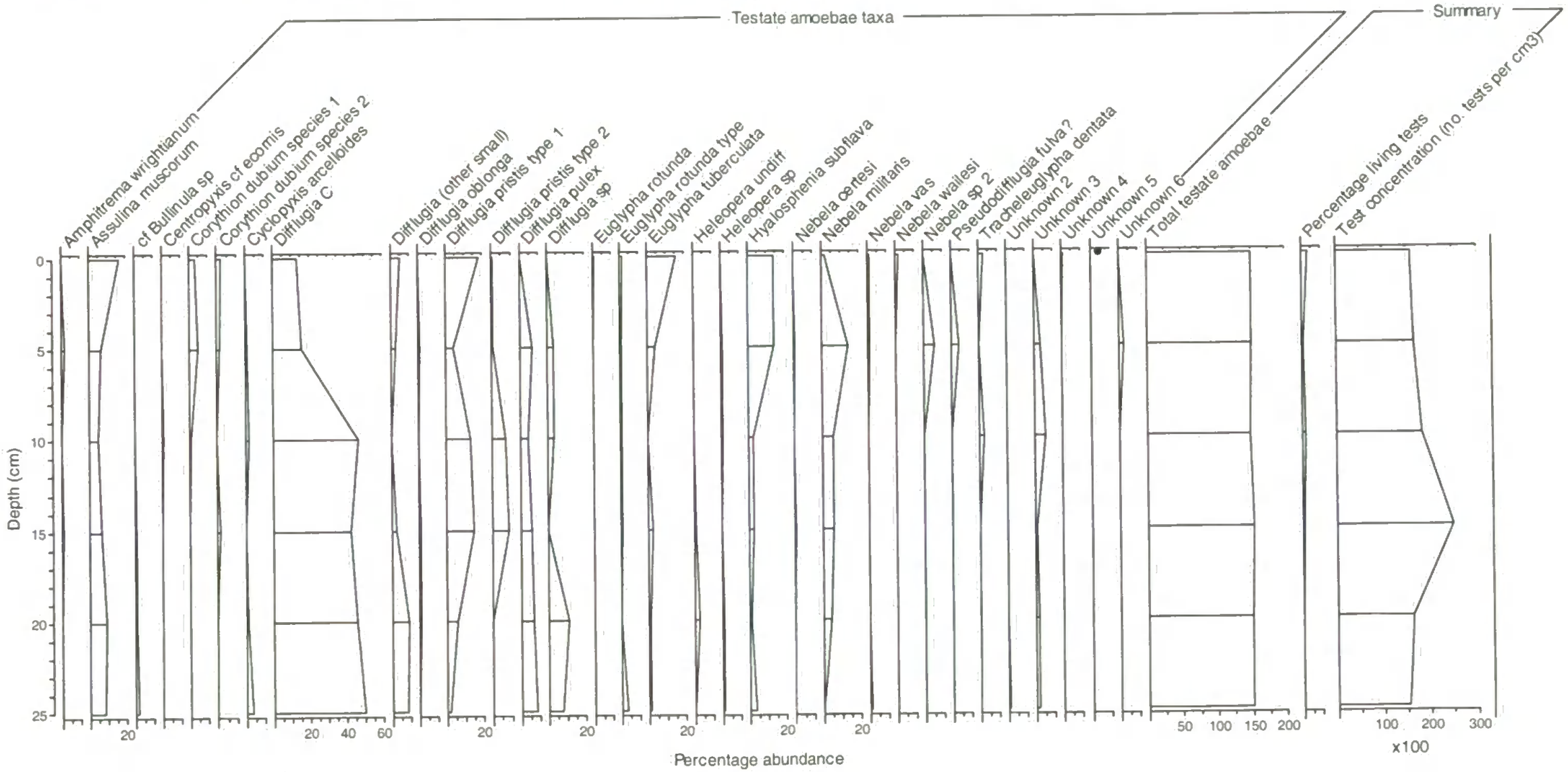

Figure 5.13 Short core testate amoebae counts from Z0106. • indicates values <1%.

Short core Z0108 (*Sporadanthus* and *Empodisma* dominant, *Gleichenia* and *Epacris* also present)

Difflugia C is by far the dominant taxon in this short core (*Figure 5.14*), increasing down-core where it contributes to almost 85% of the assemblage at 25 cm. *Nebela tubulata* and *Nebela militaris* are both present at higher occurrences in the upper core, as are the *Euglypha* and *Corythion dubium* taxa. Similar to its distribution in Z0106, *Hyalosphenia subflava* is present in the surface sample only.

Although counts are low throughout, test concentrations clearly increase down-core. Living tests are, again, very low in abundance at less than 5%, with the deepest occurrence at 15 cm.

Testate amoebae counts Z0108 Kopouatai

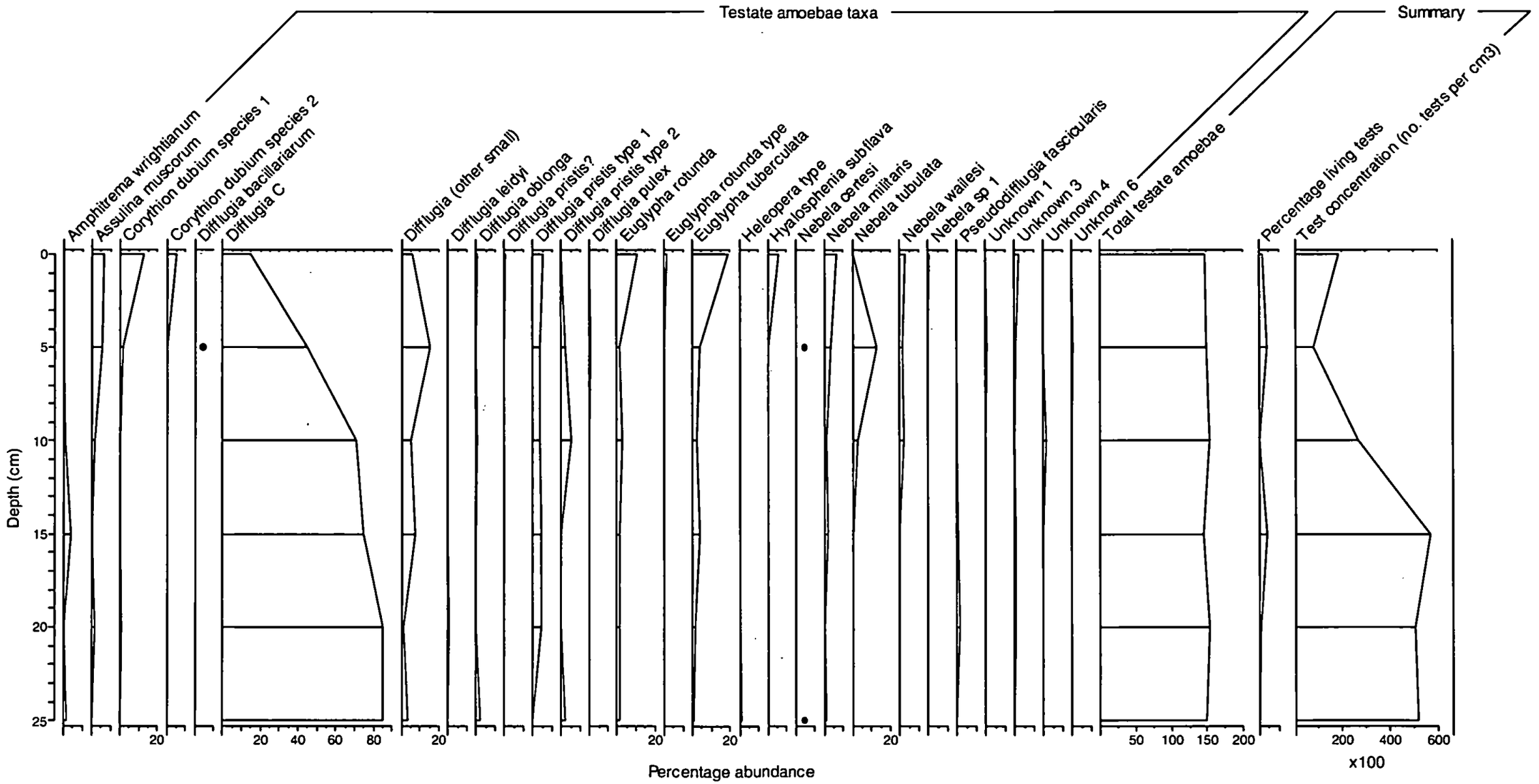

Figure 5.14 Short core testate amoebae counts from Z0108. • indicates values <1%.

Short core Z0103B (*Empodisma* and *Gleichenia* dominant, with some *Epacris* and *Sporadanthus*)

Hyalosphenia subflava is the dominant taxon in this short core (*Figure 5.15*). It is present up to almost 85% abundance at 5 cm and fluctuates throughout the core. The next dominant taxon is *Cyclopyxis arcelloides*, peaking at 10 cm with between 60-70%. The small *Difflugia pulex* is highly abundant below 20 cm, peaking at 60%.

Test concentrations are very low except for a large maximum of 40,000/cm^3 at 10 cm. Living tests are present at low percentages, only in the 10 cm sample and above.

Testate amoebae counts Z0103B Moanatuatua

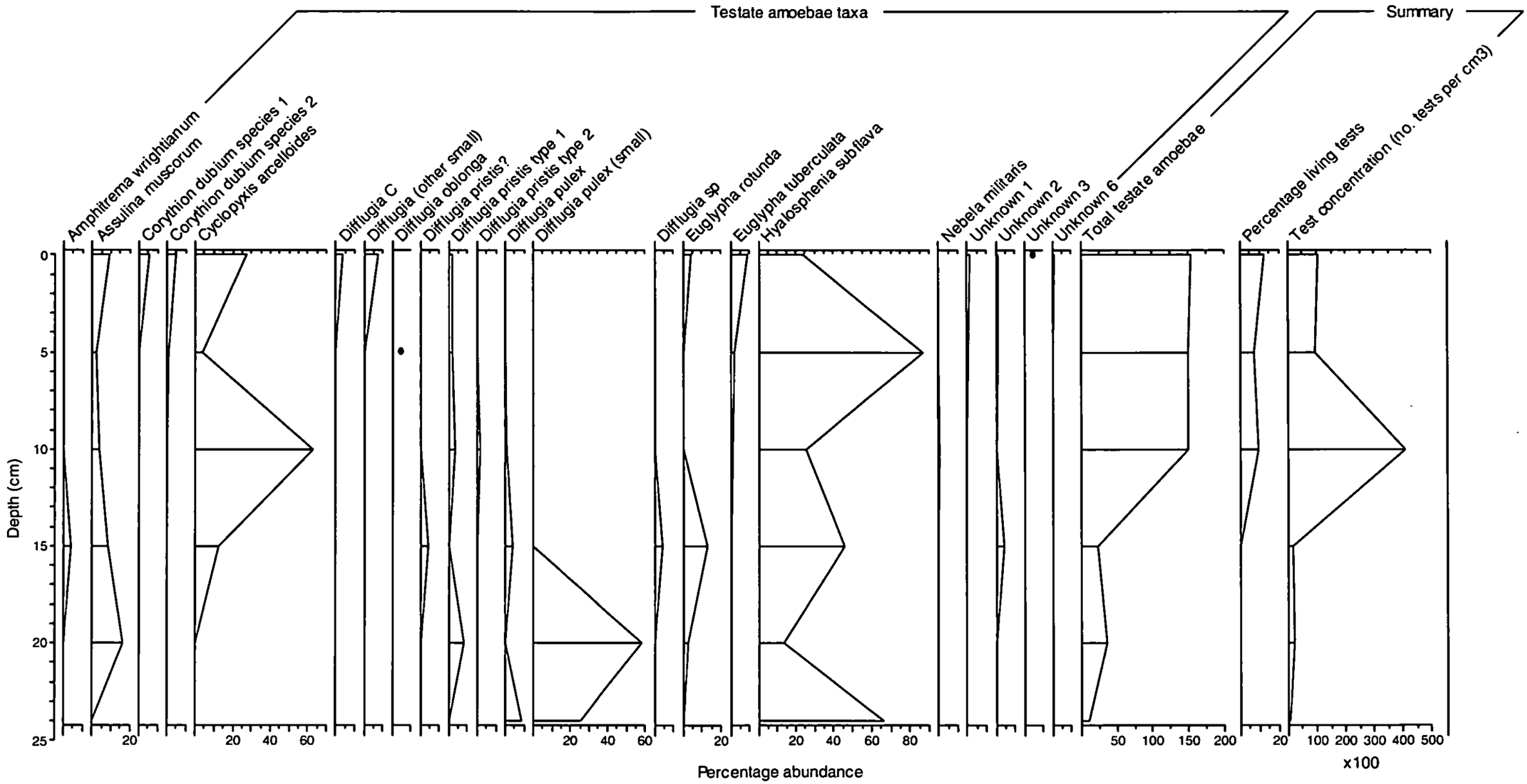

Figure 5.15 Short core testate amoebae counts from Z0103. • indicates values <1%.

Short core Z0104#2 (*Empodisma* and *Gleichenia* dominant, *Sporadanthus* nearby)

Difflugia pulex dominates in the lower half of this core (*Figure 5.16*), from 15 cm downwards, with abundances of up to approximately 40%. *Centropyxis cassis* is highly abundant at values reaching 30% in the surface 10 cm. *Assulina muscorum* is present throughout the core, increasing towards 60% at the base. *Euglypha* taxa are present, as usual, in the upper parts of the core, dominated by *Euglypha tuberculata*.

Test concentrations are generally high throughout the core, with a trough in values between 5 and 10 cm, and then falling off from 30 cm downwards. Living test percentages are very low throughout the core, at less than 5%.

Testate amoebae counts Z0104#2 Moanatuatua

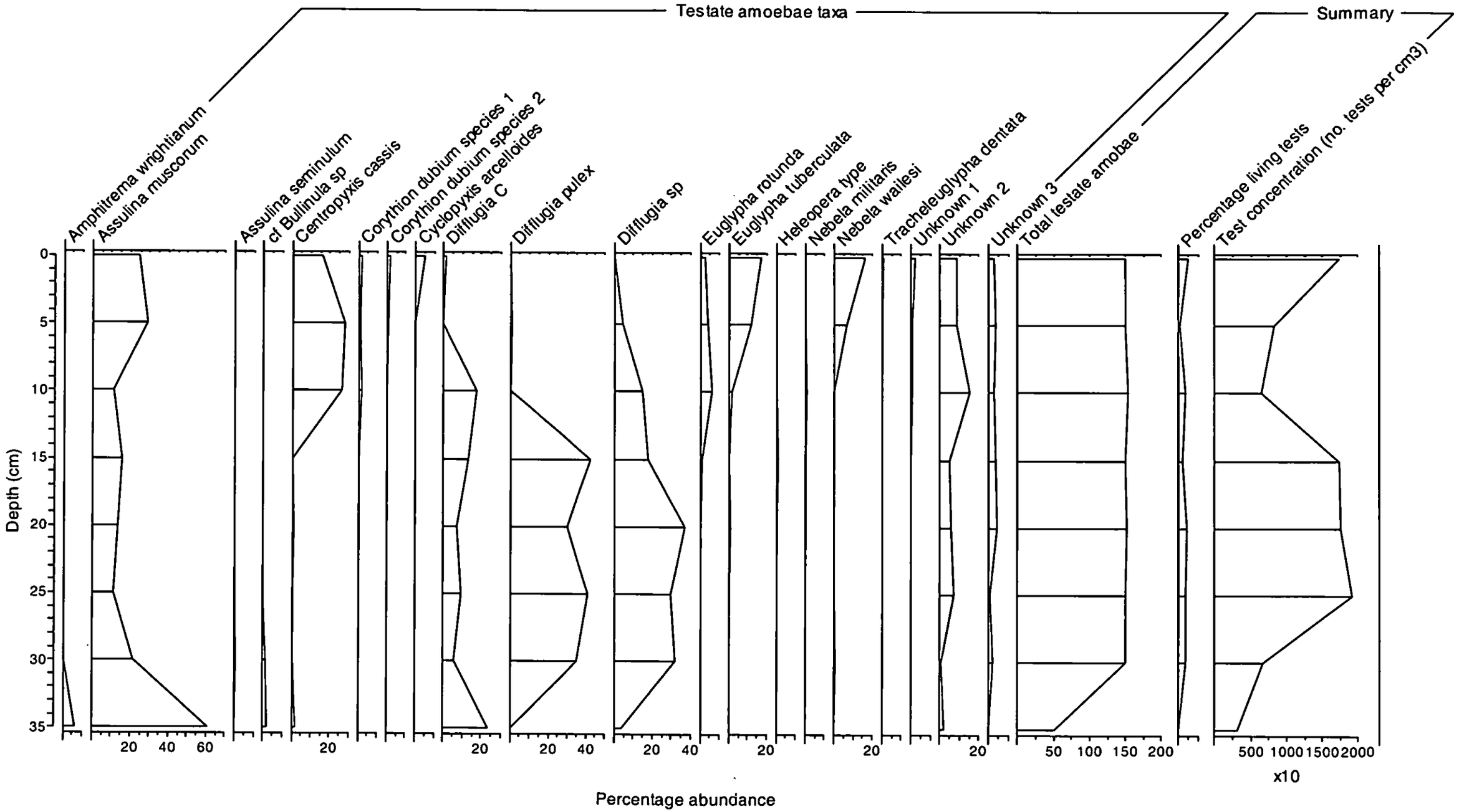

Figure 5.16 Short core testate amoebae counts from Z0104.

5.3.5 Site summaries and comparisons

Maximum test abundances vary greatly between surface samples, from between peaks of approximately 17,500 per cm^3 from M5 (Moanatuatua) to 100,000 per cm^3 from K2 (Kopouatai). There does not seem to be any consistent pattern between abundances and the downward decline in tests in these short cores. It has been shown (*Table 5.3*) that a time/depth factor appears to be strongly related to test concentration. The absence of a clear downward decline in test abundance in these short cores might possibly be due to the comparatively short interval encompassed by these 20-30 cm cores, which might be insufficient length for the downcore decay pattern to become established.

Samples from the short cores from Moanatuatua contain a larger abundance of the drier indicators *Assulina muscorum*, *Hyalsophenia subflava* and *Difflugia pulex* than at Kopouatai, probably due to the fact that, in general, Moanatuatua has a drier bog surface because of its lower water table. Kopouatai contains more taxa associated with wet conditions, for example, *Amphitrema wrightianum*. However, this taxon is also present at very low abundances in Z0204A where the presence of *Gleichenia*, together with a low water table would rather suggest relatively dry conditions. *Euglypha strigosa* is particularly abundant in the *Sphagnum*-dominated sample as well as those of *Empodisma-Sporadanthus*, even though Charman (1997) found its optimum abundance in dry conditions. *Difflugia oblonga* prefers wet conditions (Charman, 1997) and is seen to be most abundant at Kopouatai, in particular at K2 dominated by *Sphagnum*. The small *Difflugia* C taxon is present in much higher abundances (up to 50%) in Kopouatai, suggesting that it prefers wetter conditions. *Assulina muscorum*, found by Charman (1997) to be associated with relatively drier conditions, is present in all cores, even at high abundances in the wetter *Empodisma-Sporadanthus* sites, but at the *Sphagnum* dominant site it fits the predicted pattern, as it is much less abundant at this very wet site.

Often, the number of living tests stained pink by rose bengal was found to be very low (only one or two tests per species) in each sample. General observations identified that living tests of *Corythion dubium* spp. and *Sphenoderia fissirostris* tend to be present only in the upper samples nearest the surface (usually the top 10 cm). *Euglypha* spp. were dominant in the upper surface samples, usually down to 8 cm. *Difflugia pulex* tends to be associated with lower samples, most frequent below 12 cm. The remaining species did not appear to show any systematic patterns with depth, particularly when compared between cores.

In order to investigate the possible downcore trends in test concentrations, the results of each short core were normalised using:

$$\text{normalised value} = \text{concentration} - \frac{\text{mean concentration}}{\text{standard deviation}}$$

Patterns were investigated for both concentrations 'per cm^3' and 'per dry g', although only the results of the former are shown below (*Figure 5.17*) due to the fact that this concentration had been calculated for every short core, whereas the latter had not. Even so, results were very similar between cores.

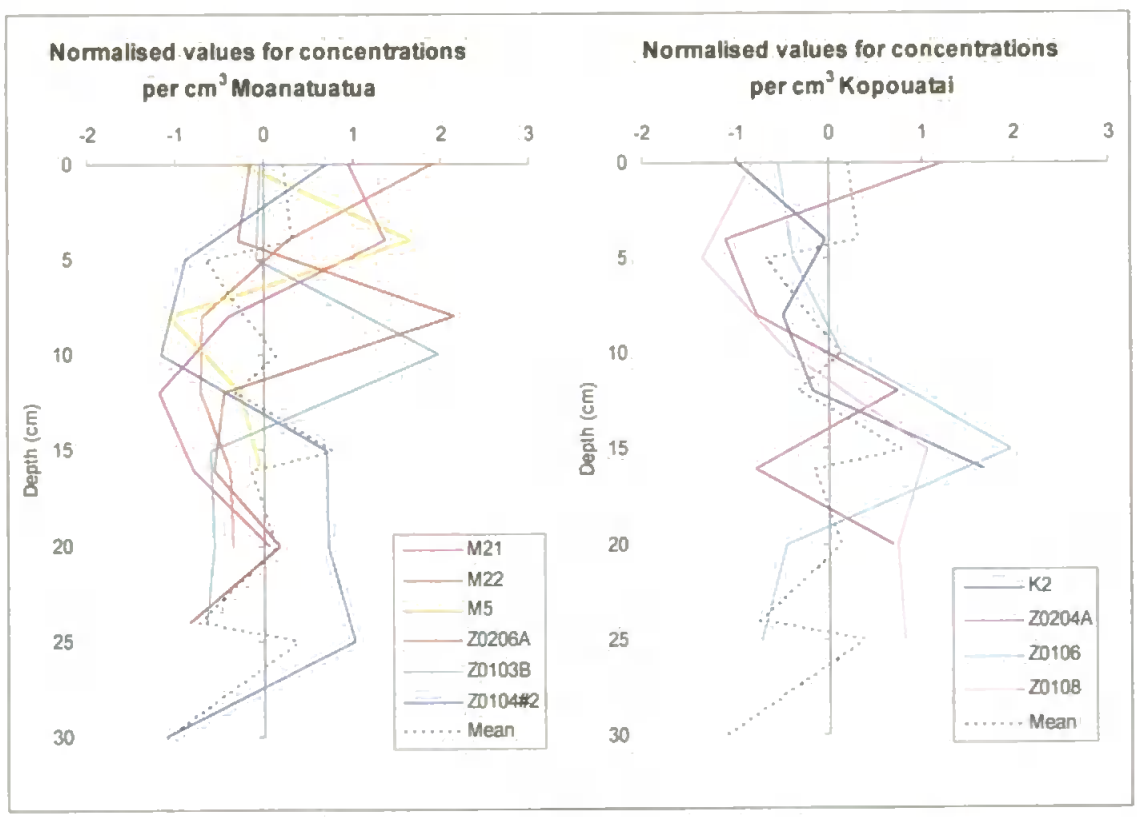

Figure 5.17 Normalised test concentrations (per cm^3) for Kopouatai and Moanatuatua. The mean was calculated from both sites combined.

From Moanatuatua, all the cores, excluding Z0206A and Z0103B, show a similar pattern particularly above 15 cm. The main features (downcore) are an initial decline from positive normalised values above average at the surface, to a trough in values below average between approximately 5 to 15 cm, followed by a subsequent rise. Cores Z0206A and Z0103B show a peak in values between 5 to 10 cm, opposing the trend shown by the other cores. At Kopouatai, normalised values shift from negative to positive between 10-12 cm, and then values drop, with Z0106 values falling below zero.

To investigate the relationships further, depth and normalised concentrations (the mean) were correlated (*Table 5.6*).

	Pearson		Spearman's rank	
	r	p value	r_s	p value
Concentration per cm^3	-0.334	0.076	-0.231	0.471
Concentration per dry g	-0.485	0.270	-0.571	0.180

Table 5.6 Correlation coefficients for normalised concentrations and depth.

For the abundances measured per cm^3, there appears to be only a weak negative correlation. However, the correlation coefficient for sample abundances per dry g are more strongly correlated with depth, although the r values are still not very high. This suggests that there is some degree of correlation between test abundance (normalised compared to the average value across the same depths of every core). A possible reason for this relatively low correlation is that the sampled depths have been shown to still be within the living zone of testate amoebae. The observation of living tests within the top 20 cm of peat is unusual compared to Northern Hemisphere work that has observed the living zone be limited to only the top 5 cm (Charman *et al.*, 2004). It is possible that the difference is due to the relatively less compacted structure of the surface restiad peat compared to that of *Sphagnum*, relating to light availability and/or the availability of mineral and peat matter for test formation (Heal, 1962). These results imply that deeper sampling at the surface is required to fully investigate their decline. However, when considering the p values, none of the correlation coefficients are significant at the 95% level, and only the Pearson value for the per cm^3 data is significant at the 90% level.

Low counts at the surface (i.e. 0-1 cm) of M5 and M21 could be explained by the fact that these samples comprised a large amount of accumulated leaf litter, particularly plant stems and leaves. This material that was much drier would be inhospitable to testate amoebae, thus reflected in low test counts.

It is also interesting to note that the slides from Moanatuatua took much longer to count due to a very high amount of fine organic detritus on the slides, and this could be due to the lower water table causing increased humification of the peat matrix.

5.3.6 Test abundances and down-core trends: a summary

This section addresses the initial questions posed regarding the abundance and concentrations of testate amoebae at the two sites.

Abundance of testate amoebae at surface and depth

It has been clearly shown that testate amoebae *are* present at both these sites, both at the surface and at depth. However, concentrations overall are low when compared to their Northern Hemisphere equivalent *Sphagnum* bogs. From the fact that testate amoebae are found in adequate abundances at the surface, it can be reasonably inferred that living tests have been present throughout the development of the bogs, particularly since there have been no significant changes in bog development over time, for example, in vegetation composition. Fossil tests *are* also found at depth, albeit in very low abundances.

Samples near the surface show typical test concentrations to be 10-20,000/cm^3, whereas fossil samples from depth reach a maximum of 8500/cm^3. The disparity between surface and fossil counts suggests that poor test preservation is an issue, together with high levels of fine, highly-decomposed organic matter 'diluting' the samples.

There also seems to be a difference in test counts between sites, with higher counts, together with higher assemblage diversity, at Kopouatai than at Moanatuatua. This is most likely due to the lower water table at Moanatuatua affecting test abundance and preservation.

Depth of test concentration decline

Within the short cores it can be seen that for some, such as M22, test abundances decrease down-core, but that for a few cores, for example Z0204A, counts actually increase. For the latter category, most of which are from Kopouatai, and for those where changes in abundance are minimal, deeper sampling is required to determine more clearly the depth of their decline.

5.4 Surface environmental variables and their relationships to testate amoebae

Exploratory analysis was carried out to investigate how the testate amoebae taxa related to the measured environmental variables: pH, conductivity, depth to water table and percentage moisture content. Only six samples had been counted, so because of this low number, this work is only preliminary. Canonical correspondence analysis (CCA), a direct

ordination method that uses both the species and environmental data to derive a relationship (ter Braak, 1986), was performed on the testate amoebae assemblages and the measured variables from the surface samples (0-1 cm) from K2, M5, M21, M22, Z0204A and Z0206A (with no down-weighting of rare species). The ordination programme used was CANOCO for Windows version 4.51 devised by ter Braak and Smilauer (1997-2003), and that for plotting was Canodraw for Windows version 4.1 (Smilauer, 1999-2003).

	Axis 1	Axis 2
pH	0.1038	**-0.4603**
Conductivity	0.2967	-0.0043
Depth to water table	0.3629	0.1574
Percentage moisture content	**-0.8413**	-0.2055
Eigenvalue	0.513	0.191

Table 5.7 Correlation coefficients for CCA between the first two axes of taxa variation and the four measured variables.

These results (*Table 5.7*) show that Axis 1 explains most of the species variation, and it is interpreted that this axis primarily reflects percentage moisture content. Axis 2 explains the next largest proportion of variation, and this is associated with pH. Together, the first two axes explain the majority of the variation. Although based on a small sample size, these results agree with previous work that has identified moisture content and pH as strong factors influencing testate amoebae distributions e.g. Charman and Warner (1997), Charman (1997).

The relationship between individual taxa and these inferred environmental variables is illustrated in *Figure 5.18*. Depth to water table and moisture content are, as expected, opposing, since their arrows point in opposite directions i.e. samples with greater depth to (i.e. a lower) water table will have a lower moisture content. Arrows aligned at 90° to each other indicate that the variables that they represent are uncorrelated e.g. pH and moisture content. Here, moisture and then pH are the most important variables. Generic groups tend to be plotted in similar regions of the plot e.g. *Nebela* taxa in the bottom right region, and *Difflugia* in the top left quarter. Under the original aims of this thesis, these testate-environmental relationships would have provided a basis for reconstructing past conditions at the two study sites.

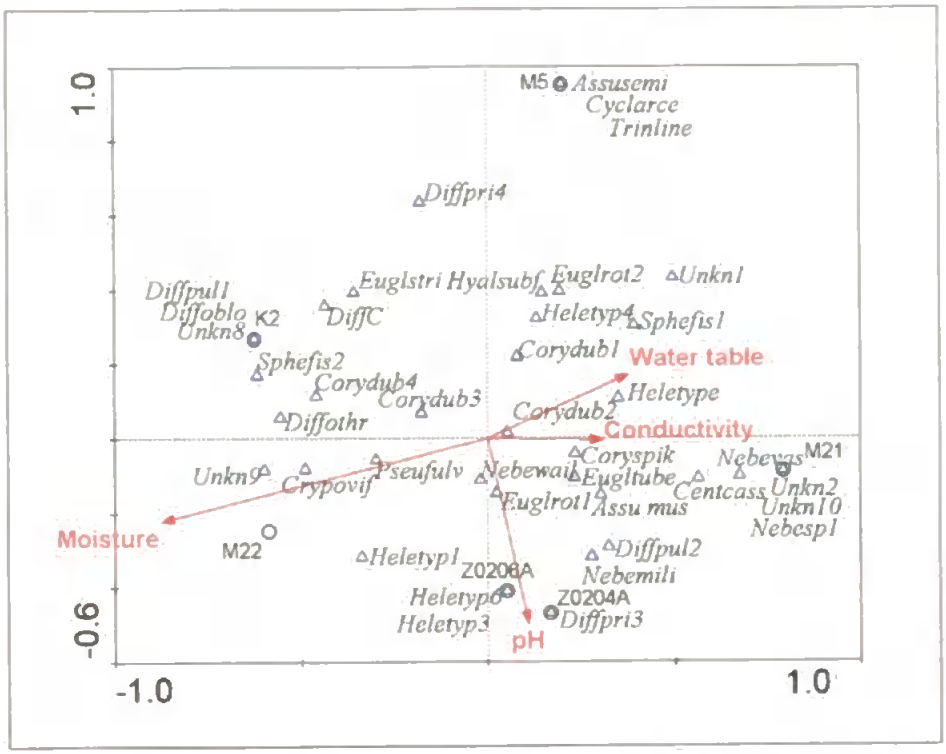

Figure 5.18 A CCA environment-species-site triplot for the 6 sites M5, M21, M22, K2, Z0204A and Z0206A. Testate amoebae taxa are shown as Δ and the sites as ○. The length of the arrows is proportional to the amount of species variation that they explain and a taxon's perpendicular position along an environmental arrow demonstrates the preferred conditions of that variable. See Table 5.8 for full taxa names.

Code	Full taxa name	Code	Full taxa name	Code	Full taxa name
Assu mus	*Assulina muscorum*	Diffpri4	*Difflugia pristis* 4	Nebemili	*Nebela militaris*
Assusemi	*Assulina seminulum*	Diffpul1	*Difflugia pulex* 1	Nebesp1	*Nebela* species 1
Centcass	*Centropyxis cassis*	Diffpul2	*Difflugia pulex* 2	Nebevas	*Nebela vas*
Corydub1	*Corythion dubium* 1	Euglrot1	*Euglypha rotunda* 1	Nebewail	*Nebela wailesi*
Corydub2	*Corythion dubium* 2	Euglrot2	*Euglypha rotunda* 2	Pseufulv	*Pseudofifflugia fulva*
Corydub3	*Corythion dubium* 3	Euglstri	*Euglypha strigosa*	Sphefis1	*Sphenoderia fissirostris* 1
Corydub4	*Corythion dubium* 4	Eugltube	*Euglypha tuberculata*	Sphefis2	*Sphenoderia fissirostris* 2
Coryspik	*Corythion* spiky	Heletype	*Heleopera* type	Trinline	*Trinema lineare*
Crypovif	*Cryptodifflugia oviformis*	Heletyp1	*Heleopera* type 1	Unkn1	Unknown 1
Cyclarce	*Cyclopyxis arcelloides*	Heletyp3	*Heleopera* type 3	Unkn2	Unknown 2
DiffC	*Difflugia* C	Heletyp4	*Heleopera* type 4	Unkn8	Unknown 8
Diffoblo	*Difflugia oblonga*	Heletyp6	*Heleopera* type 6	Unkn9	Unknown 9
Diffothr	Other small *Difflugia*	Hyalsubf	*Hyalosphenia subflava*	Unkn10	Unknown 10
Diffpri3	*Difflugia pristis* 3				

Table 5.8 Explanation of taxa abbreviations for Figure 5.18.

5.5 Summary

This chapter has demonstrated the paucity of testate amoebae at the two study sites, and investigated the possible reasons for this. Fossil test abundances are likely to have been affected by a combination of a) decay processes, b) original peat conditions (wet/dry) and c) original abundances. Analysis of test abundances downcore shows the strongest negative correlation to be with the depth of the more humified peat samples, statistically significant at 95%. Down-core counts from surface short-cores showed some decline in concentration, but this was by no means consistent between cores. This is probably due to insufficient depth of sampling, as this was still often in the zone of living testate amoebae. The lack of tests at depth compared to their surficial abundance seems to suggest that their preservation is being detrimentally affected by unsuitable environmental conditions, and that this is a very gradual process over depths greater than those covered by the short cores. Wilmshurst *et al.* (2003) also experienced difficulties involved with the use of testate amoebae in a New Zealand palaeo study. They could not produce credible palaeomoisture reconstructions due to the taxa disparities between surface and fossil test assemblages.

Due to the inappropriateness of the application of this method at these sites, focus of the project will shift to the remaining palaeoecological techniques, particularly that of peat humification. The results of the remaining palaeomoisture proxies (peat humification, plant macrofossils and charcoal) are presented in the following two chapters, where Kopouatai (Chapter 6) and Moanatuatua (Chapter 7) are considered separately.

CHAPTER SIX – RESULTS: KOPOUATAI

6.1 Introduction

The previous chapter presented the testate amoebae results and concluded that they will not be useful as a palaeomoisture indicator at these sites. With peat humification now the main focus of this project, the remaining analytical results are presented here for cores Z0106, Z0108 and Z0204 from Kopouatai. Core stratigraphies are presented in Appendix 2.

6.2 Core Chronologies

Core chronologies were derived using a combination of tephra and radiocarbon ages.

6.2.1 Tephras

The main tephra layers used in this study are the Taupo and Tuhua tephras, retrieved from all cores from Kopouatai. They were identified on the basis of their appearance and relative stratigraphical position, but also from their chemical constituents determined by microprobe analysis (University of Waikato) (all tephra confirmations are from Lowe, 2004, pers. comm.). Other additional identifiable tephras were found, and are described below. 'Cryptic' tephra layers i.e. those not visible to the naked eye, were also found later by Ballinger (2003). However, the identifications of these have not yet been confirmed.

Kaharoa (655±15 ^{14}C years BP (Lowe *et al.*, 1999); 550-650 cal. years BP; AD 1314±12 (Hogg *et al.*, 2003))

This creamy-white coloured, pumiceous tephra (*Plate 6.1*) was retrieved coherently only in core Z0204 due to the very wet and fibrous nature of the upper sediments (grains were often washed down through sections of core). It is outside the age range of this project, as it is too young, but is mentioned for general interest nonetheless.

Plate 6.1 Kaharoa Tephra from core Z0201 (the top of the core is to the left of the picture).

Taupo (1,850±10 ^{14}C years BP (Lowe *et al.*, 1999); 1,650-1,800 cal. years BP)

At Kopouatai Bog, the Taupo Tephra is an orangey-brown, pumiceous tephra, with pumice fragment sizes commonly reaching 1-3 mm in diameter (*Plate 6.2*). This deposit was typically 2-3 cm thick, and its depth from the surface varied over a range of 1 m between cores (between depths of approximately 0.5 m and 1.5 m).

Plate 6.2 Taupo Tephra from core Z0204 (the top of the core is to the left of the picture).

Digital images were taken of tephra shards from this layer (*Plate 6.3*)

Taupo Tephra 3.71-3.72 m

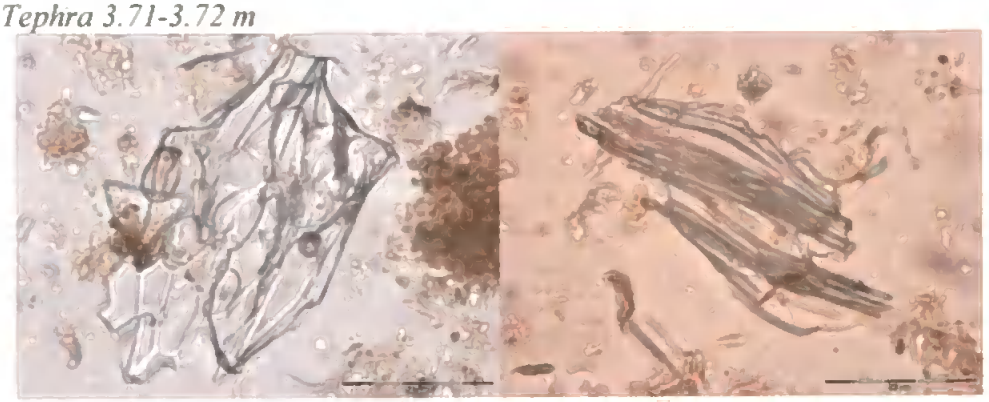

Plate 6.3 Tephra shards from the Taupo Tephra layer from core Z0204. Scale bar = 50 µm.

Egmont-derived

This white, fine tephra deposit was only visible in core Z0204, just below the lowest clay facies. It is thought to originate from an Egmont eruption due to the proportions of K_2O (relatively high) and SiO_2 (relatively low) (Lowe, 1988a). As this tephra layer has not been identified and was not observed in other cores from this site, it was not useful for core chronology or correlation.

Tuhua (6,130±30 ^{14}C years BP (Lowe *et al.*, 1999); 6,800-7,150 cal. years BP)

At Kopouatai, the grey Tuhua Tephra (*Plate 6.4*) was a very thick layer (10-15 cm) comprised of two layers of differently sized eruptive separated by a sharp boundary. This feature is thought to result from the nature of the eruption; a two-phase eruption emitting smaller particles first, followed by larger eruptives.

Plate 6.4 Tuhua tephra from core Z0204 (the top of the core is to the left of the picture). Note the coarser layer overlying the finer layer.

Digital images were taken of tephra shards from this layer (*Plate 6.5*)

Tuhua Tephra (coarse layer) 8.76-8.77 m.

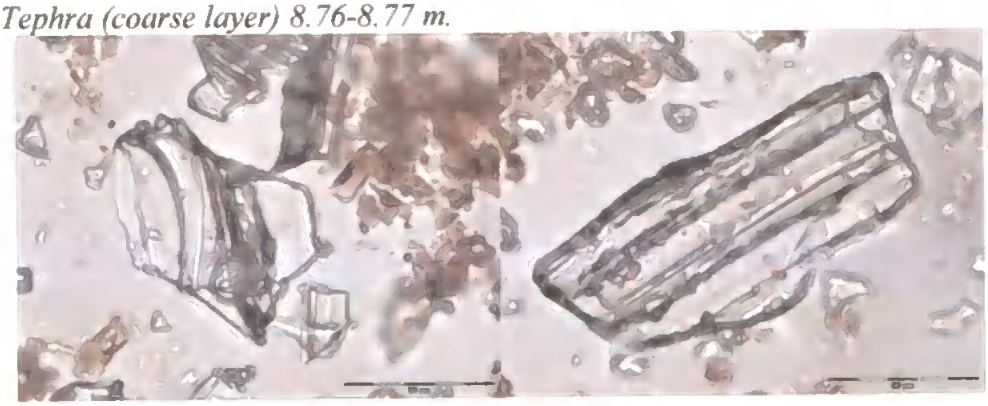

Tuhua Tephra (fine layer) 8.81-8.82 m.

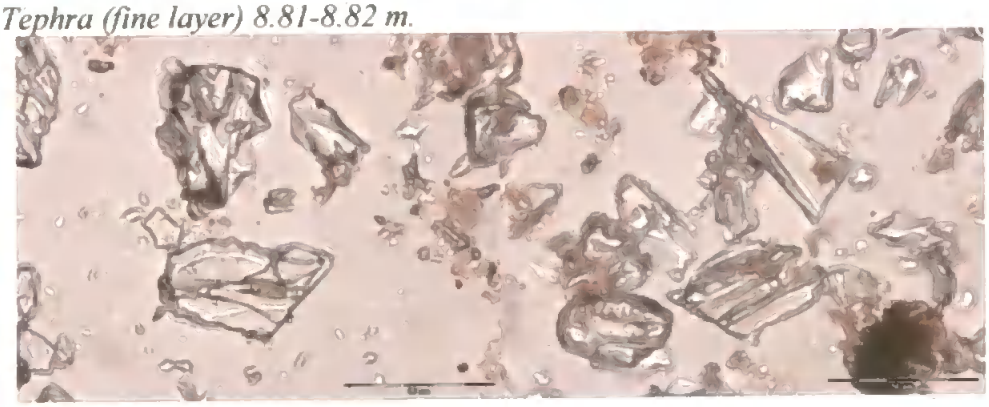

Plate 6.5 Tephra shards from the Tuhua Tephra layer from core Z0204. Scale bar = 50 µm.

Mamaku (7,250±20 ^{14}C years BP (Lowe *et al.*, 1999); 7,950-8,100 cal. years BP)

This (white) tephra layer was only found in cores Z0106 and Z0108 and is beyond the time-frame of this project. Microprobe analysis suggests that this tephra could possibly also be the Rotoma Tephra. The chemical constituents are the same in the tephras from both cores, suggesting that they can be joined by tie-lines as they represent the same event. Because the Rotoma has been identified as a possibility in Z0108 where it underlies this white layer (see below), it is most likely that this tephra is the Mamaku Tephra.

Rotoma (8,530±10 ^{14}C years BP (Lowe *et al.*, 1999); 9,450-9,550 cal. years BP)

This tephra layer found in core Z0108 is thought to possibly be the Rotoma Tephra, on the basis of its geochemistry and its relationship to other tephras and the ^{14}C ages in the core (see previous paragraph).

Waiohau (11,850±60 ^{14}C years BP (Lowe *et al.*, 1999); 13,450-15,150 cal. years BP)

This tephra was found only in core Z0108, as a fine sand-like brown deposit. It is provisionally identified as the Waiohau Tephra on the basis of age relationships, geochemistry and its known distribution limits, but lies well beyond the time frame of this project.

A summary of the tephra geochemistry for Kopouatai is presented (*Table 6.1*).

	Z0106 2.81-2.82 m	Z0106 7.85-7.86 m	Z0106 8.09-8.10 m	Z0108 3.36-3.37 m	Z0108 7.37-7.38 m	Z0108 7.78-7.79 m
Constituents	Percentage content (normalised)					
SiO_2	i/g	78.64	78.31	75.86	74.60	78.06
Al_2O_3	-	12.13	12.28	13.21	9.58	12.35
TiO_2	-	0.10	0.13	0.23	0.26	0.12
FeO	-	0.73	0.81	1.82	5.44	0.88
MnO	-	0.08	0.07	0.10	0.15	0.06
MgO	-	0.10	0.11	0.24	0.02	0.11
CaO	-	0.71	0.71	1.42	0.24	0.72
Na_2O	-	3.66	3.78	4.07	5.26	3.93
K_2O	-	3.64	3.63	2.88	4.20	3.61
Cl	-	0.19	0.17	0.16	0.25	0.15
n	-	1	13	13	10	12
Tephra ID	**Taupo**	**Tuhua**	**Mamaku** (or Rotoma)	**Taupo**	**Tuhua**	**Mamaku** (or Rotoma)

	Z0108 7.94-7.95 m	Z0108 8.18-8.19 m	Z0108 8.74-8.75 m	Z0204 3.70-3.71 m	Z0204 8.42-8.43 m	Z0204 8.75-8.76 m
Constituents	Percentage content (normalised)					
SiO_2	77.95	i/g	77.91	75.88	70.15	73.51
Al_2O_3	12.41	-	12.62	13.40	15.66	9.92
TiO_2	0.10	-	0.14	0.25	0.47	0.27
FeO	0.74	-	0.84	1.75	1.77	5.57
MnO	0.08	-	0.11	0.08	0.11	0.19
MgO	0.07	-	0.12	0.26	0.39	0.03
CaO	0.52	-	0.77	1.42	1.28	0.28
Na_2O	4.03	-	3.97	3.99	4.61	5.64
K_2O	3.93	-	3.38	2.82	5.32	4.36
Cl	0.17	-	0.15	0.17	0.25	0.23
n	2	-	13	13	7	16
Tephra ID	**Rotoma** (possible)	-	**Waiohau** (possible)	**Taupo**	**Egmont-derived**	**Tuhua**

Table 6.1 The main geochemical indicators of the Kopouatai tephras, as identified from microprobe analysis by D. Lowe. i/g indicates insufficient glass counts for microprobing. Identifications made even with insufficient glass were based on a combination of stratigraphical position and physical characteristics.

6.2.2 Radiocarbon ages

All ages were calibrated (*Table 6.2*) using the Southern Hemisphere dataset of CALIB v.4.4.2 (Stuiver and Reimer, 1993) as recommended by McCormac *et al.* (2002). The well-established tephra ages as given in section 2.4.2 were also calibrated. All calibrated ages are quoted in the text to the nearest 50 years.

Sample number	Laboratory code	Depth (m) (corrected)	Type	Conventional age	Calibrated age (2 sigma)	Mid-point age	$\delta^{13}C$
Core Z0106							
17	AA-54136	3.406-3.424	AMS	2,347±38	2,154-2,426	2,290	-26.4
18	AA-54137	3.895-3.905	AMS	2,962±38	2,947-3,209	3,078	-29.1
19	AA-54138	4.444-4.456	AMS	3,618±39	3,721-3,981	3,851	-29.8
20	AA-54139	4.982-4.993	AMS	4,116±41	4,422-4,809	4,616	-29.9
21	SUERC-1481	5.556-5.567	AMS	4,433±37	4,851-5,255	5,053	-30.2
22	SUERC-1482	6.090-6.100	AMS	4,925±34	5,492-5,708	5,600	-30.1
23	SUERC-1483	6.633-6.656*	AMS	5,039±39	5,613-5,889	5,751	-30.0
24	SUERC-1517	7.361-7.371	AMS	6,017±34	6,682-6,890	6,786	-30.9
Core Z0108							
25	AA-54140	3.791-3.802	AMS	2,404±40	2,211-2,707	2,459	-29.8
26	AA-54141	4.252-4.262	AMS	2,832±37	2,780-2,969	2,875	-29.7
27	AA-54142	4.635-4.650	AMS	3,352±38	3,450-3,675	3,563	-30.2
28	AA-54143	5.121-5.132	AMS	4,145±40	4,446-4,819	4,633	n/a
29	AA-54144	5.586-5.597	AMS	4,514±41	4,890-5,299	5,095	-28.5
30	SUERC-1484	6.021-6.041*	AMS	4,999±37	5,600-5,855	5,728	-29.0
31	SUERC-1485	6.476-6.497*	AMS	5,707±33	6,314-5,646	6,430	-28.9
32	SUERC-1486	6.879-6.900*	AMS	6,101±30	6,760-6,999	6,880	-27.3
Core Z0204							
41	SUERC-1496	4.17-4.18	AMS	2,165±28	1,999-2,296	2,148	-28.6
42	SUERC-1497	4.62-4.63	AMS	2,543±28	2,363-2,739	2,551	-28.8
43	SUERC-1501	5.06-5.07	AMS	3,056±28	3,079-3,333	3,206	-30.7
44	SUERC-1502	5.51-5.52	AMS	3,484±29	3,593-3,827	3,710	-29.3
45	SUERC-1503	5.95-5.96	AMS	3,992±32	4,261-4,518	4,390	-30.7
46	SUERC-1504	6.40-6.41	AMS	4,344±34	4,827-4,967	4,897	-30.2
47	SUERC-1505	6.84-6.85	AMS	5,084±33	5,662-5,905	5,784	n/a
48	SUERC-1507	7.29-7.31*	AMS	5,429±31	6,000-6,282	6,141	n/a
ZOE-6	Wk-11111	7.76-7.78	Bulk	5,983±185	6,354-7,245	6,800	-
ZOE-5	Wk-11110	8.26-8.28	Bulk	6,526±174	6,953-7,676	7,315	-
ZOE-4	Wk-11109	8.44-8.46	Bulk	6,571±151	7,031-7,678	7,355	-
ZOE-3	Wk-11108	9.28-9.30	Bulk	7,624±165	7,981-8,929	8,455	-

*Table 6.2 AMS and bulk radiocarbon ages from Kopouatai (conventional and calibrated). * indicates those samples where macrofossils were picked from intervals greater than 1 cm due to scarcity of suitable material in the 1 cm interval. AA- and SUERC- samples were processed as two separate batches at the NERC Radiocarbon Laboratory (East Kilbride) and Wk- samples at the University of Waikato (New Zealand). n/a indicates no result due to insufficient sample.*

From these results, a composite diagram was constructed showing the calibrated radiocarbon ages (cal. years BP) together with their stratigraphic positions, and linking the three core chronologies (*Figure 6.1*).

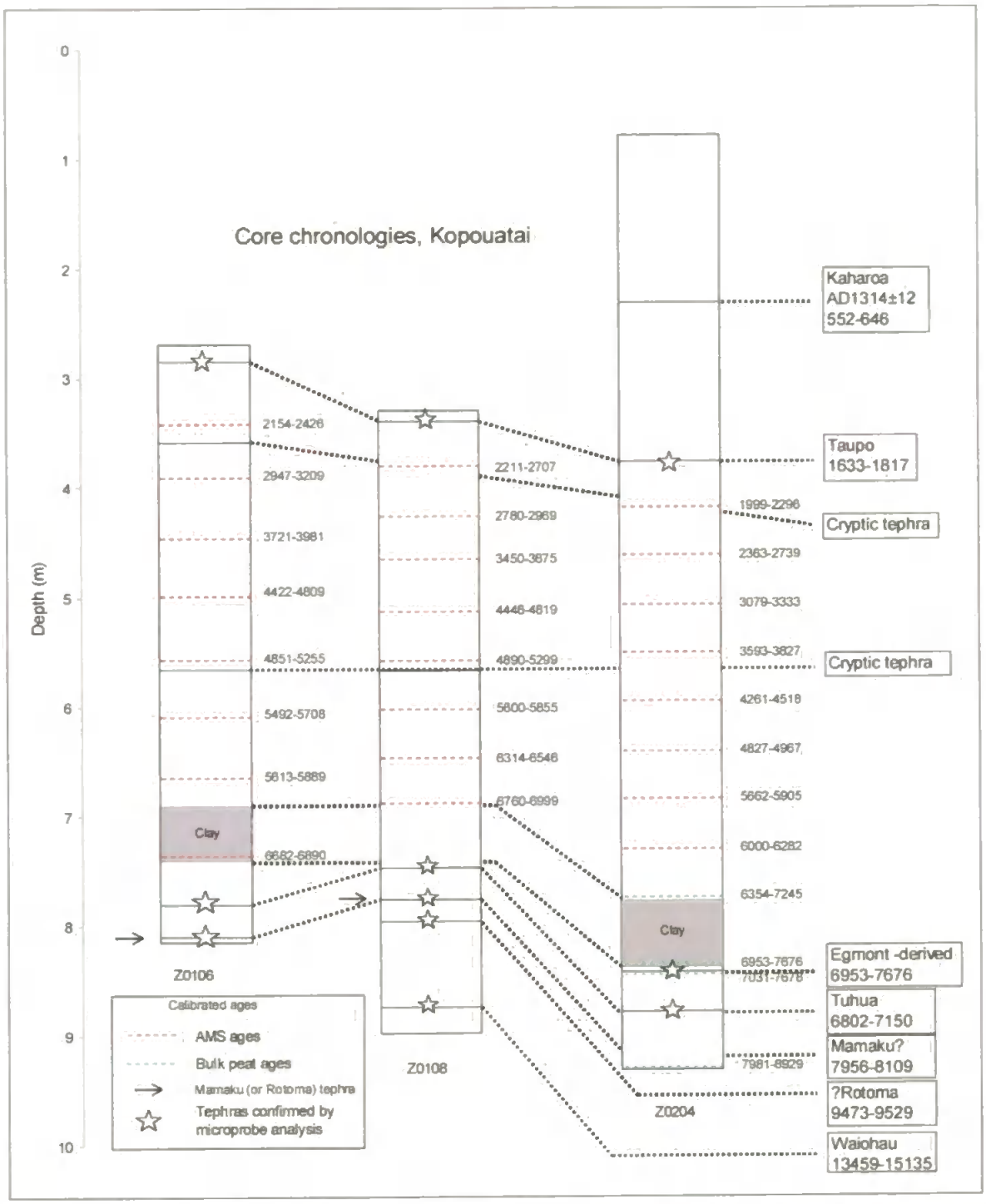

Figure 6.1 Core chronologies from Kopouatai, showing the tephra and calibrated radiocarbon ages. The tie-lines drawn between cores join levels of the same age, mainly tephra layers. Tephras are drawn at the depth of their peak in mineral content.

6.2.3 Age-depth models

From the suites of calibrated ages, a selection of age-depth models were produced using the mid-point value of the calibrated age range (as Hughes *et al.* (2000) and Chambers and Blackford (2001) employed) plotted against the mid-point depth value. Other work suggests alternative methods to derive a summary age value, for example, using the median value (Telford *et al.*, 2004b), but it is thought that this would produce negligible difference in the final age model. Several models were produced since no single age-depth model exists for any profile (Telford *et al.*, 2004a) and these were subsequently compared. However, for the tephra layers, which represent instantaneous events, the lower peat-tephra boundary of the Taupo Tephra was used as the depth for its 1,850±10 ^{14}C years BP age (i.e. the start of the eruption), and the upper boundary of the Tuhua Tephra was used as the depth for its 6,130±30 ^{14}C years BP age (i.e. the end of the eruption). The cut-off point for the tephras was determined using the (corrected) TOC results; for all the cores, tephras were considered to begin where the TOC values fell below 50%. However, in cores Z0106 and Z0204, the clay layer (*Figure 6.1*) added complication by lowering TOC values in the peat between the clay layer and the Tuhua Tephra to values that were lower than those above the clay layer. So, for this core, the Tuhua Tephra was considered to begin where TOC values fell below 35%. Similarly for Z0204, the Tuhua Tephra was considered to begin below 30%. Both were where the sharpest change in TOC occurred.

Experimental work was undertaken to develop the most appropriate age-depth model for each core. Only the AMS radiocarbon ages between the Taupo and Tuhua tephras, and the tephras themselves, were used, as this is the period of focused study. The bulk peat ages were omitted as they were too old relative to the AMS ages (based on their mid-point ages) and also had much larger errors associated with them (*Table 6.2*).

The different approaches used to derive age-depth models were:

a) using a single best-fit trendline (e.g. linear or polynomial) that passed through the most ages ranges. However, this most straightforward approach demonstrated that lines did not necessarily pass through the tephra age ranges, and often bypassed AMS ages too.
b) joining each age (AMS and tephra) to adjacent ages with separate linear relationships i.e. linear interpolation. Any linear relationship assumes that all changes in peat deposition rates occur exactly at the depth of the dated point, which is unrealistic, and that peat accumulation is constant between these dates.

c) fitting a single linear relationship through the AMS dates only, and then joining the ends of this trendline to the tephra ages using a linear relationship. This assumes that the majority of the core accumulates constantly, apart from the end sections where tephra layers have altered the accumulation rates. This effect is apparent in several cores.

d) fitting two linear regression lines through parts of the core that, by eye, seem to show constant accumulation rates. At this site, all three cores suggest an increase in accumulation rates at approximately mid-core.

The selection of age-depth models were derived for each core and the applicability of each was assessed. For the chosen method, it was decided that the same approach for each core's age-depth model should be used to ensure consistency, despite it being unlikely that profiles have been subjected to exactly the same post-depositional processes, such as rate of decomposition given different vegetation composition.

Below, the age-depth models are discussed for each core, commenting on their individual merits and applicability.

Z0106

The calibrated radiocarbon ages of Z0106 are presented (*Figures 6.2 and 6.3*).

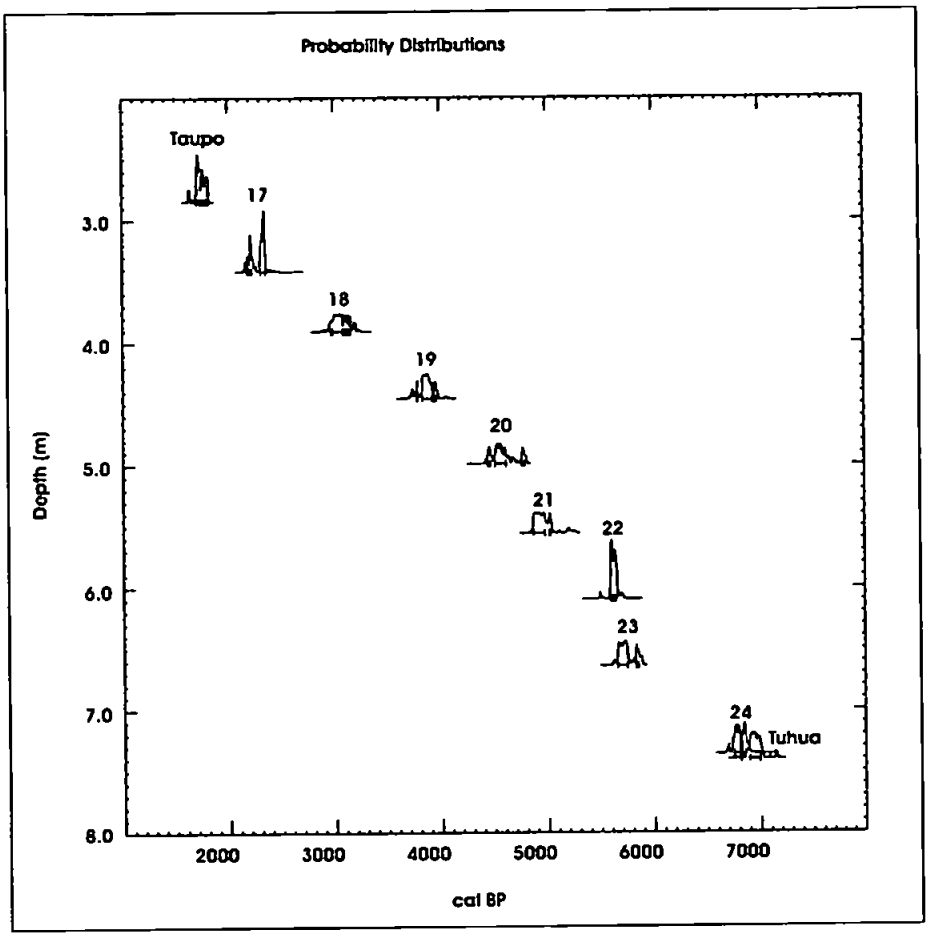

Figure 6.2 Probability plots for the calibrated radiocarbon ages for Z0106.

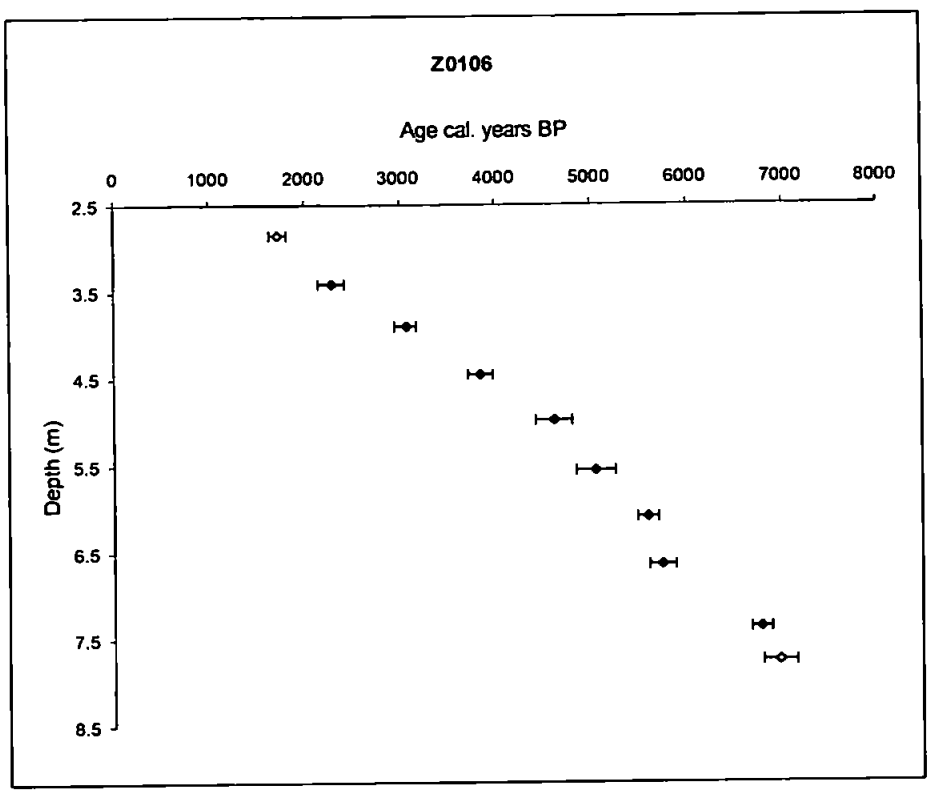

Figure 6.3 Age-depth plot with error bars for all radiocarbon ages obtained from core Z0106. Blue symbols are AMS ages and yellow symbols are the well-established radiocarbon ages of the Taupo and Tuhua tephras.

These age-depth plots show that there are no age reversals within the core, so, all the ages can be incorporated when deriving the age-depth models.

The four possible age-depth models are shown together in *Figure 6.4*.

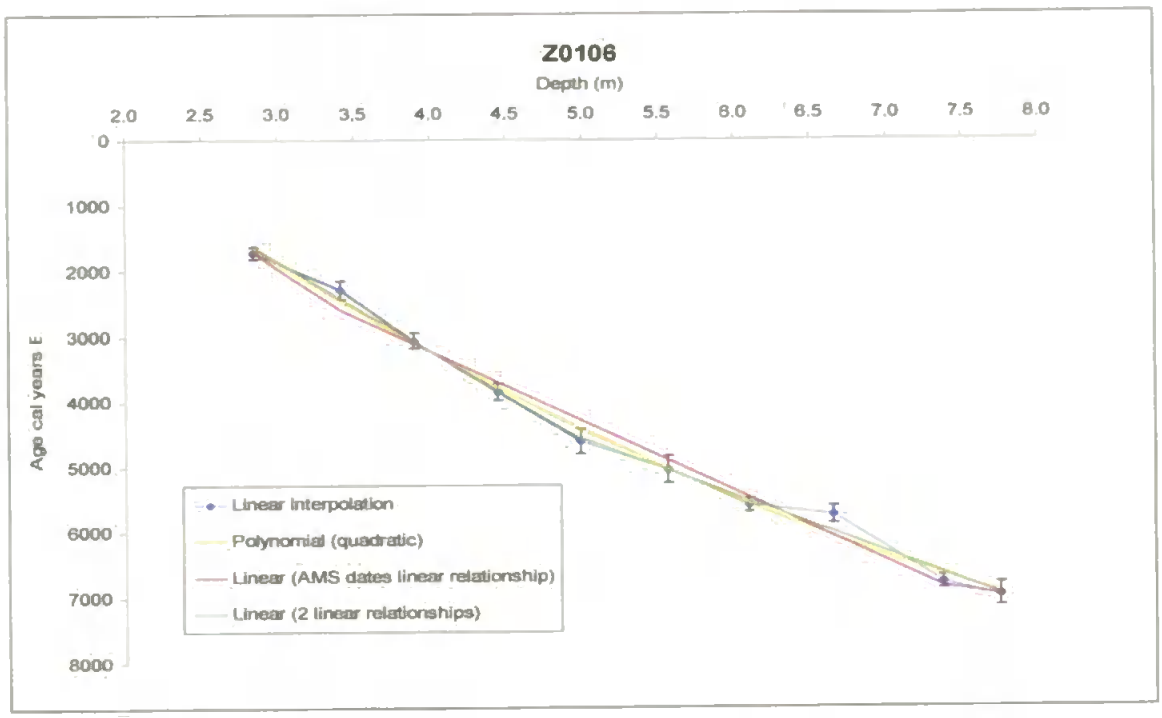

Figure 6.4 The age-depth models for Z0106 plotted on the same axis.

The curvilinear relationship (a 2nd-order polynomial i.e. quadratic) seems to perform well, passing through the age error ranges of both tephras and also passing through the majority of AMS age ranges. However, this relationship is poor due to the systematic distribution of residuals around the line. The linear interpolation method joins each point with a straight line relationship resulting in quite a complex model because it uses nine separate lines. Using the AMS ages separately from the tephra layers shows a steep change in gradient at the tephra layers compared to the section of core between these points, suggesting that this model is unrealistic. Fitting two linear relationships (between 2.845-4.988 m and 4.988-7.752 m) through the data shows a good fit with the data. However, there is no discernible change in sediment stratigraphy (Appendix 2) to suggest that a consistent change in accumulation rates occurs at this point, implying that the model cannot be justified.

Figure 6.5 shows the reconstructed light humification values plotted against the ages calculated from the selection of age-depth models. This was done to assess whether the choice of age model significantly affected the chronostratigraphic pattern of the principal

analytical parameter of this study (peat humification). It also provides an easily visualised way of identifying which parts of the profile are most and least affected by the choice of age-depth model.

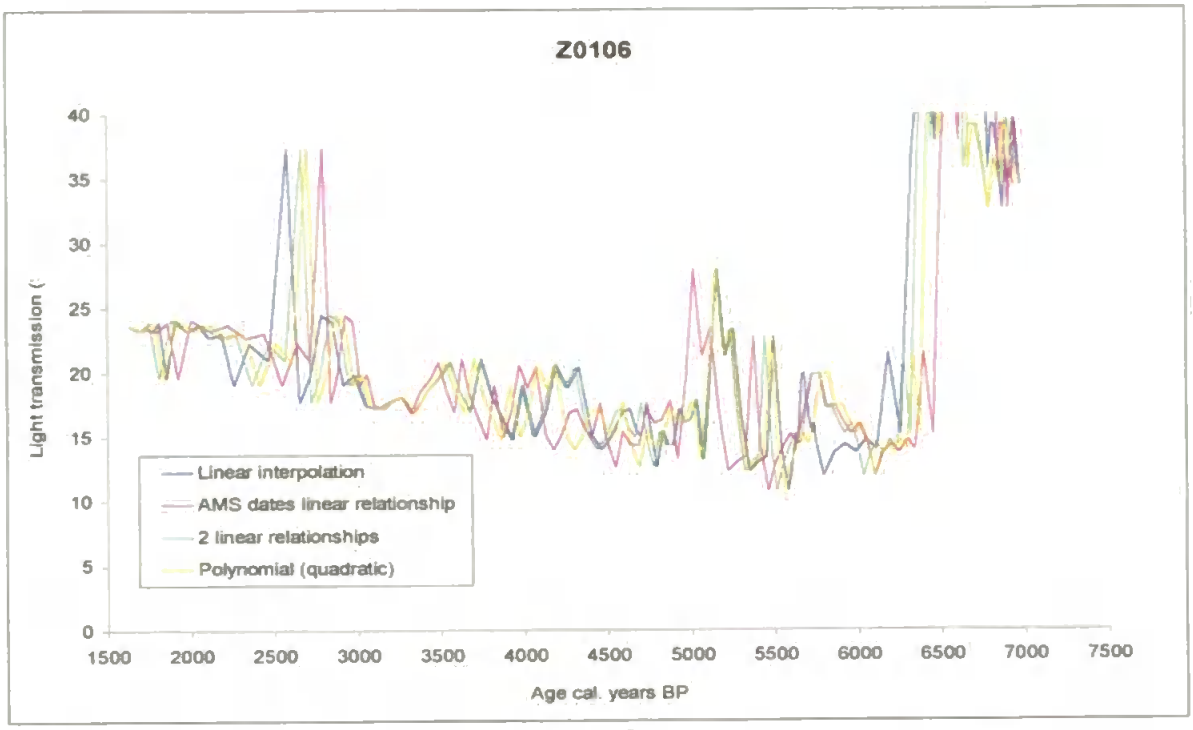

Figure 6.5 The peat humification record plotted against the ages derived from the four main age-depth models for Z0106.

This plot suggests that overall there is little difference in the calculated ages of the four different age-depth models. The largest difference in ages is of 212 years, calculated for the tephra peak (indicated by high light transmission values) occurring between 2,500-3,000 cal. years BP. There are also numerous points on the curves where two models (the linear interpolation model and the model using two linear relationships) are overlaying each other almost exactly e.g. between 3,000-4,000 cal. years BP.

Z0108

The age-depth plot and model for Z0108 are presented below (*Figures 6.6* and *6.7*).

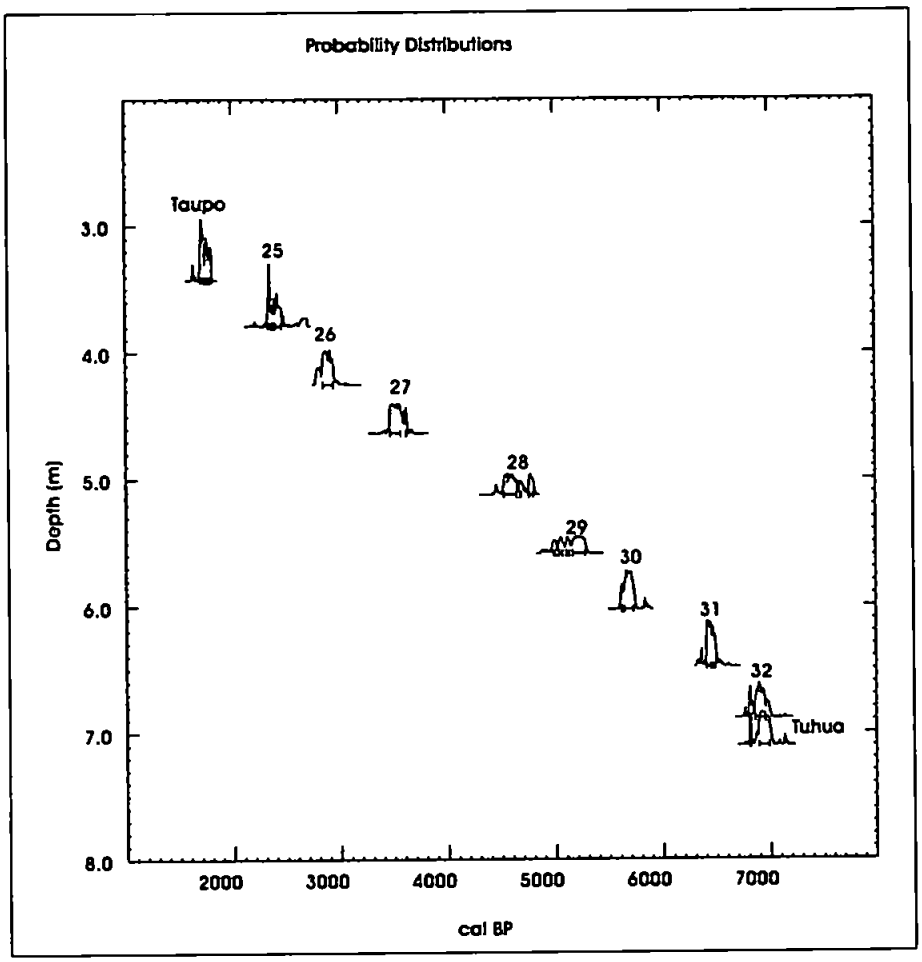

Figure 6.6 Probability plots for the calibrated radiocarbon and tephra ages for Z0108.

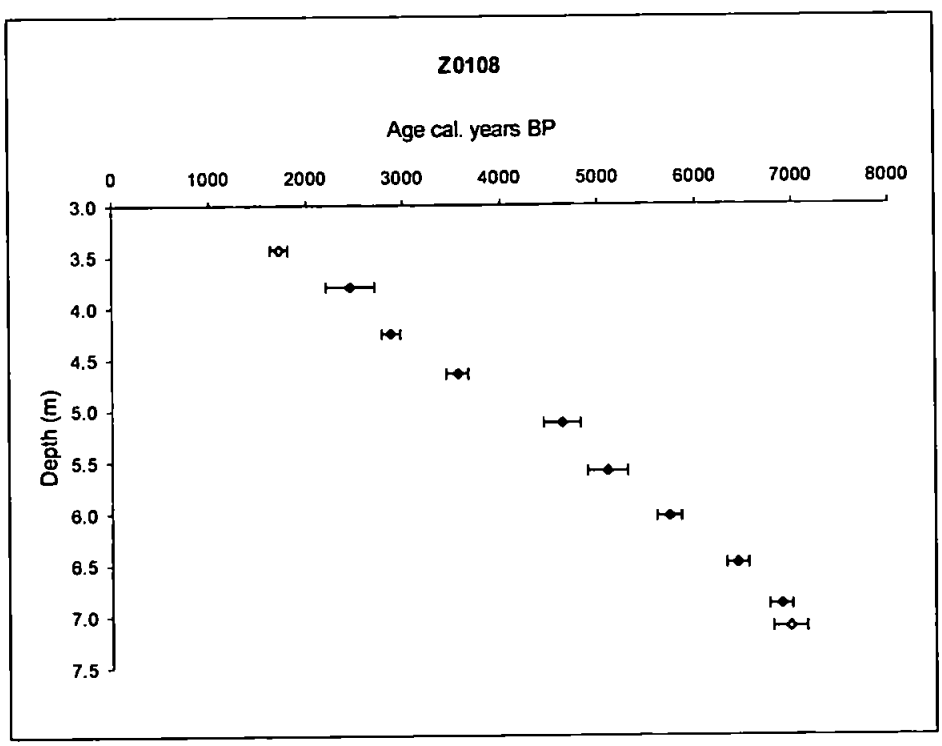

Figure 6.7 Age-depth plot with error bars for all radiocarbon ages obtained from core Z0108. Blue symbols are AMS ages, and yellow symbols are the well-established ages of the Taupo and Tuhua tephras.

Again, these calibrated AMS ages suggest that there are no age reversals within the core. All age-depth models are shown in *Figure 6.8*.

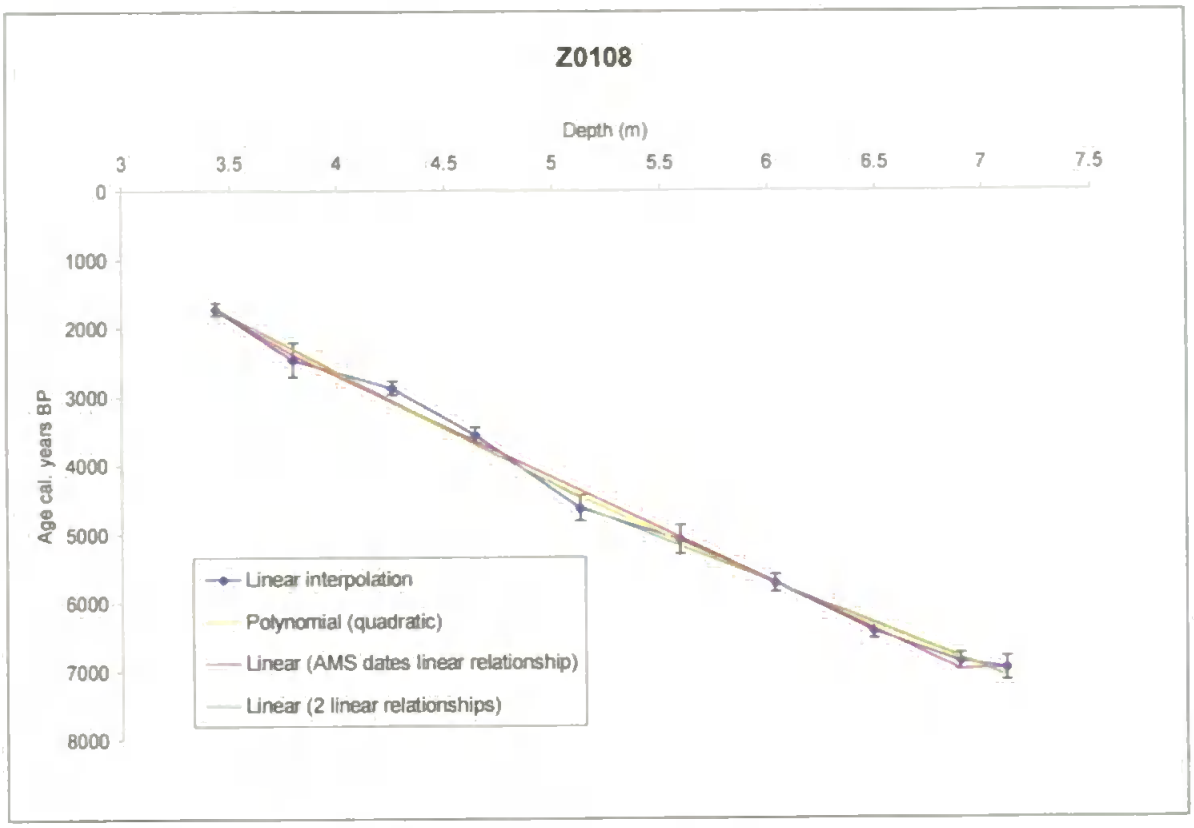

Figure 6.8 The age-depth models for Z0108 plotted on the same axis.

The quadratic relationship passed through both tephra age ranges and also the majority of AMS ages, and it seems that there is no pattern to the residuals, suggesting that the use of this model can be justified. Linear interpolation between the mid-point values resulted in nine separate lines joining the ages. Using the AMS ages separately resulted in negative peat accumulation at the base of the core, suggesting that this method is not suitable due to this age reversal. The data could also be described well by fitting two linear relationships (between 3.434-5.127 m and 5.127-7.107 m) however no stratigraphic change could be identified at this point.

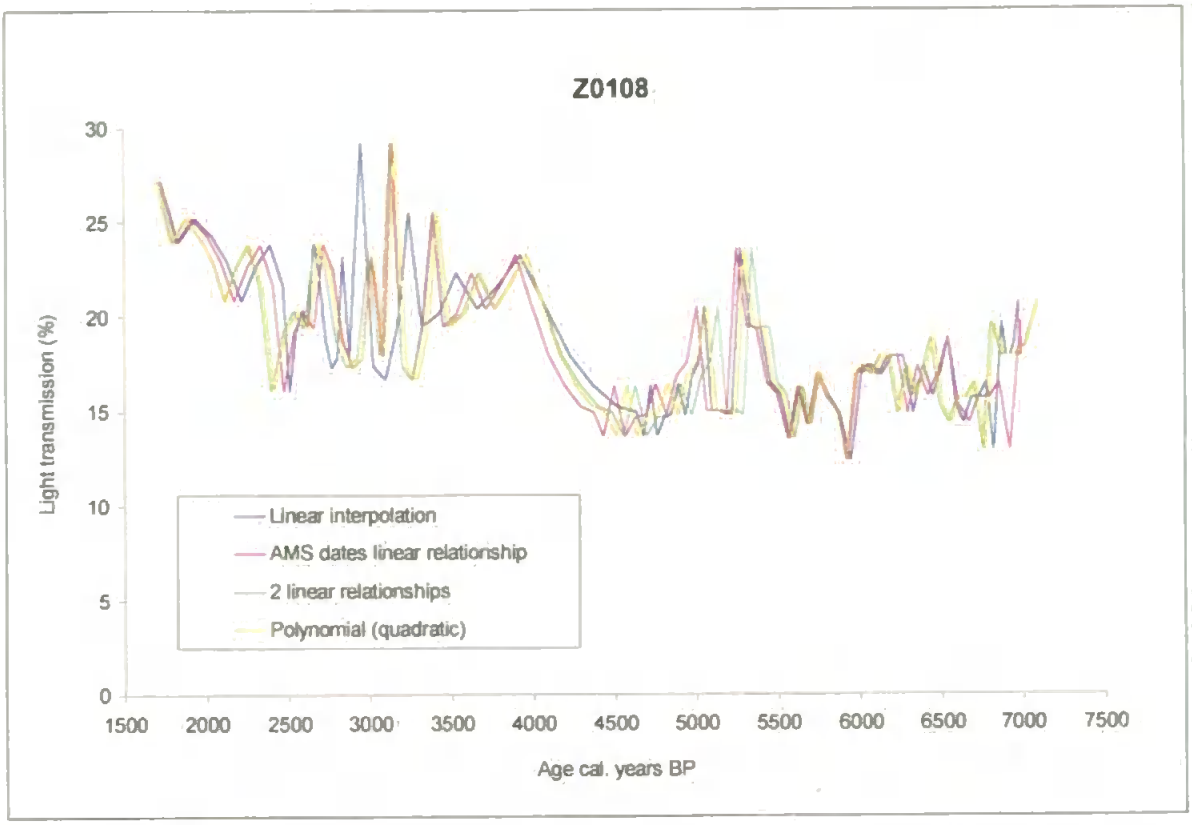

Figure 6.9 The peat humification record plotted against the ages derived from the four main age-depth models for Z0108.

The peat humification record plotted against the selection of age-depth models (*Figure 6.9*) shows that all four of the age-models construct very similar ages throughout the majority of the core. The biggest difference occurs for the peak between 2,500-3,000 cal. years BP, with the timing varying by 207 years.

Z0204

The calibrated radiocarbon ages of Z0204 are presented below (*Figures 6.10 and 6.11*).

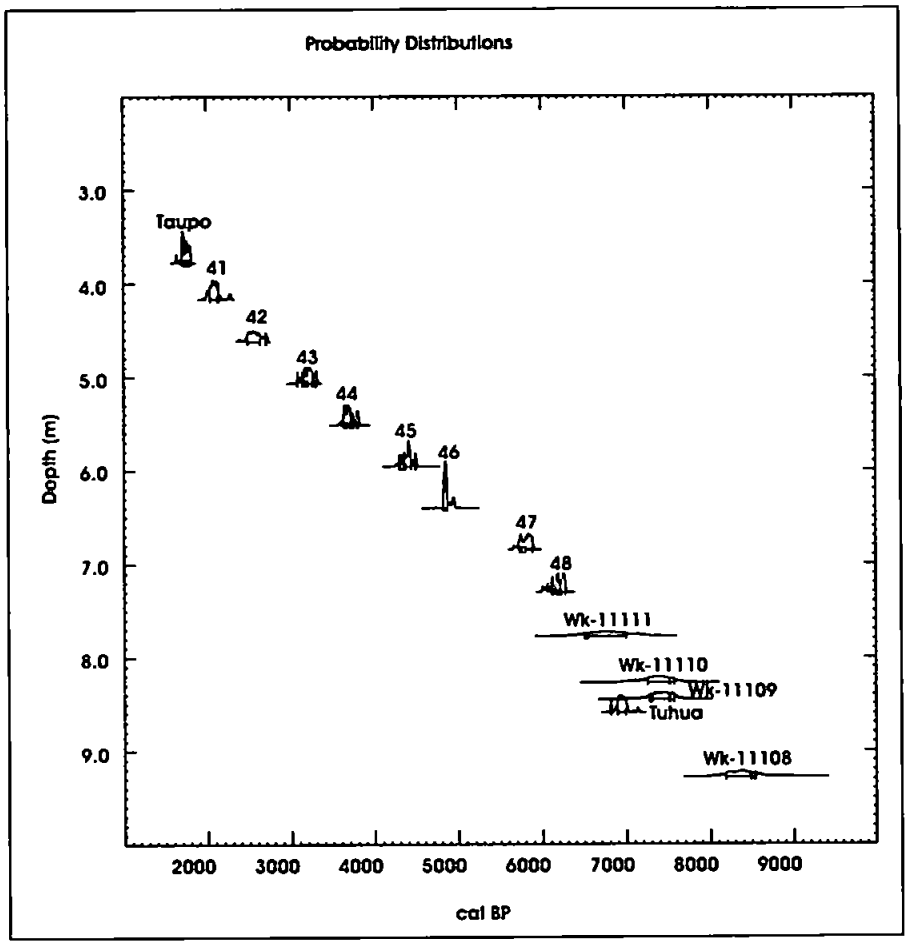

Figure 6.10 Probability plots for the calibrated radiocarbon and tephra ages for Z0204. Wk-11108 to Wk-11111 are bulk peat ages; the others are AMS ages on plant macrofossils.

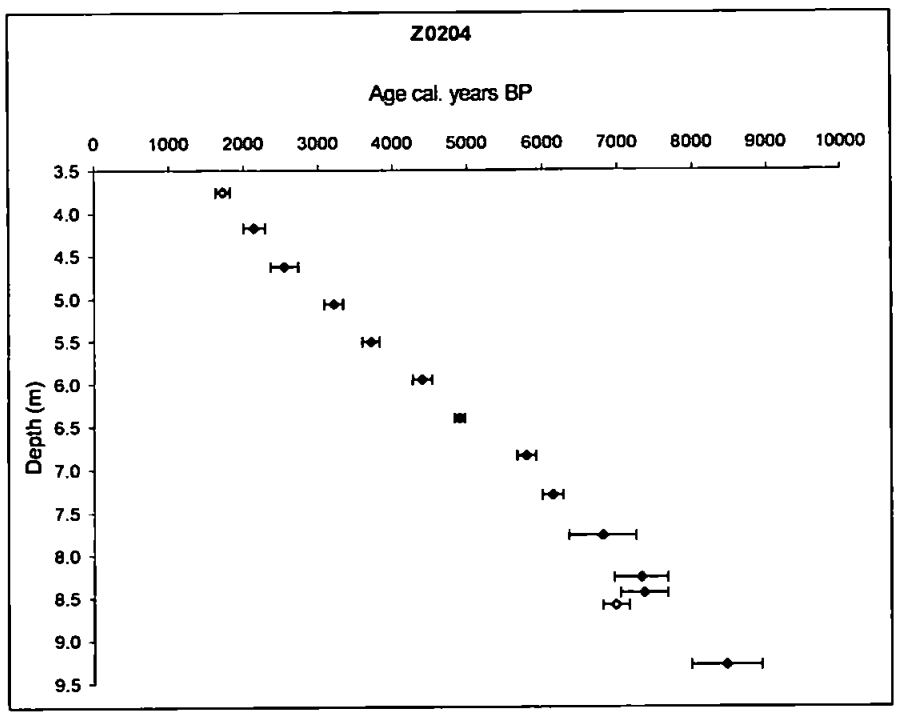

Figure 6.11 Age-depth plot with error bars for all radiocarbon ages obtained from core Z0204. Blue symbols are AMS ages, red symbols are the bulk peat ages and yellow symbols are the well-established ages of the Taupo and Tuhua tephras.

From this core, all the bulk peat ages were omitted from the age-depth models because they generally seemed to be too old in relation to the Tuhua Tephra, even though they seemed to be 'in line' with the AMS ages.

All the age-depth models are shown together in *Figure 6.12*.

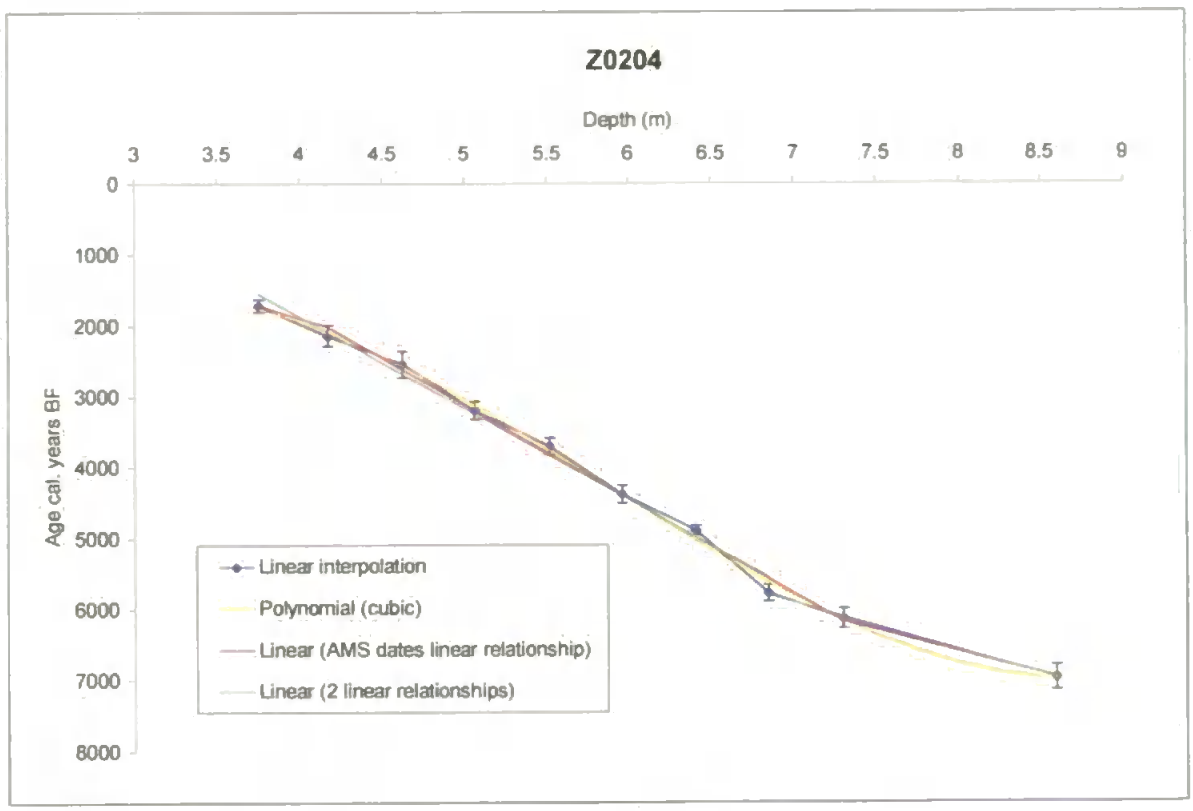

Figure 6.12 The age-depth models for Z0204 plotted on the same axis.

The cubic relationship passed through both tephra and most of the AMS age ranges. This curve could be justified because, when compared to a simple linear curve, the majority of points at the top end of the graph were below the line, and vice versa at the lower end of the graph. Linear interpolation is a more complex model, using nine separate relationships to explain the data. AMS ages considered separately from the tephras resulted in steep changes in peat accumulation rates towards the tephra layers. Two linear relationships were fitted to the data (between 3.755-6.845 m and 6.845-8.595 m). However they suggested a decline in accumulation rates in the middle section that could not be linked to any changes in the peat humification results (this period actually coincides with inferred wet conditions, from which *increased* peat accumulation would be expected) (section 6.3.3).

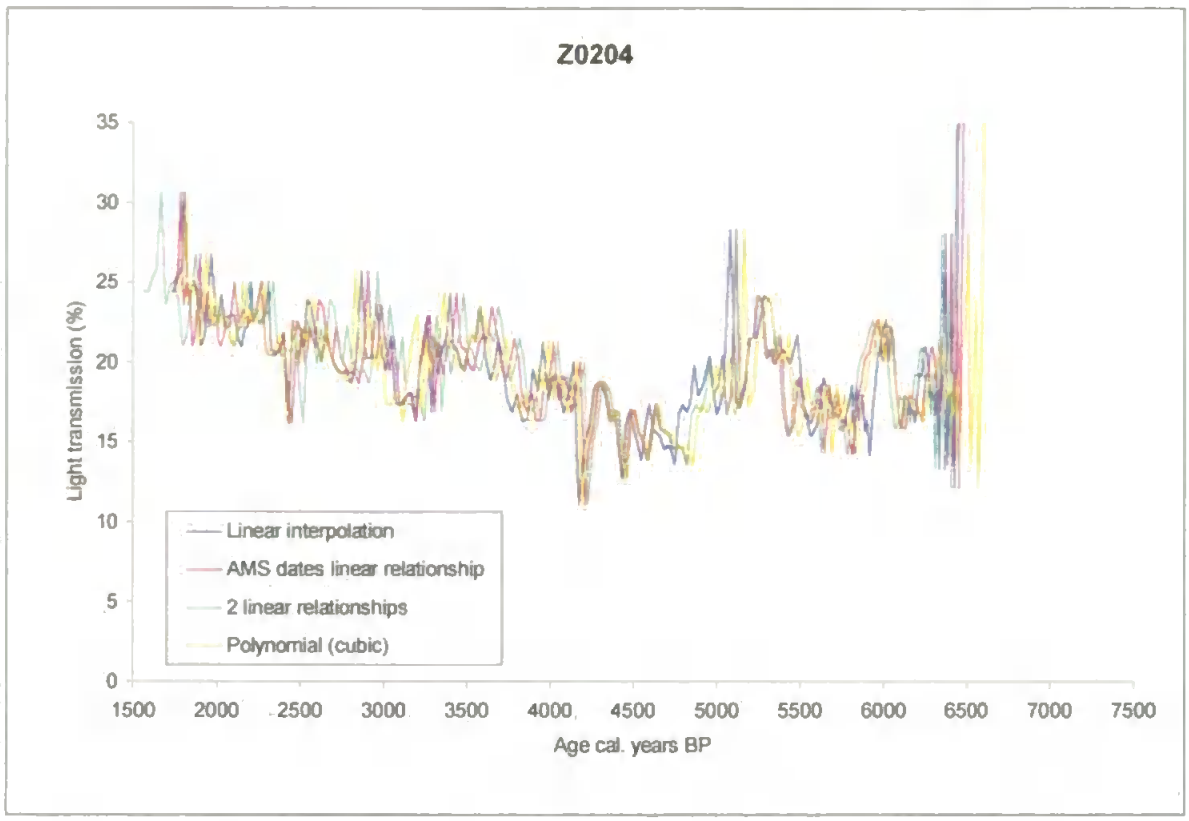

Figure 6.13 The peat humification record plotted against the ages derived from the four main age-depth models for Z0204.

By comparing the different peat humification records (*Figure 6.13*) the greatest difference between ages calculated from the models is of 180 years, and that is at the middle of the clay layer peak, that varies between approximately 6,800 and 6,600 cal. years BP depending on which model is used. Before 4,000 cal. years BP, the linear interpolation and AMS linear curves are very similar, particularly from 5,500-5,000 cal. years BP. At the clay layer, the model that was derived using a cubic relationship is the most different from the other three models.

The final models

Because there is no single correct way to determine the best age-depth model to be used, choosing the most appropriate in terms of palaeoclimate reconstruction can be difficult (see Telford *et al.*, 2004a). However, after considering all the possible age-depth model options, and comparing their performances, it was decided to use the linear interpolation method for each core using the mid-point value as a good age estimate, both of which are advocated by Chambers and Blackford (2001). This method was chosen because each profile has the same number of ages, and it takes into account changes in the stratigraphy (tephra and mineral layers e.g. the clay layers in Z0106 and Z0204) that will have altered the accumulation rates of the substrate, rather than averaging them out. It also provides a

relatively straightforward relationship between ages that is simple to apply to the various proxies that use this chronology. In addition, none of the other methods could be applied to every core successfully. For example, a) Z0108 did not fit the age-depth model using a linear relationship through the AMS ages, due to the age reversal at the Tuhua, b) cubic trendlines could not be justified for all and even where it could, for example in Z0204, the age of the clay layer was calculated as being too old compared to Z0106, and c) sudden changes in accumulation rates as demonstrated by the models using two linear regression lines, could not be justified by any changes within the stratigraphy.

The chosen age-depth models are now presented (*Figure 6.14*) and are shown to be generally similar to each other.

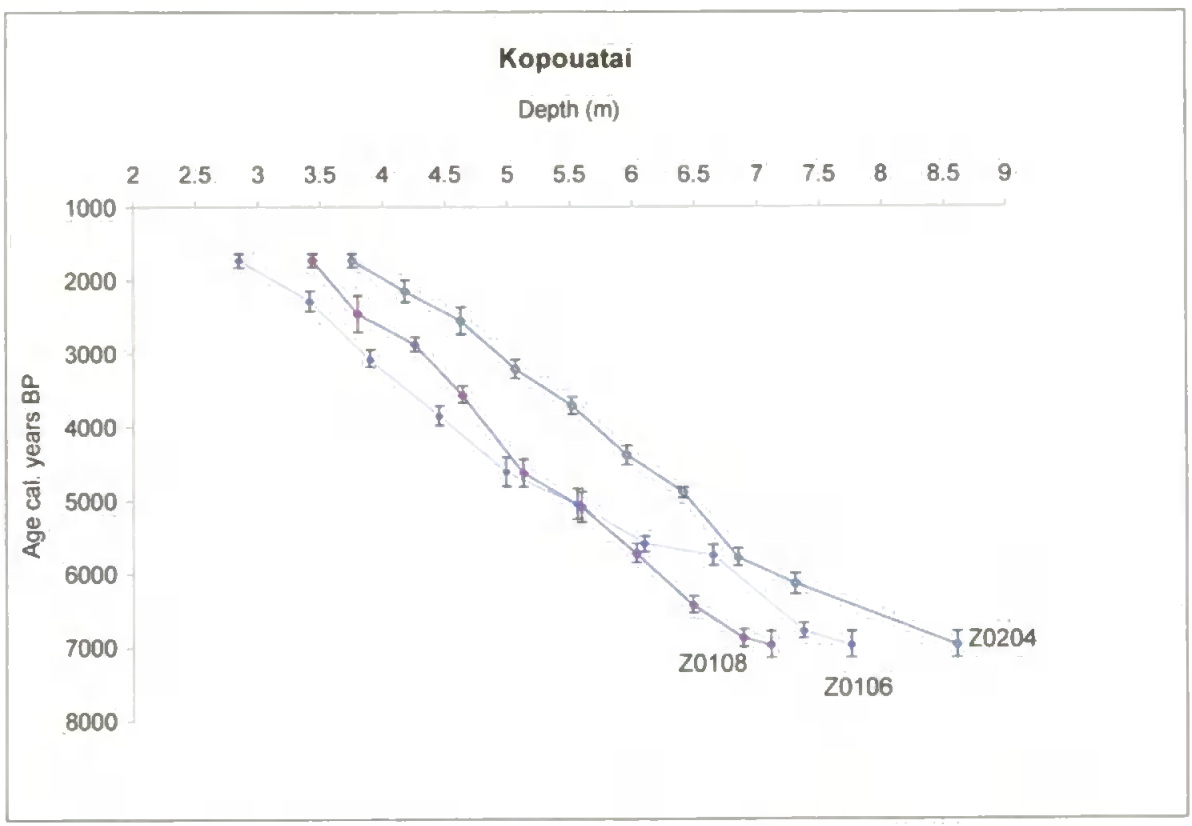

Figure 6.14 Linear interpolation age-depth models for Z0106, Z0108 and Z0204 from Kopouatai.

It is also necessary to consider the errors that are associated both with the radiocarbon ages themselves and with the derivation of the age-depth models. It has already been shown that the maximum time difference between models for the Kopouatai cores is of approximately 200 years. The effect of the error ranges of the radiocarbon ages on the humification records is shown below in *Figure 6.15*.

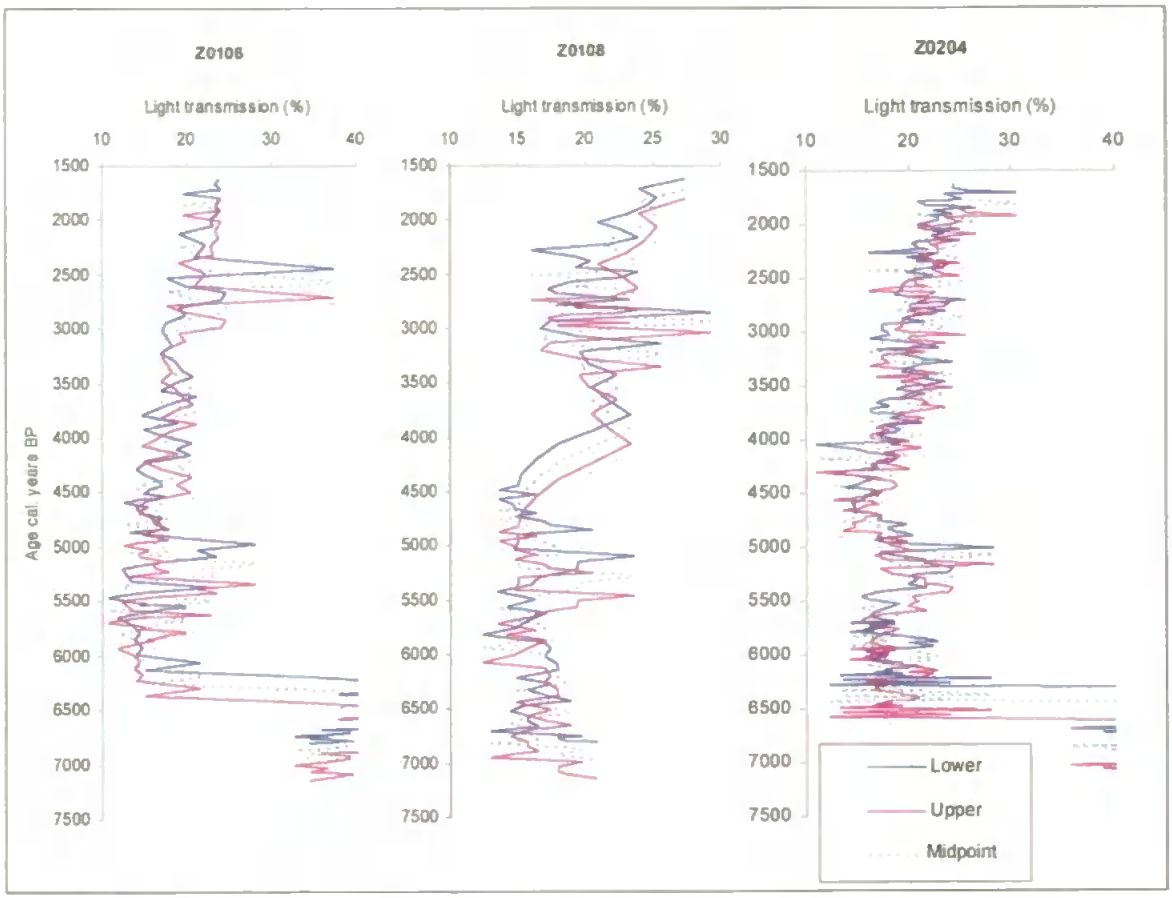

Figure 6.15 The effect of radiocarbon age ranges on humification profiles. The range in ages between the lower, mid-point and upper 2□ values of the calibrated radiocarbon ages using the same linear interpolation approach for each.

Figure 6.15 demonstrates that the largest age ranges are of approximately 370, 370 and 340 years for Z0106, Z0108 and Z0204 respectively. This could have important implications when comparing the cores to determine which shifts could be happening simultaneously, given their age ranges resulting from the radiocarbon errors.

Having decided on the most applicable age-depth model, the analytical results will now be discussed in terms of both depth and age.

6.3 Analytical results

In this section, results are presented for each core individually. All results are presented on composite diagrams. Initially peat humification values are uncorrected, but corrected results are presented later. See Section 4.4 for details on the correction procedure. Core stratigraphies shown here are simplified. For a detailed description of the cores' constituents and colour, see Appendix 2. All ages are discussed to the nearest 50 years, and depths are corrected to the nearest cm.

6.3.1 Core Z0106 (*Figure 6.16*)

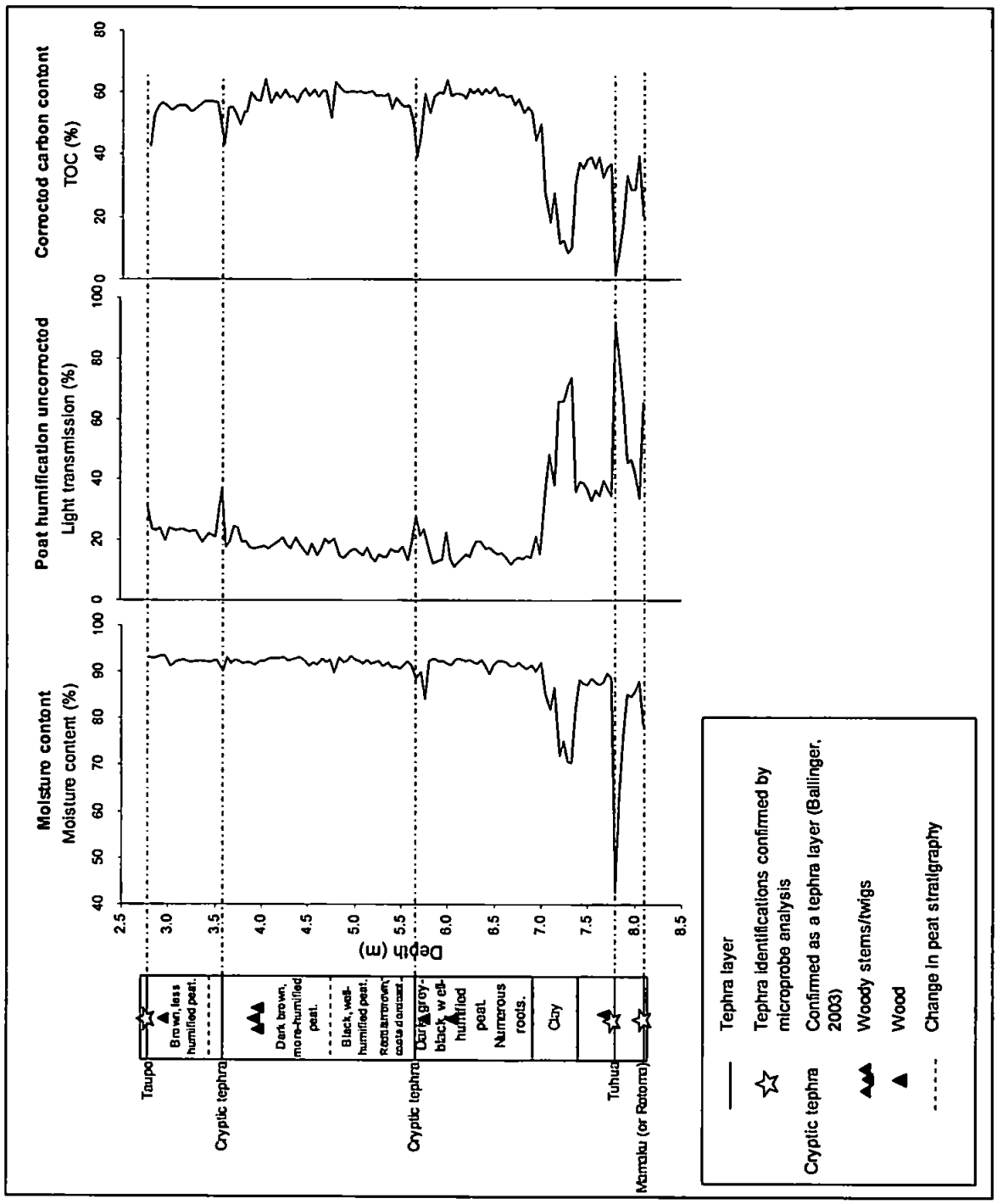

Figure 6.16 Z0106 core stratigraphy, moisture content, raw peat humification and corrected TOC results. (All sample depths are plotted on graphs as the mid point of the sample, where necessary, the middle of the corrected depth range).

Core stratigraphy (*Figure 6.16* and Appendix 2)

The stratigraphy of Z0106 shows that the peat becomes progressively less decomposed up-core, grading from a dark grey/black, well humified peat at the base of the core to a red/brown, more fibrous peat at the top. Within the core there are wood remains at approximately 2.98 m, 5.76 m, 6.08 m and 7.68 m, in addition to a layer of woody remains

at 3.99 m. Roots are abundant in the lower half of the core, from the base up to approximately 5.30 m. The main changes in core composition are the tephra layers and the fine, blue/grey clay layer from 6.89-7.41 m, thought to originate from freshwater ponding at the time of the mid-Holocene sea-level rise in the region. There are no marine indicators, such as foraminifera, within the layer. Pollen analysis was carried out on this layer by R. Newnham (University of Plymouth) and the results are presented later in section 6.3.4 and Appendix 4.

Moisture content (*Figure 6.16*)

Variations in moisture content throughout the core are small, fluctuating around 90-95%, except for the layers of high mineral content which do not hold as much water as the peat. Moisture content falls considerably at such levels, particularly the Tuhua tephra layer, which is much drier than the clay layer. The smaller cryptic tephra layers, detected by Ballinger (2003), stand out in the moisture record, with that at 5.66 m more clearly observed.

Carbon analysis (*Figure 6.16*)

Throughout the core there is a trend towards declining TOC content up-core, which is expected due to the stronger decay of nitrogen relative to carbon with increasing depth. In the lower half of the core, values are relatively constant, but from around 4.7 m upwards, TOC values start to decline. This appears to be an opposing trend to the peat humification results.

TOC results clearly identify units of high mineral content, found to coincide with the tephra and clay layers. At 4.74 m there is a sudden drop in carbon content. When this sample (4,600 cal. years BP) was sieved through 300 and 15 μm meshes and examined under the light microscope it was seen to contain a considerable amount of glass shards, indicating that the presence of a micro-tephra layer is responsible for the drop in carbon content at that depth.

Peat humification (*Figure 6.17*)

Both the uncorrected and corrected peat humification results are plotted here. It seems that the peat correction formula does not work well at high mineral contents, as falls in TOC are still evident in corrected values. This is probably exacerbated by the TOC correction that also had to be performed, together with the transformation from TOC to LOI, the

relationship between which might not be constant down-core. However, corrected light transmission results are generally an improvement on uncorrected results, so results will be discussed in detail in terms of these corrected light transmission values.

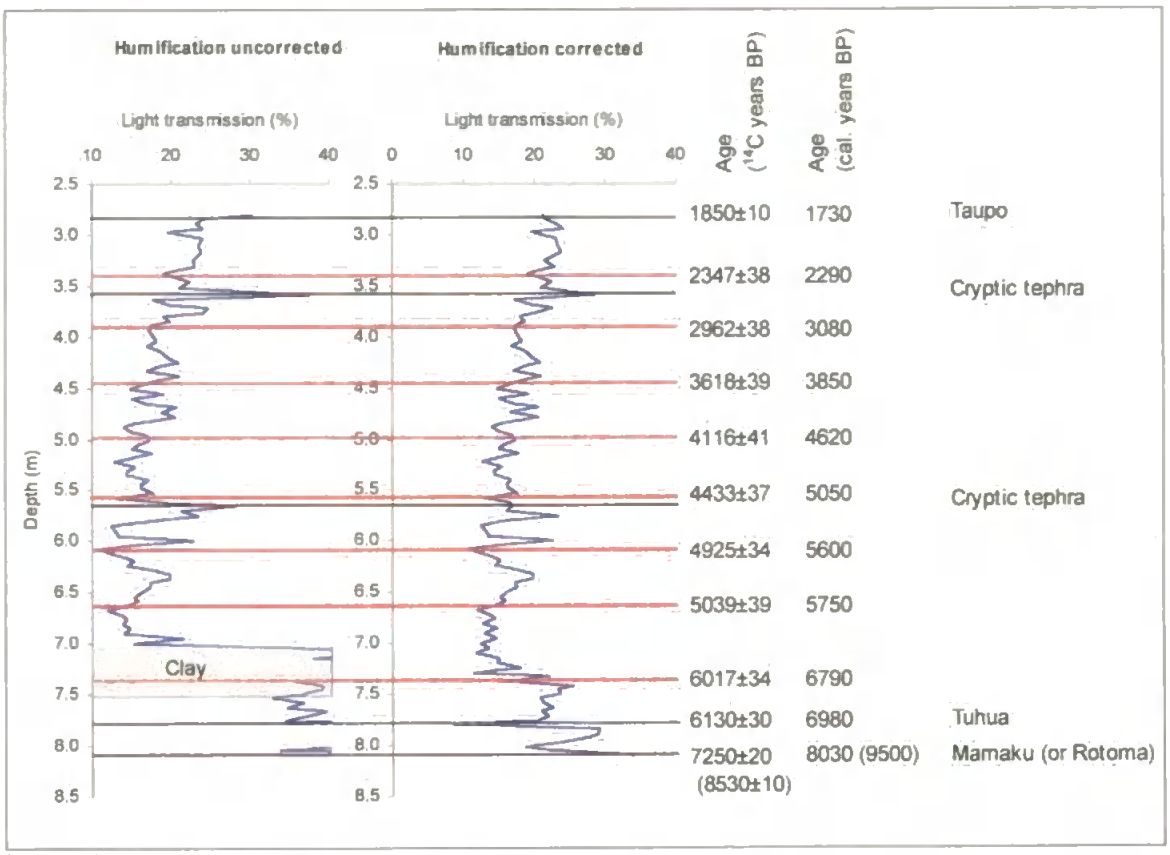

Figure 6.17 Results for core Z0106: raw light transmission values and corrected light transmission.

The raw peat humification values (*Figure 6.17*), uncorrected for varying mineral content, also clearly distinguish the layers with high mineral content (with the reverse pattern to that of moisture content) since there is less humic acid available for extraction in a sample where the peat content is less. In both the uncorrected and corrected records there is an overall trend towards increased light transmission up-core. This is to be expected, as younger peat is less decomposed than older peat. However, this age-decay effect will complicate any climate signal – and is therefore a potentially severe limitation of the peat humification technique when applied over long timescales that is not always recognised (e.g. McGlone and Wilmshurst, 1999b). It is possible to detrend for this age effect (see, for example, Langdon *et al.* (2003)), as will be done for all cores later (*Figures 8.2, 8.5* and *8.8*).

The corrected light transmission record is now described in terms of short-term climate shifts, both wet and dry, identifying the relative changes compared to the preceding

conditions i.e. to wetter/drier conditions. These oscillations are independent of any long term age-decay effect. Only the shifts that appear to be completely unrelated to changes in TOC are described, as only these have any value for climatic interpretation. The depth (or age) given for each climate shift is that of the start of the shift. First, shifts were determined by eye as beginning where significant deviations from baseline values were observed, and then they were dated using the first data point in the direction of the signal change. Changes of only one data point have been excluded as a single value cannot substantiate a shift. Depths are corrected to the nearest cm, and ages of significant changes are rounded to the nearest 50 years. All shifts in parentheses indicate tentative shifts that could still be related in part to a drop in TOC, even after applying the correction for mineral content.

Fluctuations in light transmission between samples are clearly visible. From *Figure 6.17* it can be seen that shifts to values of higher light transmission (i.e. inferred wet conditions) occur at approximately 6.63 m, (5.80 m), 5.18 m, (4.84 m), 4.46 m, and 3.76 m. Shifts of reduced light transmission, suggesting relatively dry periods occur at (7.37 m), 6.28 m, 5.40 m, 4.97 m, (4.64 m), 4.19 m and 2.89 m.

The shifts are shown and discussed in terms of ages below (*Figure 6.18*).

The wet shifts occur at 5,750, (5,300), 4,750, (4,400), 3,850 and 2,850 cal. years BP. The dry shifts are dated to (6,800), 5,650, 4,950, 4,600, (4,150), 3,500 and 1,750 cal. years BP.

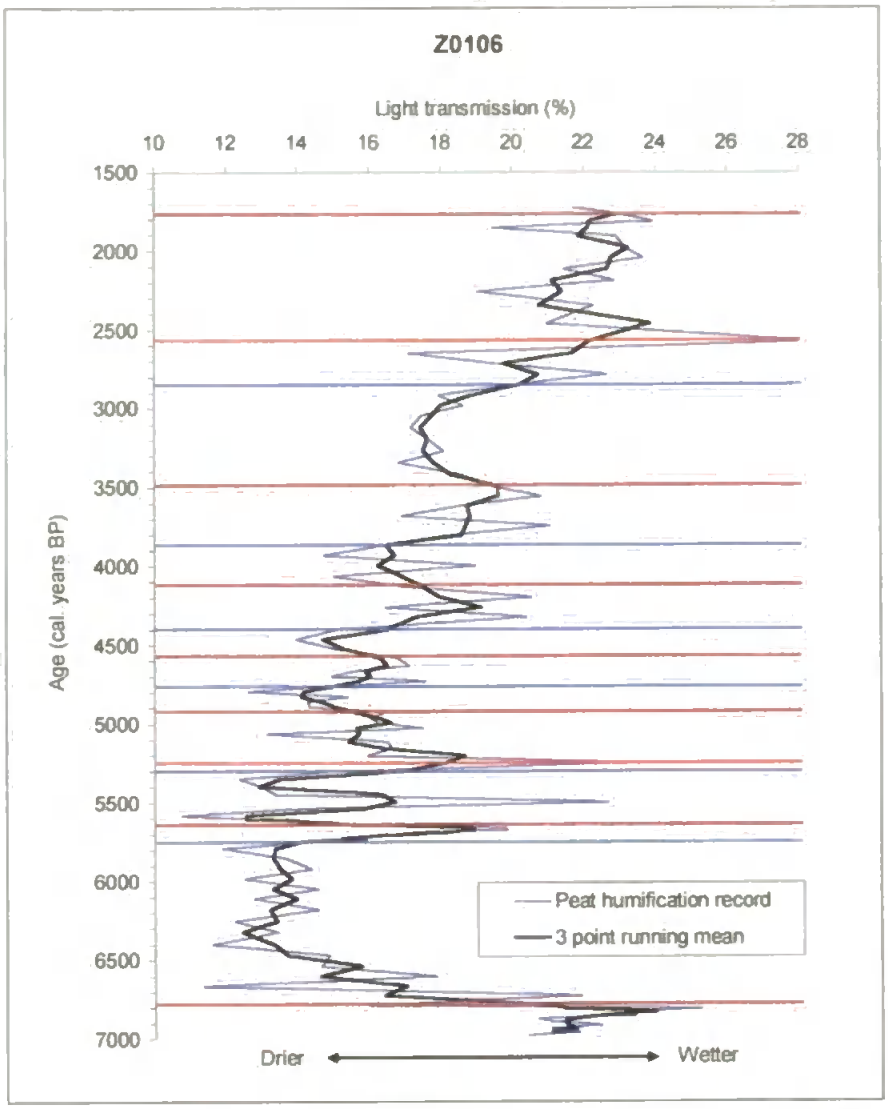

Figure 6.18 Corrected light transmission plotted against age for Z0106. Blue lines indicate wet shifts, brown lines indicate dry shifts and red lines indicate the location of tephra layers.

Within the general up-core trend in increasing light transmission values, a change in baseline values can be seen to occur at approximately 4,500 cal. years BP. Below this point, light transmission values fluctuate between 15 and 20% (excluding mineral layers), but upwards throughout the core, light transmission values gradually increase to vary between 25 and 30%. Although this dichotomy is thought to be partly due to the age-decay effect, it is nevertheless still apparent after removing this effect by detrending the curve (*Figure 8.2*).

Accumulation rate

An overall accumulation rate was calculated for the whole core, between the Taupo and the Tuhua Tephras, and was 0.93 cm/10 years (2dp).

6.3.2 Core Z0108 (*Figure 6.19*)

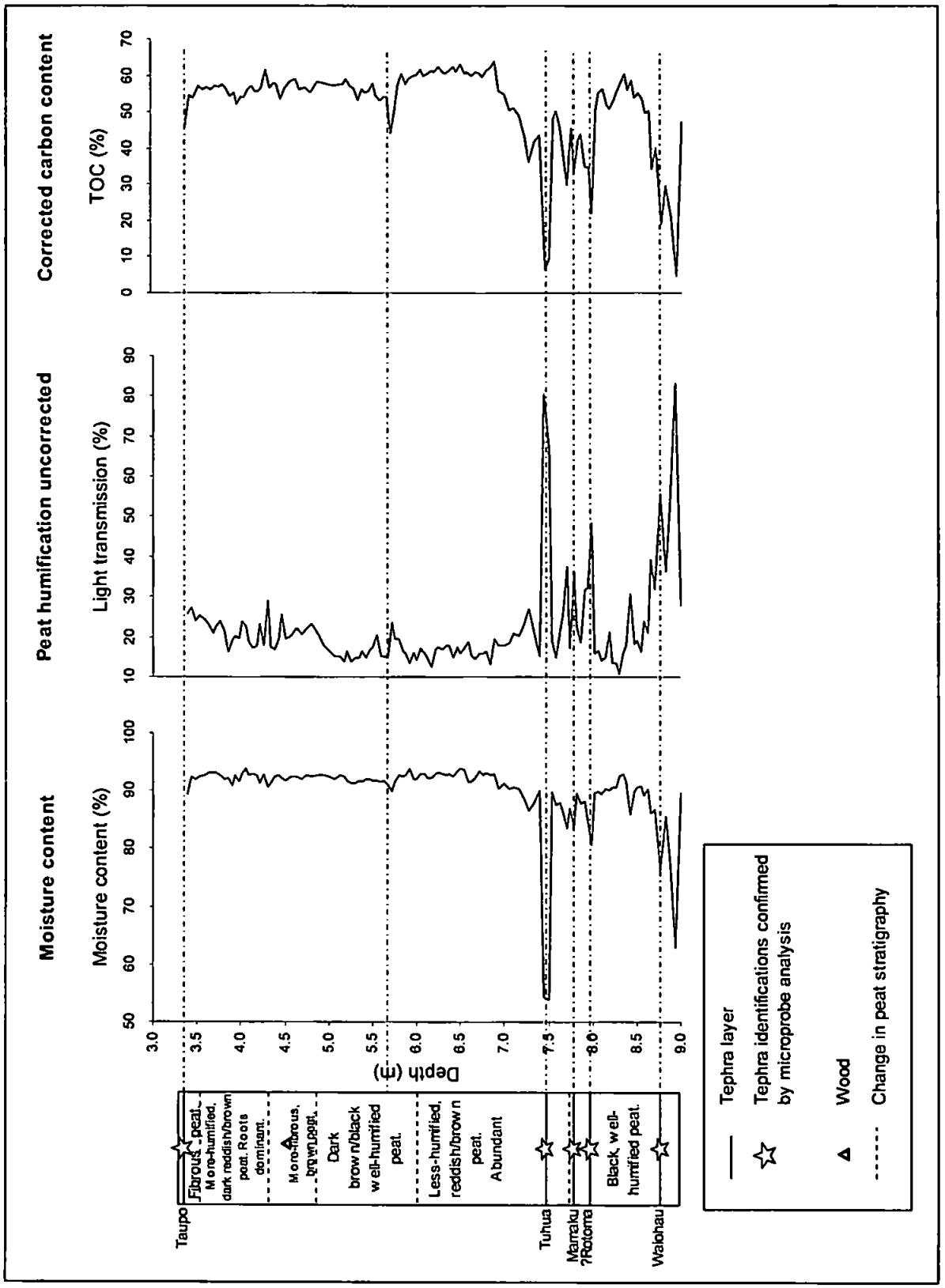

Figure 6.19 Z0108 core stratigraphy, moisture content, raw peat humification and corrected TOC results.

Core stratigraphy (*Figure 6.19* and Appendix 2)

The stratigraphy shows dark, more humified peat at the base of the core, which changes at approximately 6.00 m to a less humified peat containing abundant roots. There is then a return to more humified peat, which becomes more reddish coloured and fibrous. Wood is present at 3.54 m, 4.55 m and 4.83 m. There are numerous tephra layers identified in the core, most of which are below the Tuhua Tephra, and therefore outside the temporal range of this project. In this core the clay layer is absent.

Moisture content (*Figure 6.19*)

There is little variation in moisture content throughout the core, with values in the peat zones varying between 90-95%. The tephra layers are clearly differentiated from the peat, with the Tuhua Tephra having the greatest drop in moisture content, falling to approximately 55%.

Carbon analysis (*Figure 6.19*)

The TOC curve shows a gradual decrease in carbon content up-core that appears to mirror the overall trend in peat humification. Below approximately 5.00 m, TOC values are relatively constant, but above this depth there is a gradual decline in values towards the top of the core.

TOC results show the tephra layers clearly as horizons of reduced organic content. There seems to be a slight fall in carbon content up-core, presumably due to the nitrogen effect (section 6.3.1), however, there is little variation in values for the peat samples. The most noticeable features are small peaks in TOC at 4.30 m and 6.88 m. Sample from 7.28 m, where there is a fall in TOC, was examined under a light microscope and was observed to contain numerous tephra shards.

Peat humification (*Figure 6.20*)

Seen in both the uncorrected and corrected results, an underlying up-core trend towards increased light transmission (i.e. less humified peat) is present above approximately 5.00 m (*Figure 6.20*). Below this, light transmission values remain quite constant, and perhaps even increase down-core towards the tephras. The lower-most humification values could be affected by the underlying tephras through increased mineral content or indirectly by the tephras inhibiting drainage. The visible tephra layers are clearly marked by increased

light transmission values. However, the effect of the cryptic tephras on light transmission values are less obvious.

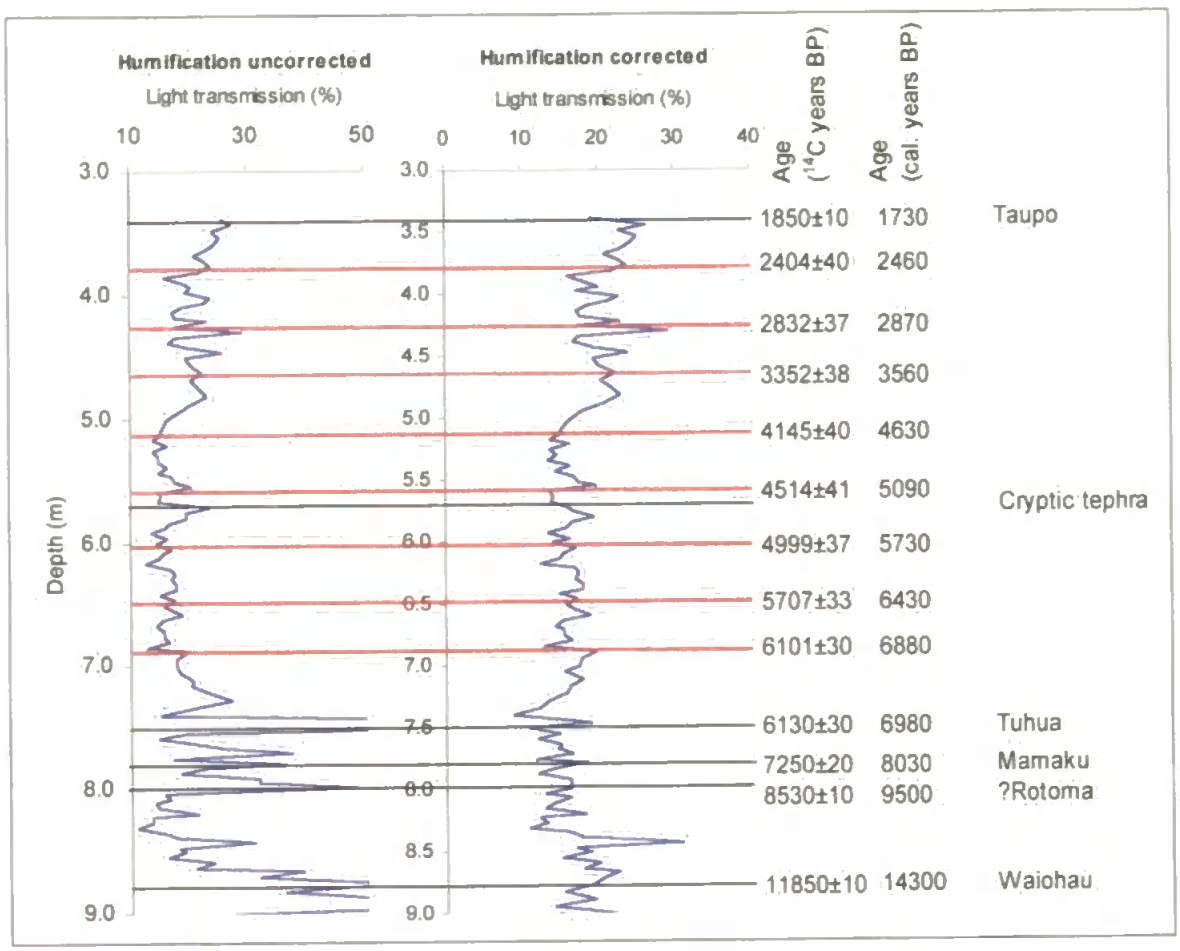

Figure 6.20 Results for core Z0108: raw light transmission values and corrected light transmission.

Shifts to high light transmission values occur at 6.63 m, 5.88 m, (5.63 m), 5.13 m, 4.34 m, (4.10 m) and 3.81 m. Shifts to reduced light transmission (i.e. dry periods) occur at 6.84 m, 6.21 m, 5.76 m, (5.51 m), 4.42 m, 4.26 m and (3.98 m).

The overall trends up-core are of decreasing light transmission values at the lower part of the core, to a minimum at approximately 5.20 m, and then an increase in light transmission values from this point upwards throughout the core, increasing strongly at the top of the core.

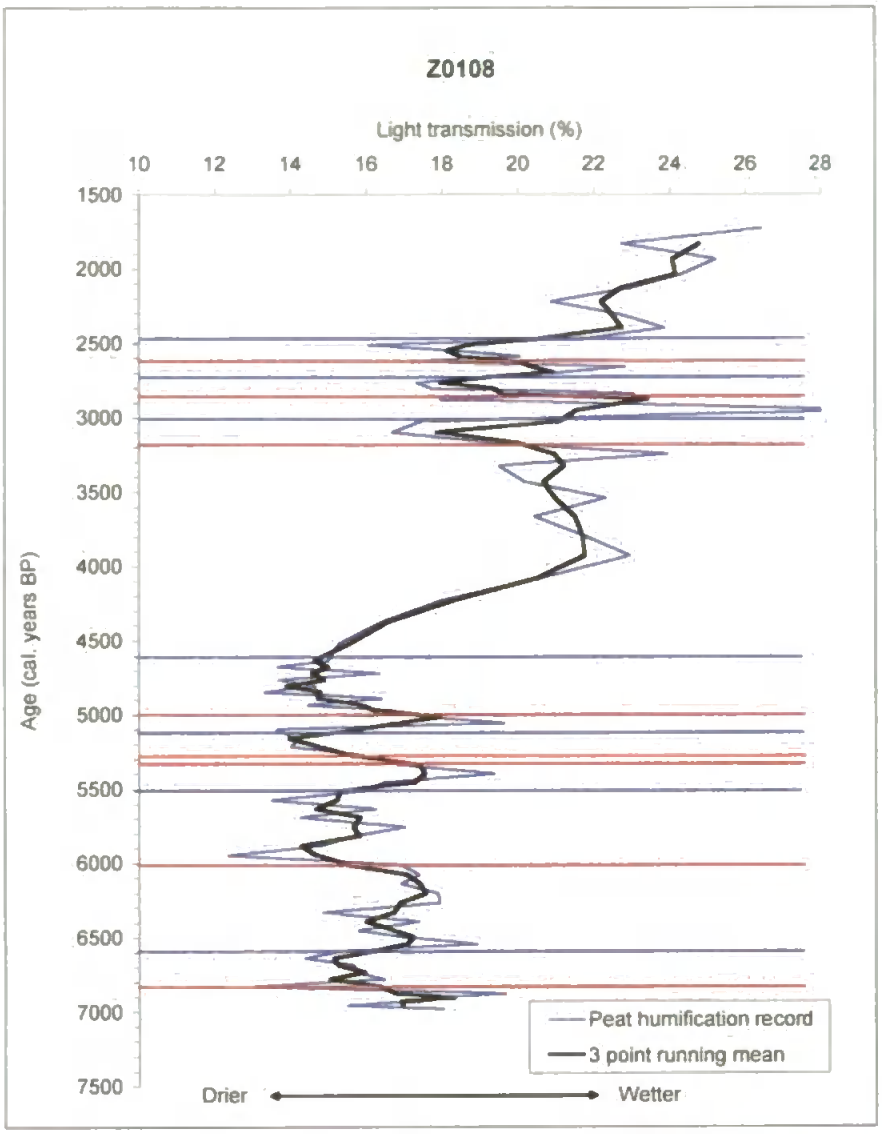

Figure 6.21 Corrected light transmission plotted against age for Z0108. Blue lines indicate wet shifts, brown lines indicate dry shifts and red lines indicate the location of tephra layers.

The main wet shifts occur at 6,600, 5,500, (5,150), 4,650, 3,000, (2,750) and 2,450 cal. years BP. The dry shifts occur at 6,850, 6,000, 5,350, (5,000), 3,150, 2,850 and (2,600) cal. years BP.

Figure 6.21 also indicates that the change in light transmission values from a lower to a higher baseline that occurs at approximately 5.20 m occurs between 4,500-4,000 cal. years BP. This same directional trend as that observed in core Z0106 is of a very similar timing.

Accumulation rate

The average accumulation rate calculated between the Taupo and Tuhua Tephras was 0.70 cm/10 years (2dp).

6.3.3 Core Z0204 (*Figure 6.22*)

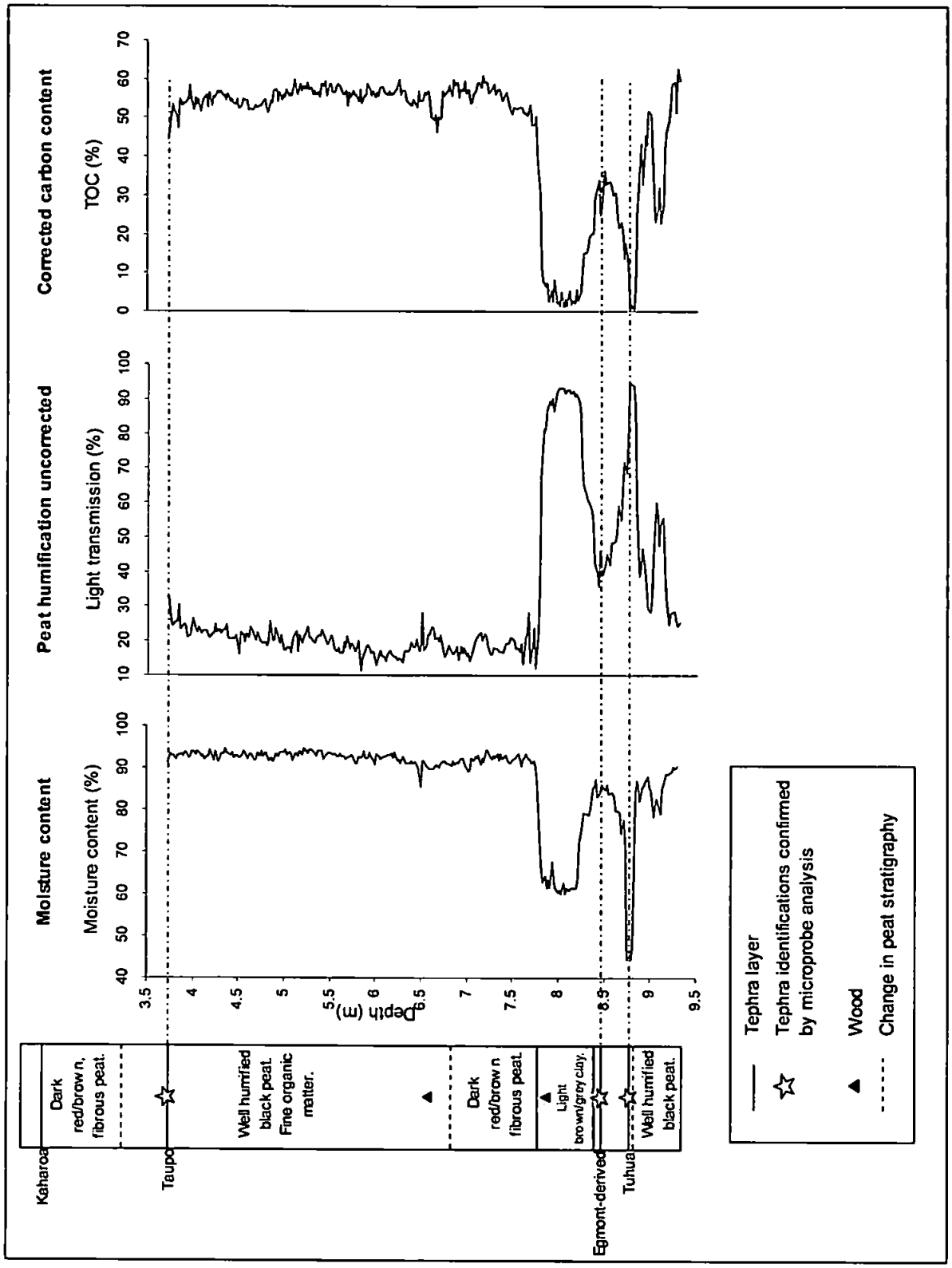

Figure 6.22 Z0204 core stratigraphy, moisture content, raw peat humification and corrected TOC results.

Core stratigraphy (*Figure 6.22* and Appendix 2)

The stratigraphy of this core alternates between dark, humified peat and red/brown less-humified peat, interrupted by a clay layer of similar characteristics to that found in core

Z0106. Pollen analysis was carried out on this layer by R. Newnham (University of Plymouth), the results of which are presented in section 6.3.4 and Appendix 4. The first layer of more-humified peat is present at the very base of the core, and is overlain by more fibrous peat up to just above 7.00 m. There is then a return to more degraded peat, until above the Taupo Tephra layer, when more fibrous, less humified peat is present. Wood is present in the upper part of the clay layer at 7.85 m and then also at 6.55 m.

Moisture content (*Figure 6.22*)

There is only small variation in moisture content throughout the peat sections of the core, except at 6.50 m, where there is a sudden, short-lived fall in moisture value. The clay layer and the tephra layers are clearly evident from dramatic falls in moisture content.

Carbon analysis (*Figure 6.22*)

Again, the overall upwards trend in TOC is of declining values from approximately 5.50 m upwards, with comparatively constant values in the lower half of the core.

There are minor fluctuations in TOC values throughout the core, but centred on 6.66 m is a clear fall in carbon content. The clay layer and the tephras are, again, picked out by their very low TOC contents. The peat at 6.66 m was examined for glass shards, and a small but not significant amount was found.

Peat humification (*Figure 6.23*)

Due to the higher sampling resolution of this core (at every 2 cm) there appears to be more variation between samples, particularly in the upper section of core. An up-core trend in increasing light transmission values, similar to the other records at this site, occurs above approximately 6.00 m.

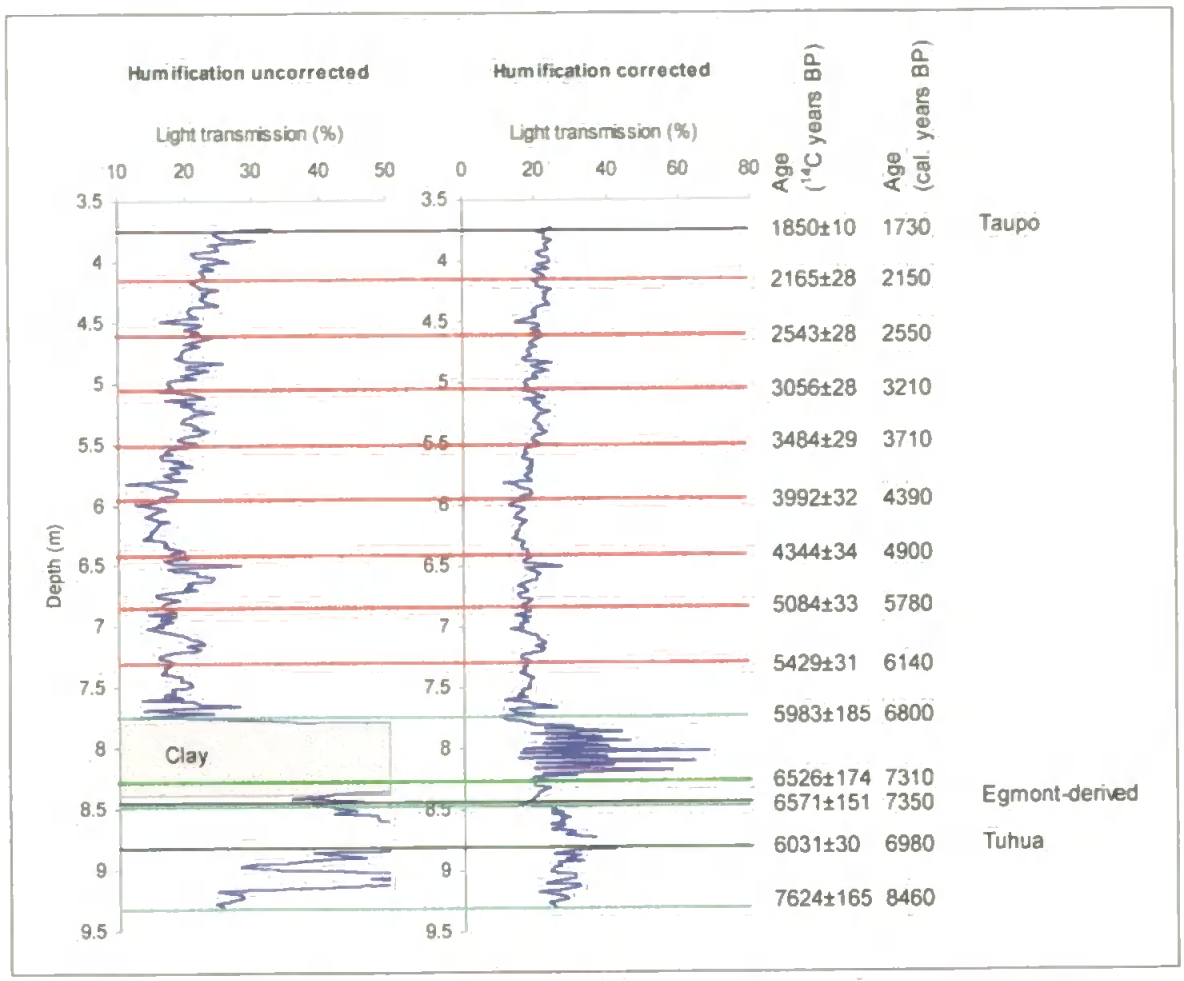

Figure 6.23 Results for core Z0204: raw light transmission values and corrected light transmission.

The major shifts (*Figure 6.23*) towards higher values of light transmission (wet periods) occur at 7.58 m, 7.22 m, (6.64 m), 6.26 m, 5.80 m, 5.54 m, 4.98 m, 4.78 m, 4.40 m and 4.14 m. The main shifts to reduced light transmission (dry periods) occur at 7.40 m, 7.12 m, (6.54 m), 5.88 m, 5.62 m, 5.10 m, 4.82 m, 4.52 m and 4.22 m. A prolonged period of reduced light transmission occurs between 6.40-5.50 m and a peak of reduced values at 4.50 m.

From *Figure 6.24* the wet shifts identified occur at 6,300, 6,050, (5,350), 4,750, 4,150, 3,750, 3,050, 2,750, 2,350, and 2,100 cal. years BP. The dry shifts correspond with 6,200, 6,000, (5,150), 4,250, 3,850, 3,250, 2,850, 2,450, and 2,200 cal. years BP.

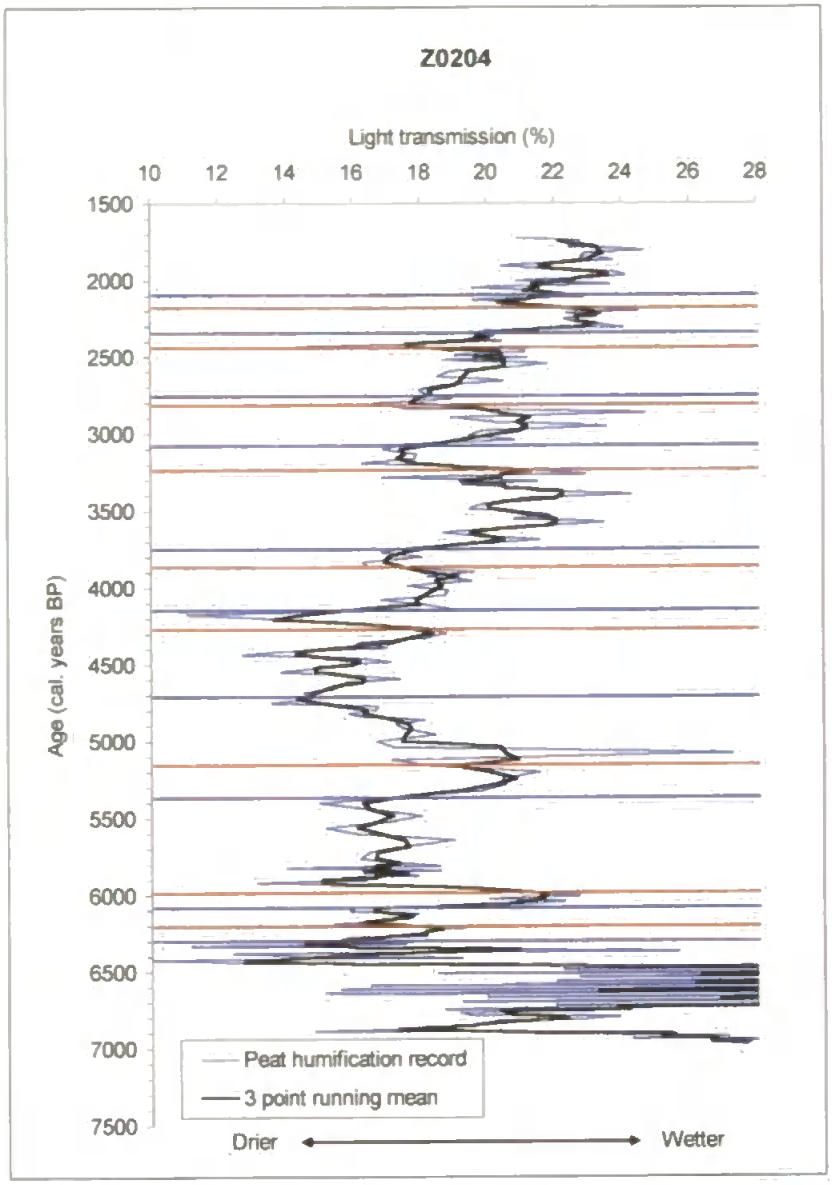

Figure 6.24 Corrected light transmission plotted against age for Z0204. Blue lines indicate wet shifts and brown lines indicate dry shifts.

Figure 6.24 also identifies the same mid-core change in light transmission trends as experienced in Z0106 and Z0108. The range of reduced values in the lower half of the core also seems to be manifest here as an upwards decline. This then changes to an increase in the baseline of values at a similar time period (4,500-4,000 cal. years BP) to the change in the other cores. These results also show an increase in variability in the upper half of the core, with more fluctuations in values after approximately 3,700 cal. years BP. These common trends between the three cores will be discussed further in Chapter 8.

Accumulation rate

The peat accumulation rate was calculated between the two tephra layers as 0.92 cm/10 years (2dp).

Plant macrofossils

The main vegetation trends, determined from plant macrofossil analysis of core Z0204 (*Figure 6.25*) are described here.

Four main zones were identified (by eye): a) pre-Tuhua to 6,500 cal. years BP (8.94-7.85 m) (Zone A), b) 6,500 to 5,300 cal. years BP (7.85-6.60 m) (Zone B), c) 5,300 to 2,800 cal. years BP (6.60-4.80 m) (Zone C) and d) 2,800 cal. years BP to post-Taupo (4.80-3.58 m) (Zone D).

The highest presence of dry-indicator *Gleichenia* remains, mainly leaves and sporangia, is between 7.80-6.80 m i.e. in Zone B, where leaves, sporangia and roots are all at their most abundant at the same time. There is a solitary peak in leaves at 5.10 m, coinciding with a charcoal peak, consistent with increased burning during dry periods. There is a dramatic increase in the abundance of other plant remain types at approximately 6.50 m (the start of Zone C), particularly *Epacris* and *Leptospermum* (suggesting very dry conditions) that coincides with a small peak in mineral content – possibly a tephra layer that was not visible for subsampling. *Epacris* and *Leptospermum* remains tend to peak synchronously, reinforcing the idea that they respond to the same environmental factors. However, *Epacris* seeds are present at lower depths, suggesting that their differential presence is perhaps a preservation issue, with the more resistant seeds better preserved. By comparing it to the peat humification curve, there is a slight trend to a lower baseline of humification values (relative to the rest of the core) below 6.50 m. *Sporadanthus* and *Empodisma* (wet indicator) remains are mainly preserved as seeds and seed-case parts, and are most common above approximately 7.70 m. *Sphagnum* remains, indicative of very wet conditions, are found sporadically throughout the core, only at five different sampling depths, but overall, numbers increase up-core. *Campylopus* is also present infrequently in the core, with a solitary peak at 5.58 m. Other remains, such as the (as yet) unidentified small, smooth brown seed, is present throughout the upper core section in a similar fashion to the *Epacris* and *Leptospermum* remains. The index of unidentifiable organic matter shows smooth fluctuations throughout the core, with no sudden peaks or changes.

Mid point ago (cal. years BP)

2
2
3
3
4
4
5
6

Fi

In order to facilitate the interpretation of the plant macrofossil counts, the separate counts of the various components of the main wetness indicator species were amalgamated to derive one value per species (*Figure 6.26*). For example, for *Epacris* the individual leaf, seed and bud counts were added together to produce a single value. Counts of the small, broken leaf fragments were omitted for each species, as they would have resulted in unrepresentatively high counts.

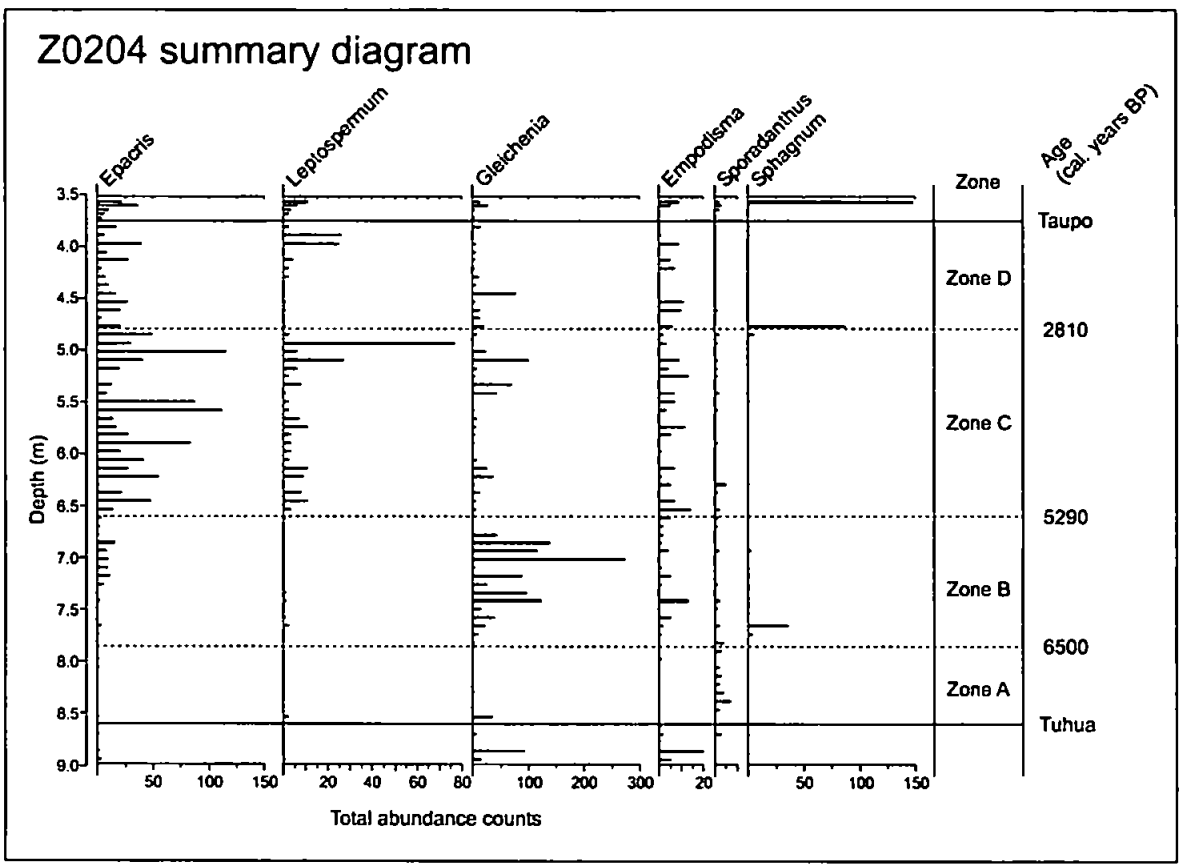

Figure 6.26 Combined abundance counts of the main plant macrofossil wetness indicator species.

In terms of palaeomoisture record, the plant macrofossil counts seem to suggest a lower-core dominance of dry species between 6,500 to 5,300 cal. years BP, followed by a dominance of drier species from 5,300-2,800 cal. years BP. However, wet indicator species are common throughout, and increase in relative abundance from 2,800 cal. years BP onwards, when the dry indicators decline. *Sphagnum*, indicating very wet conditions, is most abundant at the very top of the core. It should be noted that it is likely that the dry-indicator species are over-represented in the plant macrofossil record, due to their abundance of above-ground remains relative to the wet, restiad species.

To investigate further the relationship between the main indicator plant species (section 2.2.2) a CCA was performed using the surface environmental variable measurements and the plant species found at the sampling locations. The CCA plot is shown (*Figure 6.27*).

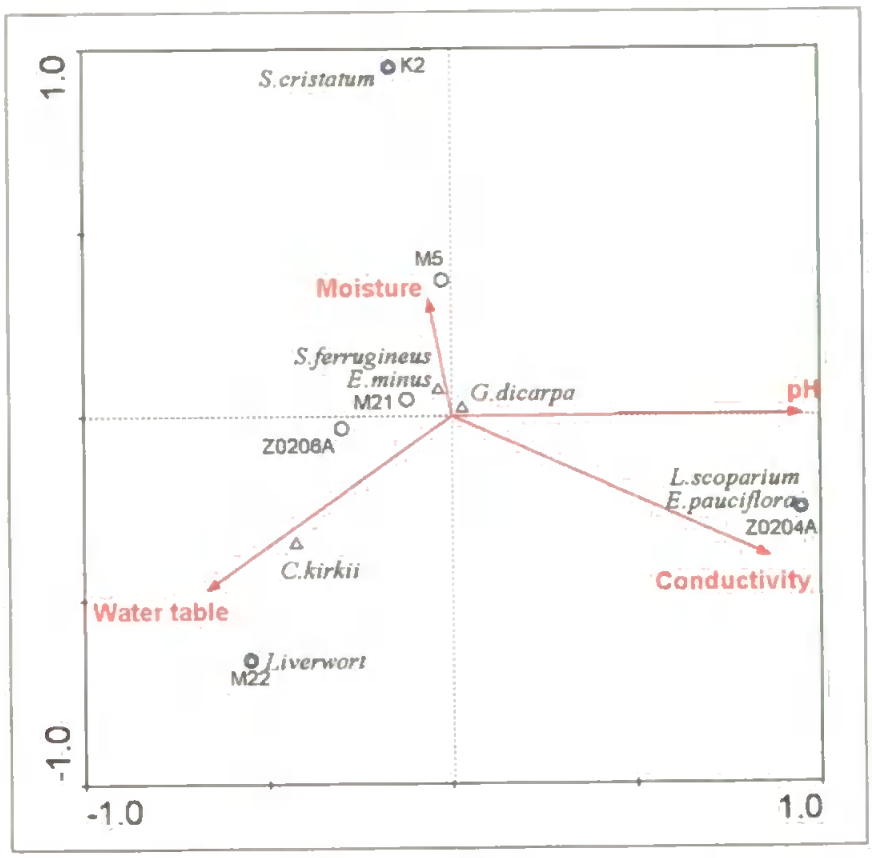

Figure 6.27 CCA plot of the surface plant macrofossils and environmental variables. Samples are also plotted.

	Axis 1	Axis 2
pH	**0.9415**	0.0052
Conductivity	0.8559	-0.3778
Depth to water table	-0.6631	**-0.4631**
Percentage moisture content	-0.0618	0.3129
Eigenvalue	0.390	0.276

Table 6.3 CCA results of the surface plant macrofossils and environmental variables.

Table 6.3 suggests that Axis 1 is explained by pH, and Axis 2 by the depth to the water table. The comparatively low level of explanation attributed to moisture-related variables (depth to water table and percentage moisture) was unexpected and perhaps is due to the small sample size. As a consequence, quantitative moisture reconstruction using these correspondence analysis results was not attempted. Instead, a macrofossil wetness indicator

was derived following Dupont (1986). Based on the previous knowledge of the indicator species' preferred moisture conditions (section 2.2.2), values were assigned according to a wetness gradient (*Table 6.4*). Value '3' was omitted to accentuate the difference between the wet and dry species.

Plant species	Moisture value
Epacris/Leptospermum	1
Gleichenia	2
Empodisma/Sporadanthus	4
Sphagnum	5

Table 6.4 Moisture indicator plant species and their assigned moisture value.

The plant macrofossil counts for these six species were then amalgamated into a total count for each species, and then weighted according to their abundance:

$$\text{Wetness index} = \left(\frac{\text{Abundance}_{S1}}{\text{Total abundance}} \times \text{value}_{S1}\right) + \left(\frac{\text{Abundance}_{S2}}{\text{Total abundance}} \times \text{value}_{S2}\right) + \ldots$$

where: abundance_{S1} = abundance of species 1

total abundance = combined abundance of indicator species

value_{S1} = moisture value of species 1

The results were compared to the light transmission record (*Figure 6.28*). These records show some degree of coherency, particularly between 5,000 to 3,700 cal. years BP, when the records both show relatively dry periods. These are preceded by a relatively wet phase peaking at approximately 5,300 cal. years BP, and followed by a wet phase peaking at approximately 3,500 cal. years BP. After approximately 4,000 cal. years BP, signals appear to be more variable and wetter than previously, suggesting agreement with the general peat humification trend from the site. The mid-Holocene trend to wetter conditions is clear in the peat humification record, but not so in the plant macrofossil index record.

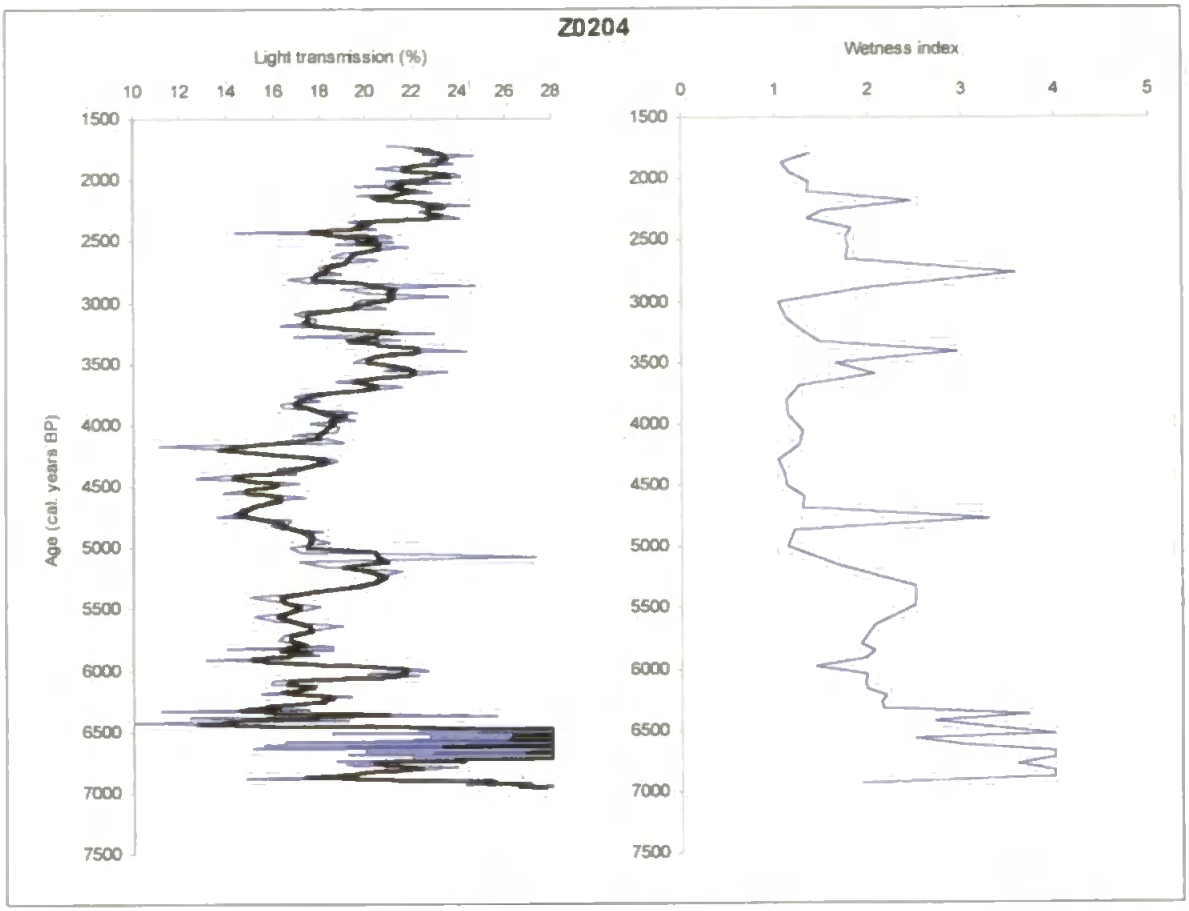

Figure 6.28 Peat humification record and plant macrofossil-derived moisture index. The black line indicates the 3-point running mean.

Charcoal

The plant macrofossil diagram (*Figure 6.25*) shows the fluctuations of charcoal throughout the core, with the main peaks occurring at 8.22 m, 7.18 m, 5.90 m, 5.26 m, 4.30 m and 3.70 m. Most of these peaks coincide either with a peak in *Gleichenia* remains or with those of *Epacris* and *Leptospermum* (*Figure 6.25*), all of which are relatively dry indicator species. The absolute count results of the group of fragments less than 1 mm matches well that of the fragments larger than 1 mm, and these in turn also show the same trends as the field-of-view percentage cover technique, suggesting that both methods can identify the same relative changes. Overall, the frequency and amplitude of charcoal peaks increase in the upper half of the core, after approximately 4,000 cal. years BP.

The charcoal record is compared with the peat humification record (*Figure 6.29*).

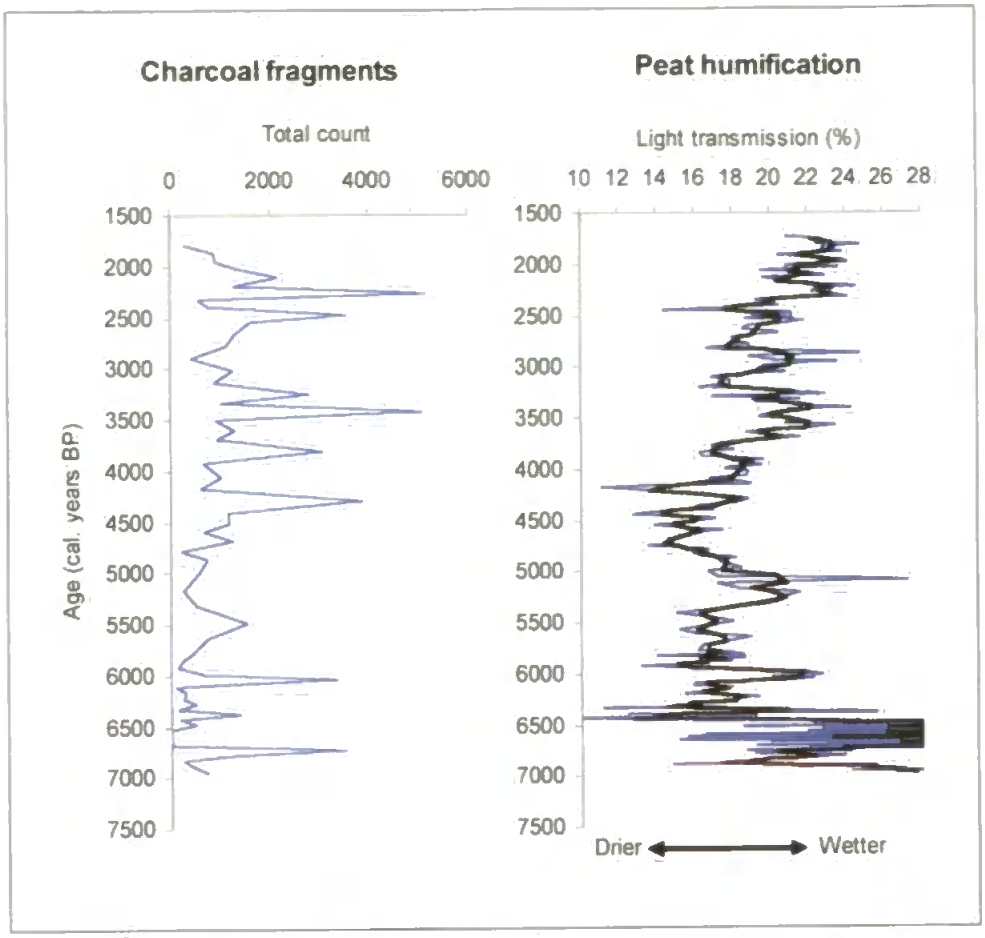

Figure 6.29 Charcoal and corrected peat humification records for Z0204 (with 3-point running mean represented by the black line).

Comparing the charcoal and peat humification records shows that there is a clear coincidence between the increased charcoal frequency (presumed to be related to drier conditions) and increased light transmission values (i.e. wetter conditions) commencing between 4,500 to 4,000 cal. years BP. This would initially appear to be contradictory in terms of palaeoclimate, but is nevertheless consistent with suggestions that the late Holocene climate became more variable (e.g. McGlone, 1988). The relationship between charcoal and humification results for Z0204 will be considered further, and in the context of other results presented in this thesis, in Chapter 8 (section 8.3). Prior to 5,000 cal. years BP, the main sustained charcoal peak coincides with a period of relatively drier conditions between approximately 6,000-5,400 cal. years BP. This would be expected, with drier peat burning more readily. In addition, from 5,400-4,700 cal. years BP, where there is a period of relatively wet conditions, there are very low charcoal counts. An exception to this trend is at around 6,000 cal. years BP where a peak in charcoal coincides with a peak in light transmission values.

Charcoal values typically show a sudden large increase directly above the tephra layers, particularly the Taupo Tephra (*Figure 6.25*), suggesting that the volcanic eruption could be responsible for initiating fire. The substantial charcoal band above the Taupo Tephra layer was clearly observed in the field (*Plate 6.6)*.

Plate 6.6 Taupo tephra and the thick charcoal band above it, clearly visible to the naked eye (the top of the core is to the left of the picture).

6.3.4 Palynology

Five samples were analysed for pollen from the clay layer of each core Z0106 and Z0204 by R. Newnham (University of Plymouth). Results indicate that the clay layers were deposited during the time of a marine incursion to the northern part of the bog, and as such cannot be used for the application of peat-based palaeo-proxies (Newnham, 2004, pers. comm.). For a detailed description of the results see Appendix 4.

6.4 Summary

This chapter has described the main palaeomoisture features from the three cores from Kopouatai, focusing on the peat humification records, and related these features to calibrated radiocarbon ages using appropriate age-depth models. Various age-depth models were derived for these cores, the most appropriate of which was considered to be joining the mid-points of the age ranges with linear interpolations. Further discussion and analysis of results is found in Chapter 8.

The main wet and dry periods identified consistently in either all or two of the three cores, were at approximately 6,000-5,500 (dry), 5,500-5,000 (wet), 5,000-4,500 (dry), 4,000-3,000 (wet) and 3,000-onwards (increasingly wet) cal. years BP. There is also a consistent longterm shift towards overall wetter conditions, commencing at 4-5,000 cal. years BP. A table of shifts is presented in Chapter 8, comparing results from Kopouatai with those from Moanatuatua.

The plant macrofossil results show a lower-core dominance of *Gleichenia* remains, suggesting dry conditions, which are then replaced by *Epacris* and *Leptospermum* at approximately 5,300 cal. years BP. As for the restiad remains, although their counts do not vary much throughout the core, they finally dominate after around 2,800 cal. years BP when *Epacris* and *Leptospermum* dramatically decline.

Charcoal results show that there is a clear increase in the frequency of charcoal after approximately 4,500 cal. years BP, suggesting increased fire occurrence from dry conditions. This does, however, coincide with the light transmission results from the same core, that show an increase in values at this time, indicating wetter conditions. This would agree with the development of a more variable climate in the late-Holocene i.e. wetter winters and drier summers, which has been suggested by McGlone (1988).

The next chapter presents and describes the results obtained from Moanatuatua.

CHAPTER SEVEN – RESULTS: MOANATUATUA

7.1 Introduction

Chronologies and analytical results are presented here for the three cores (Z0102 (Z0203/Z0205), Z0103 and Z0206) from Moanatuatua. The analytical approaches, methods and techniques employed are the same as those used in the previous chapter for the cores from Kopouatai (as described in detail in section 4.3).

7.2 Core chronologies

Identified tephra layers, together with the radiocarbon ages were used to derive the core chronologies.

7.2.1 Tephras

The chronological limits of the study period are defined by the Taupo and Tuhua tephras that were retrieved in all cores, and identified based on a combination of microprobe analysis and stratigraphical position (D. Lowe, University of Waikato).

Taupo (1,850±10 ^{14}C years BP (Lowe *et al.*, 1999); 1,650-1,800 cal. years BP)

This tephra layer was much nearer the surface in core Z0102 than any of the other cores because of drainage and farming practices that have removed the surface metre of peat. The layer was of similar physical characteristics to that deposited in Kopouatai; a distinctive yellow/brown pumiceous deposit only a few centimetres thick (*Plate 7.1*).

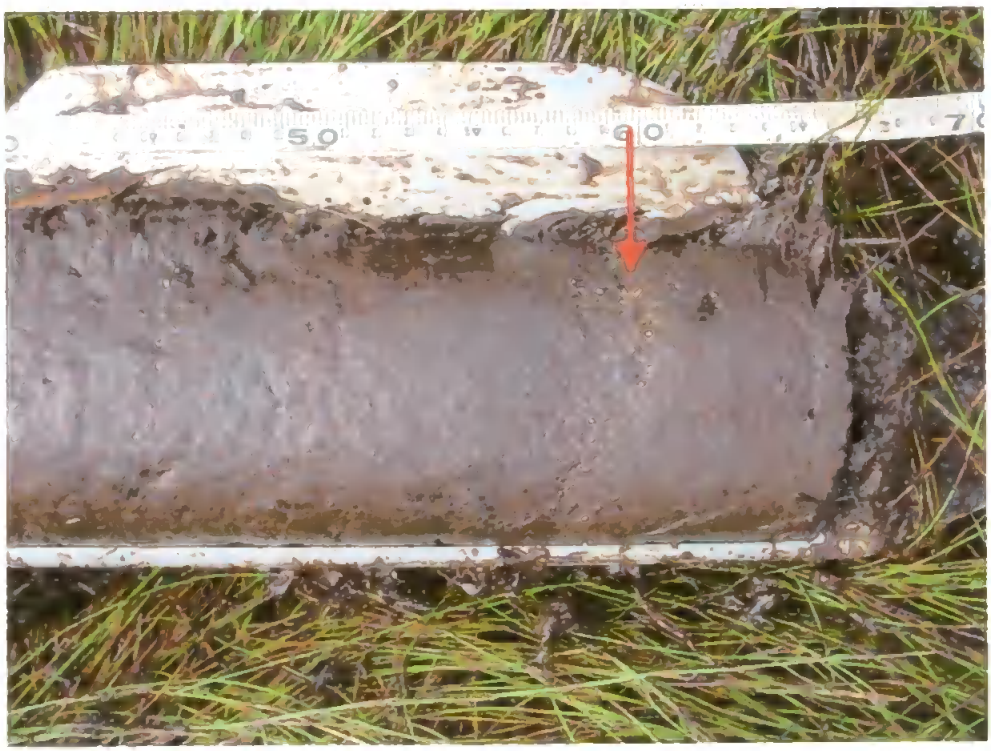

Plate 7.1 Taupo tephra from core Z0206 (the top of the core is to the left of the picture).

Whakaipo (2,685±20 ^{14}C years BP (Froggatt and Lowe, 1990); 2,750-2,800 cal. years BP)

This tephra was only found in core Z0102, approximately 0.50 m below the Taupo Tephra. It was a very fine, cream/white coloured tephra, and is thought to be the Whakaipo tephra. This provisional identification fits well with the radiocarbon ages obtained for the core (*Figures 7.2* and *7.3*).

Tuhua (6,130±30 ^{14}C years BP (Lowe *et al.*, 1999); 6,800-7,150 cal. years BP)

At this site, the Tuhua Tephra is very different in appearance to that deposited at Kopouatai. Here, it is a dark red/brown fine layer that grades into the peat (*Plate 7.2*). A sample from this tephra at Z0102 was identified by microprobe analysis. In the other two sites, identity is inferred on the basis of stratigraphical position and similar visual characteristics.

Plate 7.2 Tuhua Tephra in core Z0206 (the top of the core is to the right of the picture).

Mamaku (7,250±20 ^{14}C years BP (Lowe *et al.*, 1999); 7,950-8,100 cal. years BP)

The chemical composition of the tephra underlying the Tuhua Tephra found in cores Z0102 and Z0103 shows that it is most likely the Mamaku, or possibly the Rotoma (8,530±10 ^{14}C years BP; 9,473-9,529 cal. years BP) and that it is the same tephra as the possible Mamaku/Rotoma from Kopouatai.

A summary of the tephra geochemistry for Moanatuatua is presented (*Table 7.1*).

	Z0102 0.50-0.51 m	Z0102 1.02-1.03 m	Z0102 3.07-3.08 m	Z0102 3.36-3.37 m	Z0102 4.50-4.51 m	Z0102 5.22-5.23 m
Constituents	Percentage content (normalised)					
SiO_2	i/g	77.45	74.63	78.14	i/g	i/g
Al_2O_3	-	12.40	9.98	12.57	-	-
TiO_2	-	0.16	0.27	0.11	-	-
FeO	-	1.45	5.40	0.82	-	-
MnO	-	0.09	0.14	0.08	-	-
MgO	-	0.14	0.02	0.11	-	-
CaO	-	0.98	0.23	0.71	-	-
Na_2O	-	4.05	4.92	3.70	-	-
K_2O	-	3.13	4.16	3.59	-	-
Cl	-	0.15	0.24	0.17	-	-
n	-	4	11	11	-	-
Tephra ID	**Taupo**	**Whakaipo** (possible)	**Tuhua**	**Mamaku** (or Rotoma)	-	-

	Z0103 1.59-1.60 m	Z0103 4.895-4.905 m	Z0203 3.45-3.46 m	Z0206 1.57-1.58 m	Z0206 5.37-5.38 m
Constituents	Percentage content (normalised)				
SiO_2	75.47	78.20	77.52	75.32	77.59
Al_2O_3	13.43	12.36	12.57	13.50	12.62
TiO_2	0.26	0.11	0.11	0.21	0.10
FeO	1.94	0.85	0.88	1.81	0.92
MnO	0.12	0.08	0.06	0.12	0.09
MgO	0.27	0.10	0.14	0.26	0.13
CaO	1.49	0.72	0.75	1.40	0.73
Na_2O	4.08	3.82	3.99	4.32	4.00
K_2O	2.77	3.60	3.81	2.90	3.65
Cl	0.17	0.17	0.16	0.15	0.16
n	9	7	10	16	16
Tephra ID	**Taupo**	**Mamaku** (or Rotoma)	**Mamaku** (probably)	**Taupo**	**Mamaku** (probably)

Table 7.1 The main geochemical indicators of the Moanatuatua tephras, as identified from microprobe analysis by D. Lowe. i/g indicates insufficient glass counts for microprobing.

7.2.2 Radiocarbon dates

As before, all dates (AMS and bulk) were calibrated (*Table 7.2*) using the Southern Hemisphere dataset of CALIB v.4.4.2 (Stuiver and Reimer, 1993) as recommended by McCormac *et al.* (2002).

Sample number	Laboratory code	Depth (m) (corrected)	Type	Conventional age	Calibrated age (2 sigma)	Mid-point age	$\delta^{13}C$
Core Z0102							
1	Not available	0.79-0.80	AMS	n/a	Not available	n/a	n/a
2	SUERC-1508	1.08-1.10*	AMS	2,825±28	2,785-2,949	2,867	-28.0
3	SUERC-1511	1.38-1.39	AMS	3,434±29	3,483-3,805	3,644	-28.2
4	SUERC-1512	1.63-1.65*	AMS	3,789±29	3,985-4,230	4,107.5	n/a
5	SUERC-1513	1.92-1.93	AMS	4,474±29	4,871-5,276	5,073.5	-27.8
6	SUERC-1514	2.21-2.22	AMS	4,340±27	4,827-4,964	4,895.5	-28.2
7	SUERC-1515	2.48-2.49	AMS	5,574±29	6,282-6,403	6,342.5	-28.5
8	SUERC-1516	2.77-2.78	AMS	6,106±36	6,758-7,137	6,947.5	n/a
Core Z0203							
ZOE-1	Wk-11106	3.47-3.50	Bulk	6,071±127	6,568-7,244	6,906	-
Core Z0205							
ZOE-7	Wk-11112	5.32-5.35	Bulk	9,454±206	10,215-11,194	10,704.5	-
Core Z0103							
9	AA-54133	1.950-1.962	AMS	2,408±38	2,212-2,707	2,459.5	-28.5
10	SUERC-1473	2.370-2.382	AMS	3,111±28	3,171-3,360	3,265.5	-29.1
11	SUERC-1474	2.672-2.686	AMS	3,574±32	3,694-3,893	3,793.5	-28.2
12	SUERC-1475	3.015-3.025	AMS	3,801±33	3,988-4,237	4,112.5	-27.8
13	SUERC-1476	3.306-3.329*	AMS	4,386±35	4,835-5,031	4,933	-29.0
14	AA-54134	3.660-3.672	AMS	4,817±43	5,329-5,597	5,463	-28.4
15	SUERC-1480	4.025-4.036	AMS	5,466±40	6,001-6,302	6,151.5	-29.1
16	AA-54135	4.395-4.405	AMS	6,240±46	6,950-7,247	7,098.5	-28.2
Core Z0206							
33	SUERC-1490	1.96-1.97	AMS	2,139±24	1,993-2,147	2,070	-29.0
34	SUERC-1491	2.34-2.35	AMS	2,899±28	2,871-3,135	3,003	-28.5
35	SUERC-1492	2.71-2.72	AMS	3,256±26	3,362-3,473	3,417.5	-29.4
36	SUERC-1493	3.08-3.09	AMS	3,609±30	3,724-3,974	3,849	-28.3
37	SUERC-1495	3.46-3.47	AMS	4,294±32	4,650-4,868	4,759	-29.0
38	SUERC-1518	3.83-3.84	AMS	4,755±25	5,324-5,579	5,451.5	-29.3
39	SUERC-1521	4.21-4.23*	AMS	5,381±31	5,993-6,268	6,130.5	-28.1
40	SUERC-1522	4.58-4.59	AMS	6,079±37	6,751-6,990	6,870.5	-29.0
ZOE-2	Wk-11107	5.42-5.43	Bulk	5,952±152	6,358-7,176	6,767	-

*Table 7.2 AMS and bulk radiocarbon dates from Moanatuatua (conventional and calibrated). * indicates those samples where macrofossils were picked from intervals greater than 1 cm due to scarcity of suitable material in the usual 1 cm interval. AA- and SUERC- samples were processed in two separate batches at the NERC Radiocarbon Laboratory (East Kilbride) and Wk- samples at the University of Waikato (New Zealand).*

A series of chronologies were developed, tying together records between cores (*Figure 7.1*).

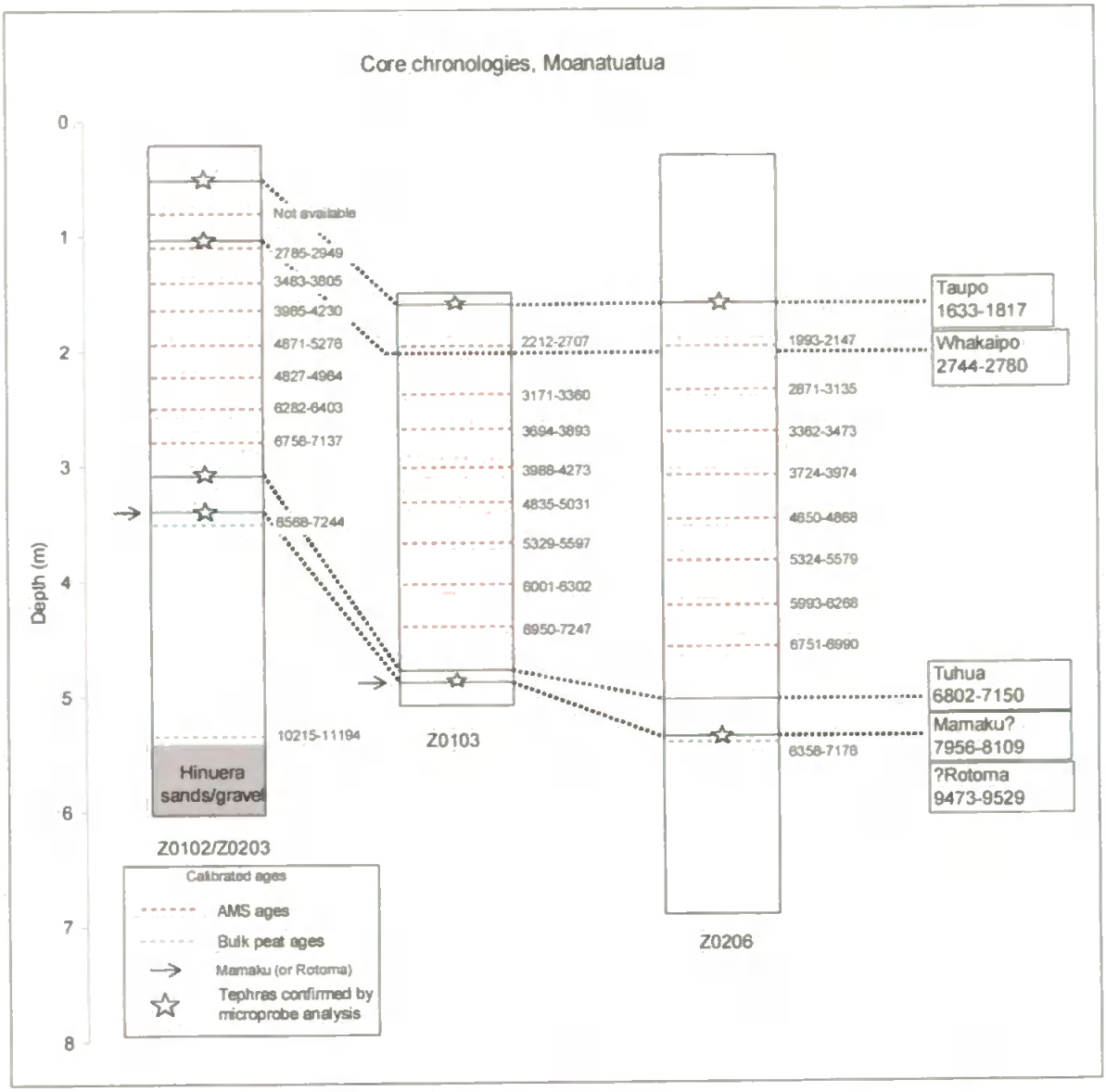

Figure 7.1 Core chronologies from Moanatuatua, showing tephra and radiocarbon ages. Tie-lines drawn between cores join tephra layers of the same age. Tephras are drawn at the depth of their peak in mineral content (hence the lowest AMS age in core Z0204 appears to be above the Tuhua Tephra). Some tephras were sub-sampled for microprobe analysis before transit i.e. before they suffered compression. Depths of these are plotted as near to their original depth as possible, based on comparisons with the TOC curves.

7.2.3 Age-depth models

Age depth models were derived for each core from the AMS and tephra ages obtained, using the same criteria as the cores from Kopouatai – including the mid-point age value and the mid-point depth. Tephras were considered to begin where TOC values fell below 45% in Z0102 and Z0206, and below 50% in Z0103. The bulk peat ages were omitted from the age-depth models for a variety of reasons that are explained below for cores Z0102 and Z0206.

The same selection of age-depth models was used as for Kopouatai – a) a polynomial, b) linear interpolation, c) fitting linear relationships to the AMS dates separately from the tephra dates, and d) fitting a number of linear relationships to the data by eye. Below, each core and their age-depth models derived are discussed.

Z0102

In this core, there are only seven AMS ages (rather than the usual eight) between tephra layers, due to an error in processing for one of the samples (0.79-0.80 m). This depth was resampled, but the age was not returned in time for this project write-up. Its age was 1962±24 (with a $\delta^{13}C$ value of -27.8) which appears to fit in well with the other AMS and tephra ages.

The calibrated radiocarbon ages of Z0102 are presented (*Figures 7.2* and *7.3*).

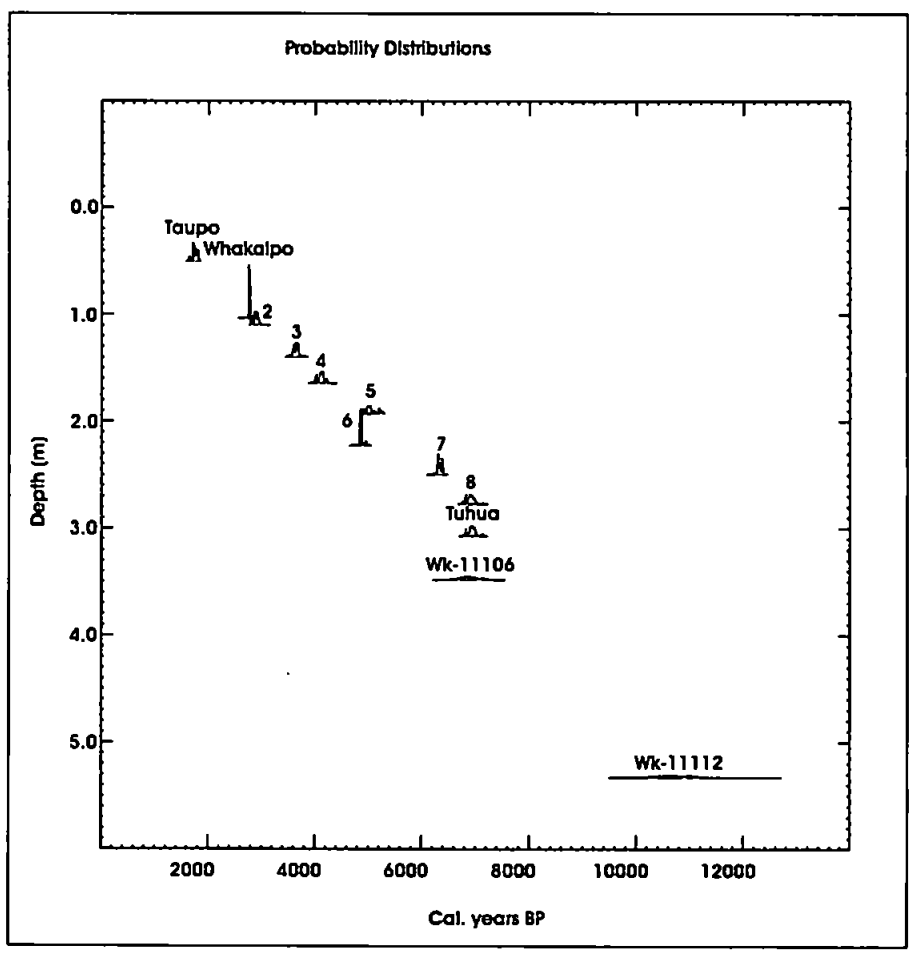

Figure 7.2 Probability plots for the calibrated radiocarbon and tephra ages of Z0102. Wk-11106 and Wk-11112 are bulk peat ages; the others are AMS ages on plant macrofossils.

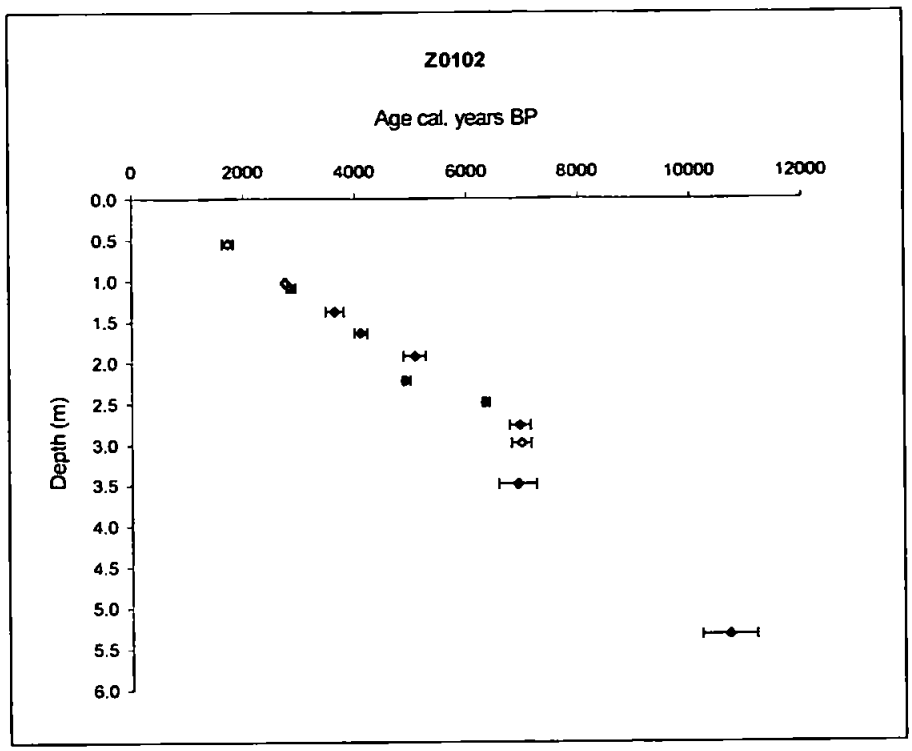

Figure 7.3 Age-depth plot with error bars for all radiocarbon ages obtained from core Z0102 (Z0203 and Z0205). Blue symbols are AMS ages, yellow symbols are the well-established radiocarbon ages of the Taupo and Tuhua tephras, red symbols are bulk peat ages, and the green symbol is the additional Whakaipo Tephra.

These plots suggest that the radiocarbon age (SUERC-1514) at 2.215 m is an age reversal, so this age will be omitted from the age-depth models. The bulk peat ages were omitted because they were not taken from core Z0102, but from a parallel core (Z0203/Z0205) and so it is not guaranteed how these cores exactly tie up to each other. They also appear to be slightly young compared to the rest of the ages.

All age-depth models are shown in *Figure 7.4*.

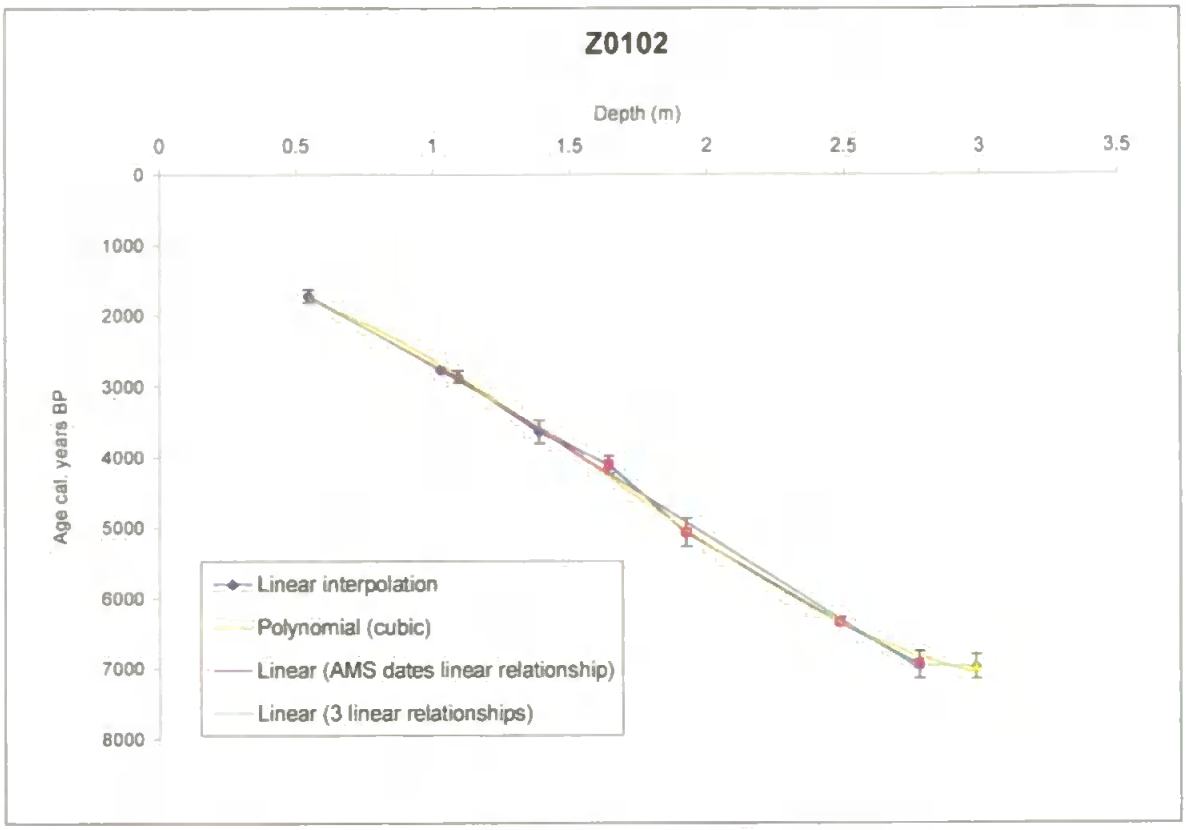

Figure 7.4 The age-depth models for Z0102 plotted on the same axis.

The cubic trendline passed through both the tephra age ranges as well as the majority of AMS ages. However, its use could not be justified because the distribution of ages were scattered to both sides. The linear interpolation model was passed through the mid-point of each age range. When considering the AMS ages separately from the three tephra layers, this resulted in a high accumulation rate around the Tuhua Tephra that is very different to rates throughout the rest of the core, suggesting that this model is not ideal. (The trendline fitted between the Taupo Tephra and the end of the AMS trendline was also fitted through the Whakaipo tephra). Using a series of linear relationships through the ages, three lines were fitted (0.545-1.640 m, 1.640-2.775 m and 2.775-2.985 m) that showed a slight increase in accumulation rates mid-core. However, the best fit of lines meant that there was a substantial difference in accumulation rates at the base of the core.

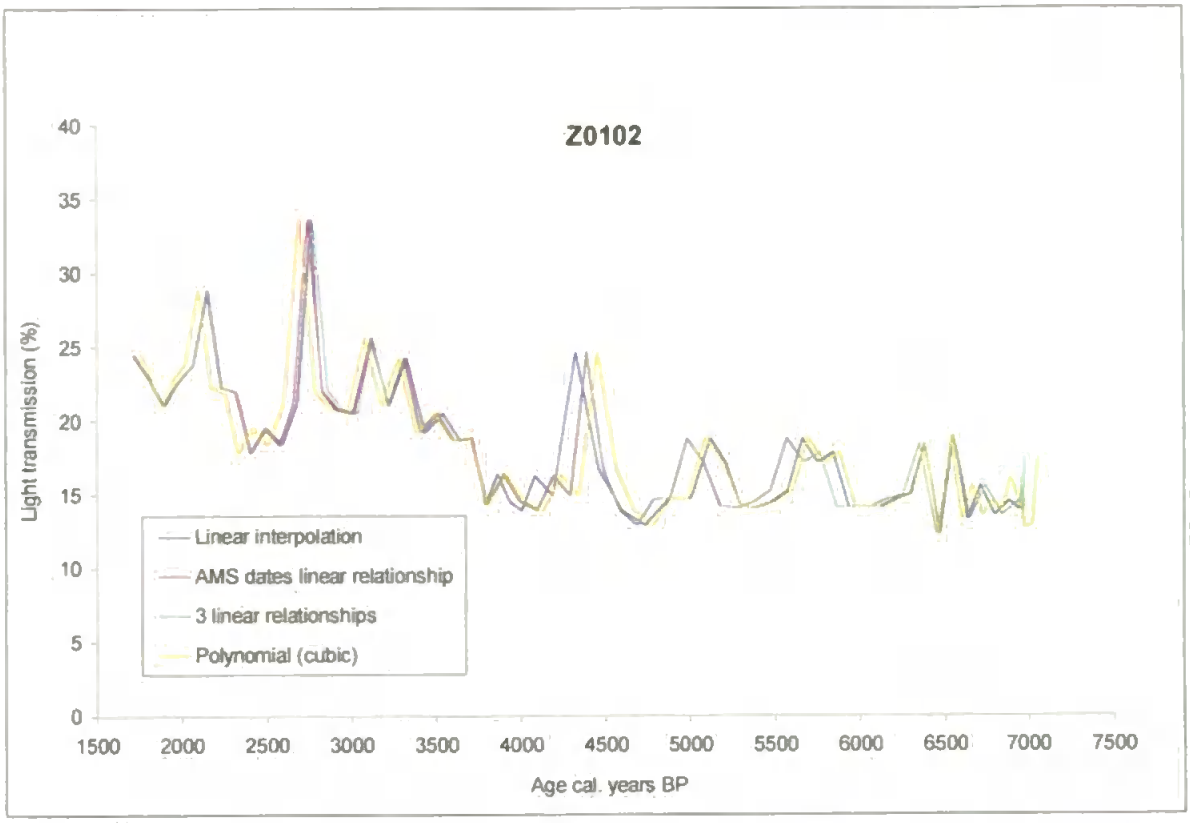

Figure 7.5 The peat humification record plotted against the ages derived from the four main age-depth models for Z0102.

In all the models the calculated ages are very similar (*Figure 7.5*). The greatest difference between models at any one point is approximately 140 years and that is for the peak occurring around 5,000 cal. years BP. The model that used using three linear relationships (determined by eye) and that which joined the AMS ages with a single linear model are almost exactly the same as each other throughout the core, and the linear interpolation and cubic models are also quite similar to each other in most places.

Z0103

The calibrated radiocarbon ages of Z0103 are presented (*Figures 7.6* and *7.7*).

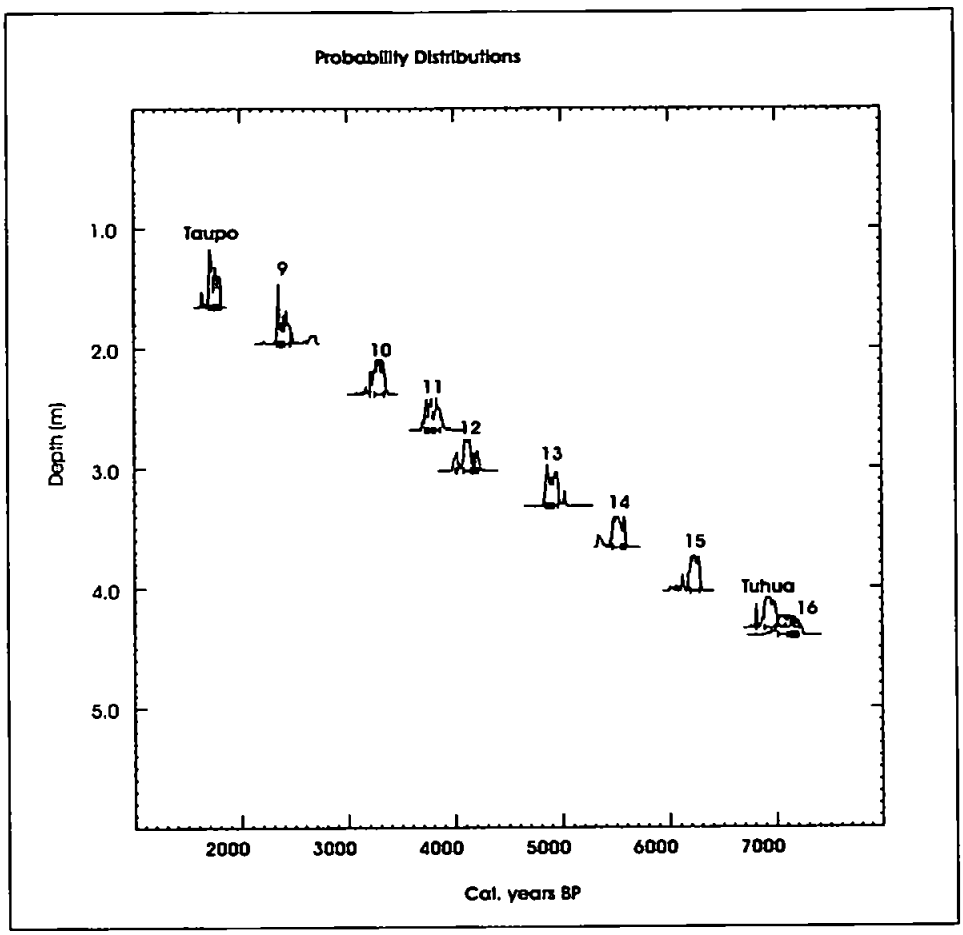

Figure 7.6 Probability plots for the calibrated radiocarbon and tephra ages for Z0103.

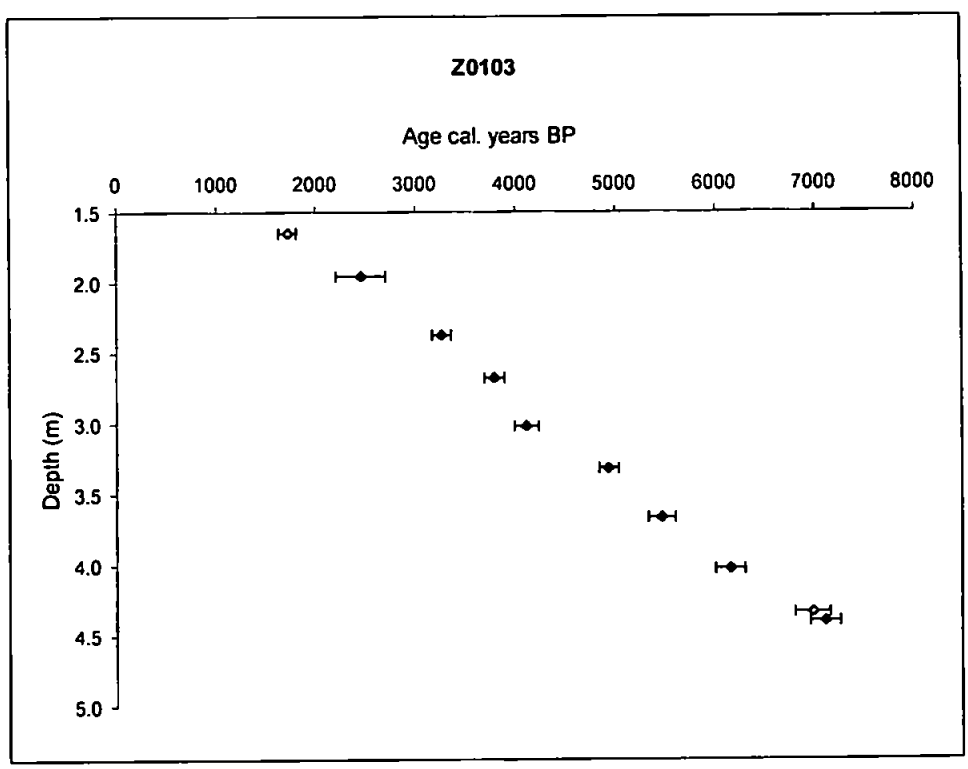

Figure 7.7 Age-depth plot with error bars for all radiocarbon ages obtained from core Z0103. Blue symbols are AMS ages and yellow symbols are the well-established ages of the Taupo and Tuhua tephras.

There are no age reversals in this suite of radiocarbon ages. However, using the TOC values to identify the extent of the tephra layers, the AMS age at 4.4 m (AA-54135) actually falls below the top of the Tuhua Tephra layer and is older. This AMS age was excluded from the age-depth model, since it is in fact beyond the timescale of this study. (Note that in *Figure 7.1* this age appears to be plotted above the Tuhua Tephra, as the tephra layer was drawn where its maximum concentration occurred).

All age-depth models are shown in *Figure 7.8*.

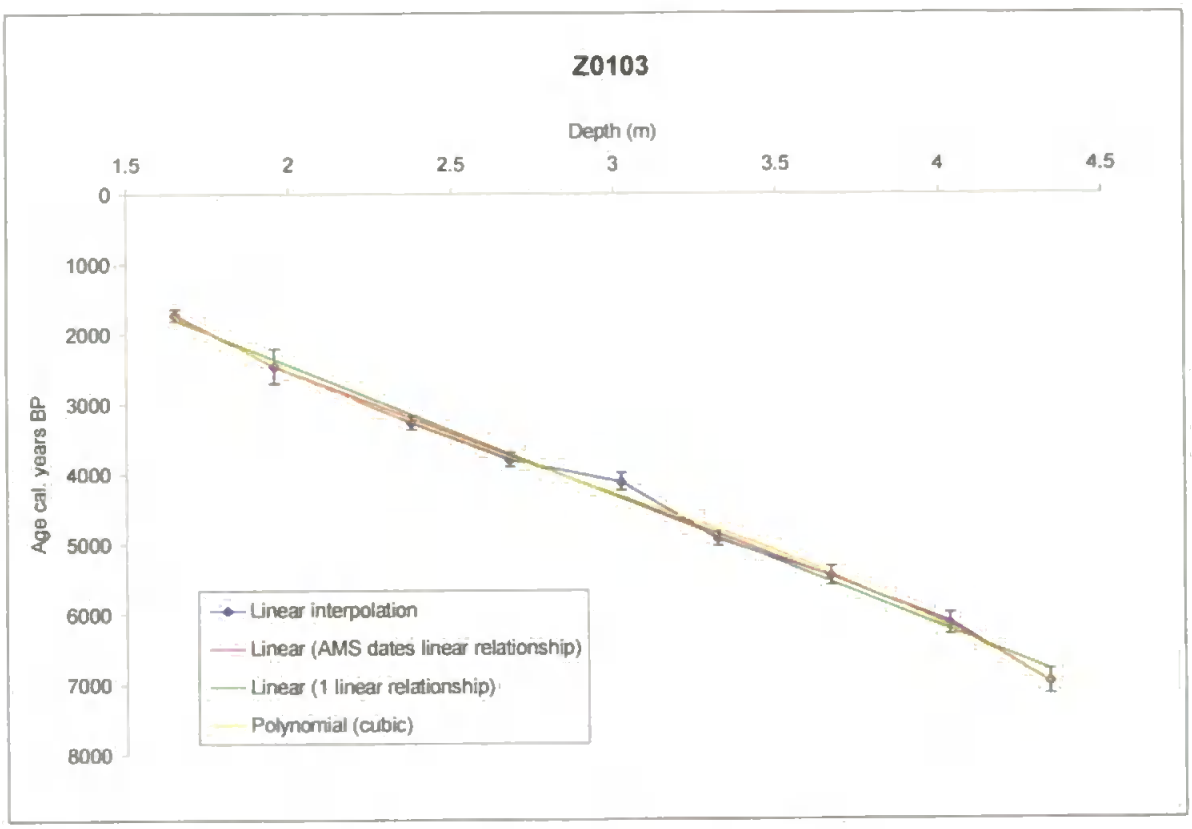

Figure 7.8 The age-depth models for Z0103 plotted on the same axis.

The cubic, best-fit line passes through the mid-points of the tephra age ranges, and through most of the AMS age ranges. The residuals are scattered either side of the line, suggesting that this model is appropriate for this data. Because one of the AMS ages falls outside the tephra-defined period, there are only eight separate linear relationships when applying linear interpolation to the series. When considering the AMS data from the rest of the series, the best-fit linear regression line passes through all but one of the AMS age ranges. When fitting multiple regression lines on the series, the best option is a single line. Using two lines meant that the Taupo Tephra age range was missed, even though it did show the same mid-core increase in accumulation rate as for Z0102.

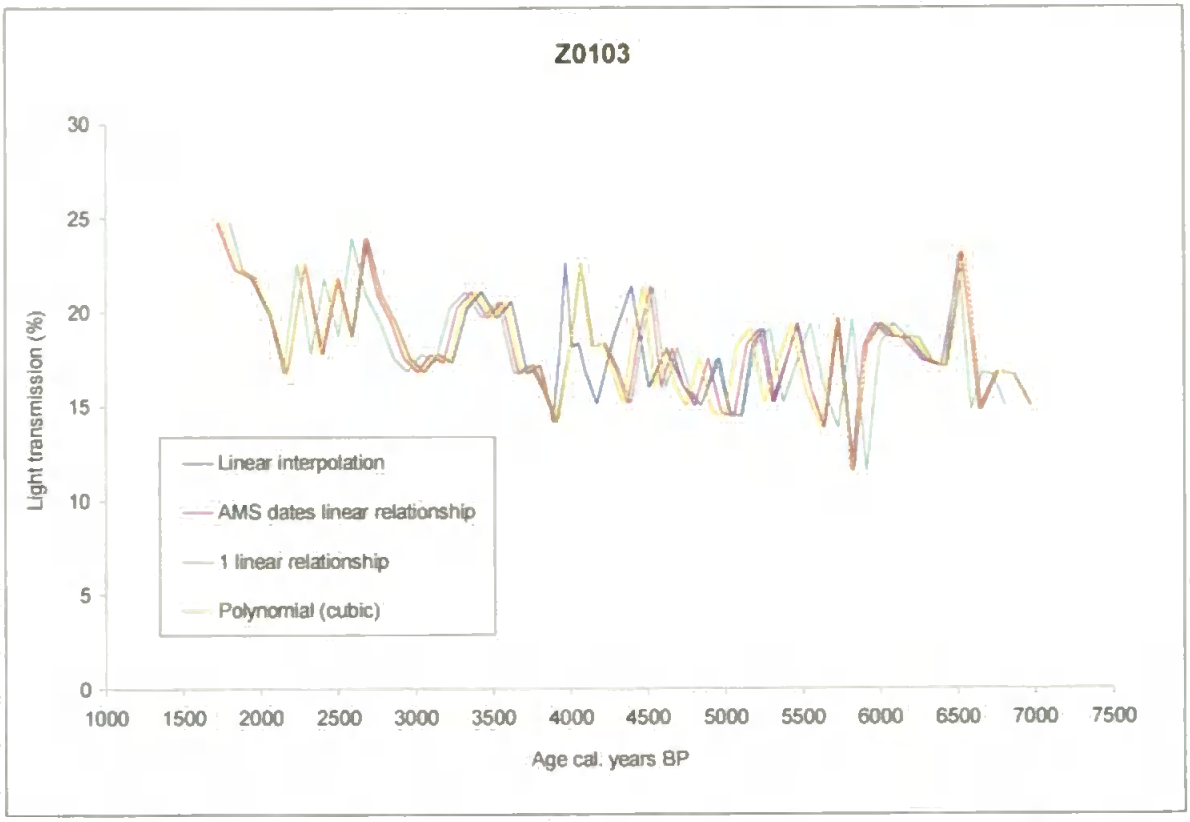

Figure 7.9 The peat humification record plotted against the ages derived from the four main age-depth models for Z0103.

Overall the age-depth models perform similarly throughout (*Figure 7.9*). The linear regression line fitted through all the data shows stronger variance with the other models for the upper and lower thirds of the series. However, in the middle section of core, linear interpolation shows the strongest variance – the greatest difference at any point is approximately 145 years at the 4,500 cal years BP peak.

Z0206

The calibrated radiocarbon ages of Z0206 are presented (*Figures 7.10 and 7.11*).

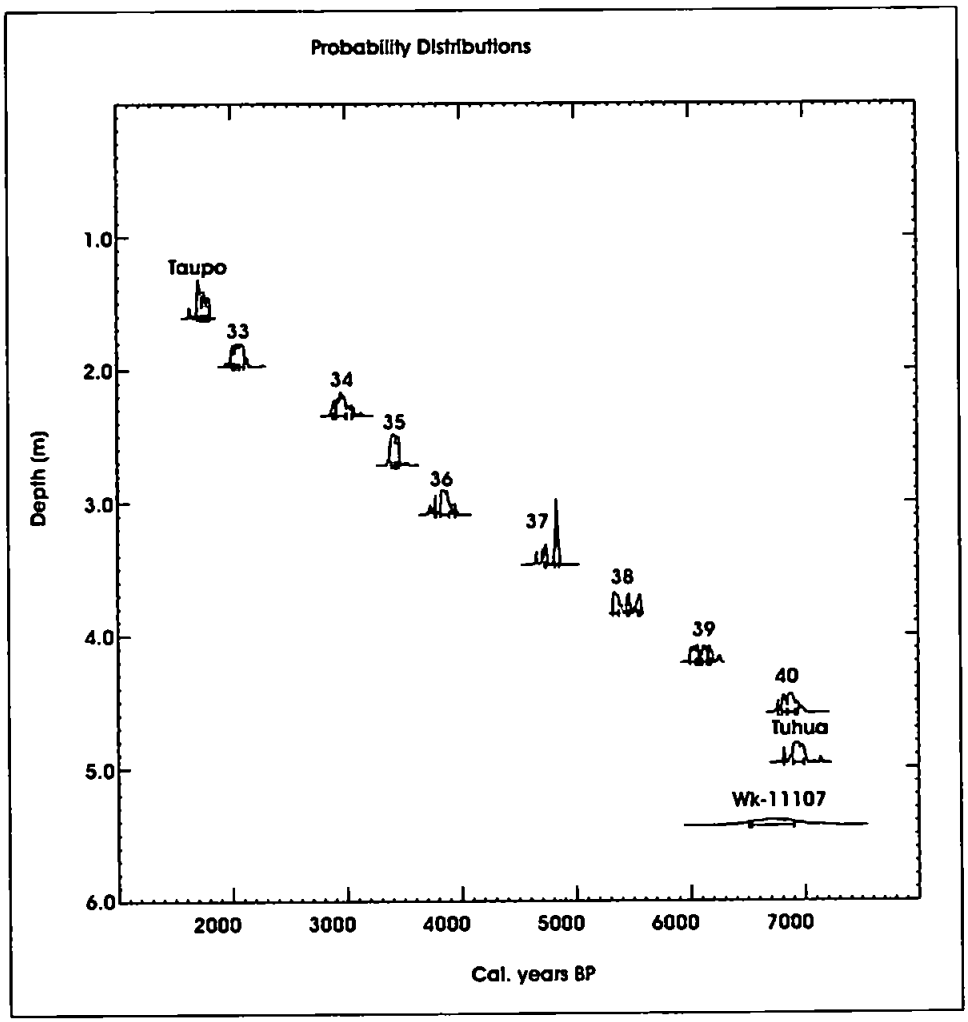

Figure 7.10 Probability plots for the calibrated radiocarbon and tephra ages for Z0206. Wk-11107 is the bulk peat age; the others are AMS ages on plant macrofossils.

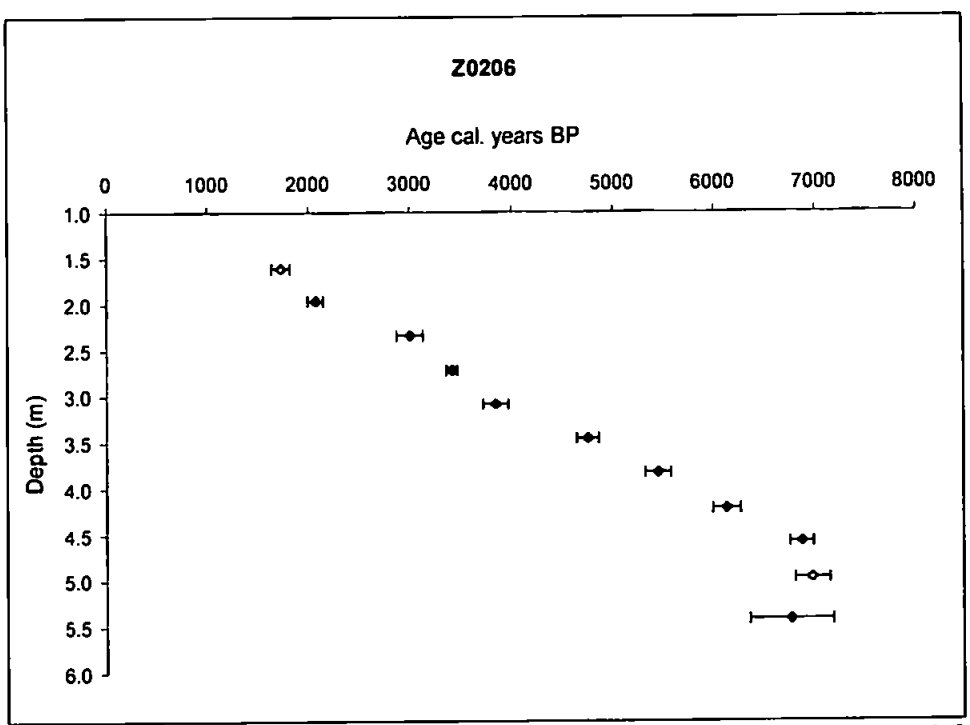

Figure 7.11 Age-depth plot with error bars for all radiocarbon ages obtained from core Z0206. Blue symbols are AMS ages, yellow symbols are the well-established ages of the Taupo and Tuhua tephras, red symbols are bulk peat ages

Excluding the bulk date that appears to be too young for the rest of the sequence, there are no age reversals within this core.

All the age-depth models are shown in *Figure 7.12*.

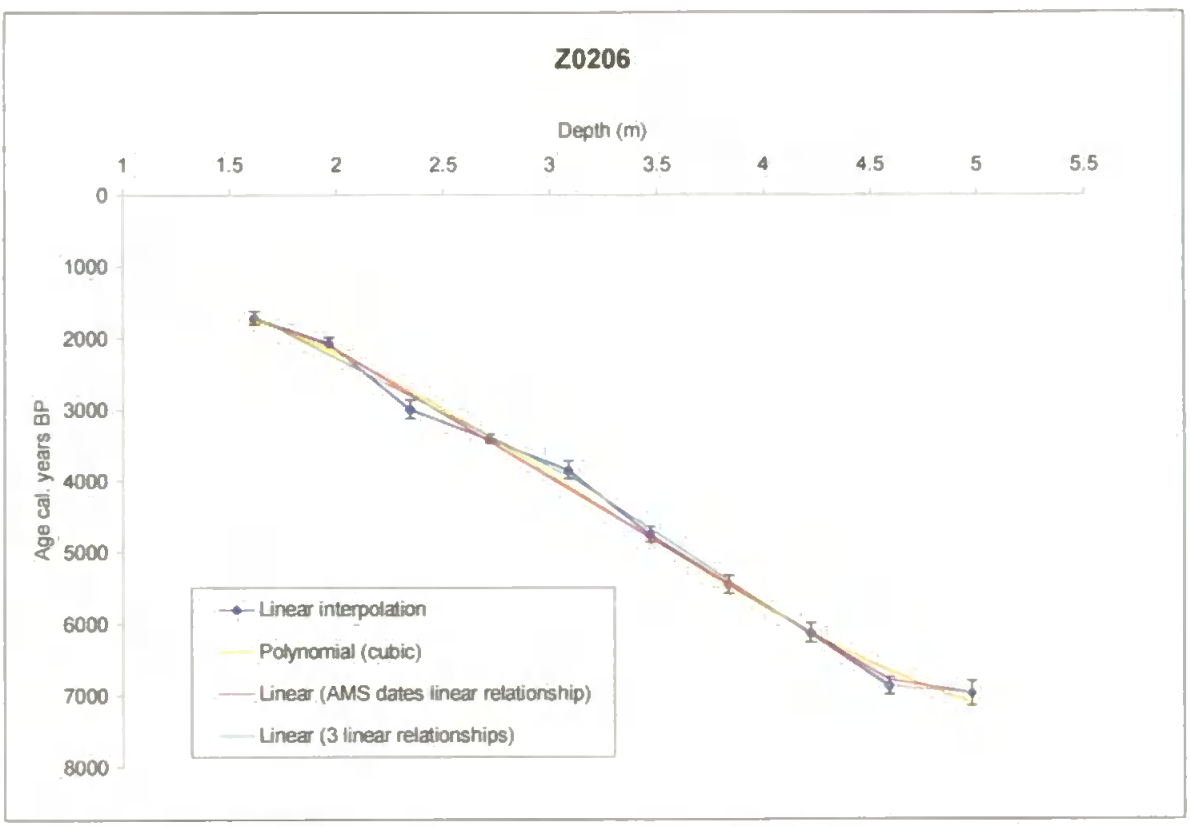

Figure 7.12 The age-depth models for Z0206 plotted on the same axis.

The cubic model passed through the majority of AMS age ranges, as well as through both tephra error ranges. However, the majority of ages plotted above the model, suggesting that there is some pattern in the residuals, and hence it should not be used since it is a poor model for this data. Because all the AMS ages are used, the linear interpolation method resulted in nine separate linear relationships. The model using the AMS ages separately from the tephras was straightforward, with no age reversals or steep changes in accumulation rates. Using three linear models (4.975-4.585 m, 4.585-3.085 m and 3.085-1.615 m) within the same model shows a mid-core increase in accumulation rates as demonstrated in all cores, but it also shows a very high accumulation rate at the base of the core. Using three lines was, however, the best way of fitting linear relationships to the ages.

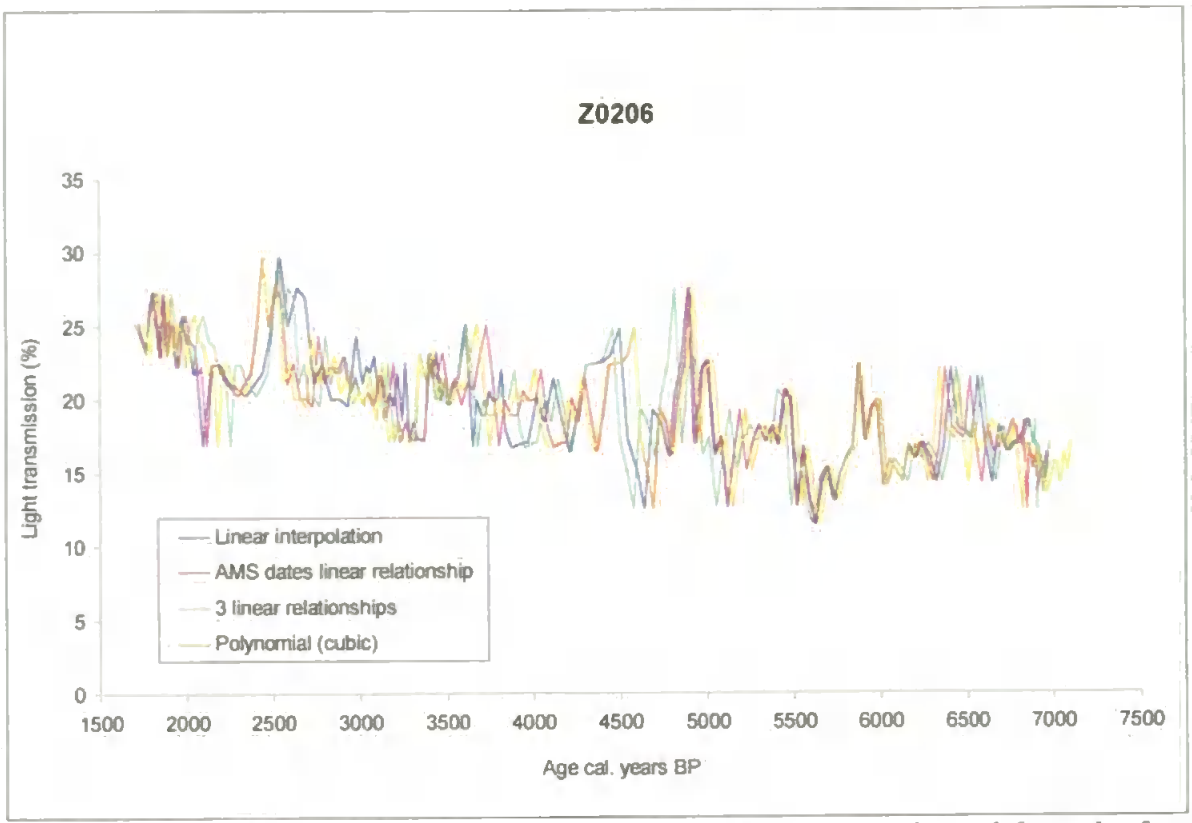

Figure 7.13 The peat humification record plotted against the ages derived from the four main age-depth models for Z0206.

Comparing the four models (*Figure 7.13*) shows that they all perform similarly. Throughout the majority of the core, the cubic and 'AMS linear' methods are most similar to each other, as are the linear interpolation model and that derived from three separate linear models. Between approximately 6,500-5,500 cal. years BP all four models are extremely similar. The greatest difference between models at any point is approximately 155 years at the sharp fall in values between 2,100-2,200 cal. years BP.

The final models

As with the cores from Kopouatai and for the same reasons given in the final section of section 6.2.3, the preferred age-depth model chosen was that of linear interpolation. The selected age models for the three cores are presented in *Figure 7.14*.

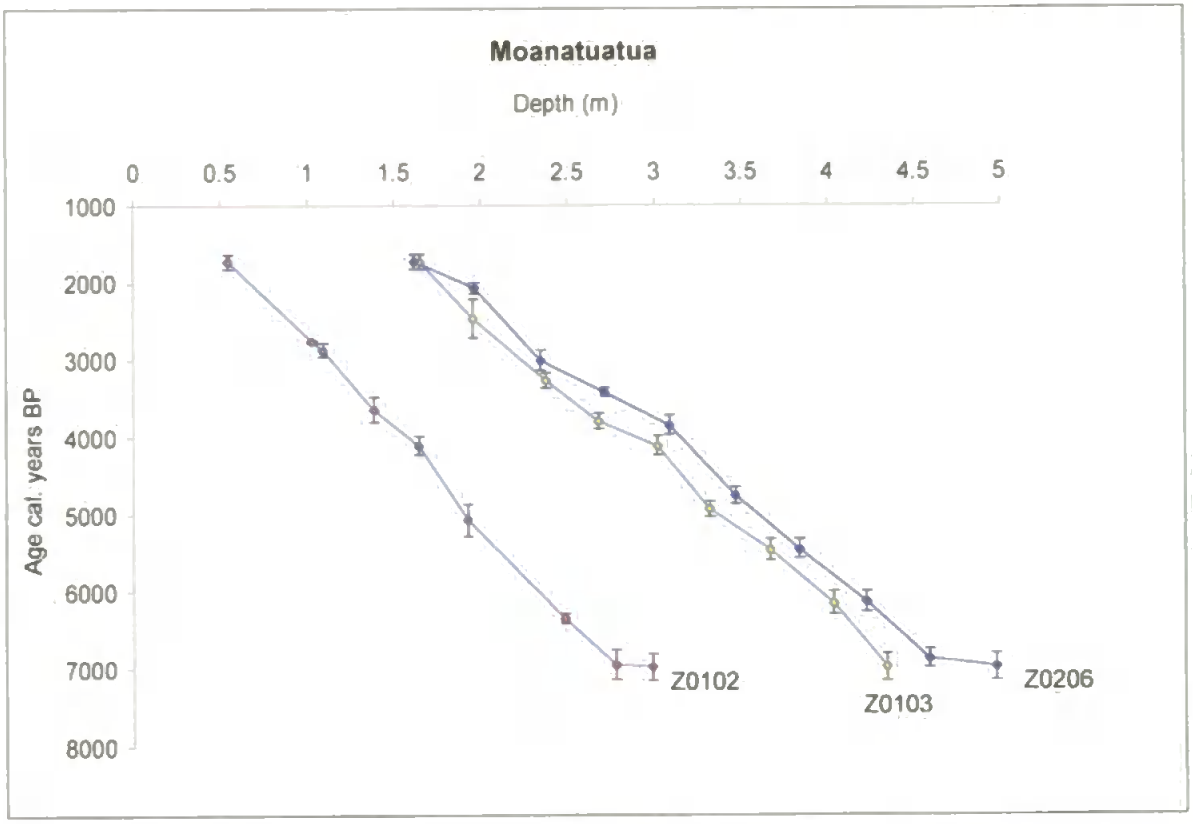

Figure 7.14 Linear interpolation age-depth models for Z0102, Z0103 and Z0206 from Moanatuatua.

All three age-depth models are similar to each other, with similar trends and changes in accumulation rates. The most noticeable difference is at the very base of the cores, where Z0102 and Z0206 show very high accumulation rates compared to Z0103. This is explained by the presence of the tephra layers. Although the definition of the top of the Tuhua Tephra layer is consistent between cores, it is likely that the input of tephra affects the apparent rate of peat accumulation in the peat immediately above the tephra.

In addition to the errors involved with the age-depth models, there are those associated with the radiocarbon ages themselves (*Figure 7.15*).

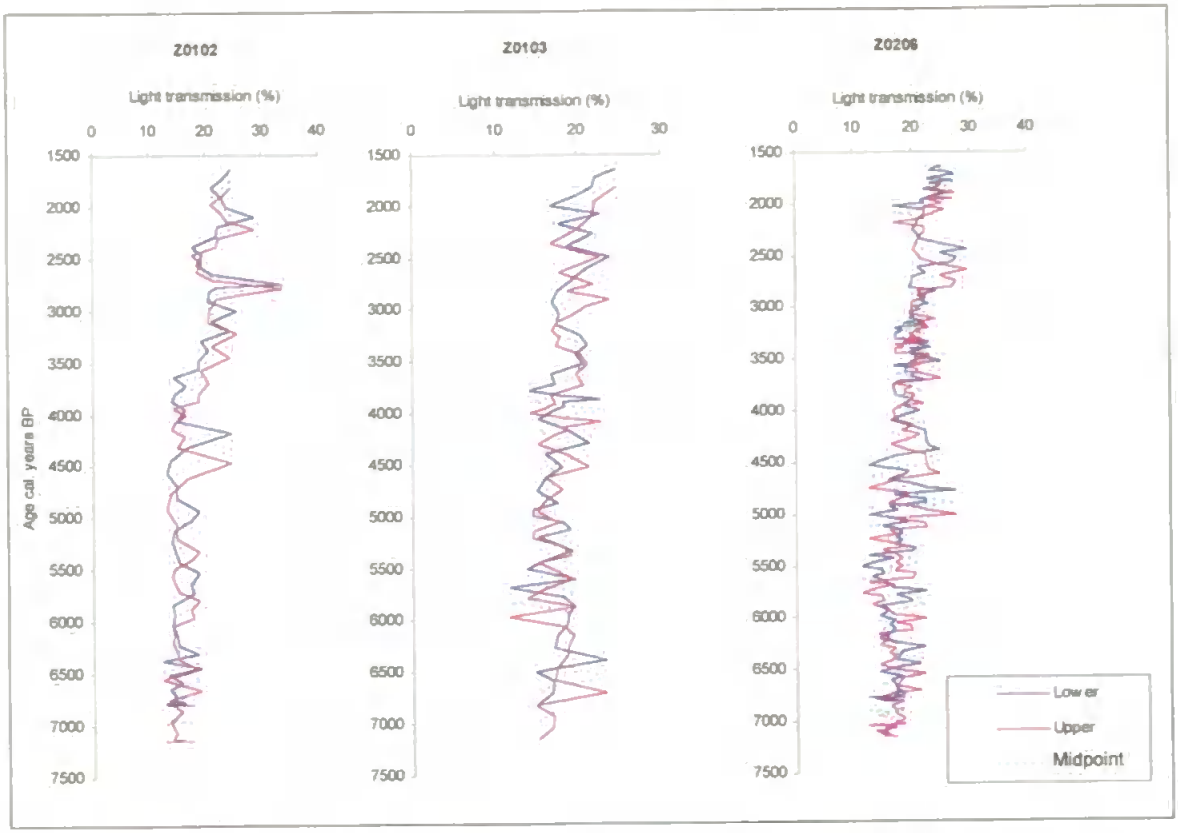

Figure 7.15 The effect of radiocarbon age ranges on humification profiles. The range in ages between the lower, mid-point and upper values of the calibrated radiocarbon ages using the same linear interpolation approach for each.

For each core, the maximum range between using the lower and upper calibrated age ranges are 395, 407 and 267 years for Z0102, Z0103 and Z0206 respectively (*Figure 7.15*). From this it is possible to see that shifts/events that initially might not seem to coincide, could actually be present in multiple cores within the error ranges.

These age-depth relationships are used in the next section which presents the analytical results for each core.

7.3 Analytical results

In this section results are presented for each core individually. Peat humification results are shown in their uncorrected and corrected form. Simplified core stratigraphies are presented here; for a detailed description see Appendix 3. All shifts are discussed to the nearest 50 years.

7.3.1 Core Z0102 (*Figure 7.16*)

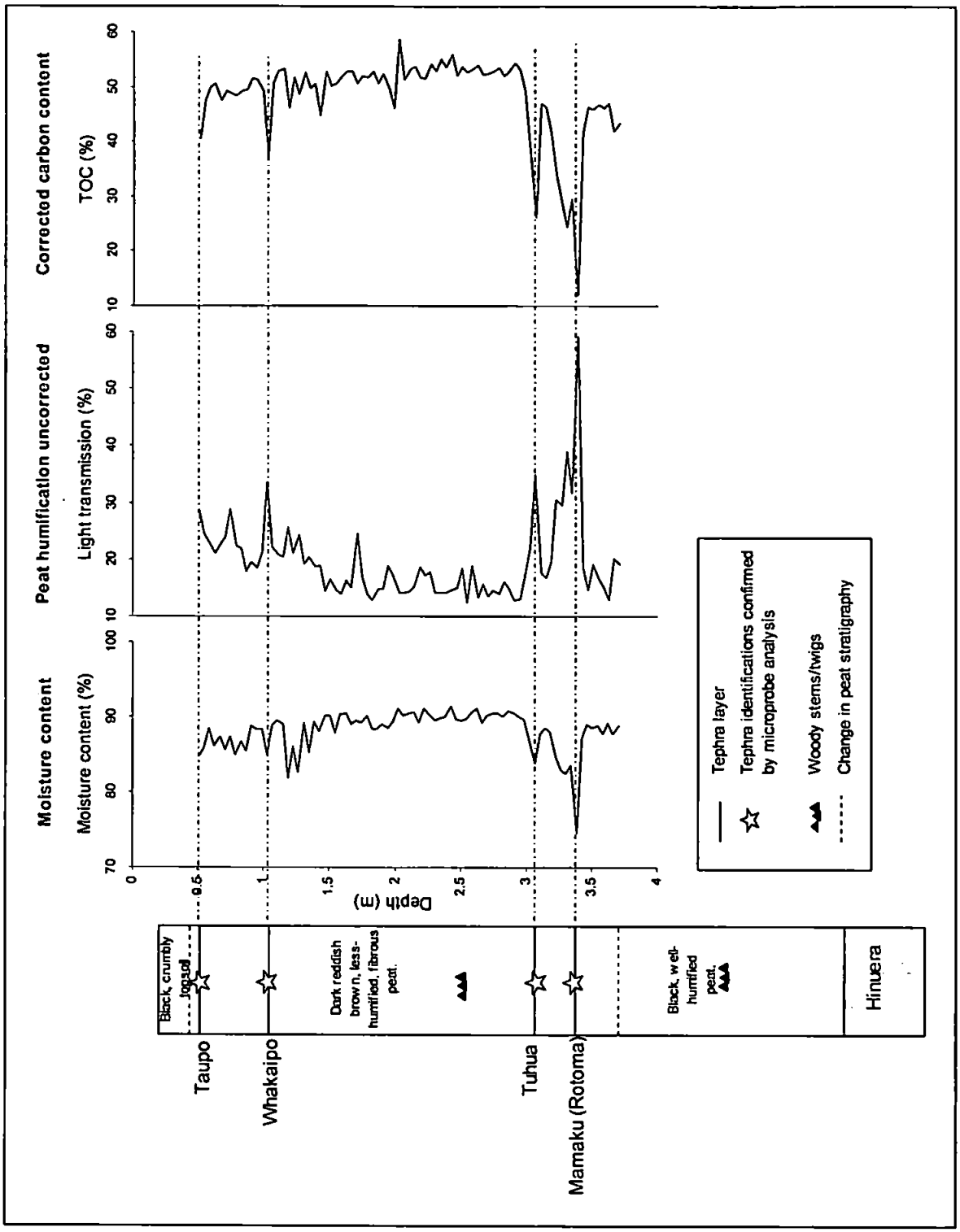

Figure 7.16 Z0102 core stratigraphy, moisture content, raw peat humification and corrected TOC results.

Core stratigraphy (*Figure 7.16* and Appendix 3)

This core is the only core that retrieved the full Holocene peat record of Moanatuatua, extending back to the bog's inception on top of the basal Hinuera sediments. There are no major changes in peat composition through the core – the main change is at 3.70 m, where

the boundary between the deeper, more humified peat and the upper, more fibrous red-coloured peat, was identified. The uppermost 0.50 m, from the Taupo Tephra layer upwards, is comprised of dry, crumbly topsoil, formed from drainage and farming of the area. The mid-core Tuhua and Mamaku tephra layers are clearly visible, and woody remains were found at 2.50 m and 4.50 m.

Moisture content (*Figure 7.16*)

Peat values generally vary around 90% moisture content, with a general up-core trend of declining moisture content. A marked change to lower overall moisture content occurs at around 1.50 m, coincident with changes in TOC and humification.

Carbon analysis (*Figure 7.16*)

The overall trend in the TOC record is of a decline in content upwards throughout the core. The fall is more pronounced above approximately 2.1 m, before which TOC values remain relatively constant. This pattern mirrors that of the peat humification record.

The more-minerogenic samples (with low TOC content) also have low moisture content, since they are not able to hold as much water as peat. TOC values also clearly identify the tephra layers within the peat, including the relatively obscure Whakaipo layer that is situated between the Taupo and Tuhua tephras. There is a large increase in TOC at 2.03 m (but only in this one data point) reaching nearly 60%, and two sharp falls at 1.99 m and 1.43 m. There is an overall trend of declining TOC values upwards through the core. As for Kopouatai, samples with relatively low carbon content were viewed under the microscope for the presence of glass shards. At 1.19 m there were extremely low counts, at 1.99 m there were more significant counts, but at 1.43 m there was a large amount, suggesting that the presence of tephra is responsible for affecting the carbon content.

Peat humification (*Figure 7.17*)

Raw and corrected light transmission values are presented here. Light transmission values increase up-core, part of which is likely related to the decrease in peat age, but which also might reflect increasingly wetter conditions. Also of interest, is that whilst moisture content declines upwards, light transmission values increase, suggesting wetter conditions caused by a lower water-retention capacity of less-decayed peat.

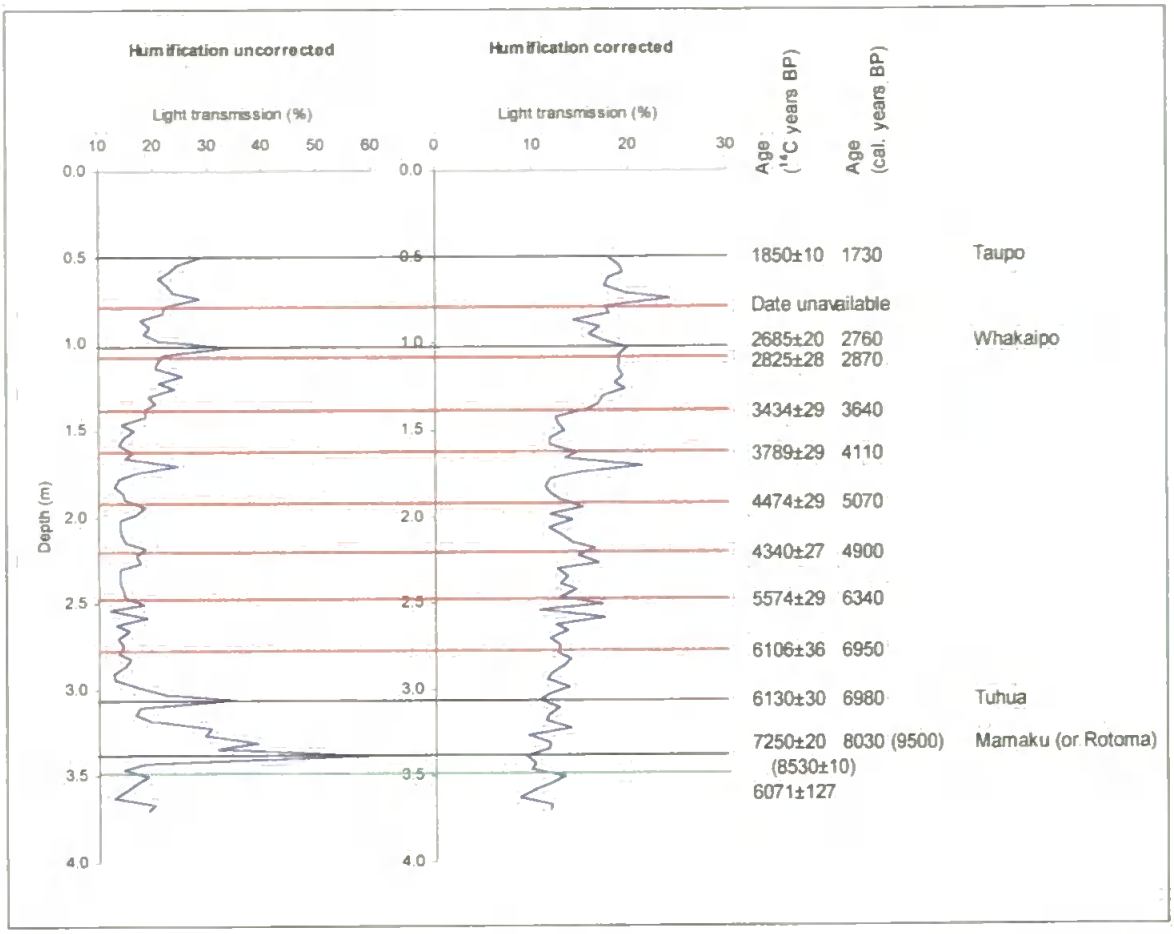

Figure 7.17 Results for core Z0102; raw light transmission values and corrected light transmission.

Any changes in light transmission that are certain to be related to a fall in TOC values are not discussed, as they have no value in terms of representing climatic signals. Shifts in parentheses indicate shifts that could be related to a possible drop in TOC even after applying the mineral correction.

The main shifts to enhanced light transmission occur at 2.67 m, 2.27 m, (2.03 m), 1.79 m, 1.51 m, (0.83 m) and 0.63 m. Shifts to low light transmission occur at 2.47 m, 2.15 m, (1.91 m), 1.67 m, 0.99 m and (0.71 m).

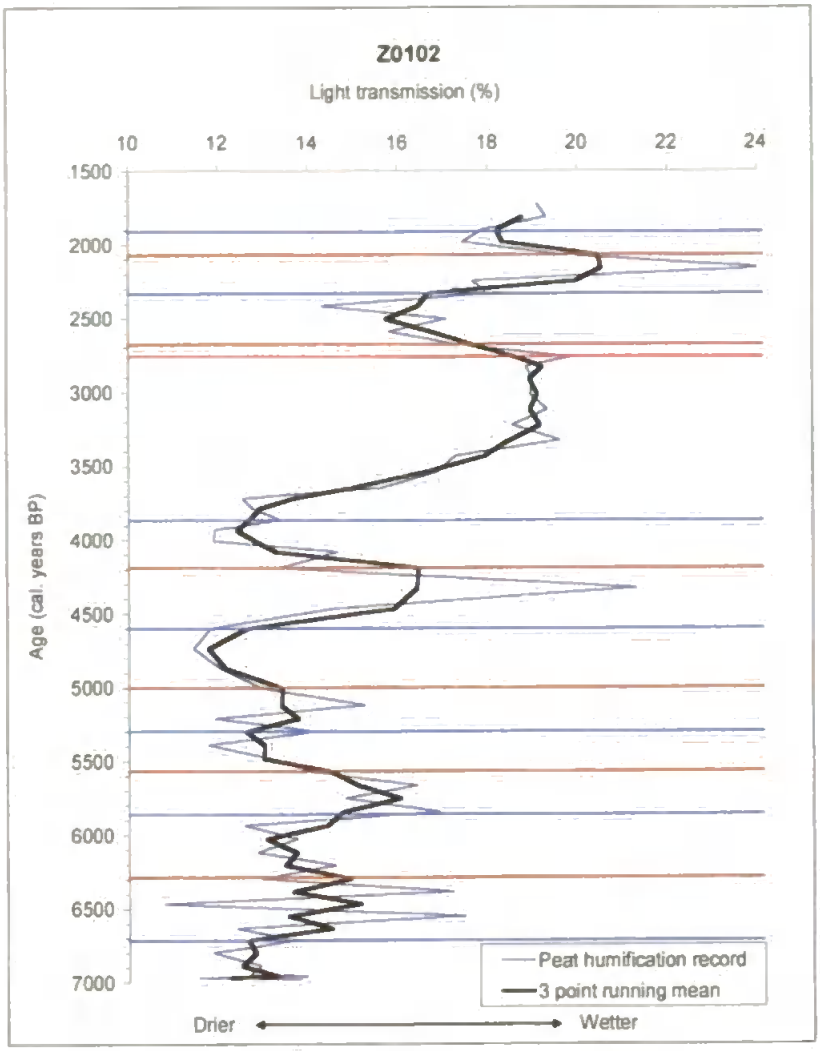

Figure 7.18 Corrected light transmission plotted against age for Z0102.

Using the age-depth model for this core, the main wet shifts identified from depth are calculated to have occurred at 6,700, 5,850, (5,300), 4,600, 3,850, (2,350) and 1,900 cal. years BP. The dry shifts occur at 6,300, 5,550, (5,000), 4,200, 2,700 and (2,050) cal. years BP.

Figure 7.18 also suggests that the baseline of light transmission values in this core seems to rise at approximately 4,000 cal. years BP. This is the same pattern and timing as observed in all three cores from Kopouatai.

Accumulation rate

A single accumulation rate was calculated between the Taupo and Tuhua Tephras, and is 0.46 cm/10 years (2dp). This rate is lower than all those calculated at Kopouatai, by approximately half. Comparisons between sites and possible explanatory reasons will be discussed in section 8.3.2.

7.3.2 Core Z0103 (*Figure 7.19*)

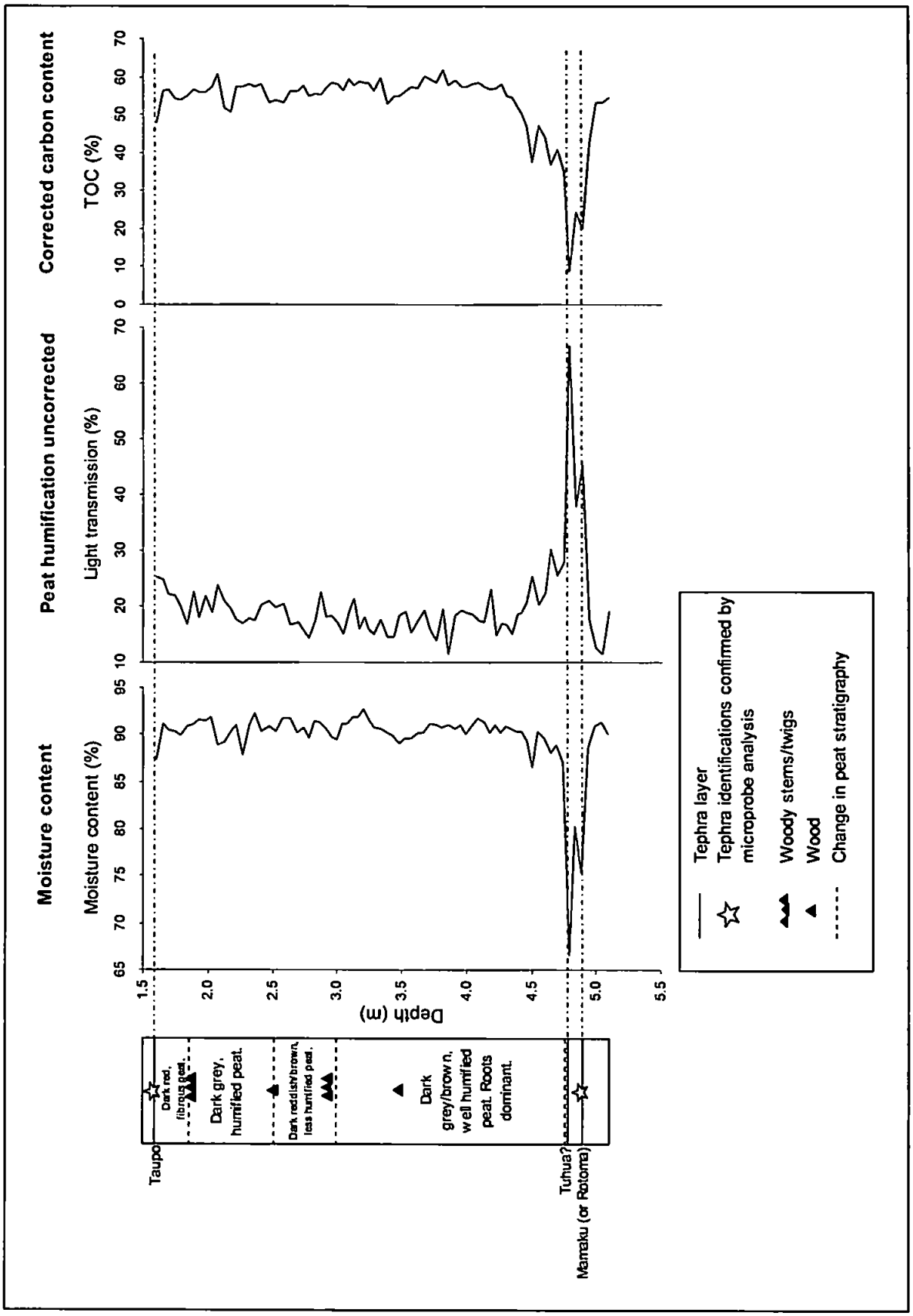

Figure 7.19 Z0103 core stratigraphy, moisture content, raw peat humification and corrected TOC results.

Core stratigraphy (*Figure 7.19* and Appendix 3)

For the majority of the core, the peat is well humified and dominated by root systems, with a layer of less humified, more red-coloured peat between 2.5-3.0 m. The most fibrous, least humified peat occurs at the top of the core. Pieces of wood were found at 2.52 m and 3.48 m and woody layers were found at 1.88 m and 2.94 m.

Moisture content (*Figure 7.19*)

Variation in moisture content is less significant in the lower half of the core than the upper half. Values vary around 90%, with peaks in tephra layers strongly distinguished from the surrounding peat. There is no distinct up-core decrease in moisture content, as observed clearly in core Z0102.

Carbon analysis (*Figure 7.19*)

A general up-core trend in declining TOC values is apparent. Above 3.4 m this trend becomes more pronounced, seemingly mirroring the peat humification curve.

TOC values of the peat samples vary between 50-60% throughout the core, with a major peak at 2.08 m and low values at 3.38 m and 2.15 m. As usual, the highly mineral tephra layers are picked out by extremely low TOC values. At 2.15 m there were very few glass shards present. However, even a small amount of mineral content can affect the TOC measurement significantly, because the values are calculated by mass and mineral weighs more than organic matter.

Peat humification (*Figure 7.20*)

Raw and corrected light transmission values are presented. The peaks of high light transmission values do not appear to relate to low values of TOC, suggesting that they are likely to be climate signals.

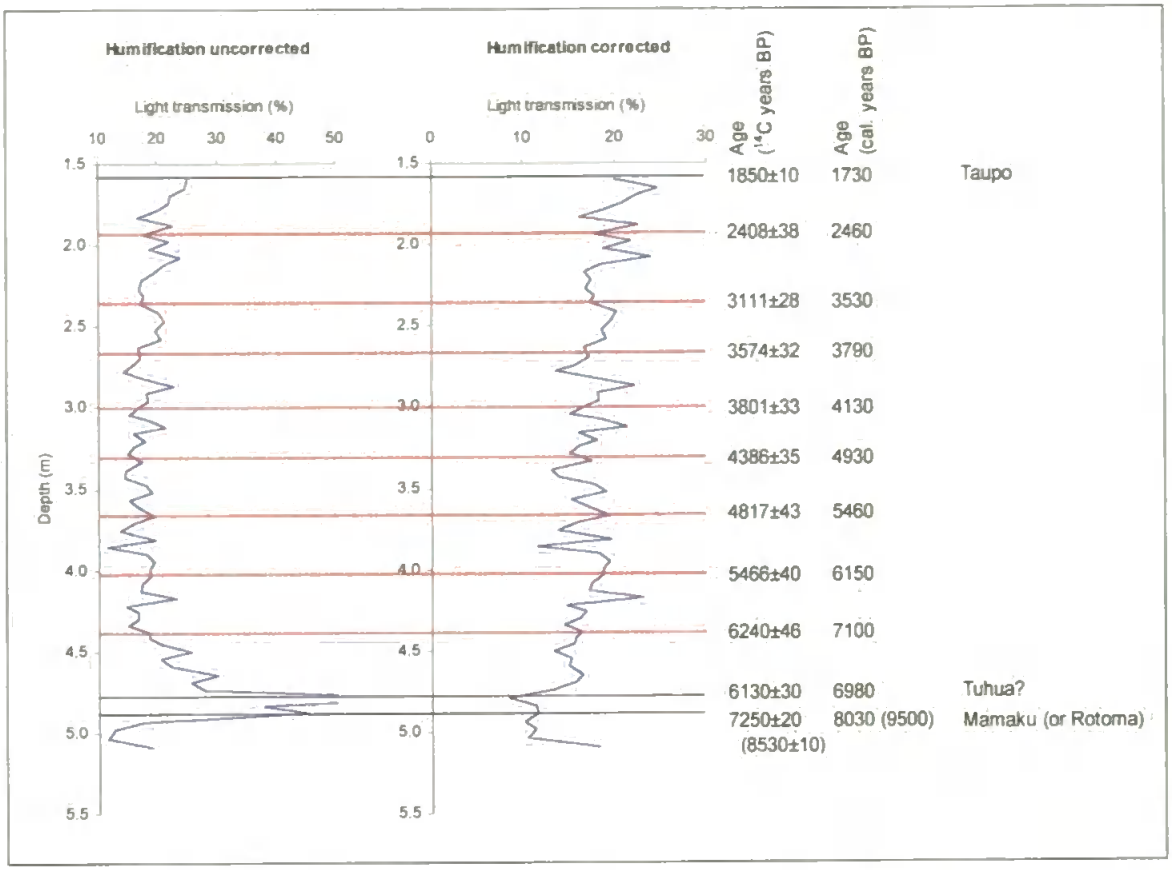

Figure 7.20 Results for core Z0103; raw light transmission values and corrected light transmission. Note the different scales used on the x-axes.

There is an overall upwards increase in light transmission values throughout the core. The main shifts to periods of higher light transmission occur at 4.30 m, 3.71 m, 3.29 m, (2.74 m), 2.12 m and 1.79 m. Shifts to reduced light transmission occur at 3.91 m, 3.48 m, 2.83 m, (2.36 m) and 1.93 m. The rise in light transmission values between 2.74-2.36 m coincides with a prolonged period of reduced TOC values, however, the shift is still clear in the corrected light transmission values.

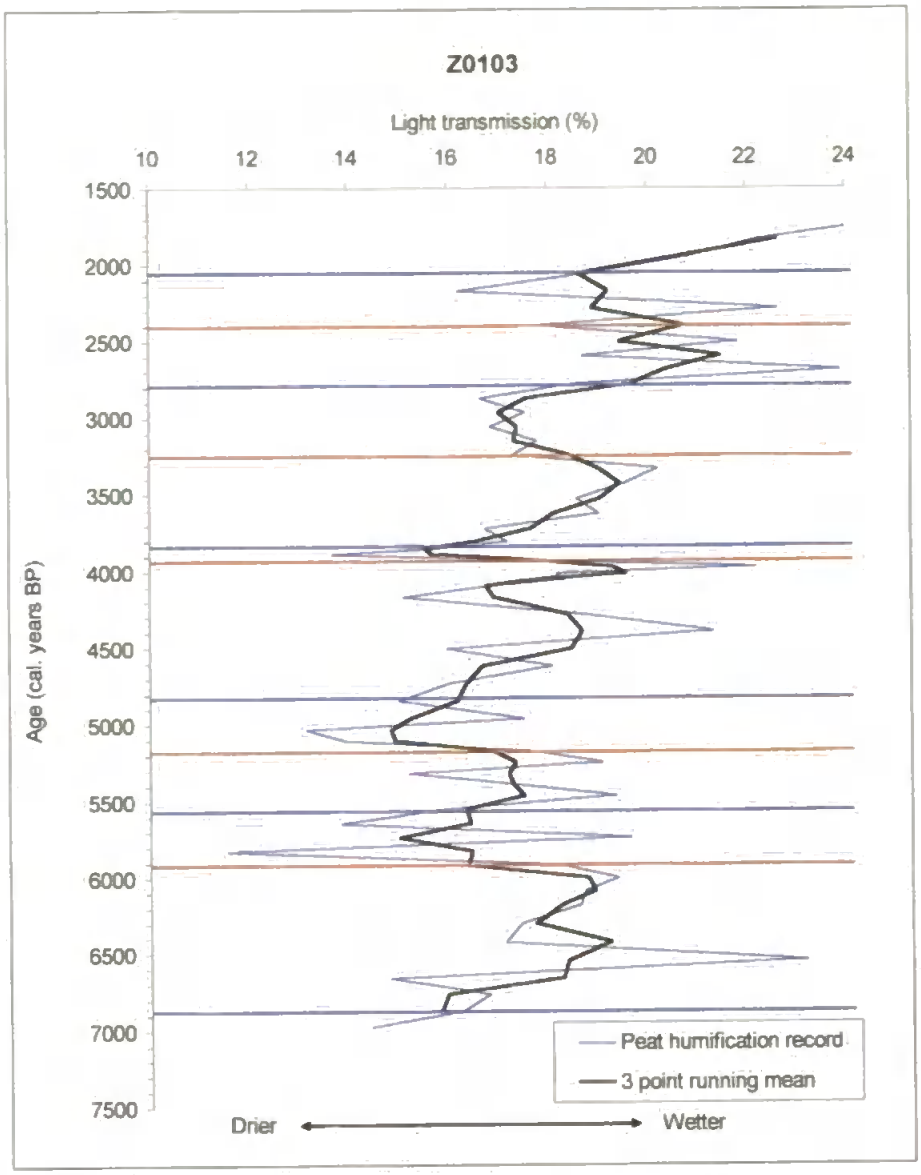

Figure 7.21 Corrected light transmission plotted against age for Z0103.

Using the age-depth model for the core, the higher light transmission (wet) shifts identified occur at 6,850, 5,550, 4,850, (3,850), 2,800 and 2,050 cal. years BP (*Figure 7.21*). Shifts to reduced light transmission (dry) occurred at 5,900, 5,150, 3,950, (3,250) and 2,400 cal. years BP.

Figure 7.21 also shows an overall change in light transmission values, occurring between 4,500-4,000 cal. years BP, from values that fluctuate around 17% increasing to values that fluctuate around 21%.

Accumulation rate

An overall accumulation rate between the two tephra layers was calculated as 0.51 cm/10 years (2dp).

7.3.3 Core Z0206 (*Figure 7.22*)

Note that this core was sampled at a higher resolution than the other two cores from this site.

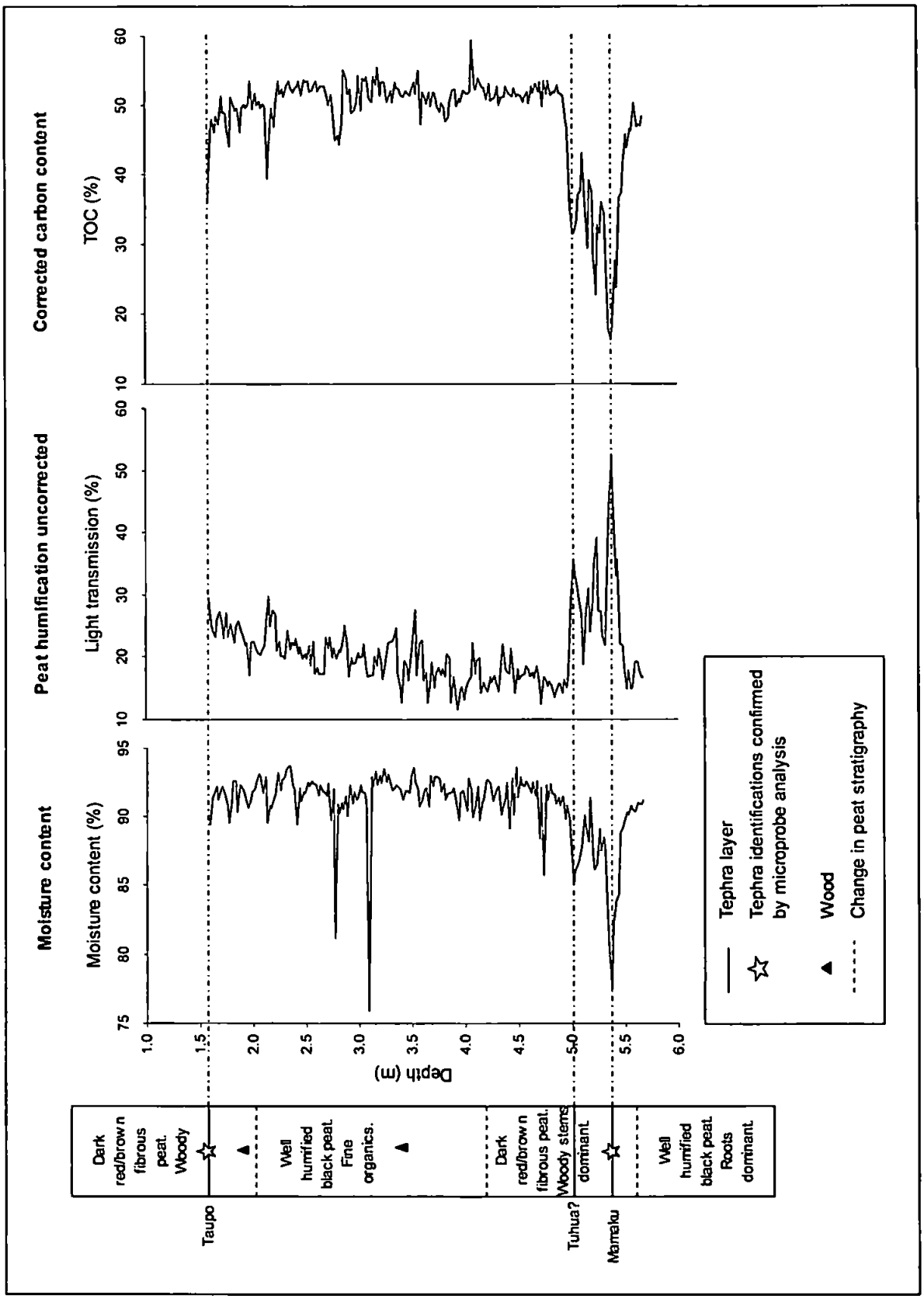

Figure 7.22 Z0206 core stratigraphy, moisture content, raw peat humification and corrected TOC results.

Core stratigraphy (*Figure 7.22* and Appendix 3)

The peat stratigraphy within this core alternates between a more humified, black, root-dominated peat (at the base) and a more fibrous, dark red peat composed of stems above. Wood remains are found at 1.91 m and 3.41 m.

Moisture content (*Figure 7.22*)

Moisture content throughout the core varies between 90-95%, with more variation than the previous cores. There is an overall slight increase from the base to *c*.3.50 m followed by a slight decline. There are major peaks of reduced water content at 4.74 m, 3.10 m and 2.78 m. It does not appear that these relate to any increases in mineral content, so they could be related to the peat composition, with more-woody peat having a lower water-retention capacity.

Carbon analysis (*Figure 7.22*)

As for the other cores, there is an upwards declining trend in TOC values. At approximately 3.2 m this decrease becomes more pronounced. Superimposed on this overall trend are several large fluctuations in TOC content.

There is a peak in high carbon content at 4.08 m, where the TOC value of the sample reaches nearly 60%. The main drops in TOC are due to the presence of the Taupo and Tuhua tephra layers. Micro-tephra analysis of certain samples was undertaken and it was found that 1.80 m, 2.16 m and 2.82 m contained no glass shards, 1.90 m contained a little, and 3.60 m contained large amounts. An alternative explanation must be sought for the fall in TOC of the samples not containing tephra shards (e.g. wind-blown dust).

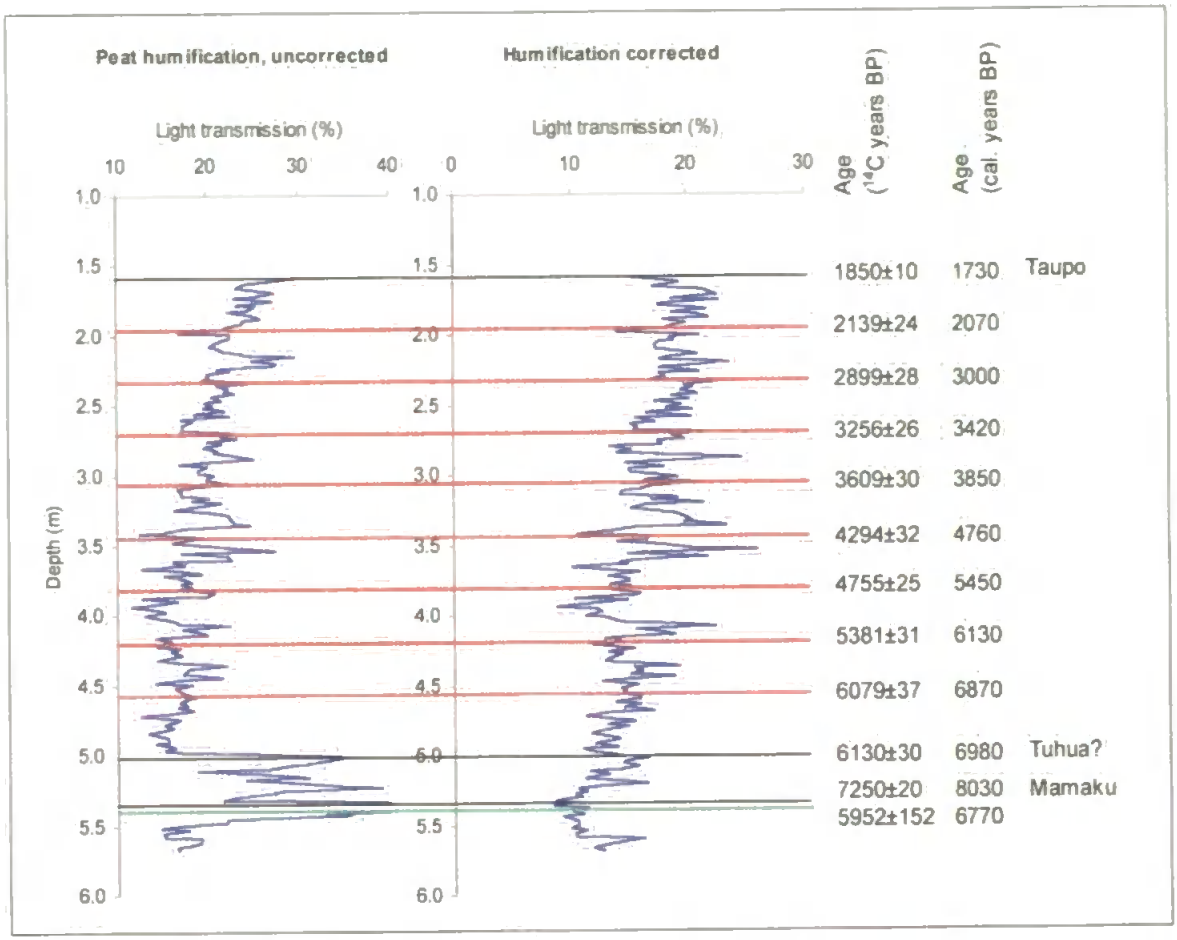

Figure 7.23 Results for core Z0206; raw light transmission values and corrected light transmission.

The peat humification record (*Figure 7.23*) shows frequent marked fluctuations superimposed on a long-term upwards trend of increased light transmission values. The shifts to increased light transmission occur at 4.46 m, 4.20 m, (3.92 m), 3.40 m, 3.22 m, 3.10 m, 2.94 m, 2.78 m, 2.58 m, (2.26 m) and 2.04 m. In terms of reduced light transmission values, shifts occur at 4.68 m, 4.34 m, 4.06 m, (3.52 m), 3.34 m, 3.18 m, 3.02 m, 2.86 m, 2.68 m, 2.32 m, (2.12 m) and 1.70 m.

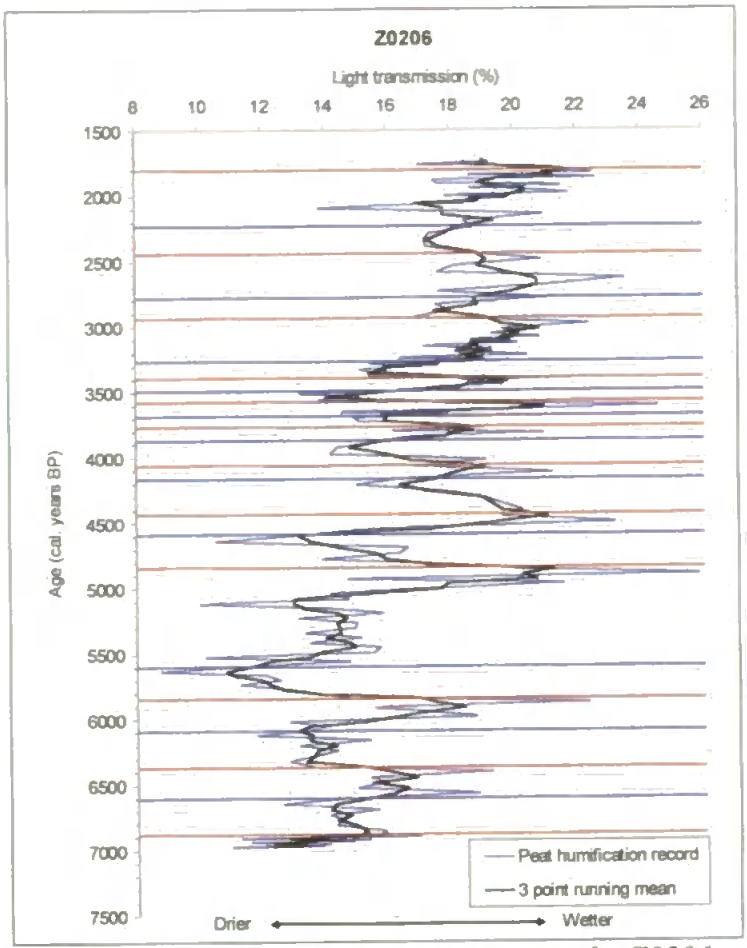

Figure 7.24 Corrected light transmission plotted against age for Z0206.

The shifts to higher light transmission (wet periods) that were identified with depth are now inferred to have occurred at 6,600, 6,100, (5,600), 4,600, 4,150, 3,850, 3,650, 3,500, 3,250, (2,800) and 2,250 cal. years BP (*Figure 7.24*). Dry shifts occur at 6,900, 6,350, 5,850, (4,850), 4,450, 4,050, 3,750, 3,600, 3,350, 2,950, (2,450) and 1,800 cal. years BP.

Figure 7.24 shows a similar mid-core transition to that observed for the other cores. Light transmission values show a steady overall increasing trend after *c.* 4,500-5,000 cal. years BP.

Accumulation rate

The accumulation rate of this core was calculated to be 0.64 cm/10 years (2dp), which is the highest accumulation rate of the three cores from this site, but is still not as high as the lowest accumulation rate from Kopouatai.

Plant macrofossils

The main vegetation trends from core Z0206 (*Figure 7.25*) are described here.

Four main vegetation groups were identified (by eye). These are a) pre-Tuhua to 6,900 cal. years BP (5.52-4.70 m) (Zone A), b) 6,900 to 3,300 cal. years BP (4.70-2.60 m) (Zone B), c) 3,300 to 2150 cal. years BP (2.60-2.00 m) (Zone C) and d) 2,150 cal. years BP to post-Taupo (2.00-1.44 m) (Zone D).

Remains of the dry indicator, *Gleichenia* are found throughout the profile at low counts, but with major peaks in leaves at 3.04 m, 3.60 m and 4.16 m. *Gleichenia* sporangia are most abundant from 4.24 m upwards where there is a sudden increase in counts. After this peak, there is a steady decline towards the top of the core. Increases in the leaf counts of *Epacris* and *Leptospermum* seem to occur at the same, or similar, depths, for example, peaks in both occur at 4.08 m and 1.92 m. This suggests that their preferred conditions are similar. They both also show a decline in abundance towards the top of the core, after peaking at 1.92 m. *Epacris* seeds are found throughout the core, with minor fluctuations. *Empodisma* and *Sporadanthus* remains are also present, but at lower abundances, with the main periods of presence peaking at 4.56 m and 1.92 m. Of the less common plant species, *Campylopus* remains are only present at one level (3.76 m) but at very high numbers (between 400-500 leaves). No *Sphagnum* was found in any of the samples in this core. The unidentified small, smooth, brown seed is found throughout the core, seeming to coincide with the fluctuations in *Epacris* seeds.

As for Kopouatai, the counts for each wetness indicator species were amalgamated (*Figure 7.26*).

The plant macrofossil results suggest a lower-core dominance at around 6,900 cal. years BP of relatively wet indicators, particularly of *Empodisma*. Throughout the majority of the core there is a general dominance in dry indicator species, although abundances fluctuate. At approximately 2,150 cal. years BP wet indicator macrofossils are at a maximum, above which drier species (notably *Epacris*) then appear to dominate.

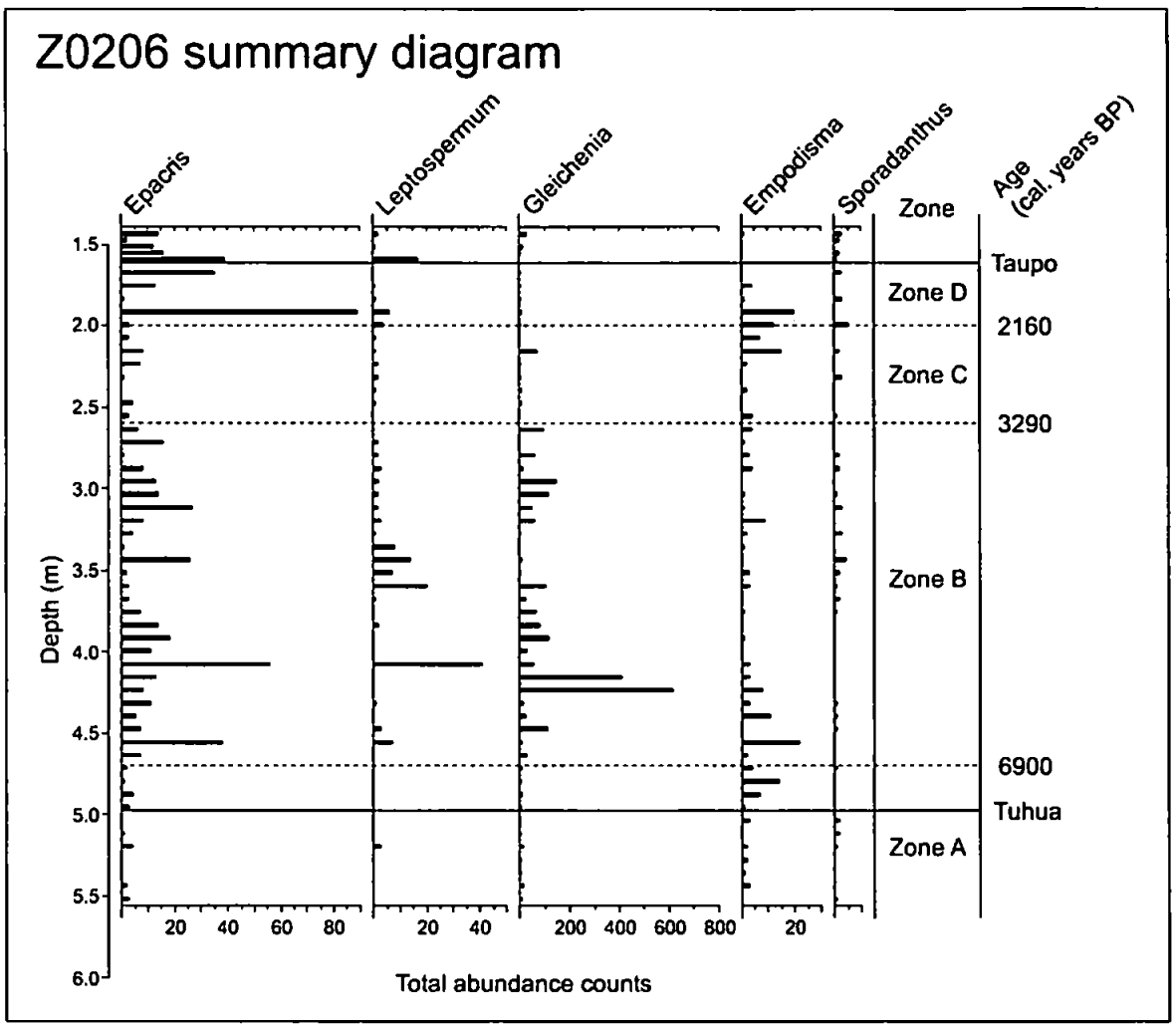

Figure 7.26 Combined abundance counts of the main plant macrofossil wetness indicator species.

Due to the inconclusive moisture relationships shown in the ordination results (section 6.3.3), a wetness index was calculated based on Dupont (1986) according to the scale in *Table 6.4*. The results are compared with the peat humification record (*Figure 7.27*).

As at Kopouatai, these results also show some degree of correspondence with each other. Both records show a clear mid-core shift in baseline values – from approximately 4,500 cal. years BP onwards there appears to be an increase in relative wetness, matching that observed in the peat humification results. The main disparity between records occurs between 2,500 to 2,000 cal. years BP, where the peat humification records imply drier conditions whereas the wetness index shows a peak in increased moisture.

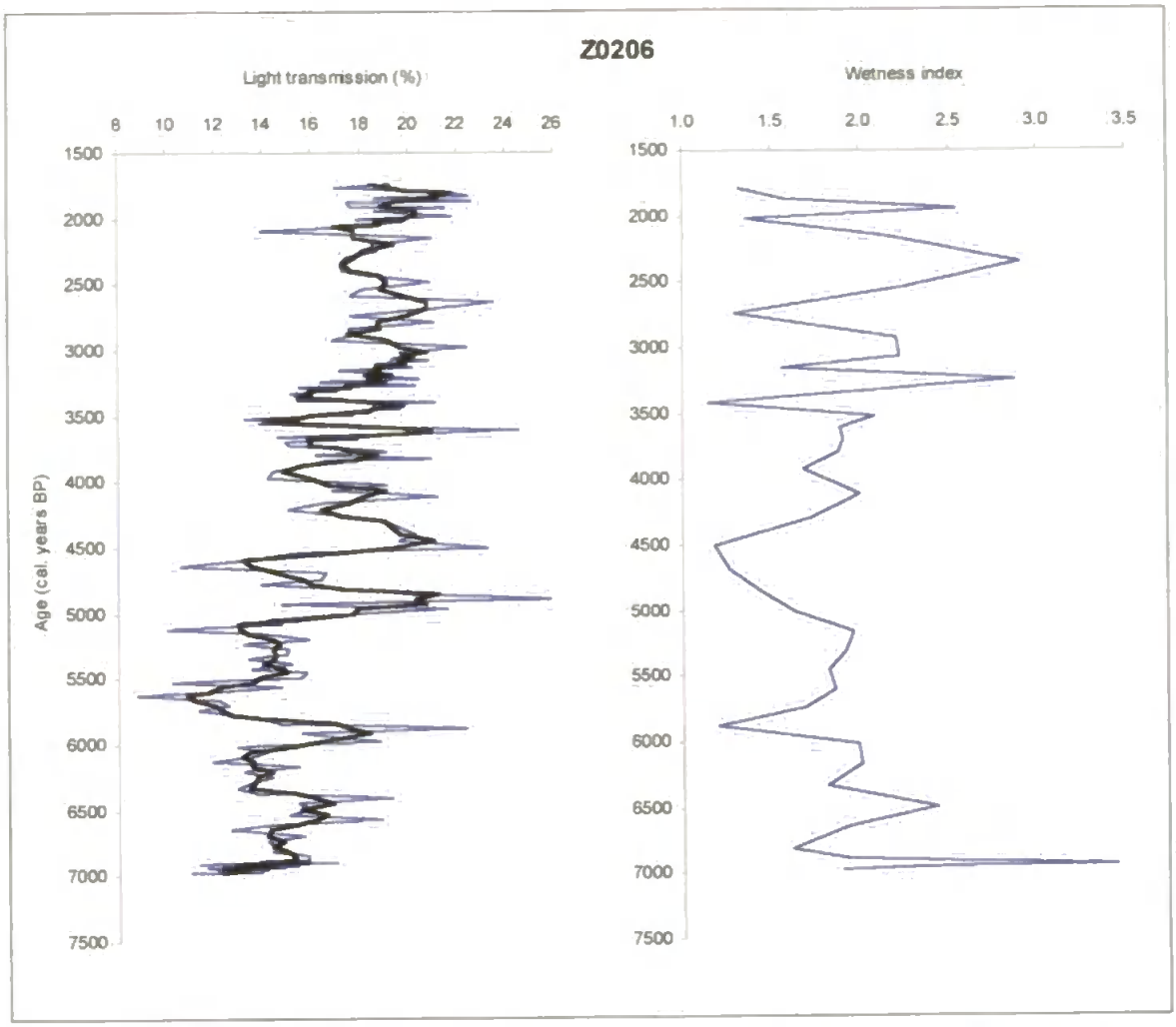

Figure 7.27 Peat humification record and plant macrofossil-derived moisture index. The black line indicates the 3-point running mean.

Charcoal

The main peaks in charcoal occur at 5.20 m, 2.72 m and 2.08 m, with the largest count of over 5,000 pieces in the sample from 2.72 m. Unlike at Kopouatai, none of the large peaks seem to coincide with any distinctive vegetation peaks. In addition to these main peaks, there is an underlying fluctuating trend in charcoal that appears to match the variations in *Epacris* seeds. There is a mid-core minimum in charcoal abundance, with counts almost reaching zero at 3.52 m, but this does not seems to coincide with any particular vegetation composition.

Charcoal results were also compared to the light transmission record (*Figure 7.28*).

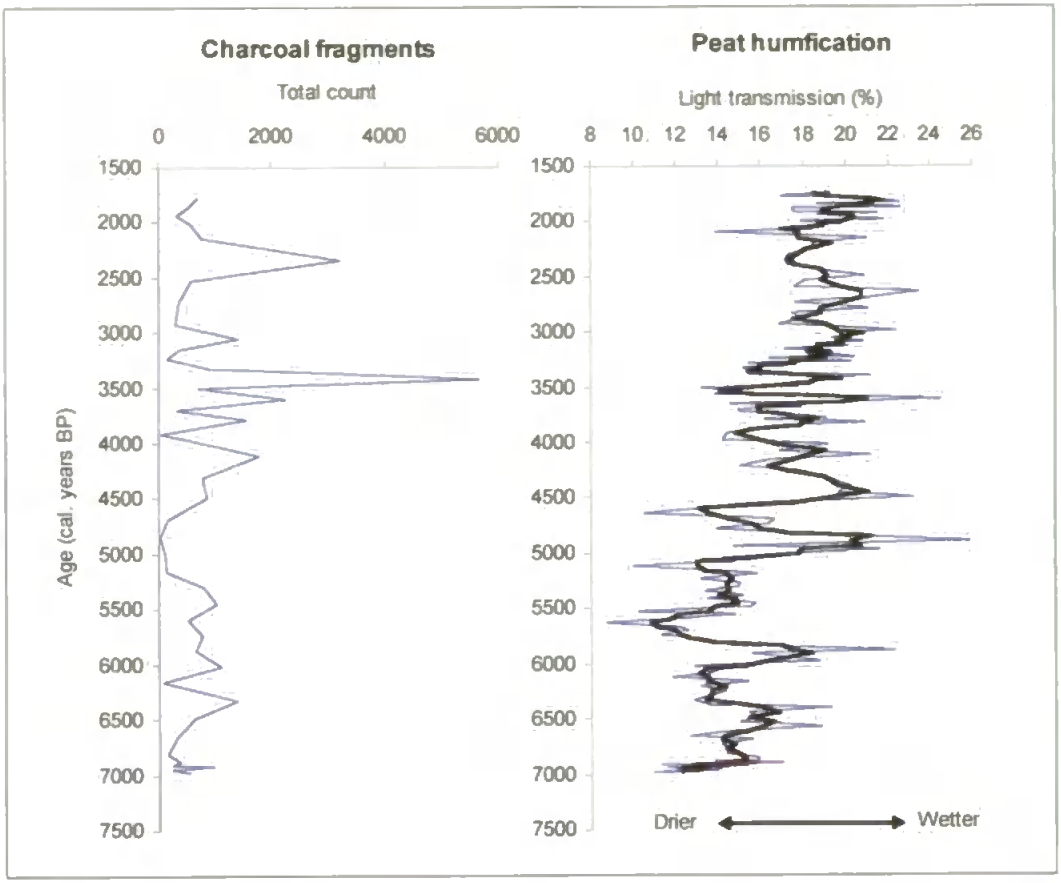

Figure 7.28 Charcoal and corrected peat humification records for Z0206 (with 3 point running mean represented by the black line).

Comparing the charcoal and peat humification records seems to suggest that there is some level of agreement between a slight increase in charcoal abundance after 5,000-4,500 cal. years BP, and an increase in light transmission values at the same time. As at Kopouatai, these can be reconciled by interpreting them as indicating a more variable climate after this time. Before this time, a drop in charcoal matches well with a peak in light transmission between 5,000-4,500 cal. years BP, as would be expected – wetter peat burns less easily. At other times, however, a definite relationship between the two variables is not clear.

The charcoal counts are also seen to increase above the tephra layers at the Tuhua and the Taupo, more so at the latter, suggesting that the volcanic ash layers or associated eruptive activity (e.g. lightning) could be responsible for helping to initiate the burning of vegetation.

7.4 Summary

This chapter has presented and evaluated the age-depth models derived for each core from Moanatuatua. The main palaeomoisture records obtained from these cores have also been presented and described in terms of depth and calculated ages. Clear changes in light

transmission can be seen in all three cores, with a major transition to increasing values occurring in all cores at 5,000-4,000 cal. years BP. The main climatic events that were observed in two or more cores, are the long term period of overall low light transmission values occurring at approximately 6,000-5,000 (dry) interspersed with short-lived periods of high light transmission, 5,500-5,000 (wet), 5,000-4,500 (dry), 4,000-3,000 (wet) and 2,750-2,500 (wet). The latter event is followed in all cores with a dry period that varies in its exact timing but is followed by a return to wetter conditions.

TOC values also follow the same trend in all three cores, with a transition to generally lower carbon values occurring at approximately the same time as the major transition observed in the light transmission record.

Plant macrofossil results seem to be less conclusive in terms of palaeoclimatic reconstruction. *Gleichenia* remains are present in large numbers throughout most of the core, but decline after approximately 3,300 cal. years BP, after which the restiads and then *Epacris* and *Leptospermum* appear to dominate, the latter of which indicate dry conditions.

The charcoal records seem to show an increase in fragment abundance after 5,000 cal. years BP, suggesting increased fire frequency/intensity and drier conditions, which coincides with the increase in light transmission values that imply wetter conditions. This would fit in well with the proposed late-Holocene increase in climate variability.

The following chapter will compare the peat humification and plant macrofossil results in detail, both between and within the two sites to examine their similarities/differences and interpret their records in terms of climatic changes.

CHAPTER EIGHT – DISCUSSION

8.1 Introduction

In this chapter the results obtained from Kopouatai and Moanatuatua are discussed, concentrating on the peat humification records as indicators of palaeomoisture history. Records are compared both within sites and between sites and discussed in terms of their possible climatic inferences, which are then examined in a regional, and where appropriate, a global context. Plant macrofossil and charcoal results are also discussed and compared between sites. The testate amoebae investigations have already been discussed in detail in Chapter 5, so here the technique is discussed in terms of its applicability to these particular sites. Throughout this chapter, ages derived from this project (in 'cal. years BP') are referred to as simply 'BP'.

8.2 Intra-site comparisons and discussion

The peat humification results are discussed separately for each site.

8.2.1 Kopouatai

Peat humification

Figure 8.1 shows the light transmission results plotted against age from all the cores from Kopouatai. When considering general trends in the peat humification results, all three cores from Kopouatai show an increase in light transmission baseline values at approximately 4,500-4,000 BP and this trend is most pronounced in Z0108 and Z0204. Before this time period, the light transmission trend of core Z0106 differs most from those of the other two cores, because it appears to show an overall increase in light transmission to this point, whereas cores Z0108 and Z0204 are decreasing.

In terms of smaller-scale, shorter-term events, it can be seen from *Figure 8.1* that there appears to be a similarity between two or more cores, manifest as a) a relatively dry period lasting from 6,000-5,500 BP, followed by b) wet conditions lasting between approximately 5,500 and 5,000 BP and c) a wet period peaking at approximately 3,000 BP (only seen in cores Z0108 and Z0204). Overall, cores Z0108 and Z0204 show the strongest level of similarity.

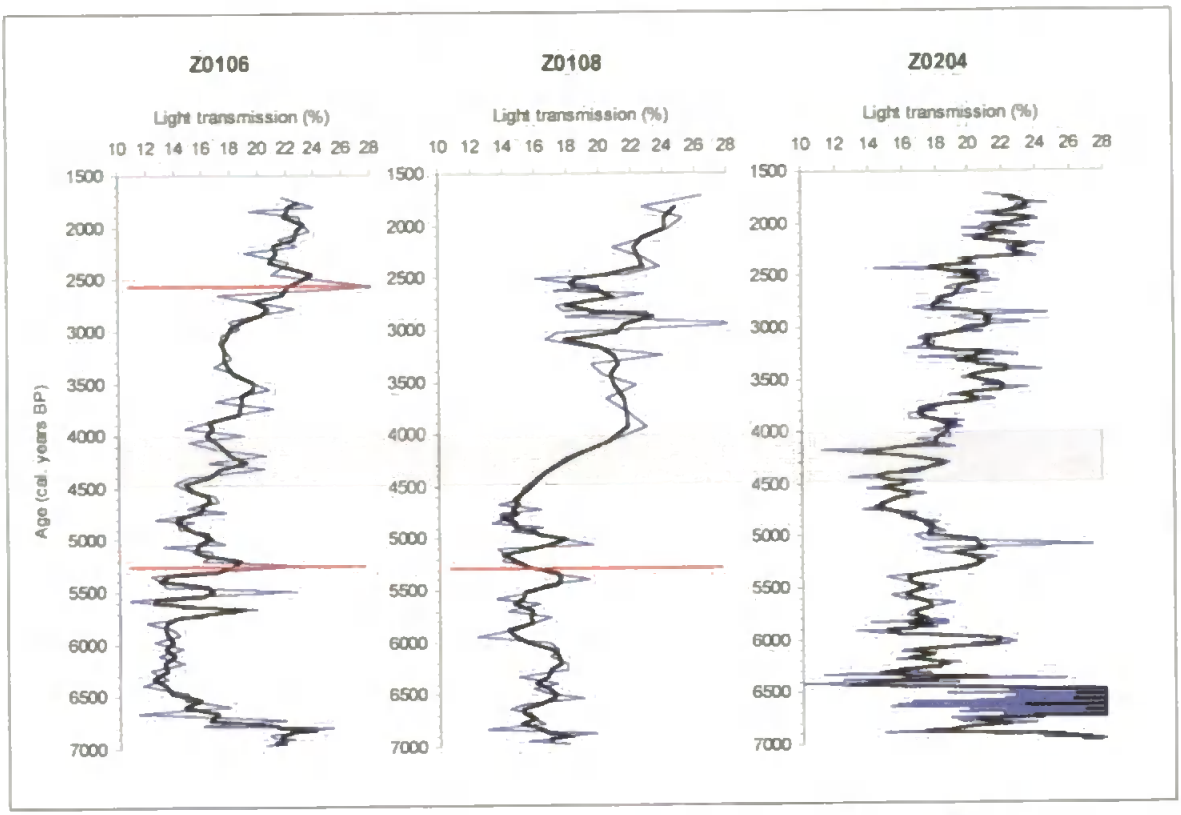

Figure 8.1 The corrected light transmission results for cores Z0106, Z0108 and Z0204 from Kopouatai with a 3-point running mean (solid black line). Tephra layers (other than the Taupo and Tuhua Tephras) are identified by the red lines and the 4,000-4,500 BP change in wetness baseline is shown by the grey band.

The main wet and dry shifts for each core (as identified in section 6.3) are listed in *Table 8.1*, where similarly-timed shifts are aligned. The age of a significant shift was determined using the first data point of the reversal in the peat humification record (section 4.3.4). It was shown in Chapter 6 that calibrated age ranges in which an event could be occurring were up to 350 years (although this varied between and throughout the cores), depending on age-depth model assumptions. This could significantly affect the timings of events and their correlation between cores.

Z0204 has the most number of shifts, both wet and dry, probably due to the higher sampling resolution for this core. However, by calculating 100-year running means, this difference in resolution can be accounted for (section 8.3.1). There is stronger correspondence in wet-shift timings between cores than in dry shifts. In terms of wet shifts, there is stronger correspondence for Z0106-Z0204 and Z0108-Z0204 than for Z0106-Z0108, again perhaps reflecting the higher sampling resolution for Z0204. Three wet shifts are seen to occur in all three cores, and only one dry shift.

	Cores		
	Z0106	**Z0108**	**Z0204**
Wet shifts (cal. years BP)			2,100
		2,450	2,350
	2,850	(2,750)	2,750
		3,000	3,050
	3,850		3,750
	(4,400)		4,150
	4,750	4,650	4,750
	(5,300)	(5,150)	(5,350)
	5,750	5,500	
			6,050
		6,600	6,300
Dry shifts (cal. years BP)	1,750		
			2,200
		(2,600)	2,450
		2,850	2,850
	3,500	3,150	3,250
			3,850
	(4,150)		4,250
	4,600		
	4,950	(5,000)	
		5,350	(5,150)
	5,650		
		6,000	6,000
			6,200
	(6,800)	6,850	

Table 8.1 Start timings of the main wet and dry shifts identified from Kopouatai cores (BP, to the nearest 50 years) as inferred from peat humification records (see Figures 6.18, 6.21 and 6.24). Shifts in parentheses refer to tentative shifts that are possibly related to an increase in mineral content.

Figure 8.2 shows the residuals of the light transmission results. These detrended results take out the long term trends of the data, such as the down-core 'age effect' on peat decomposition, but allow smaller-scale events to be seen more clearly, as well as the

longer-term climate shift at around 4,500 BP. The data was normalised by fitting a linear relationship to the light transmission results, and this trend was removed by plotting the residuals – the difference between each data value and that predicted by the theoretical curve.

The Taupo and Tuhua tephra layers and clay layers were omitted prior to plotting the linear relationship between depth and light transmission, from which the residuals were calculated. Other cryptic tephras and non-tephra low TOC samples were retained in the series when calculating the residuals, since tephra counts had not been completed on all cores, and so as to maintain consistency between them. The trends of the residuals were seen to be extremely similar, when calculated both with and without these layers.

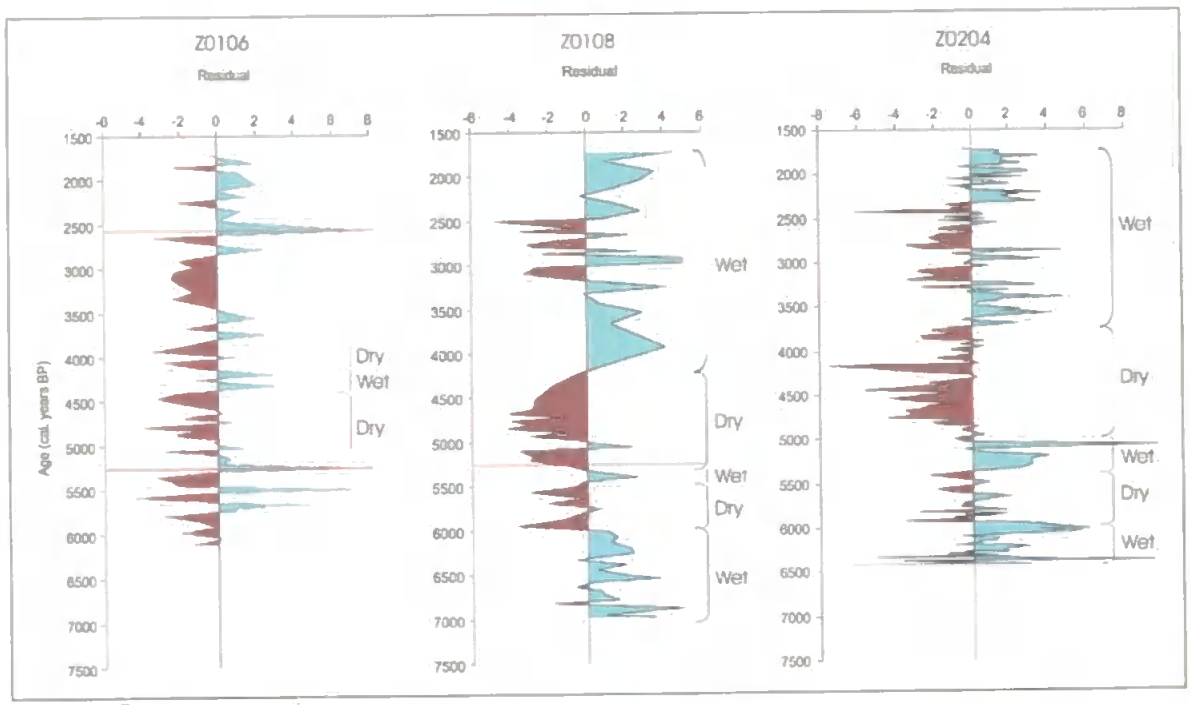

Figure 8.2 Detrended corrected peat humification results plotted against age for cores Z0106, Z0108 and Z0204 (brown residuals indicate dry periods, blue residuals indicate wet shifts and the red lines represent the confirmed 'cryptic' tephra layers). Labelled wet and dry phases are those referred to in the text.

From the residuals (*Figure 8.2*), it is possible to discuss the peat humification results as 'events'/'periods' of wet and dry, starting and ending where the zero line is crossed. The greatest degree of similarity between these cores is between Z0108 and Z0204. A prolonged dry period (the longest continual dry period at this site) is clearly observed in both cores, starting at 5,000 BP and continuing until approximately 4,000 BP. Before this dry period, the records also show similar trends with a wet, then dry, then wet pattern, although the most recent wet phase is less well defined in Z0108. After the major dry

period, a change to wetter conditions occurs at both sites, and the records remain predominantly wet throughout. Core Z0106 also shows a dry period beginning at the same time, but this event appears to be interrupted by a short-lived wet interval *c.*4,300-4,200 BP.

In order to investigate further the variability of the peat humification records a 'dissimilarity index' was derived for each core (*Figure 8.3*). This was calculated for a particular sample as the difference between the peat humification value for that sample and that of the immediately underlying sample. This gives an indication of down-core variability.

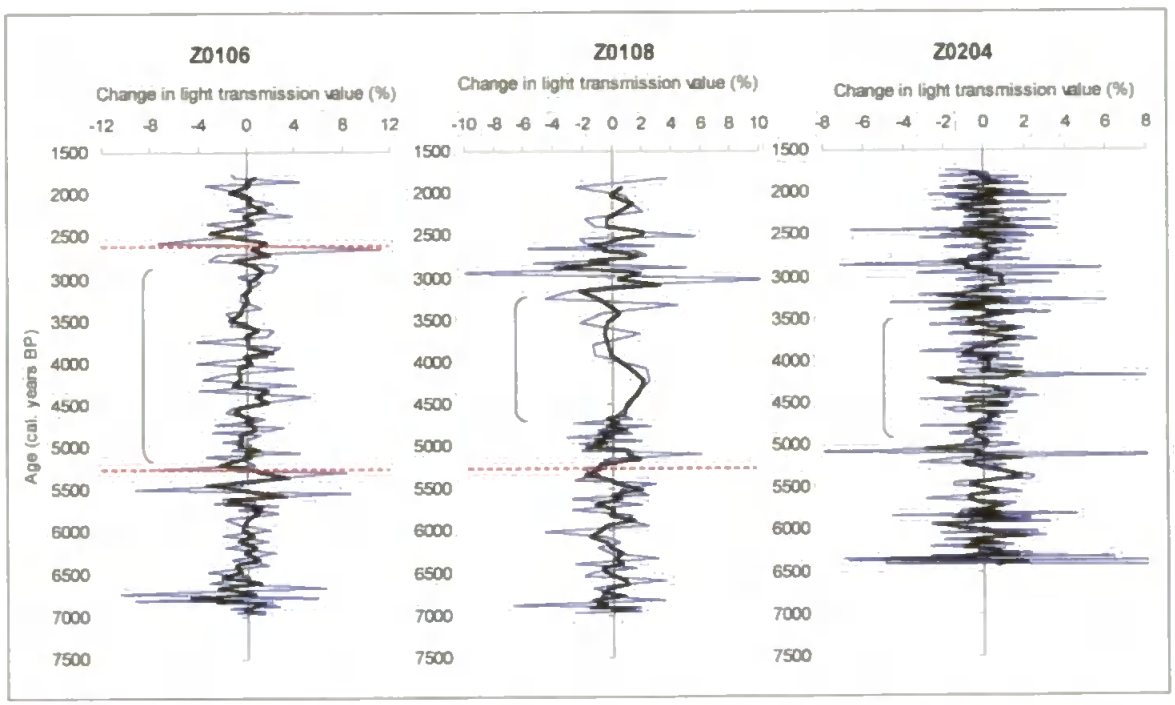

Figure 8.3 Dissimilarity indexes for Kopouatai. The blue lines represent the raw peat humification values, and the black lines are the 3-point running means. Dotted red lines represent the cryptic tephra layers and brackets highlight periods of less variability.

Z0108 appears to have least variation between 4,500-3,500 BP, after which the record becomes more varied in terms of the magnitude of the differences between successive samples. There is also considerable variability before 4,500 BP. Core Z0204, and to a lesser extent core Z0106, also seem to show an increase in the magnitude of changes after approximately 3,500 BP. Note that the index for core Z0106 is complicated around 2,600 BP by the presence of a cryptic tephra. Overall, the three records are consistent in showing greater variability between *c.*5,000-5,500 BP, less variability between *c.*5,000-3,000 BP, and greater variability after 3,500 BP.

Core replicability/representativeness

Generally, the cores replicate each other well as they all show the same trend towards increasing light transmission values i.e. wetter conditions, throughout, but particularly after around 4,500 BP. Similarly, all three records show greater variability during this post-4,500 BP interval. This similarity between records implies that within-site consistency exists between different cores i.e. that for this mid-Holocene trend, each core could be used as representative of the site. Such long-term replication work of peat-based proxies has rarely been carried out for Holocene investigations (for examples see Barber *et al.* (1998); Charman *et al.* (1999); Hendon *et al.* (2001)) and particularly not for peat humification (except on short cores by Charman *et al.* (2001)). Using replicated records is advantageous in deriving an overall site record, as individual core anomalies can be averaged out (section 8.3.1).

In contrast to the humification records, not all the cores show the same 'cryptic' tephras between the Taupo and the Tuhua layers, suggesting that even between relatively short distances within a peat bog, the deposition of volcanic ash deposits can be variable. Systematic shard counts were performed throughout both Z0106 and Z0108 by Ballinger (2003), and the uppermost 'cryptic' tephra from Z0106 was not found in Z0108 indicating that it is not present at the precise location from which this core was extracted. This is most likely due to local topographical or vegetation variations inhibiting deposition and incorporation into the substrate. In contrast, the lower tephra layer in Z0106 is matched almost exactly in age (varying by about 100 years) with a tephra layer in Z0108, suggesting that this is the same tephra layer found in both cores.

It must be kept in mind when comparing the cores that within each record inherent chronological errors exist, deriving from both the radiocarbon dating and the age-depth models. It is possible that given the age error ranges, certain events could in fact be synchronous but are not seen to be, and vice versa. Of the three cores, there appears to be least overall difference between the alternative age models for Z0204, suggesting that this core's record, in terms of its timescale, is the most reliable. For the other two cores, the largest difference between the chosen linear interpolation model and the remaining models is at 6,000-5,500 BP for Z0106 and at 3,200-2,700 BP for Z0108 (*Figures 6.5* and *6.9* respectively).

8.2.2 Moanatuatua

Peat humification

Light transmission results plotted against age, for all three cores from Moanatuatua are presented in *Figure 8.4*.

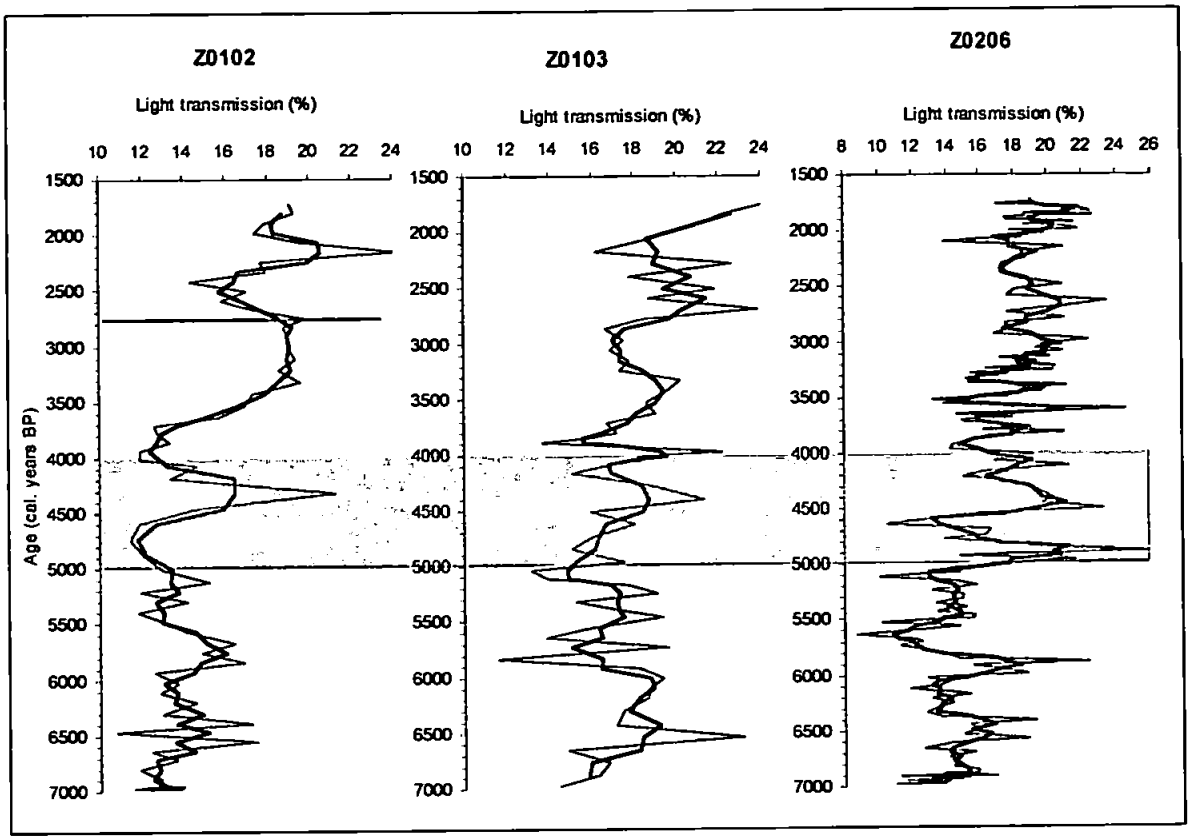

Figure 8.4 The corrected light transmission results for cores Z0102, Z0103 and Z0206 from Moanatuatua with a 3-point running mean (solid black line). The Whakaipo Tephra is identified by the red dotted line and the 5,000-4,000 BP change in wetness baseline is shown by the grey band.

As observed for Kopouatai, a consistent increase in baseline light transmission values occurs between approximately 5,000-4,000 BP. The main shifts in high/low light transmission indicating changes to wet/dry periods are listed in *Table 8.2*. Similarly-timed events are aligned, although the maximum radiocarbon age range for the site is 400 years, suggesting that there could be significant variation in the timing of events and of the ones with which they are correlated. Z0206 shows almost double the number of both wet and dry shifts as the other two cores from the same site, due to the increased sampling resolution. Three wet shifts are replicated in all cores, and two dry shifts.

As at Kopouatai, greater correspondence between cores is exhibited for wet shifts than for dry shifts. Overall, correspondence in shifts between cores appears to be similar for each pair.

	Cores		
	Z0102	**Z0103**	**Z0206**
Wet shifts	1,900	2,050	
(cal. years BP)	(2,350)		2,250
		2,800	(2,800)
			3,250
			3,500
			3,650
	3,850	(3,850)	3,850
			4,150
	4,600		4,600
	(5,300)	4,850	(5,600)
	5,850	5,550	6,100
			6,600
	6,700	6,850	
Dry shifts	(2,050)		1,800
(cal. years BP)	2,700	2,400	(2,450)
			2,950
		(3,250)	3,350
			3,600
			3,750
	4,200	3,950	4,050
			4,450
			(4,850)
	(5,000)	5,150	
	5,550		
		5,900	5,850
	6,300		6,350
			6,900

Table 8.2 Start timings of the main wet and dry shifts identified from Moanatuatua cores (BP, to the nearest 50 years), as inferred from peat humification records (see Figures 7.18, 7.21 and 7.24). Shifts in parentheses refer to tentative shifts that are possibly related to an increase in mineral content.

Figure 8.5 presents the detrended peat humification results, comparing the three cores from Moanatuatua, determined in the same way as for the Kopouatai cores (section 8.2.1).

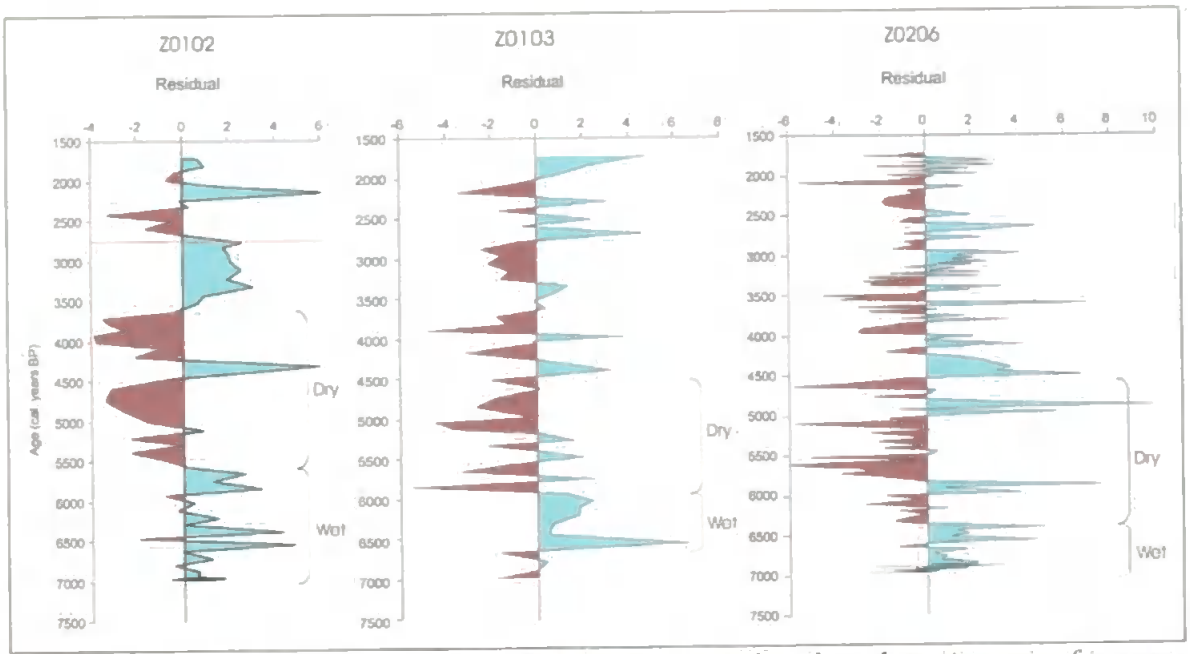

Figure 8.5 Detrended corrected peat humification results plotted against age for cores Z0102, Z0103 and Z0206 (brown residuals indicate dry periods, blue residuals indicate wet shifts and the red line indicates the Whakaipo Tephra layer). Labelled wet and dry phases are those referred to in the text.

Generally, the three cores show similar climatic patterns to each other, although Z0102 shows the most clearly defined wet and dry periods. The earliest parts of the cores show a predominance of wet conditions, until approximately 6,500-6,000 BP. This is followed by a trend towards dry events that are interspersed with smaller and shorter-duration wet periods. This period of dry dominance ends at about 3,500 BP in Z0102, and is not as clear in the remaining two cores, although there does seem to be a decrease in dry event amplitudes up-core. The largest discrete wet events that appear to be replicated in all cores are those starting at approximately 4,500 and 3,600 BP.

A dissimilarity index was also calculated for the Moanatuatua cores (*Figure 8.6*). Core Z0206 is extremely variable throughout, possibly due to the higher sampling resolution creating more 'noise' and at approximately 2,750 BP in core Z0102 the Whakaipo Tephra layer confuses the signal. Overall, cores Z0102 and Z0103 show that the interval 4,000-3,000 BP has generally lower variability compared with the parts of the record post 3,000 BP and pre 4,000 BP. Core Z0206 also shows a mid-core period of reduced variability, occurring before that seen in the other two cores, lasting between 5,000-4,000 BP. The pattern at this site is broadly consistent with that observed at Kopouatai.

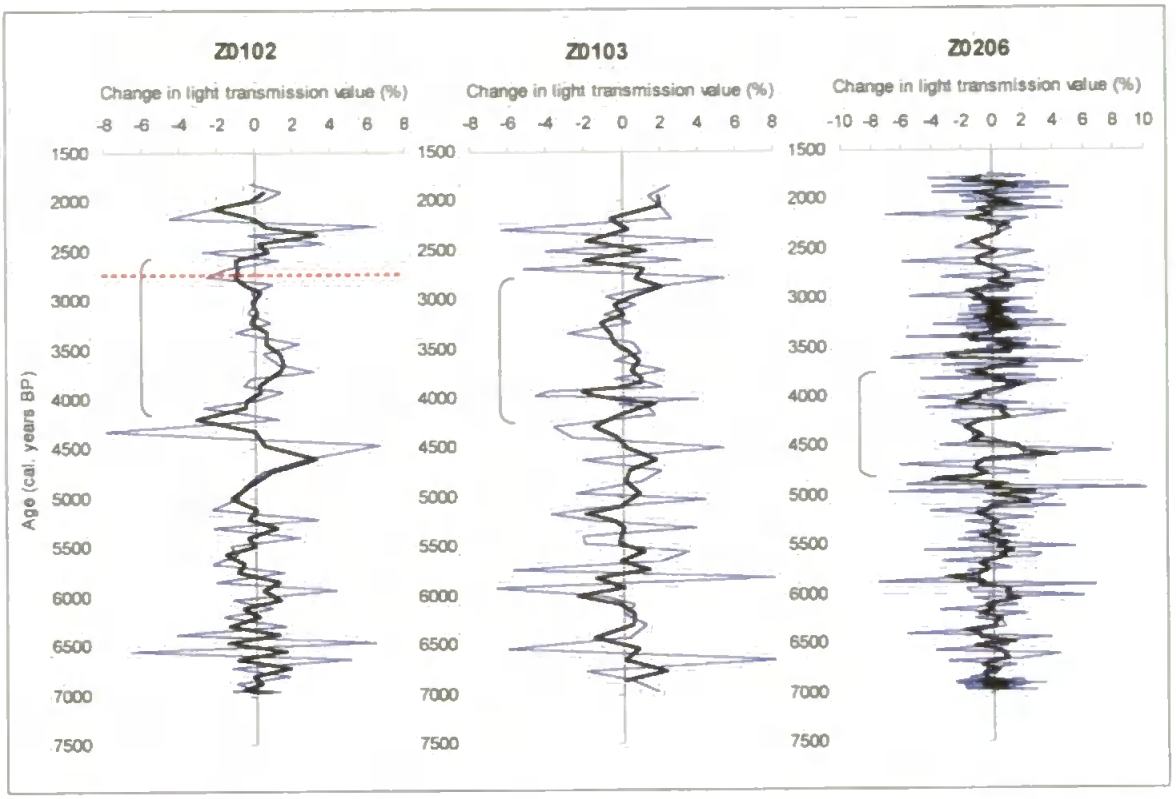

Figure 8.6 Dissimilarity indexes for Moanatuatua. The blue lines represent the raw peat humification values, and the black lines are the 3-point running means. The dotted red line represents the Whakaipo Tephra and brackets highlight periods of less variability referred to in the text.

Core replicability/representativeness

As described above, the humification results are generally well-replicated in terms of long term trends and patterns of down-core variability. For example, from each core record the main mid-Holocene wet trend can be identified. This is in spite of the fact that core Z0102 was extracted from the drained pastureland next to the scientific reserve, suggesting encouragingly that the effects of farming have not detrimentally altered the stratigraphical record.

No high resolution tephra shard counts were carried out on these cores, so it is not possible to discuss whether the same 'cryptic' tephra layers are to be found in proximal cores. However, samples from a selection of suspect tephra layers i.e. of low carbon content, have been examined under a light microscope. Of these, only Z0103 was seen to contain tephra shards and these occur at a similar age (2,850 BP) to the Whakaipo Tephra (2,750 BP).

Errors resulting from the radiocarbon dating and age-depth models are also an issue when comparing cores. Core Z0102 seems to show the least variation between age-depth models. In the other two cores, only at certain points does the chosen linear interpolation model

digress significantly from the other models, for example, between approximately 4,500-4,000 BP for Z0103 and at 3,000 BP for Z0206.

8.3 Inter-site comparisons and discussion

8.3.1 Peat humification

From the comparison of detrended results from all cores from both sites, it seems that the majority of cores show a clear initial predominance of wet conditions at the base of the core, followed by a trend towards drier conditions at approximately 6,000 BP. The exact timings vary between cores, probably due to the dating and modelling errors, but also possibly due to the varying sensitivity of the individual core locations to climatic changes, even though no core locations were noticeably different from each other e.g. on a drier hummock. The initial wet conditions could partly result from the presence of the Tuhua tephra layer (or the clay layer in cores Z0106 and Z0204) impeding drainage and resulting in increased moisture content of the peat above, causing its reduced decomposition, or by the continuing presence of small numbers of tephras shards affecting the light transmission. Hotes *et al.* (2004) found that the deposition of moderate tephra layers has no long-term changes on bog development, but that thicker or finer grained layers have stronger effects on bog vegetation.

The corrected light transmission values from both sites show a trend towards increasing light transmission values up-core, which is probably partially related to a time/age factor of peat decomposition. However, it is not known how much of this pattern results from such an 'age effect' and how much might result from a real climate signal. Nonetheless, in all cores there is a clear increase in light transmission values approximately mid-core, that all date to between 5,000-4,000 BP. This is also seen and confirmed in some of the detrended curves, particularly Z0108 and Z0204, as the residuals shift to predominantly wet conditions. The strong similarity between the palaeomoisture records of the hydrologically separate sites therefore suggests that a climatic influence is controlling surface moisture levels, since no peat properties or peat bog development processes can account for such a shift and any age/time effect is expected to be manifest as a gradual change throughout the core. Nor is the change likely to result from the choice of age-depth model, because the maximum age difference between models at this time is of only approximately 200 years. From the plots of detrended peat humification results, it can be seen that the inferred climate pattern described above is best demonstrated by cores Z0108 and Z0204 from

Kopouatai and Z0102 and Z0103 from Moanatuatua. The other cores show elements of the same patterns, but not as completely or as clearly.

Generally, the records appear to replicate well within sites. It appears that longer-term trends are better replicated between cores than the lesser fluctuations of short-lived specific events. This is not unexpected, since each core location is unlikely to have experienced exactly the same a) hydrological and microtopographical conditions during the peatland's development, b) vegetational responses and c) post-depositional decay or preservation processes. Also, the potential errors with the age-depth models lend uncertainty to any correlation of short term shifts, many of which are at a decadal time scale.

Nevertheless, the overall correspondence between the three records for each site suggests that it is plausible to amalgamate them in order to derive a single palaeomoisture record for each site. This was achieved by plotting the light transmission results from the three cores as one data series, and then calculating a 100-year running mean in order to give time equivalence to compare between sites. (For each data point, all the values that fell within the 100-year window around that central value i.e. 50 years before and after, were averaged).

Figure 8.7 demonstrates the high degree of similarity between these amalgamated records. At Kopouatai the main wet shifts start at approximately 6,150, 5,350, 4,350, 3,850, 3,050 and 2,400 BP, and the dry shifts at 6,000, 5,050, 4,250, 3,200 and 2,900 BP. At Moanatuatua the main wet shifts begin at 6,600, 6,050, 5,050, 4,550, 3,650, 2,850 and 2,350 BP and the dry shifts at 6,350, 5,850, 4,850, 4,350, 2,950 and 2,450 BP. Climate events are discussed in more detail in section 8.4.

The overall trends and patterns that seem to be replicated in both records (*Figure 8.7*) are a) an initial pre-5,500 dry phase, followed by b) a wet phase lasting until approximately 4,700 BP, c) a dry phase between 4,700-4,200 BP, d) a wet phase from 4,200-3,000 BP and e) subsequent phases of fluctuating wet and dry. Importantly, the mid-core transition to overall wetter conditions is also clearly visible in both records and is seen to occur at a very similar time (at approximately 4,500 BP). It does appear that even the lesser fluctuations are replicated in the records, although their ages do not always directly coincide. This is most likely due to the errors of the radiocarbon ages, which, at between 200 to 300 years, could easily shift the records into alignment.

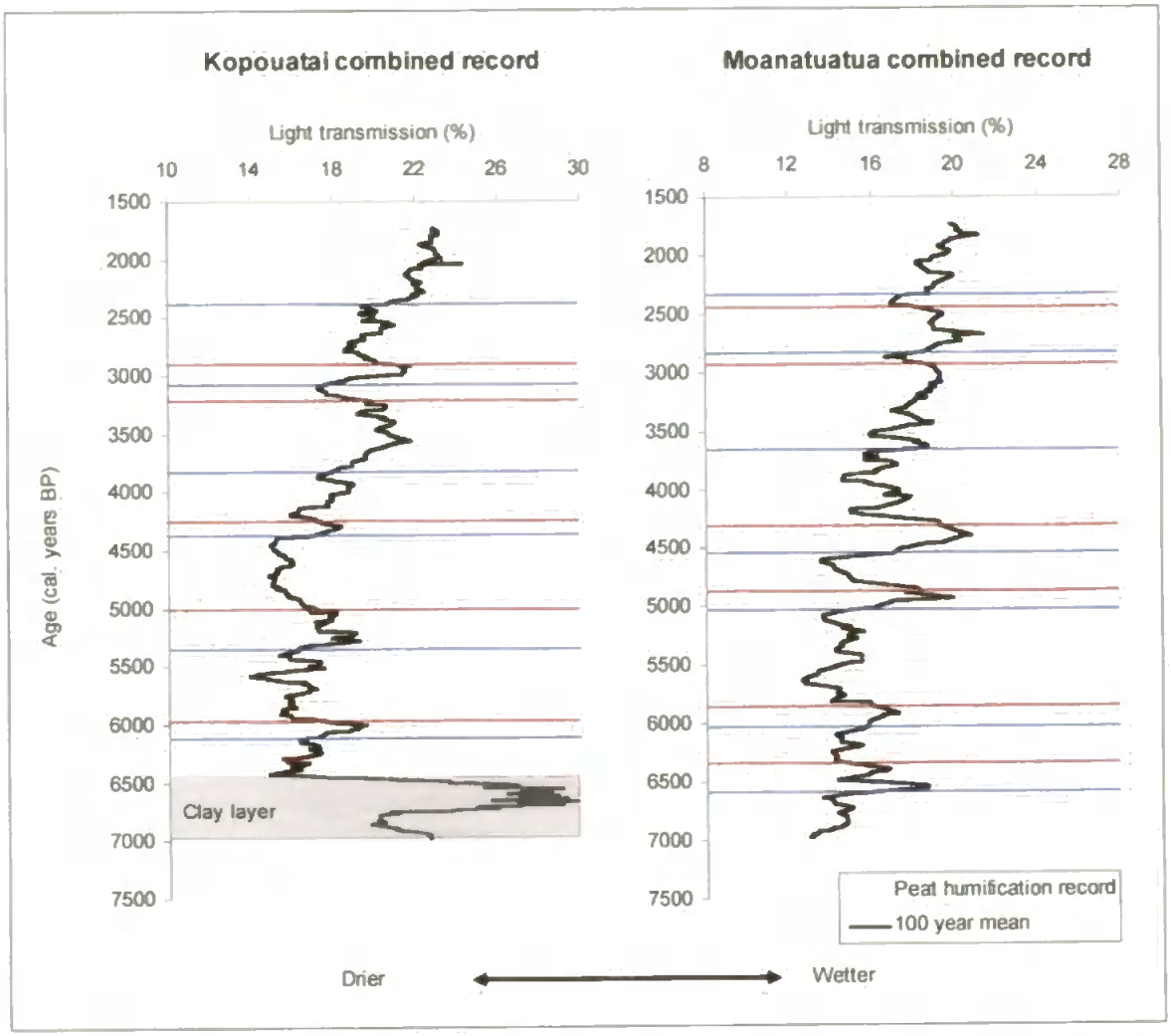

Figure 8.7 Combined corrected peat humification records of Kopouatai and Moanatuatua, with 100-year running means. Brown lines indicate dry shifts and blue lines indicate wet shifts. The wet and dry shifts have been identified from the 100-year mean curve, using the first data point in the direction of a reversal, and refer to those listed in the text.

In addition, the results were detrended in order to remove any up-core trend in light transmission values that might not be climate related (*Figure 8.8*).

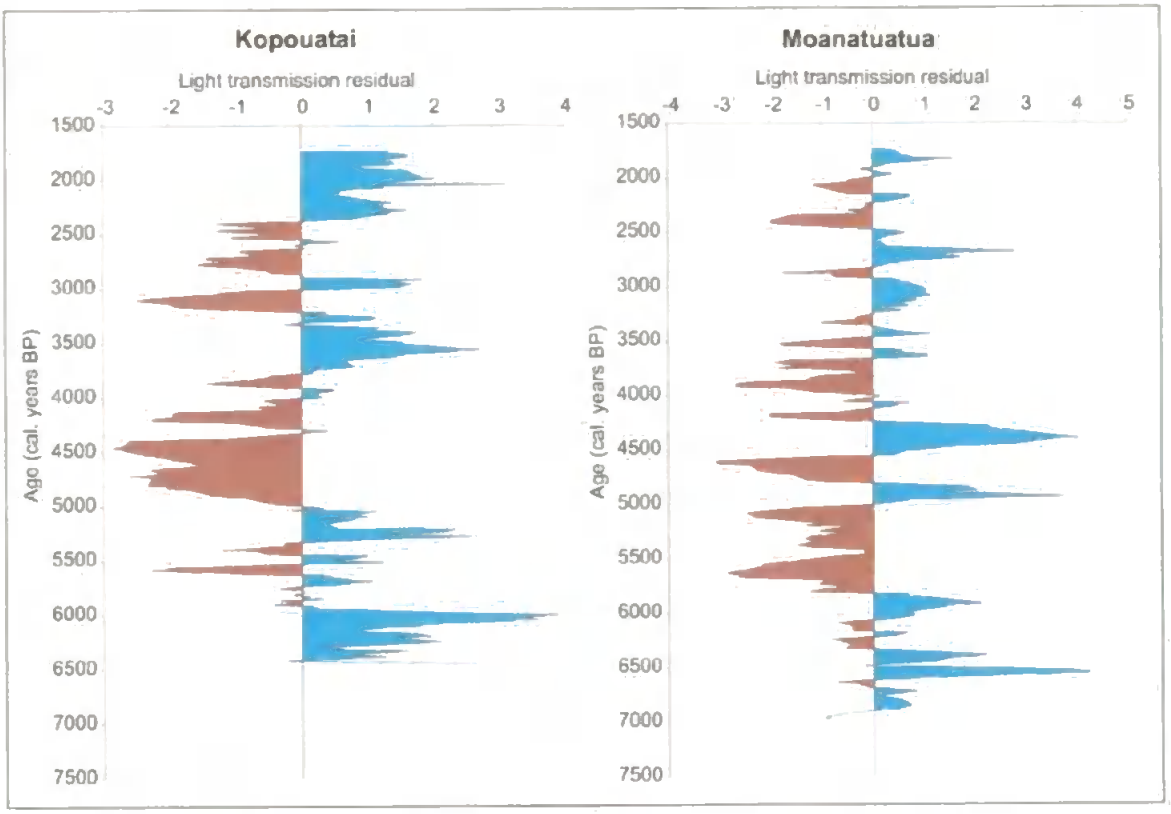

Figure 8.8 Detrended corrected peat humification amalgamated site results.

Interestingly, the detrended results (*Figure 8.8*) do not show as well a defined shift to wet values, as the individual sites better demonstrate. Of the two sites, Kopouatai shows a stronger, wetter mid-Holocene trend than Moanatuatua, which begins at approximately 3,800 BP.

Comparison of the peat humification and TOC records for each site has also identified a possible similarity. The peat humification records have been shown to increase in light transmission upwards throughout the cores, and the TOC records trend in the opposite direction, declining in carbon content. At very similar times (around the mid-Holocene) there is a shift in both types of records, where the peat humification records imply a shift to overall wetter conditions. The coinciding drop in TOC values therefore suggests that this could also be a climate signal – in wet conditions less peat decay occurs, resulting in lower carbon concentrations, as less non-carbon organic matter is mineralised.

8.3.2 Accumulation rates

Accumulation rates for each core have been calculated in previous chapters. The average accumulation rate at Kopouatai (0.85 cm/10 years) is almost double that at Moanatuatua (0.54 cm/10 years) implying that Kopouatai's peat record is more highly temporally

resolvable than that of Moanatuatua. The difference in accumulation rates is most probably due to the fact that Moanatuatua is (and has been throughout it development) generally a drier site (Kuder *et al.*, 1998), with a lower water table than Kopouatai, allowing for more degradation and therefore less peat accumulation to occur. Future work would benefit from the calculation of accumulation rates based on carbon accumulation, rather than depth of sediment accumulated. For such work, volumetric measurements are required, but were not measured as part of this project.

Changes in accumulation rates over time can be seen, with gentler gradients indicating faster accumulation rates, and steeper gradients implying reduced accumulation (*Figures 6.14* and *7.14*). The cores from Moanatuatua show striking similarities in terms of accumulation rates and their changes over time (*Figure 7.14*). They all show an increase in accumulation rates at approximately 4,500-3,500 BP. A comparable shift also occurs at Kopouatai, although earlier, between 5,000-4,000 BP (*Figure 6.14*). This increase in peat accumulation rates concurs with the observation that the peat humification records shifted to wetter inferred conditions at this point, since an increase in wetness would result in increased peat accumulation rates via the inhibition of decay.

8.3.3 Plant macrofossil and charcoal records

Both sites seem to show lower-core dominance of *Gleichenia* plant remains that is later replaced by a dominance of *Epacris* and *Leptospermum* fragments, that were previously largely absent (except for a small number of seeds). Based on their preferred environmental conditions, this would seem to suggest a shift in both cores to relatively drier conditions. However, the appearance of the *Epacris* and *Leptospermum* remains occurs at different times in the cores. At Kopouatai the main influx is just below 6.50 m (approximately 5,300 BP) and at Moanatuatua it is at around 4.70 m (approximately 6,900 BP). This difference in timing is likely to result from the drier conditions of Moanatuatua that encouraged earlier establishment of *Epacris* and *Leptospermum* (species that prefer these conditions) at this site.

Empodisma and *Sporadanthus* remains (particularly stem and root matter) were hard to identify due to the decomposed nature of the peat, although they are known to have been dominant throughout the period of study, and so are most likely to be under-represented in the cores. However, there is a clear influx of above-ground remains at approximately 7.90 m (6,500 BP) in Kopouatai, matched well in Moanatuatua following the Tuhua Tephra at

around 5.00 m. These plant remains imply wetter conditions, but they seem to be occurring simultaneously with the *Epacris/Leptospermum* and *Gleichenia* between 5,300-2,800 BP in Kopouatai and between 6,900-3,300 BP in Moanatuatua. After this time both *Epacris/Leptospermum* and *Gleichenia* decrease in presence, whereas remains of *Empodisma* and *Sporadanthus* continue at similar levels. This suggests the development of relatively wetter conditions at around 3,000 BP.

By comparing peat humification records with the Dupont plant macrofossil-derived wetness index (*Figures 6.28* and *7.27*), it can be seen that for both sites the two different types of record seem to show a degree of similarity, although better demonstrated at Kopouatai. This suggests that the plant macrofossil work holds potential for the reconstruction of palaeomoisture records, although it would be best used in conjunction with other proxy techniques.

From comparing the two charcoal records (*Figure 8.9*), it can be seen that certain peaks in charcoal occur at similar times in the two sites. Between the Tuhua and Taupo Tephra layers, the largest burning events at Kopouatai (core Z0204) as inferred from the charcoal record occurred at 6,750, 6050, 4,300, 3,400 and 2,250 BP (to the nearest 50 years) and at Moanatuatua (core Z0206) at 3,400 and 2,350 BP. Both the large charcoal peaks seen at Moanatuatua occur at very similar times to events at Kopouatai; the first at 3,400 BP and a second event that occurs within an 80 year period (at 2,250 BP in Kopouatai and at 2,350 BP in Moanatuatua). These could be reflecting the same events, but it is interesting to note that Moanatuatua, the site that is considered to be the drier of the two, actually shows *fewer* incidences of burning than Kopouatai.

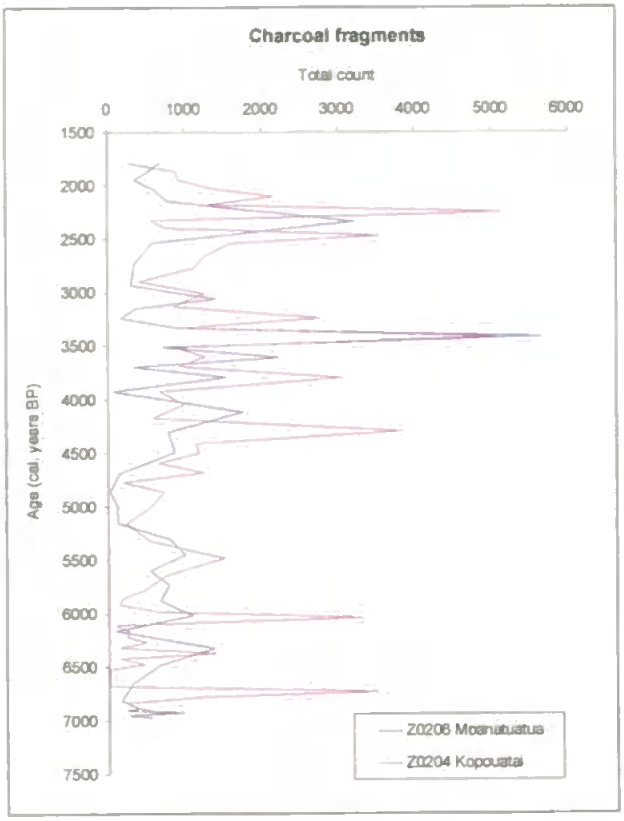

Figure 8.9 Charcoal counts from Kopouatai and Moanatuatua.

Similar to Newnham *et al.*'s (1995) late Holocene findings from the same site, core Z0204 from Kopouatai shows an increase in charcoal abundance up-core, particularly from 4,400 BP, suggesting that fire occurrence at this site was increasing throughout this period. By comparing the charcoal counts with the peat humification light transmission results, it can be seen that at both sites the increase in charcoal abundance, suggesting drier conditions, coincides closely with the increase in light transmission that suggests wetter conditions. This, together with the dissimilarity index of the peat humification records, suggests that the late-Holocene became more variable in terms of climate, particularly after 5,000-4,000 BP. Together with the overall trend in the peat humification record towards wetter conditions, these results suggest an increase in late Holocene seasonality – that the summers became drier and the winters became wetter, but that the peat humification record suggests an overall wetter signal. This Mid-Holocene Transition fits with previous suggestions of a more variable late Holocene climate e.g. McGlone (1988). This is discussed in more detail later (section 8.4).

The separate fragment counts of charcoal remains that are less than and more than 1mm are extremely similar for both sites. This suggests that either a) the charcoal record is a combination of regional and local burning signals, b) local burning is strongly controlled

by regional influences that also cause regional burning events or c) the choice of fragment size categories is unsuitable to differentiate between the two – microscopic charcoal would perhaps be a better indicator of regional burning.

8.4 Climatic inferences

This section discusses the events and trends identified from both sites in terms of their climatic interpretations, with reference to the literature already published for sites from New Zealand, other parts of the Southern Hemisphere and, where appropriate, for the Northern Hemisphere.

8.4.1 Climatic shifts/events

Below, *Table 8.3* lists the start dates of the main wet and dry climate shifts, as identified from the amalgamated peat humification records calculated for both sites. Tephra layers that confuse the light transmission record have been excluded when drawing climatic inferences.

As can be seen when taking into consideration age error ranges, the timing of events as determined from the composite peat humification records are similar between sites. Each composite record compares well with that from the other site by averaging out unusually high and low values found in only one sample and/or in only one core. The method used here to combine records, involving simply incorporating records from the same site into one large dataset, has been shown to perform very well due to the similarity achieved between sites. Shift ages were determined from the 100-year running mean.

	Timing of start of shift (cal. years BP) (to the nearest 50 years)	
Direction of shift	Kopouatai	Moanatuatua
Dry		1,800
Wet	2,050	2,050
Dry	2,200	2,150
Wet	**2,400**	**2,350**
Dry	2,500	**2,450**
Wet	2,700	2,550
Dry	**2,900**	2,650
Wet	**3,050**	**2,850**
Dry	**3,200**	**2,950**
Wet	**3,850**	3,300
Dry	3,900	3,450
Wet	4,100	3,500
Dry	**4,250**	3,550
Wet	**4,350**	**3,650**
Dry	4,550	3,750
Wet	4,650	3,850
Dry	**5,050**	3,950
Wet	5,100	4,150
Dry	5,200	**4,350**
Wet	**5,350**	**4,550**
Dry	5,450	**4,850**
Wet	5,550	**5,050**
Dry	5,650	5,200
Wet	5,750	5,250
Dry	**6,000**	5,400
Wet	**6,100**	5,600
Dry		**5,850**
Wet		**6,050**
Dry		**6,350**
Wet		**6,600**

Table 8.3 Start timings of the wet and dry shifts as calculated from composite site records (BP to the nearest 50 years). Events have not been aligned between cores. Shifts in bold indicate the main shifts as shown in Figure 8.7.

The mid-core 'Mid-Holocene Transition' trend towards wetter conditions identified at approximately 4,500 BP would be inferred to have resulted from an increase in the strength of westerly winds across the region bringing with them more rain, according to the mechanism that precipitation is controlled by the strength of the westerlies. However, this late Holocene trend appears at first to conflict with evidence from Newnham *et al.* (1989) who inferred an overall *drier* climate during the Late Holocene from a variety of proxies: a) an increase in the Waikato region of *Agathis australis* pollen – from response function analyses of *A. australis* growth and modern rainfall and temperature data, it was found that *A. australis* actually prefers drier and warm summers (Ogden and Ahmed, 1989), b) an increase in charcoal abundance, and c) a decrease in pollen of the frost and drought sensitive *Ascarina*, suggesting an increase in extreme weather conditions. The decline in *Ascarina* pollen from 5,000 years BP onwards had already been documented by McGlone and Moar (1977), with a similarly timed shift to a drought-prone climate inferred by McGlone and Topping (1977). Elliott (1998) has also contributed to records indicating an inferred drier late Holocene from a palynological investigation of a site in Northland. Lake-level reconstructions from Lake Rotorua are also thought to represent a change from wetter to drier conditions at 4,000 years BP (McGlone, 1983). However, Lake Rotorua is situated in a tectonically active area and McGlone (1983) could not discount the blocking of the lake outlet by ash deposits as a possible mechanism that would have resulted in elevated lake levels before this time, rather than a climatic factor.

In contrast, Rogers and McGlone (1989) identify the start of increased wetland (e.g. bog, lake) development in eastern parts of the North Island at approximately 5,000 years BP. This would imply a shift to wetter climatic conditions, whose timing would be in agreement with the inferred wet shift seen in the peat humification records from Kopouatai and Moanatuatua. Rogers and McGlone (1989) account for this wetland expansion by proposing cooler wetter winters and drier summers, within an overall drier late Holocene. The records from Kopouatai and Moanatuatua suggest that the overall climate signal is that of increasing wetness, with the wet winters being sufficiently wet to override the summer dryness signal, as preserved in the peatbog archive. In other words, there seems to be general agreement that the Late Holocene became more seasonal, but Rogers and McGlone (1989) use this to defend a drier overall climate, whereas this study infers an overall wetter late Holocene climate.

The apparent difference in conclusions can be reconciled by considering the facts that a) *A. australis* is responding to the drier summers, b) the charcoal record represents burning also occurring in the drier summers, c) *Ascarina* is recording a drought signal (from drier summers) and d) the fall in lake levels are due to the tectonically active nature of the region. In this way, increased seasonality is accounting for the drying trends previously observed in the literature, but rather than using them to infer an overall drier climate, they are in fact implying drier summers. Wetter, cooler winters are therefore responsible for the overriding wetter climate signal as found in this project.

Glacier advances in southwestern New Zealand, identified from moraine evidence, are inferred to have occurred at 5,000 cal. years BP (Gellatly *et al.*, 1988). This would also seem to correspond with the late Holocene wetter climate as suggested by the peat humification records from Kopouatai and Moanatuatua. Recent historical observations suggest that glacier advances in southwestern New Zealand are primarily driven by the increased strengthening of westerly and south-westerly airflows (Fitzharris *et al.*, 1992). The glacier advances therefore suggest that a significant strengthening of these directional winds occurred at 5,000 cal. years BP, at almost exactly the same time as the Mid-Holocene Transition observed in this study. Together with the formation of wetlands around this time (Rogers and McGlone, 1989) this evidence corroborates a wetter late Holocene New Zealand climate.

ENSO

There is currently debate over the history of ENSO – in particular whether this climate cycle has been present over long timescales, or has only developed in the Holocene. Loubere *et al.* (2003) conclude that ENSO did not exist before 7,000 cal. years BP, and Sandweiss *et al.* (1996) infer the onset of ENSO at 5,000 years BP along the Peruvian coast. Evidence is now accumulating to suggest that it has been present long before this, but operating in a reduced manner. From coral oxygen isotope investigations over the last glacial-interglacial cycle, Tudhope *et al.* (2001) have determined that ENSO has been present as a climatic phenomenon over the last 130,000 years i.e. even during glacial periods. Its strength has varied over time in response to precessional forcing resulting in changes in seasonal insolation values. Clement *et al.* (2001) suggest that the timing of the perihelion (when the Earth is nearest to the Sun) is crucial in these precessional-driven ENSO variations. When the perihelion occurs during the Northern Hemisphere Summer/Winter (or Autumn/Spring), trade wind strength increases and El Niño events are

reduced (or enhanced) due to uneven heating of the Equatorial Pacific and changes in seasonal extremes between hemispheres. It was also found that ENSO activity was weakened during the mid-Holocene after which it has gradually increased in strength (Clement *et al.*, 2000). This is supported by Rittenour *et al.* (2000) who suggested a weak/absent ENSO in the early Holocene that was thought to be caused by precessional forcing. As well as finding semi-precessional climate cycles, Turney *et al.* (2004) also infer orbital-led fluctuations in ENSO from north eastern Australian records, as determined from millennial-scale dry shifts (thought to relate to El Niño phases) that match the timing of North Atlantic Dansgaard-Oeschger warm events.

Unfortunately, the sampling resolution in this investigation was insufficient to pick out the sub-decadal periodicity of ENSO events. However, the dissimilarity index seems to indicate that all cores show a greater degree of variability during the late Holocene. The younger part of the peat humification records (after 4,000-3,500 BP) is more variable than the oldest sections, and this pattern is particularly clear in core Z0204. This agrees with previous work suggesting that the increase in moisture variability between 4,000-1,000 years BP is due to stronger ENSO fluctuations (McGlone and Wilmshurst, 1999b). McGlone *et al.* (1992) proposed that such an intensification of ENSO in the mid-Holocene resulted in highly variable rainfall and the occurrence of severe droughts. This could account for the increased fire incidence occurring at Kopouatai at the same time as a generally wetter trend, because the fires most likely occurred during late summer when the bogs had been able to dry out sufficiently. ENSO intensification is most likely combined with enhanced seasonality (i.e. drier summers and wetter winters) as a possible forcing mechanism resulting in these seemingly opposing characteristics of the palaeorecord. The increased variability of New Zealand climate records in the mid Holocene that are thought to result from such enhanced ENSO activity is also matched in northern Australia after approximately 4,000 years BP (Shulmeister and Lees, 1995). Such intra-hemispheric similarity suggests a large scale forcing factor – the stronger seasonality could be explained by precessional- (i.e. orbital forcing-) driven changes in insolation values at this latitude (section 8.4.3).

8.4.2 Intra- and inter-hemispheric comparisons

In terms of the long term Holocene climate records, various studies from different global locations have also identified a wet shift similar to that of the Mid-Holocene Transition identified at Kopouatai and Moanatuatua.

From peat humification results from south west Australia, Dodson and Lu (2000) inferred initially dry conditions at approximately 5,000 years BP, after which the record becomes wetter. This, together with other Australian work referred to by them, is inferred to be due to a regional increase in the strength of the westerlies. This wet shift closely matches the New Zealand results from this study, both in direction of the mid-Holocene climate shift and in its timing. Dodson (2001) states that in southwest Australia many wetland systems started forming in the mid-Holocene, reinforcing previous work by Harrison and Dodson (1993) and Kershaw (1995) who also suggested the prevalence of warmer and wetter conditions at this time from the analysis of lake and peatland archives. Given the similarity between southwest Australia and New Zealand in terms of their southern mid-latitude location and sensitivity to the westerlies, it is not surprising that the wind regimes of both regions are similarly controlled and affected.

McGlone *et al.* (1992) produced a synthesis of South American climate work based on pollen and lake level records, summarising that southern regions of the continent were wetter but more variable from 5,000-3,000 years BP. McGlone *et al.* (1992) have suggested that general observed increased seasonality is responsible for such regions of southwest South America at similar latitudes to New Zealand becoming much wetter in the late Holocene.

Pollen work from a lake in central Chile also suggests that the regional climate became more humid during the late Holocene, with the preceding more-arid period ending at approximately 5,700 cal. years BP (Villa-Martínez *et al.*, 2003). Although this increase in precipitation, thought to result from an increase in westerly storm tracks, occurs approximately 1,000 cal. years before that observed from the New Zealand results here, it nevertheless suggests a general late Holocene coherency in climate trends within the Southern Hemisphere mid-latitudes.

Other work from central Chile (Jenny *et al.*, 2002) seems to support the findings of this study concerning linkages between New Zealand westerly and precipitation patterns compared to reconstructed insolation values. It was found that since 3,200 cal. years BP precipitation has been higher than previously, which was attributed to a weaker subtropical high pressure cell and stronger westerlies, and possibly increased ENSO activity. This in turn was found to match insolation records that suggested increased seasonal insolation (together with increased summer insolation) at a similar time. Veit (1996) previously

reported evidence from northern Chile of an increasing influence of westerlies between 5,100-3,700 years BP and 3,000-1,800 years BP. At 5,000 years BP in South America other significant climate-related events occurred, namely the end of Andean soil formation as the Holocene climatic optimum ended, the start of glacier advances, and a shift to a more variable climate (Veit, 1996). The results presented in this thesis, indicating a mid-Holocene shift to an overall wetter climate with stronger seasonality and variability, would appear, therefore, to be consistent with comparable records from elsewhere in the Southern Hemisphere.

Similar comparisons can be made with comparable records from the Northern Hemisphere. Barber *et al.* (2003) present climate records of three bogs from northern Britain and Ireland and find that they compare well with numerous other palaeoclimatic peat records from across Europe in showing a general trend towards wetter conditions that commenced at around 4,400 cal. years BP. The direction and age of this trend matches the observed increase in baseline wetness levels inferred from Kopouatai and Moanatuatua. As well as this increasing trend, both New Zealand sites show a strong wet period (of larger magnitude and duration at Moanatuatua) starting at approximately 4,500 BP at Moanatuatua and at 4,400 BP in Kopouatai. If these records from different hemispheres are responding to the same climatic event and driving force, then it could be tentatively suggested that the Southern Hemisphere is leading the Northern Hemisphere, since the Mid-Holocene Transition identified from Kopouatai and Moanatuatua starts from between 5,000-4,000 cal. years BP.

Barber and Charman (2003) summarised northern England wet shift records from different sites and identified phases of contemporaneous shifts. Of the six groups that fall within the period of study of this project, all seem to have an equivalent at Kopouatai and/or Moanatuatua (*Table 8.4*). Also, Hughes *et al.* (2000) identified wet shifts from Walton Moss in northern England, and summarised them together with previously-derived palaeomoisture records from England and Scandinavia. Those listed also show a strong correspondence with the New Zealand shifts (*Table 8.4*). Magny (2004) investigated published lake level records derived from a variety of proxies and interpreted them climatically. They show general agreement with the northern England and New Zealand sites.

Hughes *et al.* (2000)	Barber and Charman (2003)	Barber *et al.* (2003)	Magny (2004)	Kopouatai	Moanatuatua
		1,750**	1,800-1,700		
2,320-2,040*	2,150	2,250		2,400	2,350
	2,650	2,750-2,350	2,750-2,350		
3,170-2,860*	2,900			3,050	2,850
3,500	3,500	3,200	3,500-3,100		3,650
			4,150-3950		
4,410-3,990*	4,400	4,400-4,000**		4,350	4,550
			4,850-4,800		5,050
5,300	5,300		5,650-5200	5,350	
			6350-5900	6,100	6,050

Table 8.4 Major European and New Zealand wet shifts *as identified from peatland records and wet* phase *start and end ages from European lake levels. Dates are rounded to the nearest 50 years, except Hughes et al. (2000) which are corrected to the nearest 10 years. * indicates 2σ radiocarbon age ranges. ** indicates shifts only observed in two of the three records produced by Barber et al. (2003).*

In addition to the main, general shifts discussed above, comparisons of the timing of lesser shifts indicate that various other documented events from Bolton Fell Moss and Walton Moss in northern England could also be matched in timing in the New Zealand records. These are a) a dry shift in the English sites at 3,900 cal. years BP (Barber *et al.*, 2003) matched in New Zealand at 3,900 BP (Kopouatai) and 3,950 (Moanatuatua), b) a wet shift at 3,750 cal. years BP in England (Barber *et al.*, 2003) and at 3,850 BP (Kopouatai) and 3,850 BP (Moanatuatua), and c) a wet shift at 3,015 cal. years BP (Hughes *et al.*, 2000) and at 3,050 BP in New Zealand (Kopouatai). If these events are indeed linked, then they are important for detailing smaller-scale globally-felt climatic events.

Other work in the Southern Hemisphere identifies a climatic deterioration (a significant wet period) at approximately 2,700 cal. years BP from Chile (van Geel *et al.*, 2000). From the amalgamated peat humification records it can be seen that at both sites there are wet shifts occurring around this time at Kopouatai (3,050 BP and 2,700 BP) and at Moanatuatua (2,850 BP and 2,550 BP). This event is not as clear when considering each core individually, for example this time period coincides in core Z0102 with the Whakaipo Tephra layer. However, either one of these events from each site could coincide well with the South American findings, given their age errors, although it is more likely to be the earlier, larger-scale shifts. This Chilean event is thought to be due to a strengthening of

westerlies at this time, as would be the proposed mechanism of such a wet period in New Zealand. It has been connected with the occurrence of a similarly timed climatic deterioration in the Northern Hemisphere occurring in the Netherlands at 2,650 BP, other locations throughout Europe (van Geel *et al.*, 1996; van Geel *et al.*, 1998) and possibly in North America (Booth and Jackson, 2003). Van Geel *et al.* (1996) also amalgamate evidence of similarly-timed climate shifts from the Southern Hemisphere, although certain climatic anomalies are seen to be drier rather than wetter, for example, the decline of *Ascarina* from New Zealand observed by McGlone and Moar (1977). If all these events are indeed occurring at the same time, thus indicating that they are responding to the same climate phenomenon, these New Zealand results are important in reinforcing the theory of such a globally-felt event, although it is still unclear as to how such a climate signal could be transmitted globally.

Taken together, these possible teleconnections between sites from different hemispheres could be recording globally-felt climate phenomena. With regard to the Mid-Holocene Transition, the evidence presented here is consistent with a Southern Hemisphere lead over the Northern Hemisphere. A Southern Hemisphere-led global climate has been proposed by Hays (1977) and Williams *et al.* (2003), however, both these claims were in relation to large-scale climate transitions for which time lags were 2-3,000 years. Here, the 5,000-4,000 BP shift to wetter conditions, that from the amalgamated records occurs at approximately 4,500 BP at both sites, precedes the majority of the European records (grouped to 4,400-4,000 cal. years BP by Barber *et al.* (2003)) by only a few hundred years.

8.4.3 Possible forcing mechanisms

It is widely acknowledged that the strength of the westerlies is controlled by insolation differences between the Equator and the poles; larger insolation differences lead to stronger westerly flows (Dodson, 1998). A stronger gradient would displace the Subtropical Front and the associated westerly airflow northwards, resulting in stronger westerly circulation over New Zealand (Dodson, 1998) and as a consequence, more precipitation. Shulmeister (1999) considers there is sufficient evidence from New Zealand to confidently confirm increased westerly circulation at 5,000 years BP, ultimately caused by increased heat (and pressure) differences between the poles and the Equator. This would fit well with the increase in wetness reconstructed from Kopouatai and Moanatuatua. Shulmeister (1999) also proposed a precessional-driven increase in seasonality in

Australasia at around 5,000 years BP. In addition, work in South America by Markgraf (1993) also identified an increase in the strength of westerly winds at a similar time, thereby suggesting a strong intra-hemispheric similarity.

The palaeomoisture records produced for Kopouatai and Moanatuatua imply that a northerly shift in westerly airflow i.e. a strengthening of the westerlies, would have occurred at 4,500-4,000 cal. years BP. Using the same mechanism, McGlone and Wilmshurst (1999b) suggested an earlier increase in the strength of south westerly winds from 7,000 years BP onwards caused by a gradual shift north of the subtropical high throughout the Holocene. This in turn resulted in an increase in the amount of winter precipitation over New Zealand.

Berger (1992) reconstructed insolation values based on orbital forcing parameters for every 10° in latitude over the last 10Ma. These calculations are used here to investigate the strength of the westerlies over time, based on the established premise (Dodson, 1998) that their strength is driven by the difference in insolation values between the Equator and the poles.

Reconstructed summer insolation values (from Berger (Newnham, 2004, pers. comm.) from 15°S and 65°S were compared throughout the Holocene (*Figure 8.10*) and are seen to have increased over the last 10,000 years, albeit at varying rates. During the early Holocene between approximately 10,000 and 8,000 years BP the difference in insolation between the two latitudes increased only minimally. However, after approximately 6,000 years BP the difference in insolation values has been increasing progressively. Such an increase in insolation difference implies a trend in strengthening westerlies throughout the Holocene, intensifying particularly around 6,000 years BP. Stronger westerlies would have resulted in increased precipitation over New Zealand consistent with the Mid-Holocene wet shift seen in the peat humification record at both sites. The wet shift appears to be lagging that of the insolation record, and this could be due to the time taken for the wind systems to adjust and shift in response to the insolation changes.

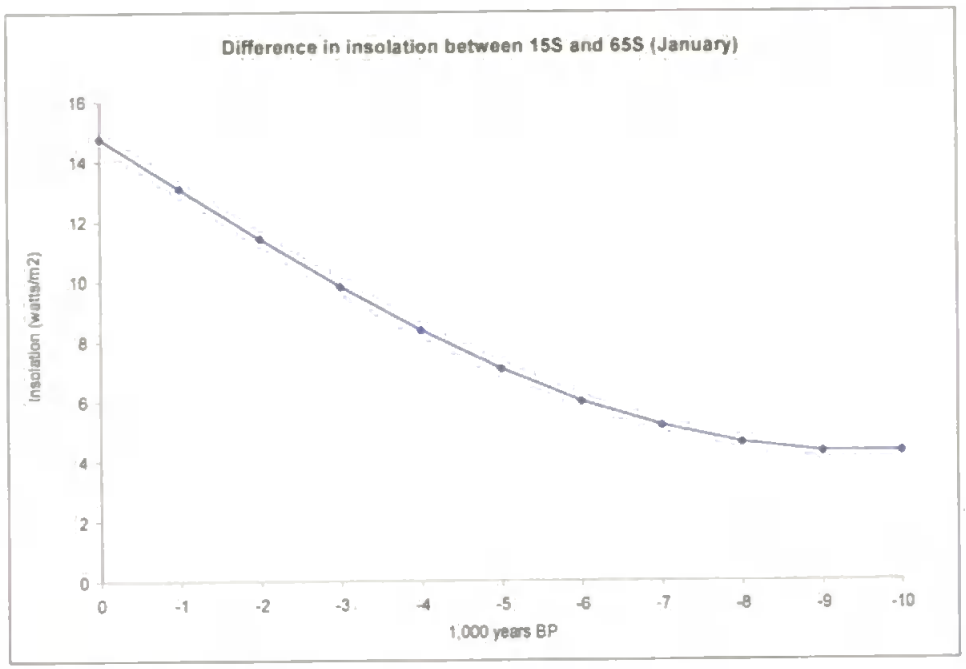

Figure 8.10 Difference in January (summer) insolation values for 15°S and 65°S over the last 10,000 years (from Berger (Newnham, 2004, pers. comm.).

In addition to changes in westerly wind circulation, orbital variations also resulted in marked changes in seasonal insolation patterns in the mid-southern latitudes during the Holocene (*Figures 8.11* and *8.12*). These changes in the seasonal strength of insolation might explain the apparent anomaly observed in the records presented here, between increasingly wet conditions and increased fire frequency, after *c.*4,500 cal. years BP observed at both sites.

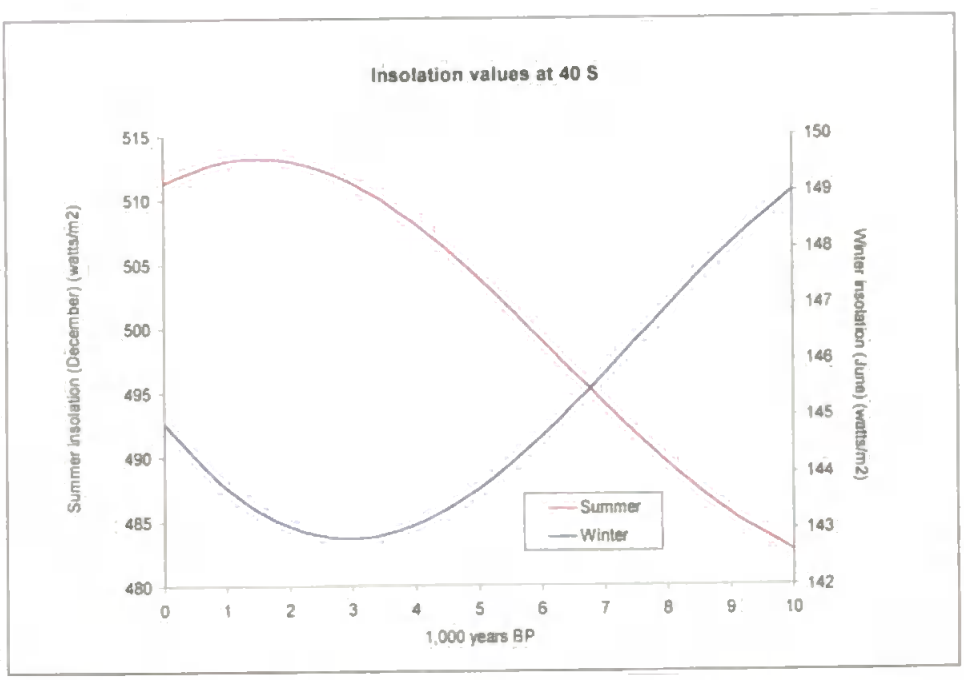

Figure 8.11 Summer (December) and winter (June) insolation values for 40°S since 10,000 years BP (from Berger, 1992).

Cooler, wetter winters resulted from a decrease in winter insolation and presumably enhanced westerly circulation after 5,000 BP, leading to overall increasing bog wetness. Warmer, drier summers are explained by the increase in summer insolation over the same period and led to increased burning of the bog. Seasonality is also shown to have increased over the same timeframe as an increasing difference between summer and winter insolation values (*Figure 8.12*).

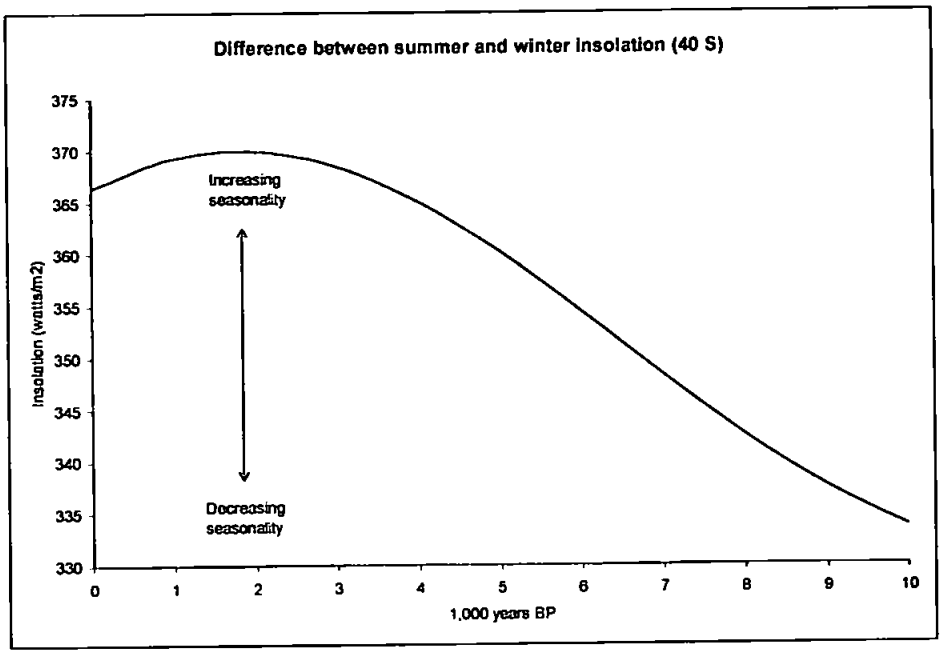

Figure 8.12 The difference between summer and winter insolation values for 40°S since 10,000 years BP (Summer minus Winter) (from Berger, 1992).

Further support for this explanation is provided by comparison of winter insolation values with present values (*Figure 8.13*). Around 6,000 years ago, winter insolation values at 40°S fell below modern values for the first time in the last 40,000 years. This is very similar in timing to the 'Mid-Holocene Transition', with the drop in insolation occurring before the change in climate trend. Such a time lag would be expected, as the westerly wind systems adjust to climatic shifts. Further support for the enhanced seasonality explanation of the Mid-Holocene Transition is provided by the evidence from both sites for increased variability in peat humification values following this transition.

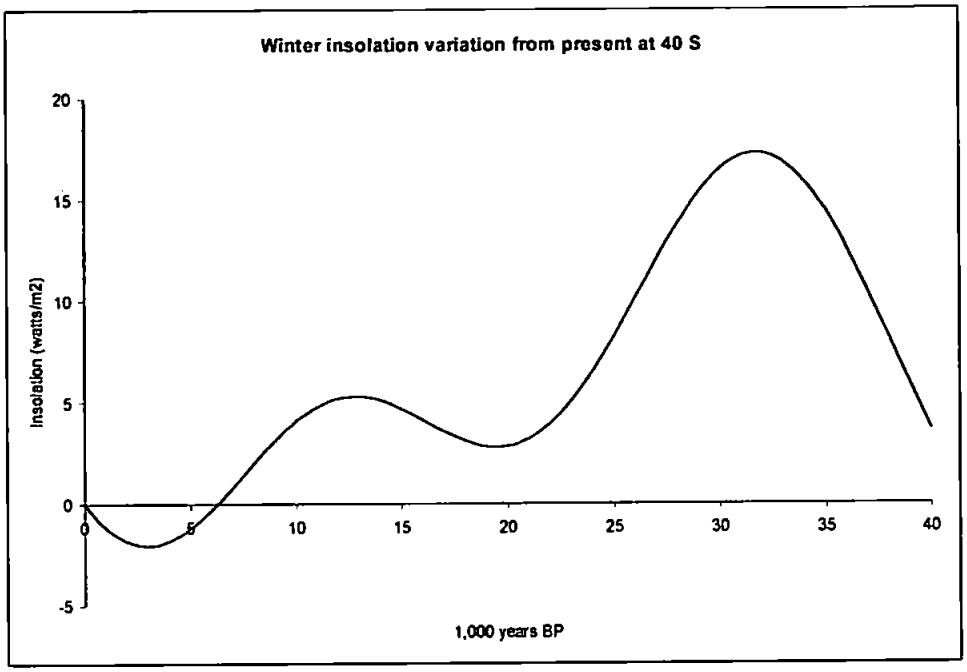

Figure 8.13 Winter insolation variation from present at 40°S since 40,000 years BP (from Berger, 1992).

Summary

There appears to be mounting evidence supporting a precessional-driven increase in the strength of the westerlies, in Australia, New Zealand and South America during the mid-Holocene. This has been demonstrated from the reconstruction and comparison of insolation values for various latitudes of the Southern Hemisphere that show a progressively increasing low-high latitude gradient since 10,000 years BP. Such a mechanism concurs with the Mid-Holocene Transition wetness trend identified from Kopouatai and Moanatuatua. This wet shift, together with enhanced charcoal abundances, can be reconciled with the previous palaeoclimate records from New Zealand that inferred a drier late Holocene, through the increase in seasonality resulting in wetter winters and drier summers.

The increase in variability throughout the Kopouatai and Moanatuatua peat humification records together with the increase in charcoal abundance could be explained by the increase in seasonality (i.e. drier summers and wetter winters), as reconstructed from the insolation records. This is also likely to be related to the strengthening of ENSO at around this time, that is suggested to be responsible for larger climatic extremes during the late Holocene (McGlone *et al.*, 1992). This enhanced ENSO activity might also be related to orbital forcing (McGlone, 1988).

8.5 Appraisal of techniques used in this investigation

8.5.1 Testate amoebae

It is clear from Chapter 5, where the testate amoebae results were presented and discussed, that at Kopouatai and Moanatuatua the use of fossil testate amoebae is not a suitable palaeomoisture technique. This is because of their low concentration at depth, thought to be mainly due to poor test preservation, combined with the high levels of degraded plant material, that together result in unproductive counts. Initial density separation work suggested that this technique might ultimately be successful in concentrating tests at abundances sufficient for counting. However, further work is required. If extracted concentrations can be increased, then testate amoebae could be used as a quantitative palaeomoisture proxy, as the modern fauna have been shown to respond to hydrological conditions (Charman, 1997). However, selective preservation would still probably remain an issue, as has been demonstrated by Wilmshurst *et al.* (2003) who found little overlap between modern and fossil test assemblages.

Samples taken from the top 20/30 cm of peat and analysed for testate amoebae showed that modern, living test concentrations are adequate for counting. These surface samples would therefore be useful for the incorporation and development of Charman's (1997) training set for New Zealand and contribute to Wilmshurst *et al.*'s (2003) work deriving a testate amoebae-based moisture record. Further work investigating the relationship of testate amoebae and environmental factors would be worthwhile.

8.5.2 Peat humification

From the clear similarity of the amalgamated site records, together with the wet and dry shifts/trends that have successfully been identified (some of which appear to match records from the Northern Hemisphere) it is concluded that the standard method of peat humification works well at these Southern Hemisphere sites. The technique appears to be as productive for the Southern Hemisphere as it is for the Northern Hemisphere bog sites on which it is regularly used as a palaeomoisture proxy. In fact, it could be better suited to restiad sites, where peat composition is less variable and mosses are largely absent However, as a criticism of the method itself, rather than on its application to Southern Hemisphere sites, peat humification is only a semi-quantitative/qualitative technique and so, unlike the application of transfer functions using testate amoebae, no actual values of moisture can be reconstructed.

It is not clear to what extent the up-core long term trends towards increased light transmission result from climate, an age effect or a combination of the two. At Kopouatai and Moanatuatua however, it seems that all the cores show a shift to higher light transmission values at the same time, thereby implying a regional climatic forcing operating at that particular time.

In peatland sites from New Zealand, light transmission results can be significantly affected by the presence of abundant tephra layers in the stratigraphy. This can influence the interpretation of the record's climate shifts unless the mineral content is corrected for. A method was devised to enable such a correction, and is seen to work well considering errors involved with the initial TOC readings (that had to be corrected) and the conversion from TOC to LOI. It is not clear whether the relationship between carbon content and LOI is constant over time, therefore it is recommended that LOI measurements should be used directly.

8.5.3 Plant macrofossils and charcoal

Plant macrofossil analysis holds great potential for the reconstruction of past vegetation assemblages, particularly as their Dupont scores appear to match the peat humification records well. Comparison of the plant macrofossil remains with the peat humification record shows a general agreement of an up-core wet trend. Regrettably, due to time constraints insufficient work was done on the samples from these sites – ideally all cores would have been investigated.

Counts of the macro charcoal fragments successfully identified peaks in abundance in both sites, indicating clear local burning events either on the bogs themselves or in close proximity. In contrast to most Northern Hemisphere investigations, in this study anthropogenic factors can be rejected and so environmental factors, including climate, must be responsible. Interestingly, the burning events recognised seemed to broadly coincide with the *wet* periods, as inferred from the peat humification record. It is most likely that the simultaneous occurrence of wet and dry indicators is due to an increase in climate variability, caused by increased seasonality and/or intensification of ENSO. Charcoal analysis has therefore been shown to be a valuable tool in reconstructing past climate and in particular for providing detailed insights into seasonal patterns, providing additional information to the general wet/dry shifts shown in the peat humification records.

8.6 Problems and limitations

This section outlines the main limitations and problems encountered with the techniques employed during the data processing and analysis, and offers possible suggestions for future work to overcome them.

8.6.1 Palaeomoisture records

As demonstrated, fossil test amoebae concentrations were inadequate for deriving palaeomoisture records. Investigation of alternative sites e.g. *Sphagnum* dominant, could prove more successful.

The effect of mineral content on the light transmission readings has been discussed above, and is especially problematic in northern New Zealand given the high frequency of volcanic eruptions. However, this problem can be resolved, and it is recommended that all such work in New Zealand at the very least carries out LOI or TOC, preferably with tephra shard counts, in order to address this problem adequately. As volcanic as well as non-volcanic minerogenic delivery to peats is not restricted to New Zealand, this recommendation could possibly apply elsewhere as well.

8.6.2 Age-depth models

As well as the methodological limitations already discussed, the main problems identified with deriving reliable palaeomoisture records are concerned with producing a reliable chronology.

Choosing an appropriate age-depth model was very problematic, as numerous issues had to be taken into consideration. As no model can give a true depiction of peat accumulation (particularly as peat is compacted over time), the task here was to choose the model that was most accurate in terms of bog accumulation.

Using standard spreadsheet programmes (e.g. Excel) to investigate the age-depth models is restrictive because it requires one value to be inputted for each level in order to be able to plot trendlines etc. However, this does not take into consideration the error ranges for each date. In fact, fitting lines completely 'by eye' could also be advocated as a viable method, as more freedom is available when aligning them despite the obvious subjectivity introduced. Alternatively, it has been suggested that rather than using the mid-point, the

probability plots of the radiocarbon ages can be used to identify the section of the age range that has the most probability of occurring (Telford *et al.*, 2004b).

Additional options for improving the age-depth models would include wiggle-matching techniques (e.g. Blaauw *et al.*, 2003) and Bayesian techniques (e.g. Buck *et al.*, 2003). However, wiggle-match dating requires a large number of radiocarbon ages in a close suite which can prove prohibitively expensive for a multi-record investigation such as this one. By providing more radiocarbon ages, moreover, the chances of them all fitting a perfect chronology with no age reversals, decrease. Dating specific changes and events within the stratigraphy is also an alternative option, as this would give a more reliable age for a particular event, rather than relying on interpolating between ages.

The Southern Hemisphere radiocarbon calibration curve used in the CALIB 4.4.2 calibration programme (Stuiver and Reimer, 1993) recognises the offset in Southern and Northern Hemisphere ^{14}C values, but applies a constant 27 year subtraction for the Southern Hemisphere throughout the Holocene prior to AD 950 (McCormac *et al.*, 2002). This is based on measurements over the last 1,000 years, and assumes that the offset has remained constant before this time, which is unlikely. This could therefore be introducing possible errors for the calibrated dates, and creating problems particularly in the comparison of dated climate shifts between hemispheres.

8.6.3 Tephra analysis

In this project, the use of tephra layers is vital in deriving the core chronologies, but a serious limitation associated with their presence is their interference with the climatic interpretation of the peat humification records. Increased mineral content (e.g. tephra layers) artificially enhances the light transmission values that are measured as a proxy of peat humification. Higher light transmission values would usually be palaeoclimatically interpreted as the prevalence of wet conditions, however, to be certain of a climatic signal confounding tephra layers must first be excluded. In addition, determining where the tephra layers start and finish is extremely important but not straight forward, because of the observation that micro-tephra can be attenuated above and below the main layer (Ballinger, 2003). In this study TOC proved to be the most reliable method for distinguishing tephra layers.

8.7 Recommendations for further work

The peat humification/plant macrofossil/charcoal record should ideally be extended to the surface of the bog because a continuous record to the present would be of great interest, particularly to see if the trend towards wetter conditions that begins at approximately 4,500 BP, continues. The Kaharoa Tephra (AD 1314±12) would be an invaluable time marker and tie-point between cores. Having a continuous record to the surface would also permit further study of testate amoebae abundances at depths extending below the limit of the surface samples studies in this project. However, it must be noted that the complete retrieval of the more-recent, less humified material is problematic. A complete Holocene record, extending the palaeomoisture record back to the Hinuera sediments when the bogs started forming would also be advantageous from a palaeoclimatic perspective. Increasing the sampling resolution of the study would also possibly enable the detection of smaller-scale climate events, particularly in relation to ENSO. Density separation work should also be carried out to determine whether or not this method holds any value in improving the yield of testate amoebae extracted from these peats.

Further work of interest would be to study the presence of testate amoebae in Torehape Bog, North Island. This site, located immediately to the north of Kopouatai and originally thought to be part of the same bog complex, is of particular interest because it is comprised of restiad-dominated vegetation overlying a *Sphagnum* substrate. This switch in vegetation layering occurred due to the start of drainage around the site for farming (Bates, 1973). Such a study would enable a direct comparison of the relative abundances of testate amoebae from the two substrates to see if the same site once had high abundances of tests. This site is preferable to Kopouatai and Moanatuatua where *Sphagnum* is only abundant in discrete clumps at the bog surface. Higher test concentrations would be expected in the *Sphagnum* layer, based on experiences from Northern Hemisphere *Sphagnum* peat bogs. However, from the limited work on the rare *Sphagnum*-dominated site of Eweburn Bog from southern New Zealand (Wilmshurst *et al.*, 2003) it appears that that site is notable for containing fewer tests than expected, with poor overlap between fossil and contemporary species.

Ideally, additional environmental variables should be measured and considered for the modern, surface testate amoebae work (such as temperature, rainfall, bulk density, nutrients, depth from surface) to investigate further the controls on test assemblages. In this project, only moisture content, depth to water table, pH and conductivity were recorded,

which, with retrospect is probably insufficient. Ideally, longterm water table measurements should be taken, rather than a one-off, single measurement. Also, the numerous short cores that were examined for the decline in test abundances need to be extended deeper, as the depths retrieved for many of them did not clearly determine the depth at which test abundances dropped to insignificant levels.

Restiad peat bogs similar to these of New Zealand are also found in Australia. Investigative testate amoebae work at these sites would be of great interest to determine, amongst other things, whether the paucity of tests is characteristic of only the New Zealand sites studied here, or whether it is typical of all restiad sites.

A broad tephrochronology was successfully derived for all cores using the upper and lower Taupo and Tuhua Tephras that were easily recognisable in the field. This chronology was improved with suites of ^{14}C dates, however further improvement could be made with the identification of cryptic tephra layers within the stratigraphy, through high-resolution shard counts. The presence of some cryptic tephra layers in certain cores was ascertained, although not directly as part of this project. If such layers could be identified by microprobe analysis, then they would be invaluable as tie-points for linking core stratigraphies together and in verifying the age-depth models. Shard counts would also help to confidently determine whether high light transmission values are 'real' climate induced signals, rather than artefacts of mineral 'contamination' diluting the organic component of the peat humification sample. As demonstrated by Ballinger (2003) tephra shards appear to have been attenuated beyond their highest concentrations. Even though TOC does contribute in determining the presence of mineral layers, it is not sufficiently sensitive to pick up minor changes. Work is currently being developed to progress the cryptic tephra records at these sites.

Statistical work, in particular spectral analysis, would be beneficial to determine whether there are any underlying temporal cycles in the light transmission records. Such work was not carried out as part of this project due to time constraints. Time-series analysis might enable the forcing mechanisms of climate change to be identified, or at least identify similar patterns in the Southern Hemisphere as have been found in the Northern Hemisphere. For example, finding a similar cycle to the approximately 200-year postulated solar cycle identified in Northern Hemisphere peat bogs from multiple studies (e.g.

Chambers and Blackford, 2001; Chambers *et al.*, 1999) would help confirm a globally acting forcing mechanism.

8.8 Summary

This chapter has discussed the palaeomoisture records from peat profiles deposited between the Tuhua (6,150±30 cal. years BP) and the Taupo (1,850±10 cal. years BP) tephra layers in terms of their climatic implications. A climate shift towards a generally wetter climate has been identified in all cores at 4,500-4,000 cal. years BP that seems to match Northern Hemisphere peatland records. This shift appears to contradict some previous work from New Zealand that inferred the late Holocene to be drier. It is proposed here that the mechanisms responsible for this and the increased charcoal abundance in the late Holocene are that the strength of the westerlies increased at approximately 4,500 cal. years BP, bringing increased winter rainfall, combined with a strengthening ENSO bringing severe summer droughts that facilitated burning events. These changes are likely to be related to precessional-driven changes in seasonal insolation received in the Southern Hemisphere.

Within this long term trend, a series of wet and dry shifts were successfully identified and found to be more or less contemporaneous between cores. This suggests that both Kopouatai and Moanatuatua are responding in the same way to a large-scale external forcing factor i.e. climate, and that peat humification is a suitable palaeomoisture proxy to be used on these raised, restiad peatland sites.

The remaining palaeomoisture proxy techniques have been shown to work with varying degrees of success on these sites, with plant macrofossil work and charcoal showing more promise than that of testate amoebae. The peat humification records however are replicated extremely well between sites, demonstrating its suitability as a proxy palaeomoisture indicator.

CHAPTER NINE – CONCLUSIONS

9.1 Conclusions

This project has successfully produced high resolution mid-to-late Holocene palaeomoisture records for the hydrologically separate peatland sites of Kopouatai and Moanatuatua, located in the North Island of New Zealand. A variety of palaeoecological techniques that are regularly applied in the Northern Hemisphere, were employed. These analyses were of testate amoebae, peat humification, plant macrofossils and charcoal, together with TOC as a measure of the peat's organic content. The raised, ombrotrophic nature of the sites allowed the interpretation of the moisture records in terms of palaeoclimate. The time interval investigated, *c.*7,000 to *c.*1,750 cal. years BP, precludes anthropogenic factors for any of the observed changes in characteristics of the peat. The profiles have been extremely well dated using a combination of AMS ages and tephras, resulting in the development of detailed age models, with consideration of inherent problems and errors with age-depth modelling.

The applicability and success of the techniques on these Southern Hemisphere sites was varied:

a) Testate amoebae analysis was found to be an inappropriate technique to be applied to these sites due to the very low fossil test abundances making counting slow, laborious and unproductive. Surface samples were relatively high in abundance, typically between 11-32,000/cm^3 (130-300,000/dry g) at Kopouatai, suggesting that the fossil tests are scarce because of their poor preservation, as well as the samples being 'diluted' by a large amount of very fine, well humified organic matter. Problems of selective preservation are also an issue. Preliminary density separation work showed potential for improving fossil test concentrations for counting, although more work is required.

b) After the exclusion of testate amoebae as a viable palaeo-technique for these sites, peat humification became the main focus of the project. This method has successfully produced credible palaeomoisture records for these restiad peat bogs of New Zealand, whilst also demonstrating the method's applicability in the Southern Hemisphere. The most highly resolved, replicated peat humification records ever produced were derived. Peat humification light transmission results of some samples were found to be severely affected by an enhanced mineral content, usually resulting from the deposition of

tephra layers. An experiment was carried out to investigate the relationship between light transmission and mineral content, which was found to be exponential. From this, a correction formula was derived to account for this 'contamination'. However, due to problems associated with a) the transformation of TOC measurements to LOI and b) the fact that a 100% mineral sample did not give a 100% light transmission reading, care still had to be taken when interpreting the corrected light transmission curves.

c) Plant macrofossil analysis was not undertaken extensively largely due to time constraints. Two cores, one from each site, were nevertheless extensively analysed for plant macrofossil content. In both cases, changes in vegetation composition related to moisture gradient in the modern bog vegetation seemed to replicate well the peat humification records from the same sites. This suggests that plant macrofossil analysis has potential in the reconstruction of past precipitation in New Zealand, at least as a complementary technique in a multi-proxy study.

d) Charcoal analysis identified discrete peaks representing major burning events in the vicinity which require non-anthropogenic explanation. The frequency and magnitude of charcoal peaks was observed to increase after *c.*4,500 cal. years BP. It is inferred that the burning events occurred during drier summers, resulting from an increase in seasonality as reconstructed from past summer and winter precessional-driven insolation values together with an inferred enhanced ENSO.

e) TOC analysis was hindered by the offset in values between runs but fortunately this was noticed and subsequently corrected for. Despite this complication, the results clearly highlighted the highly minerogenic layers that were present, most of which were explained by the presence of tephra layers.

f) Radiocarbon dating of the cores was invaluable for deriving age-depth models. Overall, the AMS ages were stratigraphically coherent, with only one age reversal from the 47 ages obtained. The bulk peat dates had much larger errors and showed greater deviation from established tephra ages and so were omitted from the age-depth models.

g) Tephra analysis and identification was also extremely beneficial for the project, mainly for clearly defining the period of study (between the Taupo and the Tuhua Tephras) but also for helping improve the chronology of core Z0102. The presence of significant cryptic tephras, hinted at by sudden drops in TOC, will also be of use as chronologic tie-points between cores if they can be identified in the future.

Intra-site comparisons between cores showed that there was a strong degree of similarity between records, particularly considering the longer term trends. All cores from both sites

showed a mid-Holocene (approximately 5,000-4,000 cal. years BP) change in trend to increasingly wet conditions. Inter-site comparisons between amalgamated palaeomoisture records additionally showed a fair degree of similarity for the shorter-term events and shifts. The main wet shifts were seen to have occurred at 6,100, 5,350, 4,350, 3,850, 3,050 and 2,400 cal. years BP at Kopouatai, and at 6,600, 6,050, 5,050, 4,550, 3,650, 2,850 and 2,350 cal. years BP in Moanatuatua. Some shifts show equivalence with Northern Hemisphere peatland work, but in particular the longer term 4,500 cal. years BP wet trend is seen to start in New Zealand prior to the Northern Hemisphere. The 2,700 cal. years BP climate event of the Northern Hemisphere (and Chile) may also occur at these sites, but unfortunately coincides with a tephra layer in Moanatuatua which interferes with the light transmission results.

The interpretation of the palaeomoisture records in terms of climatic events suggests that the late Holocene climate became more variable, with increased seasonality (i.e. warmer, drier summers and cooler, wetter winters). This would account for the combination of the inferred wet shift (termed here the 'Mid-Holocene Transition') together with increased fire incidence (inferred from the peat humification and charcoal records respectively). This climate trend can, in turn, be explained by insolation (or orbital) forcing, predominantly through the precessional cycle. Throughout the time frame of this project, the reconstruction of summer insolation at 40°S was increasing, and winter insolation decreasing (Berger, 1992) resulting in an increase in seasonal extremes. Another factor in the increase in weather extremes at this time is the intensification of ENSO, evidence for which comes from Australasia and South America. The Mid-Holocene increase in wetness is linked to the difference in insolation values between the Equator and the poles, which is thought to have increased throughout the Holocene. This was responsible for strengthening westerly wind circulation across New Zealand, bringing more precipitation to the region.

Further work is required on a) the testate amoebae method – to improve the fossil test concentrations through density separation, b) tephra analysis – mainly carrying out continuous shard counts throughout each core and analysing by microprobe the major peaks to help improve core chronologies, and c) time-series analysis of the records to investigate the periodicities of the climate shifts detected.

9.2 Summary

In conclusion, this project has successfully applied some of the palaeoecological techniques that are regularly used in the Northern Hemisphere, to Southern Hemisphere peatland sites in New Zealand. Peat humification and charcoal were the most successful techniques, with plant macrofossil results showing potential. Testate amoebae analysis does not appear to be appropriate for these sites due to very low test abundances. Possible solutions for overcoming this problem require further research.

From the selection of useful proxies, climatic inferences have successfully been made about the climate of mid North Island of New Zealand over the period between the Tuhua and the Taupo Tephras (7,000 and 1,750 cal. years BP respectively). The peat humification records are the highest resolution replicates produced so far for this region, and records between cores and between sites show remarkable similarities, particularly when comparing amalgamated site records.

Interpreting these records in terms of palaeoclimate has identified a trend towards increased wetness and seasonality in New Zealand over the mid-late Holocene, thought to result from insolation changes driven by orbital forcing, that control the strength of the dominant westerly, rain-bearing winds. As well as this longterm pattern, numerous small-scale wet and dry shifts have been identified. An apparent contradiction between a late Holocene wet trend determined here and previous inferences for dry conditions at this time is explained by increased seasonality leading to drier summers and wetter winters.

APPENDIX ONE – TESTATE AMOEBAE TAXONOMY

This section will explain the criteria used for identifying and grouping rare and unusual taxa, illustrated with images taken using the analySIS® imaging software, via a Leica DC100 camera attached to the microscope. The two images aim to show different features of the tests; between them, they focus on the surface pattern/plate configuration and the mouth, as well as displaying the tests' measurements (all the images were taken at the same magnification, so their scales are directly comparable). The following list is arranged in alphabetical order, just as the taxa are displayed in the results graphs. All identifications followed Charman *et al.* (2000), except for new taxa and divisions as described here.

A1.1 *Corythion* sp. (Trinematidae)

The tests in this genus are clear and colourless, and composed of adjoining plates separated by organic cement.

Corythion dubium (Taránek, 1881)

The plates of *Corythion* are small, rounded and arranged haphazardly. Individuals found here were divided according to the shape of the aperture (round or oval) and also according to size (greater or less than 55 μm). The aperture was round if the 'depth' of the aperture was greater than 2/3rds its width, and oval if it was less than 2/3rds. The smaller tests tended to have plates more ovoid in shape, whereas the larger tests had more irregular shaped plates. The key facilitates the categorisation of this taxon:

1. Spines present.....*Corythion dubium*, spiky
   Spines absent.....2
2. Length < 55 μm.....3
   Length > 55 μm.....4
3. Aperture oval.....*Corythion dubium* 1, small
   Aperture round.....*Corythion dubium* 2, small
4. Aperture oval.....*Corythion dubium* 1, large
   Aperture round.....*Corythion dubium* 2, large

- *Corythion dubium* 1 (oval aperture) – small

Plate A1.1 Corythion dubium 1 (oval aperture) – small (Z0108 0-1 cm).

- *Corythion dubium* 1 (oval aperture) – large

Plate A1.2 Corythion dubium 1 (oval mouth) – large.

- *Corythion dubium* 2 (round aperture) – small

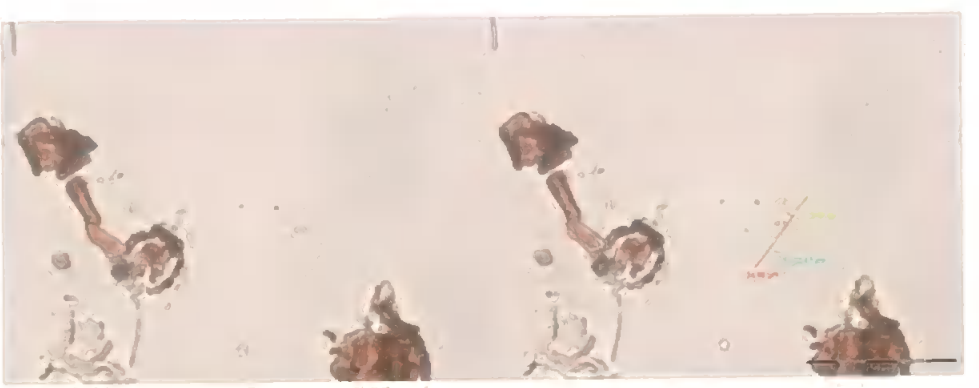

Plate A1.3 Corythion dubium 2 (round aperture) – small (Z0108 0-1 cm).

- *Corythion dubium* 2 (round aperture) – large

Plate A1.4 Corythion dubium 2 (round aperture) – large (K2 0-1 cm).

- *Corythion dubium* – spiky

A new type of *Corythion* was also seen, of the same form as the previously described individuals (tending to have an oval aperture) but covered all over with short, thin spikes 2-3 μm long. The tests were less than 45 μm long, with an aperture just less than ½ the width of the test.

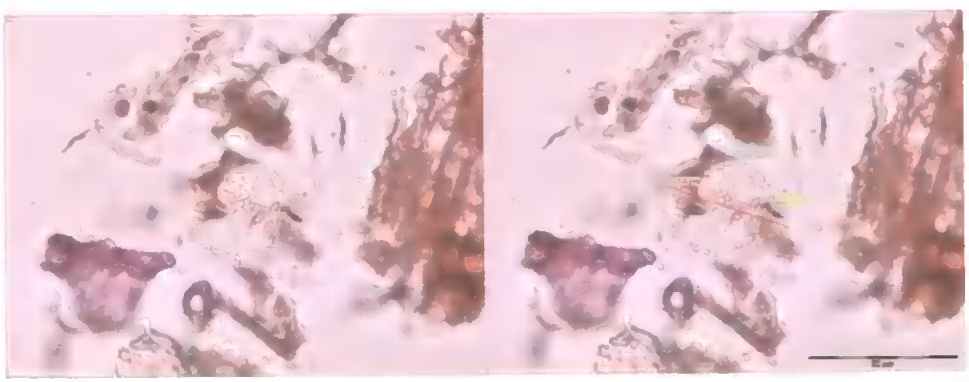

Plate A1.5 Corythion dubium – spiky (Z0204A 0-1 cm).

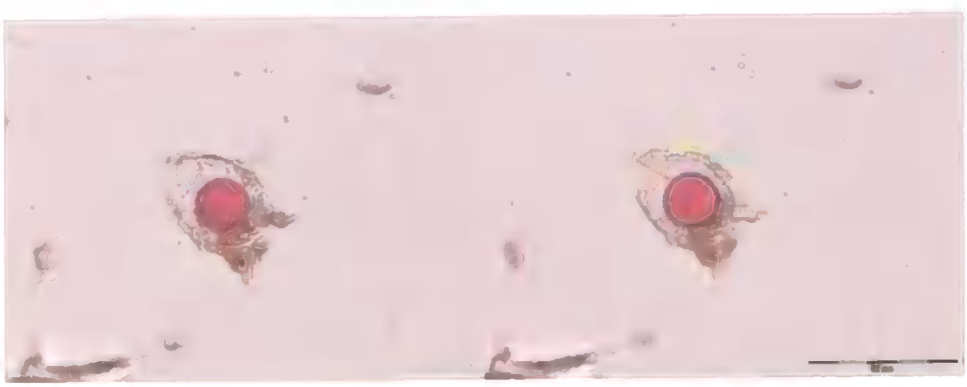

Plate A1.6 Corythion dubium – spiky (Z0204A 0-1 cm).

Plate A1.7 Corythion dubium – spiky (Z0204A 0-1 cm).

A1.2 *Cryptodifflugia* spp. (Cryptodifflugiidae)

This genus is characterised by extremely small tests that can be overlooked if careless, or easily confused with fungal detritus.

cf. Cryptodifflugia compressa (Penard, 1902)

The tests of this transparent ovoid taxon were very small (approximately 20 µm), neat and smooth, with a very small aperture. They were categorised as being less than 20 µm long, less than 18 µm wide, and with an aperture 5-6 µm.

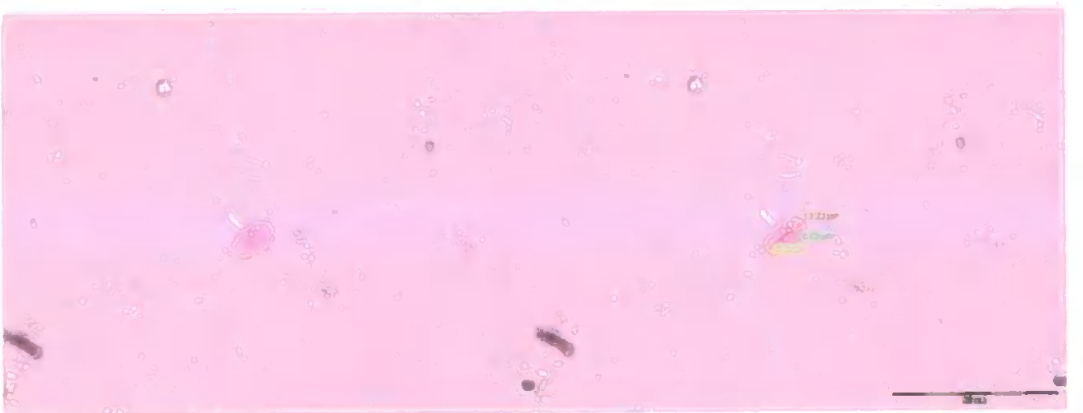

Plate A1.8 cf. Cryptodifflugia compressa.

Cryptodifflugia cf. oviformis

These tests were dark brown and uneven, with many small particles attached. They were very small (<22 µm) with a small mouth of 5 µm that was often not visible.

Plate A1.9 Cryptodifflugia cf. oviformis (Z0206A 0-1 cm).

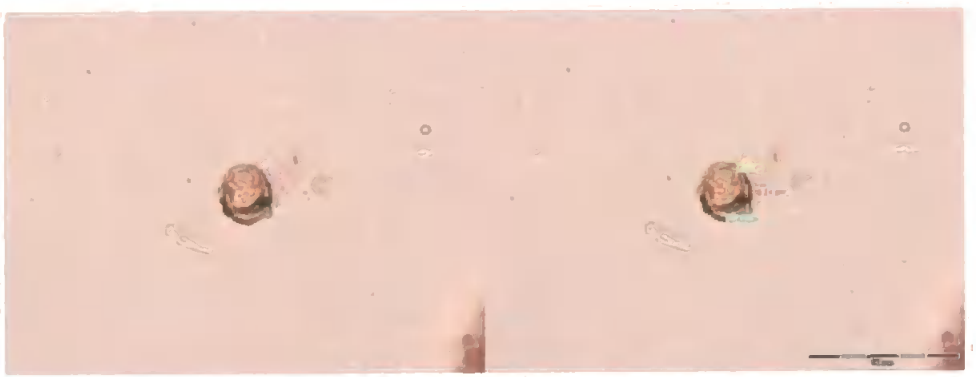

Plate A1.10 Cryptodifflugia cf. oviformis (M5 16-17 cm).

A1.3 *Difflugia* spp. (Difflugiidae)

This genus was very common in these sites, and numerous taxa were identified.

Difflugia C (Wilmshurst, 2001, pers. comm.)

This was a small (just over 20 µm long) brown coloured test with a neck constriction that flared out very slightly at the aperture (tests had to be rotated in order to see this feature). The aperture was more than ½ the width of the test, and the 'neck' flare at the aperture was 2-5 µm long.

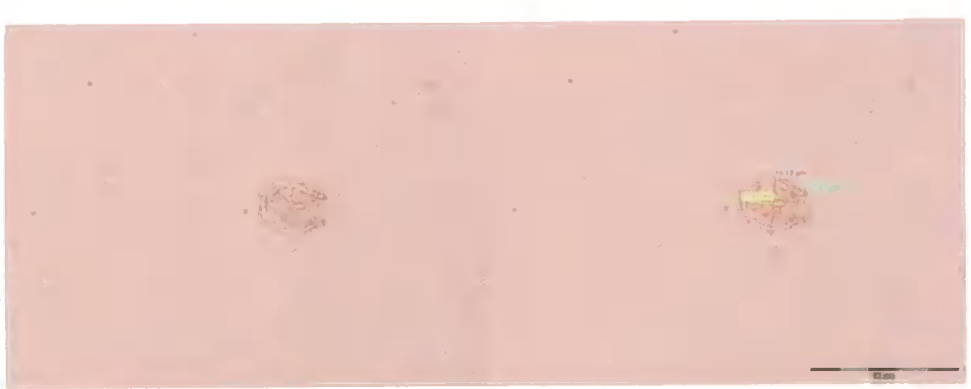

Plate A1.11 Difflugia C (M21 12-13 cm).

Plate A1.12 Difflugia C (Z0206 4-5 cm).

Other small *Difflugia*

This taxon was of a similar size (greater than 20 µm) and composition to *Difflugia* C, but it had no neck constriction. The aperture was less than ½ the test width. There seemed to be a degree of morphological continuum between this taxa and *Difflugia* C, so certain individuals were problematic to categorise.

Plate A1.13 Other small Difflugia (M5 8-9 cm).

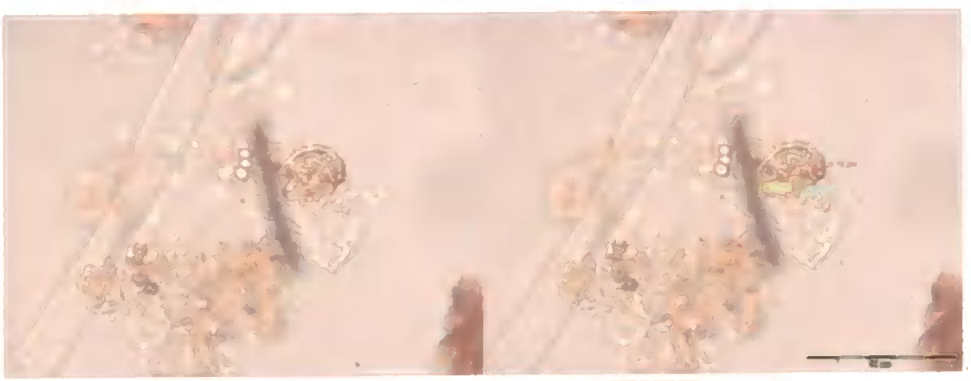

Plate A1.14 Other small Difflugia (Z0106 15-16 cm).

Difflugia pristis

A variety of different *Difflugia pristis* types were observed in these samples. During the first short core counts, they were split into two groups (type 1 and 2) according to their surface structure, and during the second phase of counting, divisions were revised, and they were subdivided according to the size of the test and the aperture. (Tests less than 30 µm were classed as *Pseudodifflugia fulva* (Charman *et al.*, 2000)). The following keys divide the taxon according to the different criteria used during the first and second phases of counting, respectively:

1. Length < 30 µm.....*Pseudodifflugia fulva*
   Length > 30 µm.....2
2. Surface structure smooth.....*Difflugia pristis* type 1
   Surface structure plate-like.....*Difflugia pristis* type 2

and:

1. Length < 30 µm.....*Pseudodifflugia fulva*
   Length 30-40 µm.....2
   Length >40 µm.....3
2. Aperture < ½ the width of test...*Difflugia pristis* type, small with small aperture
   Aperture > ½ the width of test...*Difflugia pristis* type, small with large aperture
3. Aperture < ½ the width of test...*Difflugia pristis* type, large with small aperture
   Aperture > ½ the width of test...*Difflugia pristis* type, large with large aperture

- *Difflugia pristis* type 1

This division included individuals with a smooth surface pattern.

Plate A1.15 Difflugia pristis type 1 (Z0108 0-1 cm).

- *Difflugia pristis* type 2

These had a plate-like pattern on their surface.

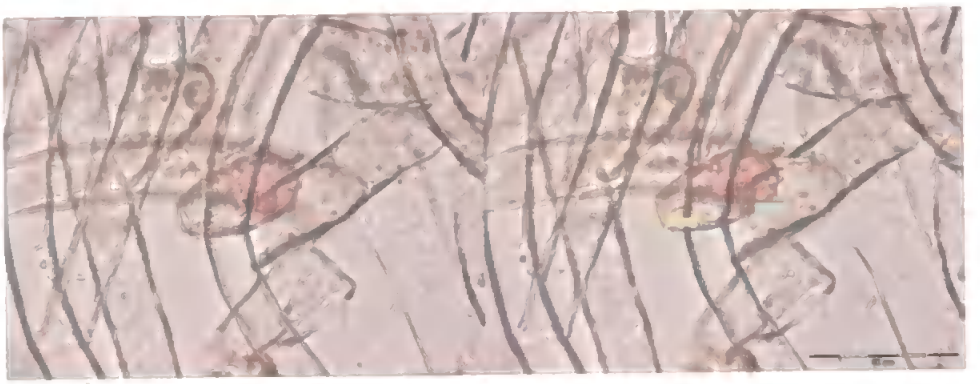

Plate A1.16 Difflugia pristis type 2 (Z0108 5-6 cm).

- *Difflugia pristis* type – small, wide aperture

These individuals were relatively small (between 30 µm and 40 µm) with an aperture that was greater than half the width of the test.

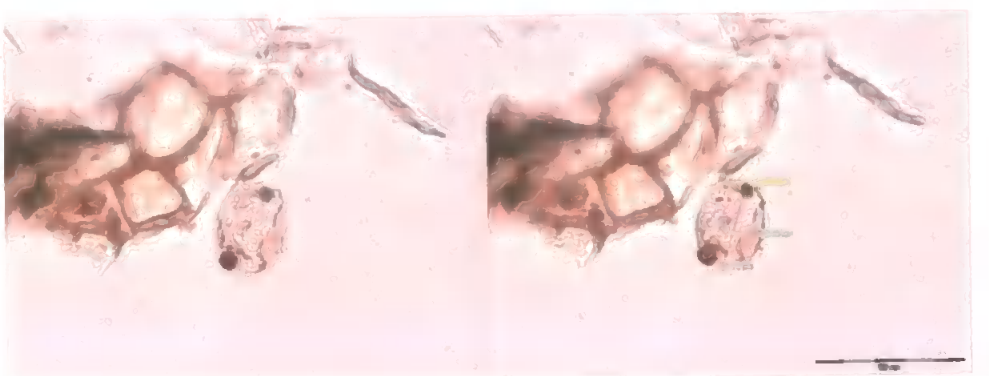

Plate A1.17 Difflugia pristis type – small, wide aperture.

- *Difflugia pristis* type – small, small aperture

These were small, but with an aperture less than half the width of the test.

Plate A1.18 Difflugia pristis type – small, small aperture.

- *Difflugia pristis* type – large, wide aperture

These were larger in length (>40 µm) and with an aperture size greater than half the width of the test.

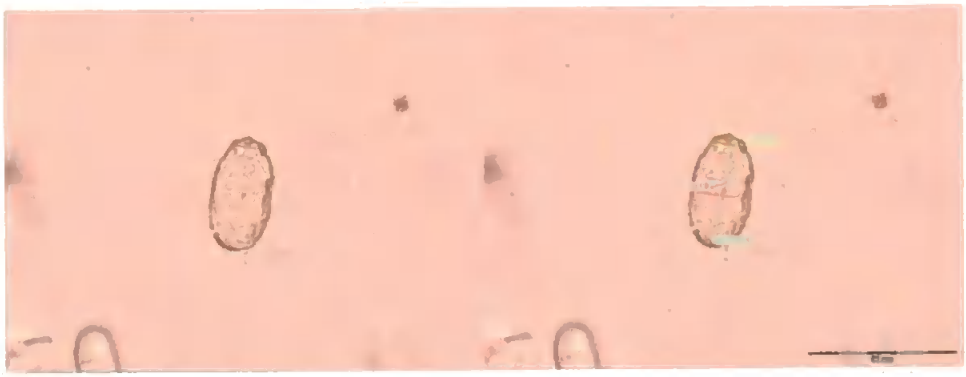

Plate A1.19 Difflugia pristis type – large, wide aperture (Z0204 8-9 cm).

- *Difflugia pristis* type – large, small aperture

These individuals were larger (>40 µm), but with an aperture less than half the width of the test.

Plate A1.20 Difflugia pristis type – large, small aperture (Z0204 0-1 cm).

Difflugia pulex

This taxon was pyriform (conical) in shape, narrowing to the aperture. Tests were composed of varying amounts of particles, and were divided according to size.

- *Difflugia pulex* – small

These individuals were less than 35 µm.

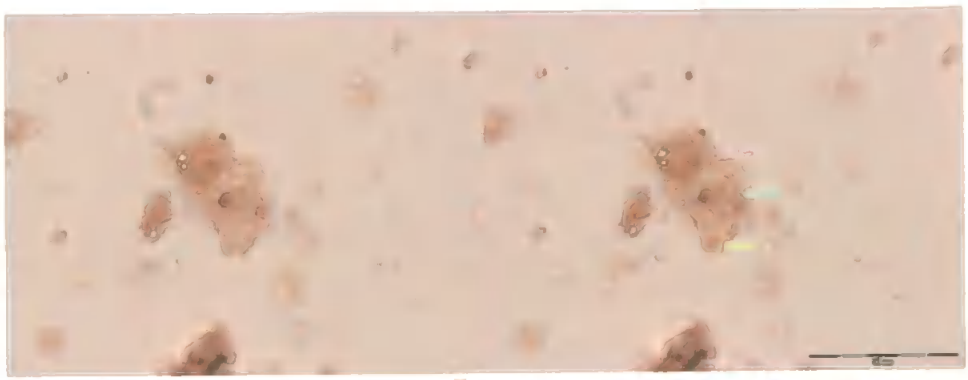

Plate A1.21 Difflugia pulex – small (Z0204 4.51-4.52m).

- *Difflugia pulex* – large

This group was greater than 35 µm.

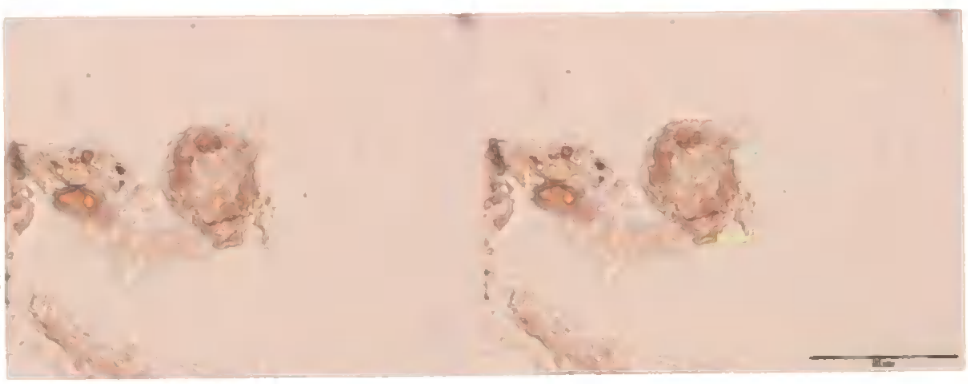

Plate A1.22 Difflugia pulex – large (M21 16-17 cm).

Difflugia sp.

This was an unidentifiable oval shaped *Difflugia* taxon.

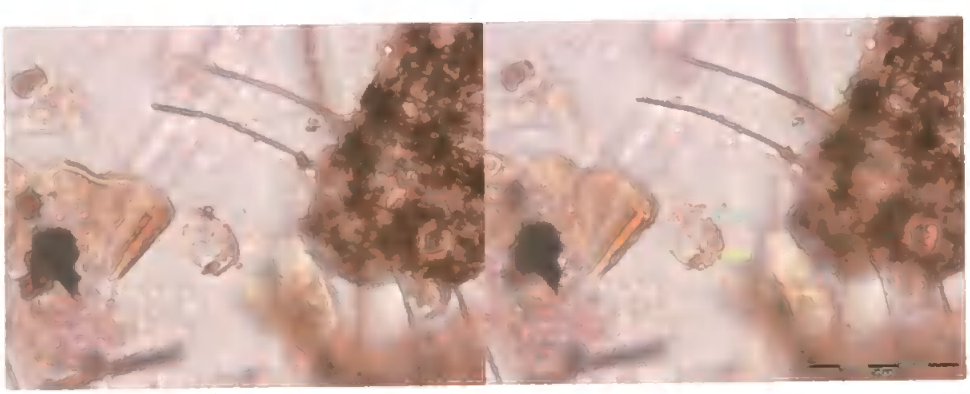

Plate A1.23 Difflugia sp (Z0106 5-6 cm).

A1.4 *Euglypha* spp. (Euglyphidae)

Like the *Assulina* genus, *Euglypha* are also composed of overlapping plates, but which appear angular and hexagonal when viewed under a light microscope. The tests are clear and colourless.

Euglypha rotunda (Wailes and Penard, 1911)

There were 2 main differences within *Euglypha rotunda*; those that clearly tapered to a smaller, pointed aperture that was less than ½ the test's width, and those that tapered more subtly to a wider aperture more than ½ the test's width. The size of plates relative to the size of the test is much smaller for the wider and flatter mouthed individuals. The length of the tests was less than 45 µm. This is described with the key:

1. Aperture < ½ the width of the test..... *Euglypha rotunda*, pointed aperture
   Aperture > ½ the width of the test..... *Euglypha rotunda*, flat, wide aperture

- *Euglypha rotunda* (pointed aperture)

Plate A1.24 Euglypha rotunda (pointed aperture).

- *Euglypha rotunda* (flat, wide aperture)

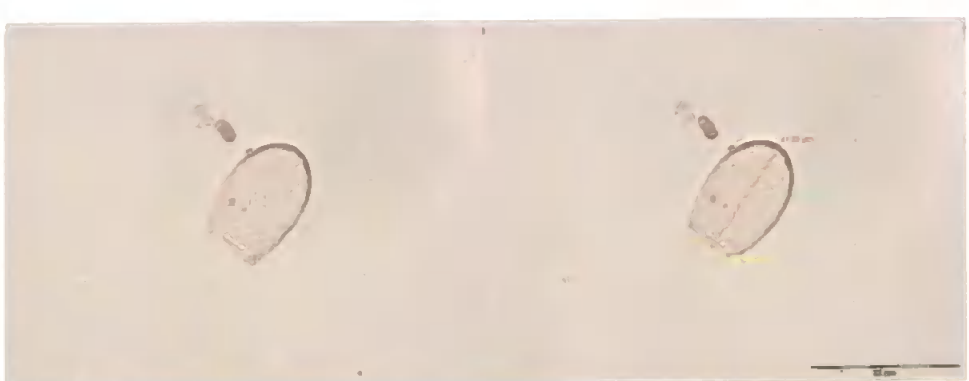

Plate A1.25 Euglypha rotunda (flat, wide aperture) (Z0108 0-1 cm).

- *Euglypha rotunda* type

This was a variation between the two main *Euglypha rotunda* taxa, with a tapering towards a concave aperture.

Plate A1.26 Euglypha rotunda type (Z0108 0-1 cm).

A1.5 *Heleopera* spp. (Hyalospheniidae)

This genus is characterised by an accumulation of particles on the far end of the test.

Heleopera undiff.

This was a type of *Heleopera*, but its exact identity was not known.

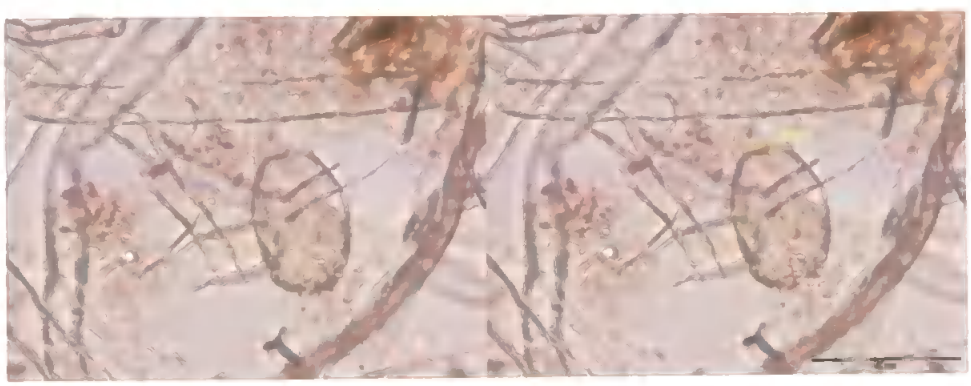

Plate A1.27 Heleopera undiff. (Z0106 15-16 cm).

Heleopera sp.

These were individuals of unknown *Heleopera*.

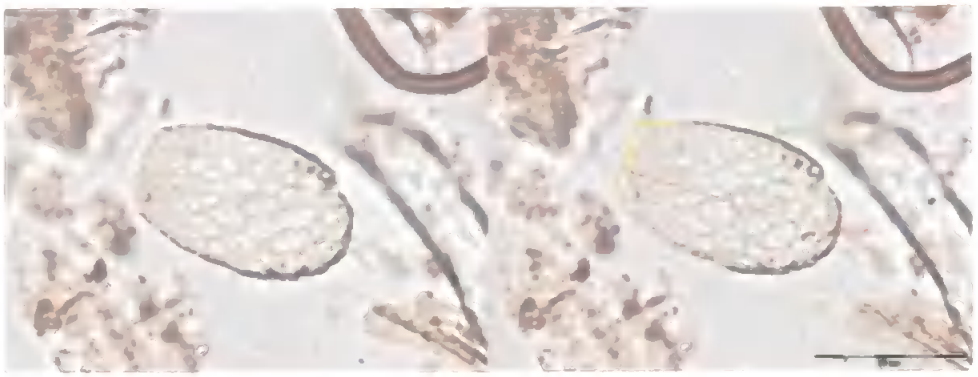

Plate A1.28 Heleopera sp. (Z0106 5-6 cm).

The following were *Heleopera* type tests, but with *Nebela*-like plate features. (They were originally classed as Unknowns 2 and 3, but the grouping was refined in the second counting phase, based on overall test size, aperture size and whether the corners of the aperture were rounded or angled). The following key facilitates their segregation:

1. Length < 50 µm.....2
   Length > 50 µm.....5
2. Aperture subangular.....3
   Aperture rounded.....4
3. Aperture < ½ the width of the test.....*Heleopera* type 8
   Aperture > ½ the width of the test.....*Heleopera* type 6
4. Aperture < ½ the width of the test.....*Heleopera* type 7
   Aperture > ½ the width of the test.....*Heleopera* type 5
5. Aperture subangular.....6
   Aperture rounded.....7
6. Aperture < ½ the width of the test.....*Heleopera* type 4
   Aperture > ½ the width of the test.....*Heleopera* type 2
7. Aperture < ½ the width of the test.....*Heleopera* type 3
   Aperture > ½ the width of the test.....*Heleopera* type 1

Heleopera type 1

These were greater than 50 µm long, with the aperture more than half the width of the test, and rounded at the aperture corners.

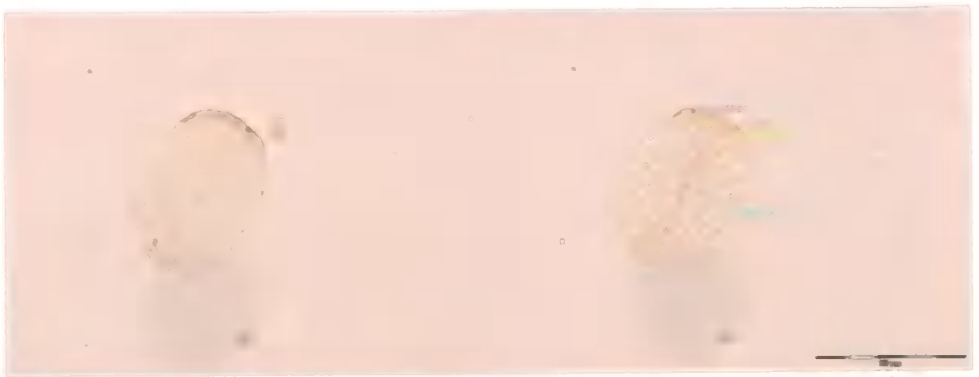

Plate A1.29 Heleopera type 1 (Z0206 8-9 cm).

Heleopera type 2

These were greater than 50 µm long, with the aperture more than half the width of the test, and angled at the aperture corners.

Plate A1.30 Heleopera type 2 (M5 8-9 cm).

Heleopera type 3

These were greater than 50 µm long, with the aperture less than half the width of the test, and rounded at the aperture corners.

Plate A1.31 Heleopera type 3 (Z0206 0-1 cm).

Heleopera type 4

These were greater than 50 µm long, with the aperture less than half the width of the test, and angled at the aperture corners.

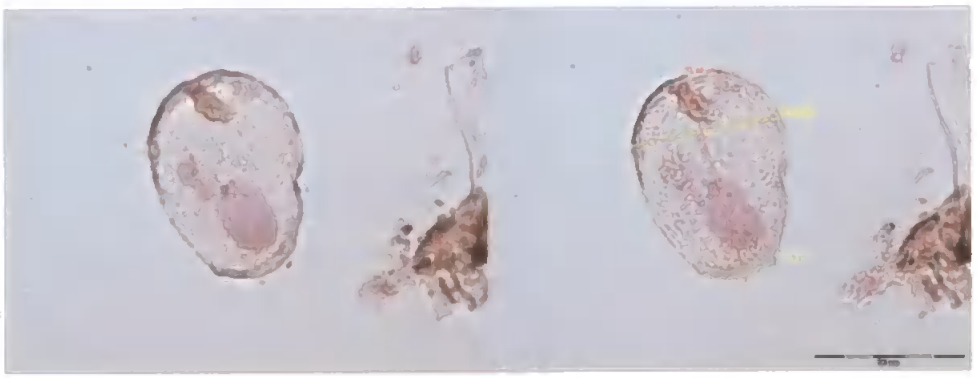

Plate A1.32 Heleopera type 4 (M21 4-5 cm).

Heleopera type 5

These were less than 50 µm long, with the aperture greater than half the width of the test, and rounded at the aperture corners.

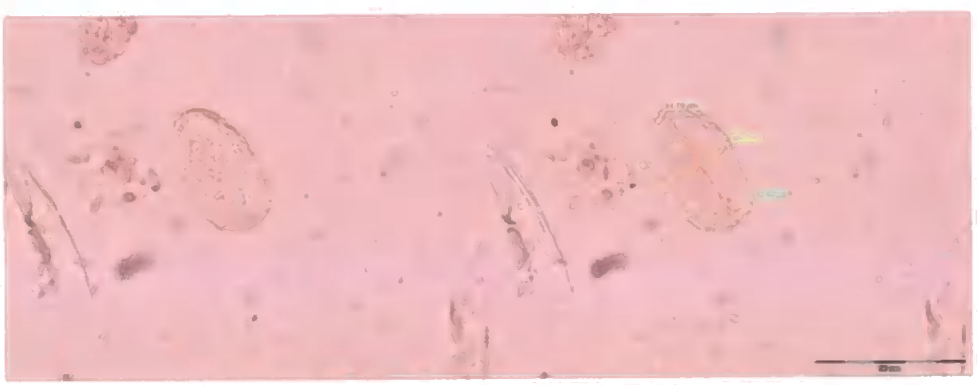

Plate A1.33 Heleopera type 5 (M21 12-13 cm).

Heleopera type 6

These were less than 50 µm long, with the aperture greater than half the width of the test, and angled at the aperture corners.

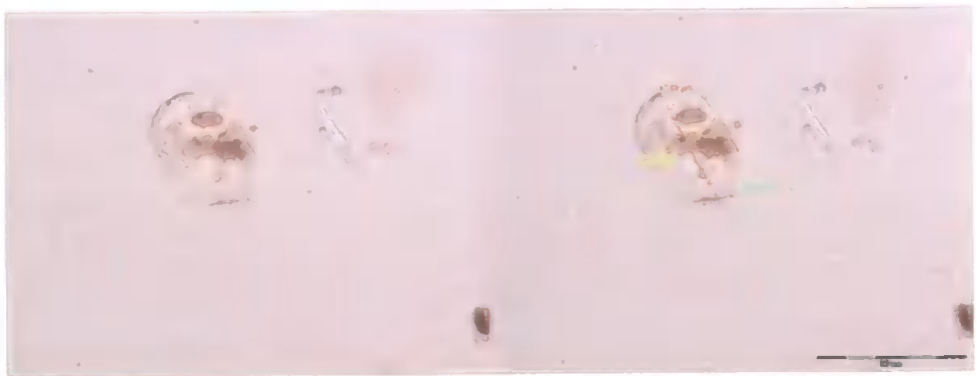

Plate A1.34 Heleopera type 6 (M21 12-13 cm).

Heleopera type 7

These were less than 50 µm long, with the aperture less than half the width of the test, and rounded at the aperture corners.

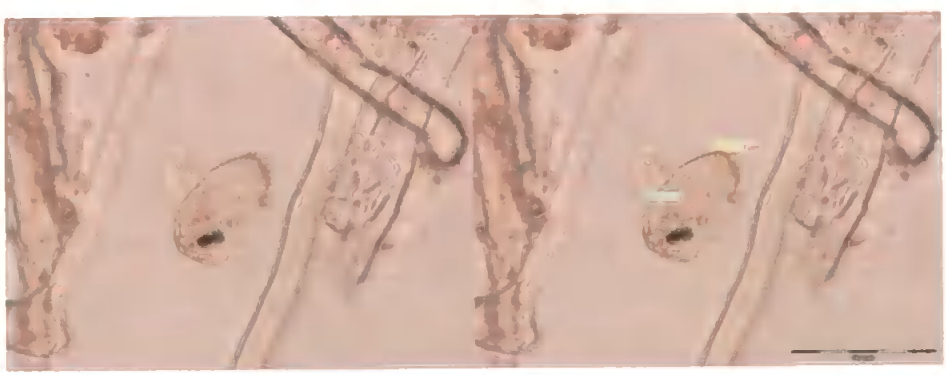

Plate A1.35 Heleopera type 7.

Heleopera type 8

These were less than 50 µm long, with the aperture less than half the width of the test, and angled at the aperture corners.

Plate A1.36 Heleopera type 8.

A1.6 *Hyalosphenia* spp. (Hyalospheniidae)

Tests from this genus have very clean, smooth surfaces, produced by secretions. They are pale yellow/brown, with a very neat terminal aperture.

Hyalosphenia minuta (Cash 1891)

This was a consistently smaller version of *Hyalosphenia subflava*. It was a smooth light brown test less than 40 µm.

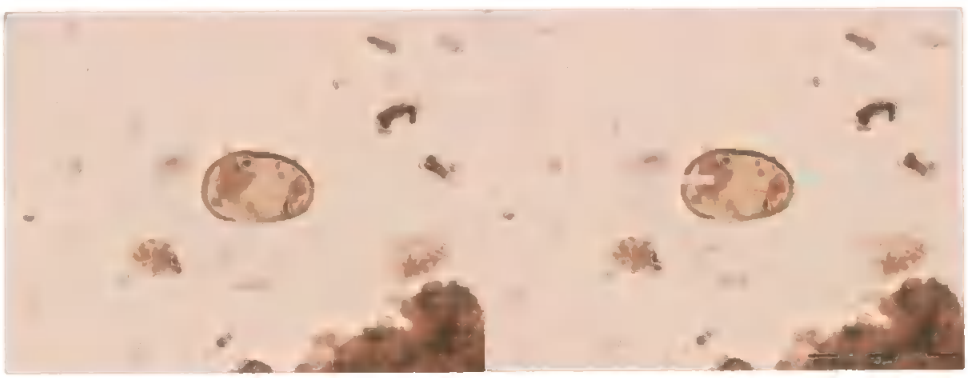

Plate A1.37 Hyalosphenia minuta (Z0204).

A1.7 *Nebela* spp. (Hyalospheniidae)

This genus has a single terminal aperture, and produces its tests from a series of distinctive, irregular, siliceous plates.

Nebela tubulata (Ellison and Ogden, 1987)

This taxon was separated from *Nebela wailesi* on the basis of its smaller size of less than 80 µm long. It had a very distinctive narrow neck that remained a constant width along its length, with a clear constriction at its base. The plates were relatively large compared to its size.

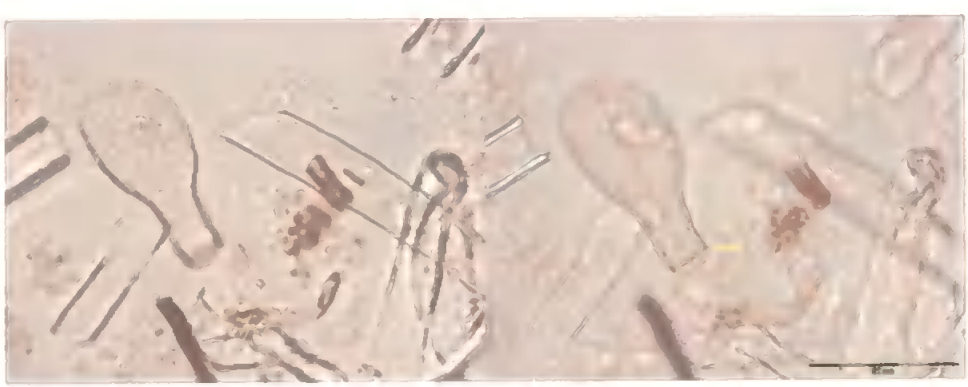

Plate A1.38 Nebela tubulata (Z0108 5-6 cm).

*Nebela sp.*1

This *Nebela*-like test was of a similar shape, with plate features, but apparently lacking the thickening around the aperture. They were approximately 50 µm long, with an aperture ¼ of the test's width.

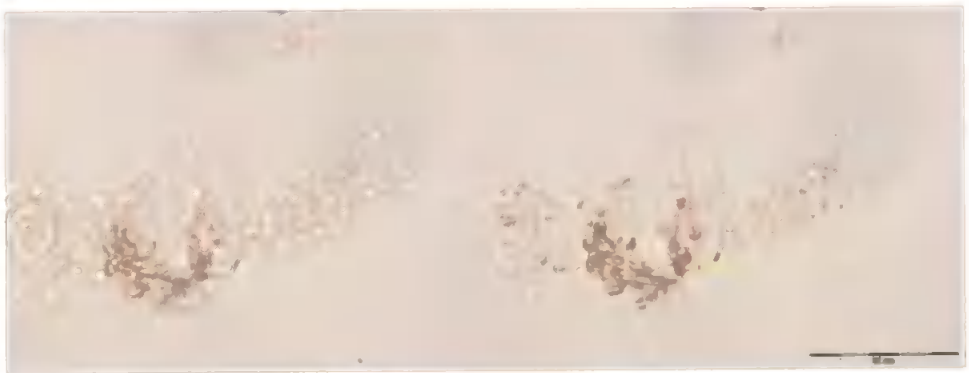

Plate A1.39 Nebela sp.1 (Z0108 0-1 cm).

*Nebela sp.*2

Again, this was probably a *Nebela*, but it was unclear which taxon. They were greater than 35 µm long, with an aperture more than ½ the width of the test.

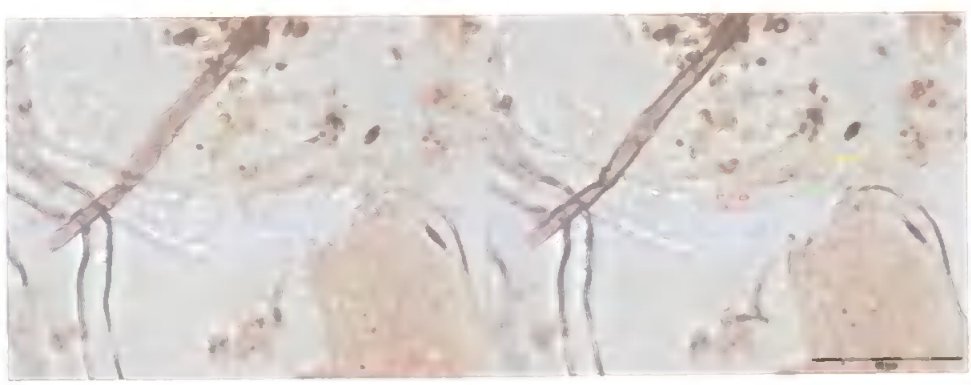

Plate A1.40 Nebela sp.2 (Z0106 5-6 cm).

A1.8 *Pseudodifflugia* spp. (Gromiidae)

This genus is comprised of small tests, very similar in form to *Difflugia*. In fact, based on the key by Charman *et al.* (2000) they are separated out from the *Difflugia* on the basis of size criteria.

Pseudodifflugia cf. fulva

This *Difflugia* shaped test was small, and similar in form to *Pseudodifflugia fulva*.

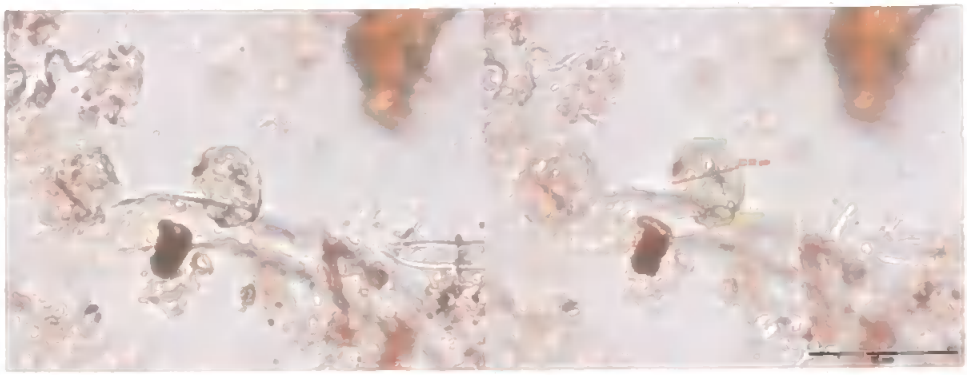

Plate A1.41 Pseudodifflugia cf. fulva (Z0106 5-6 cm).

A1.9 *Sphenoderia* spp. (Euglyphidae)

This genus is characterised by round plates that are large relative to the size of the test. They are clear and colourless, with a collar around the neck of the aperture.

Sphenoderia fissirostris (Penard, 1890)

This taxon had relatively large, oval plates, with only 2-3 across the width of the test. They possessed a smooth cemented collar at their aperture, which was covered with a fine dotted pattern. Tests were grouped into 2 sizes, separated according to those larger and those smaller than 40 µm:

1. Length < 40 µm.....*Sphenoderia fissirostris* small
   Length > 40 µm.....*Sphenoderia fissirostris* large

Plate A1.42 Sphenoderia fissirostris (large) (M5 0-1 cm).

A1.10 *Trinema* sp. (Trinematidae)

The tests are made from clear, colourless round plates, between which, unlike *Corythion*, there is no visible organic cement (Charman *et al.*, 2000).

Trinema lineare-type

These had an oval shaped test, with a round aperture bordered by serrated plates. Its circular plates were large relative to the overall test size, with only approximately 4 across the width of the test, arranged in rows. Plates here were clearly visible, opposing Corbet (1973) who suggested that they are often impossible to see.

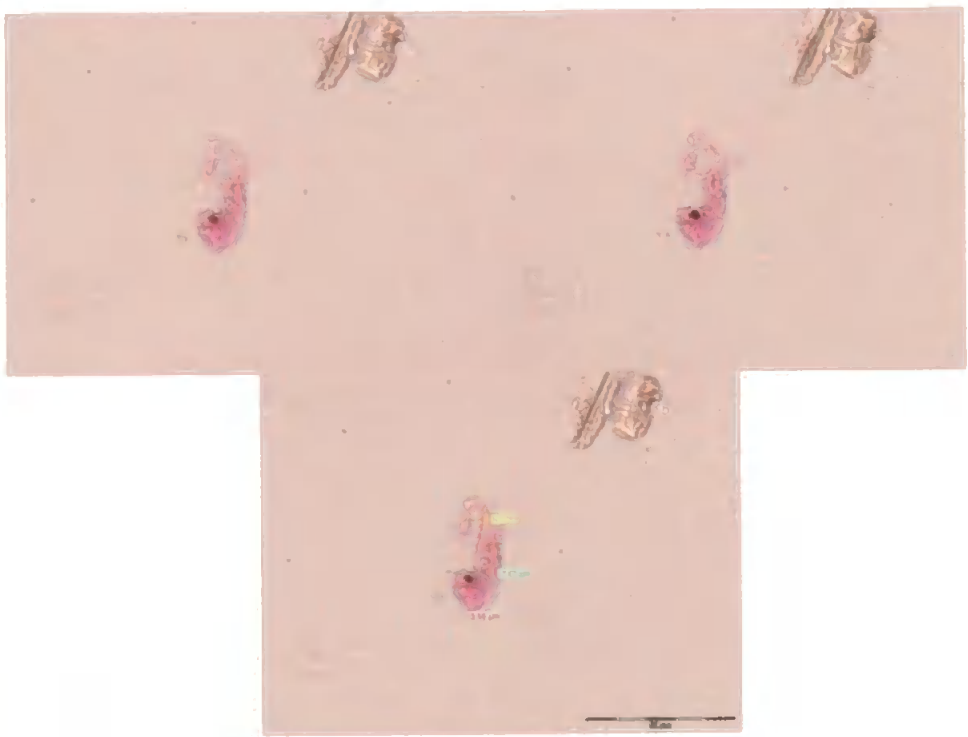

Plate A1.43 Trinema lineare-type (M5 0-1 cm).

A1.11 Unknowns

- Unknown 1

These tests had a plate-like pattern, with a row of small circular features towards the aperture. They were more than 45 µm long, and its aperture was more than half the width of the test.

Plate A1.44 Unknown 1 (Z0103B 0-1 cm).

- Unknown 2

This was an initial categorisation of the *Heleopera* types, having an angled corner at the aperture.

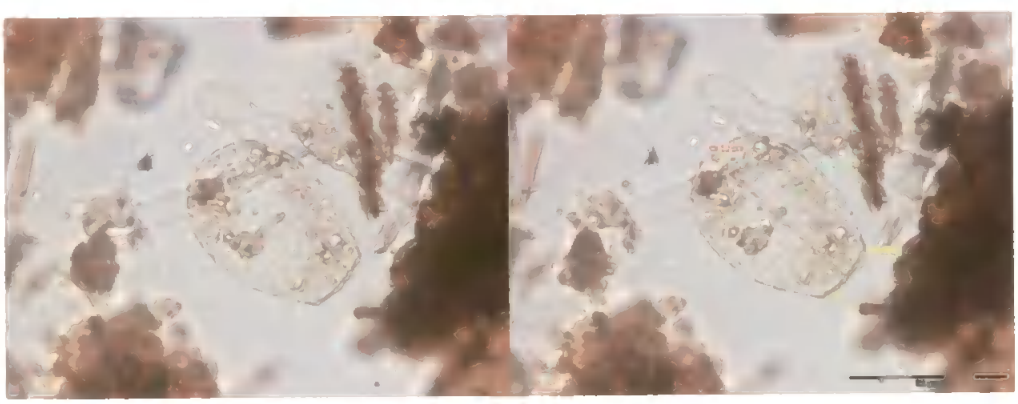

Plate A1.45 Unknown 2 (Z0103B 5-6 cm).

- Unknown 3

This was also an initial categorisation of the *Heleopera* types, but having a rounded corner at the aperture.

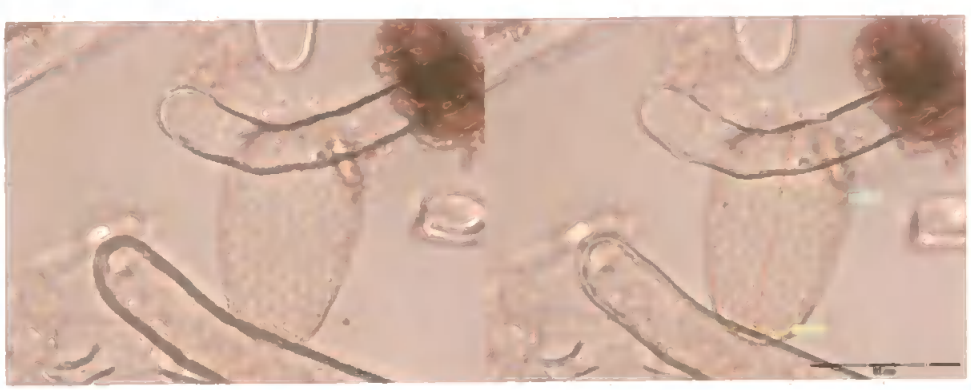

Plate A1.46 Unknown 3 (Z0108 5-6 cm).

- Unknown 4

This was a very small, messy test, greater than 20 µm long, with an aperture less than half the width of the test.

Plate A1.47 Unknown 4 (Z0108 10-11 cm).

(Unknown 5) (Pseudodifflugia fulva?)

This test, greater than 36 µm, with an aperture greater than ½ the test's width, flared out at the aperture.

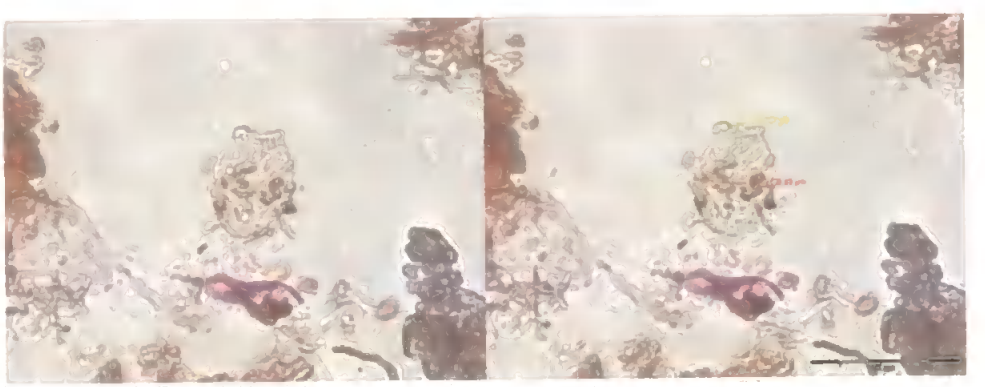

Plate A1.48 Unknown 5 (Z0106 0-1 cm).

Unknown 6

This test possibly had a plate-like pattern, but it was unclear. The main feature was the uneven edging at the aperture, as if plates were extending to the very edge. They were greater than 50 µm long, with an aperture less than ½ the test's width.

Plate A1.49 Unknown 6 (Z0108 5-6 cm).

Plate A1.50 Unknown 6 (M21 0-1 cm).

Unknown 7

This test was almost circular and had an oval aperture with a corrugated edge pattern. The test itself was disc shaped. The test was greater than 30 µm in diameter, with its aperture just less than ½ the test width. The aperture's depth was the full depth of the test.

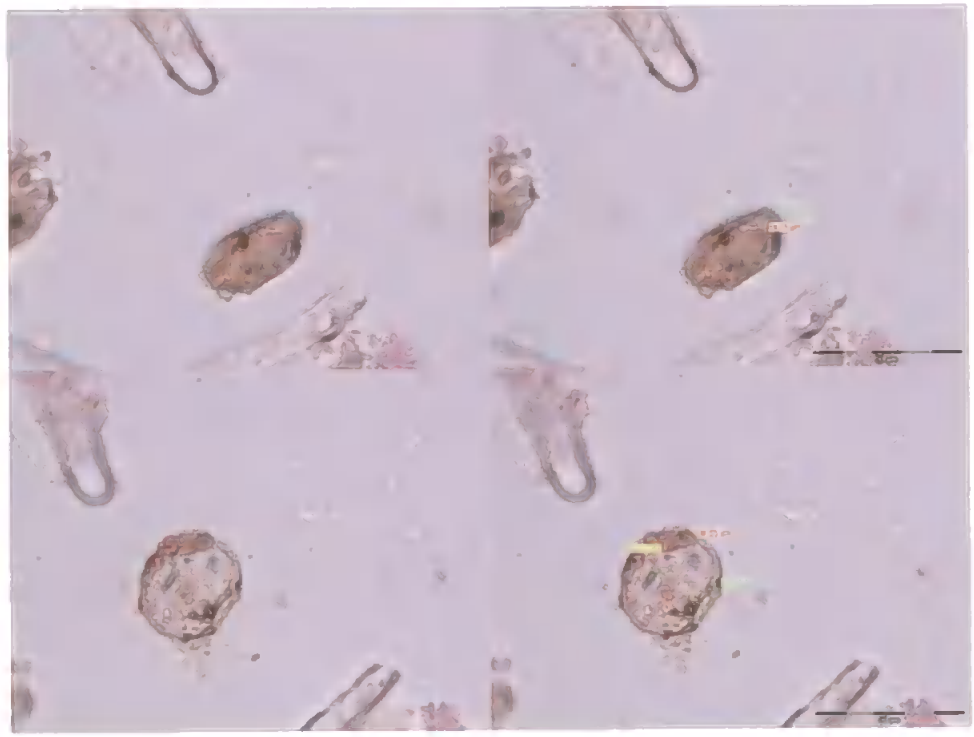

Plate A1.51 Unknown 7 (M21 12-13 cm).

Unknown 8 (large pink, spikes)

These were large (greater than 75 µm long) with an irregular plate-like structure, covered with narrow, pointed spikes 3.5-5 µm long. The aperture was ½ the test width. They were often stained pink by the rose bengal.

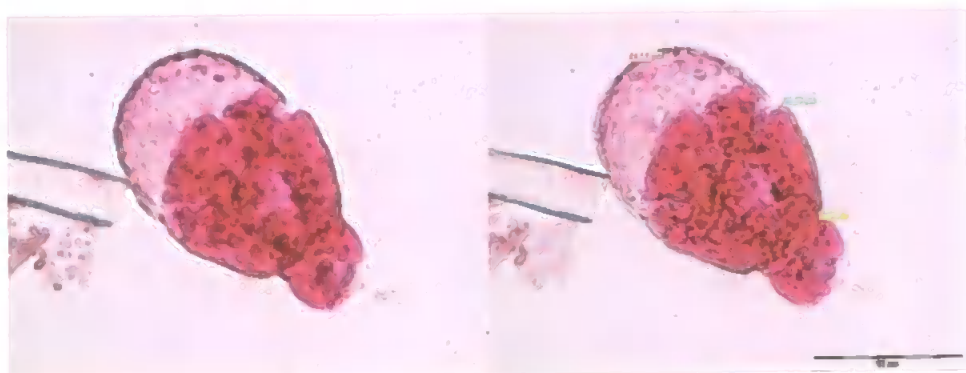

Plate A1.52 Unknown 8 (K2 0-1 cm).

Plate A1.53 Unknown 8 (K2 0-1 cm).

Unknown 9 (large pink, no spikes)

This was very similar to Unknown 8, but with no spikes.

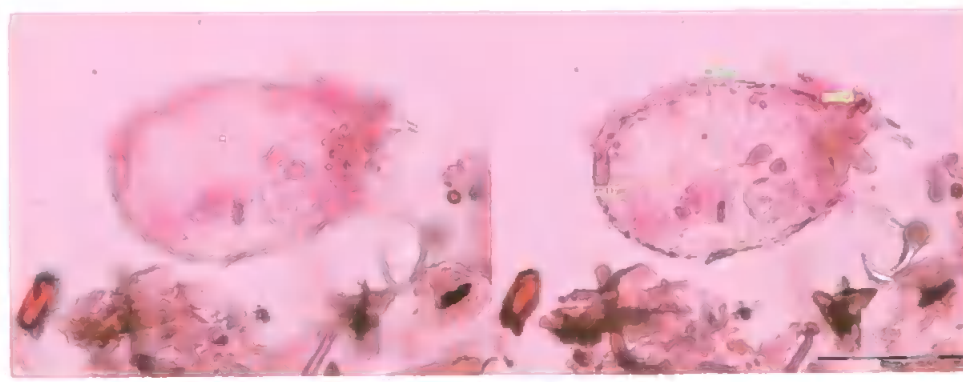

Plate A1.54 Unknown 9.

Unknown 10

This test had a fine plate-like pattern, with a flared out aperture. The length of the tests was greater than 40 µm, and the aperture was more than ½ the test's width.

Plate A1.55 Unknown 10 (M21 0-1).

Unknown 11

This brown oval test had a short collar-like narrowing at the aperture. It was greater than 35 µm long, with the aperture less than ½ the width of the test, and the collar 5 µm long.

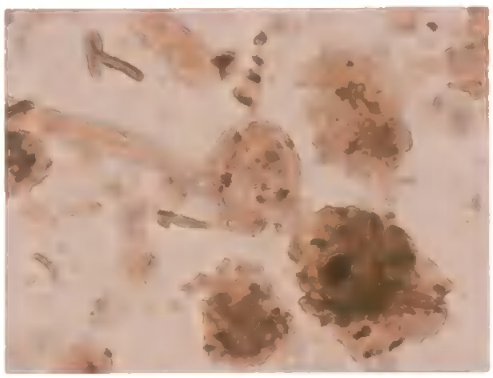

Plate A1.56 Unknown 11 (Z0204A 5.11-5.12m).

Unknown 12

This circular test was greater than 55 µm in diameter, with a round aperture of a diameter 1/5 that of the test.

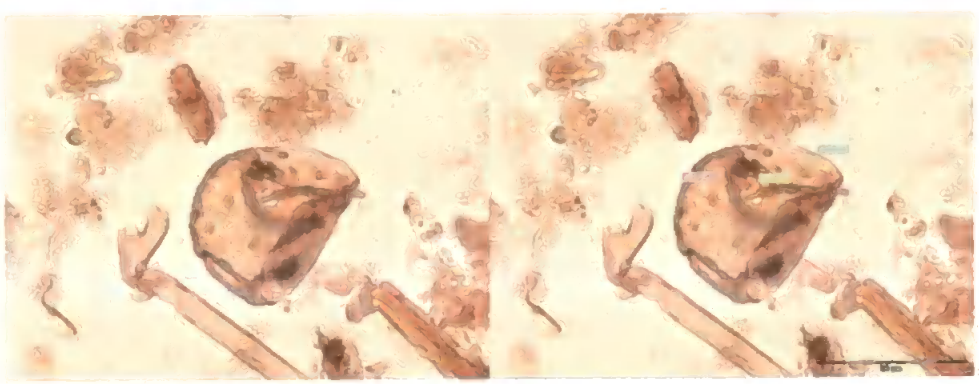

Plate A1.57 Unknown 12 (Z0204 5.70-5.80m).

A1.12 Interesting features

This section includes images of interesting features seen in samples. Firstly some broken/damaged tests are shown to demonstrate how their preservation could be being affected considering that even at the surface, they are broken.

Assulina muscorum

This test was at the very surface but was already broken.

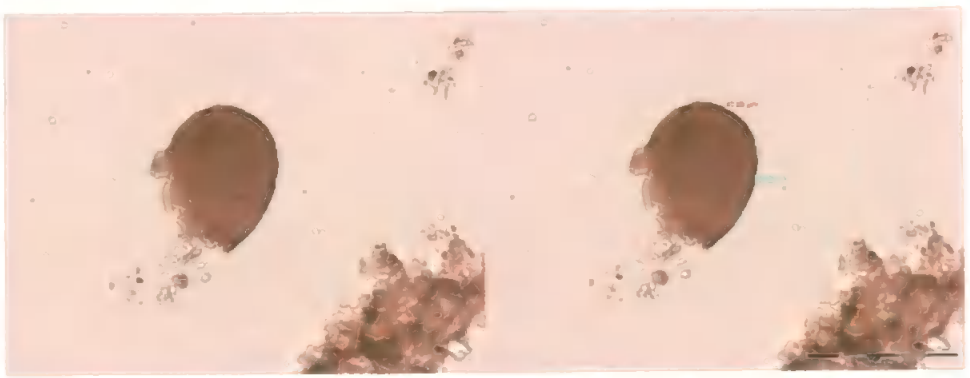

Plate A1.58 Broken Assulina muscorum (Z0206A 0-1 cm).

Euglypha tuberculata

This near surface test was degraded, becoming squashed and faded.

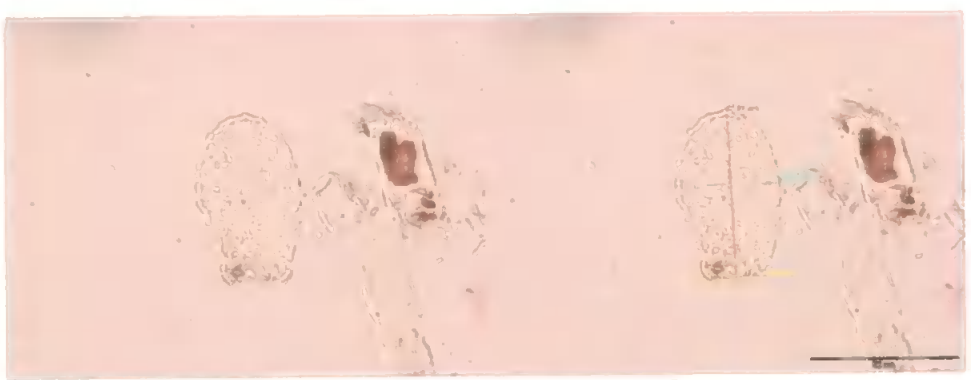

Plate A1.59 Degraded Euglypha tuberculata (Z0206 4-5 cm).

Difflugia pulex

This large test was highly decomposed, covered with and surrounded by fine structureless matter.

Plate A1.60 Decomposed Difflugia pulex (Z0206 8-9 cm).

Nebela wailesi

This surface test has been squashed out of shape.

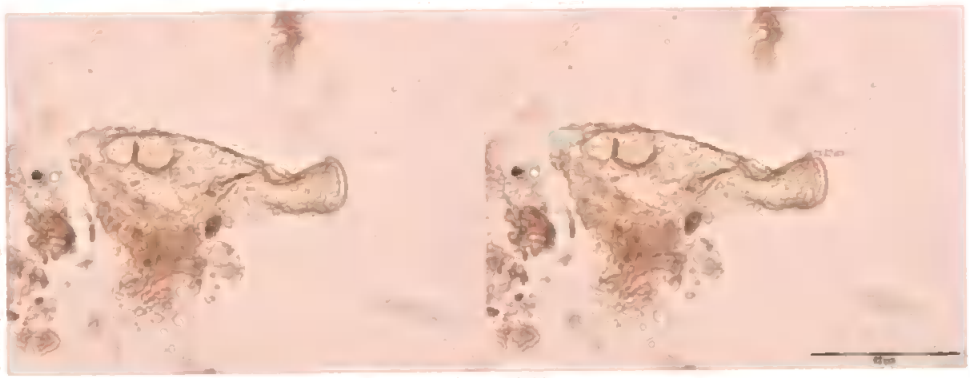

Plate A1.61 Squashed Nebela wailesi (Z0206 0-1).

Difflugia pulex

A pair of large tests was joined, probably in the process of reproducing.

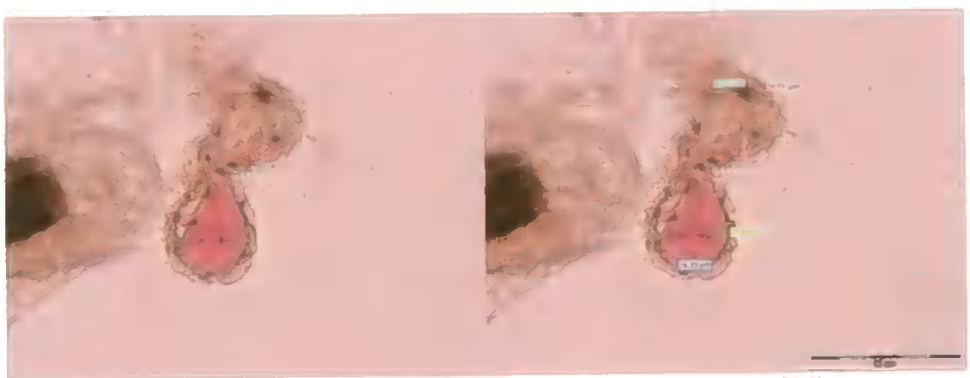

Plate A1.62 Joined Difflugia pulex (M21 16-17 cm).

Difflugia oblonga

This test illustrates that testate amoebae make use of matter in their surroundings in their test construction. This particular one has incorporated a tephra shard.

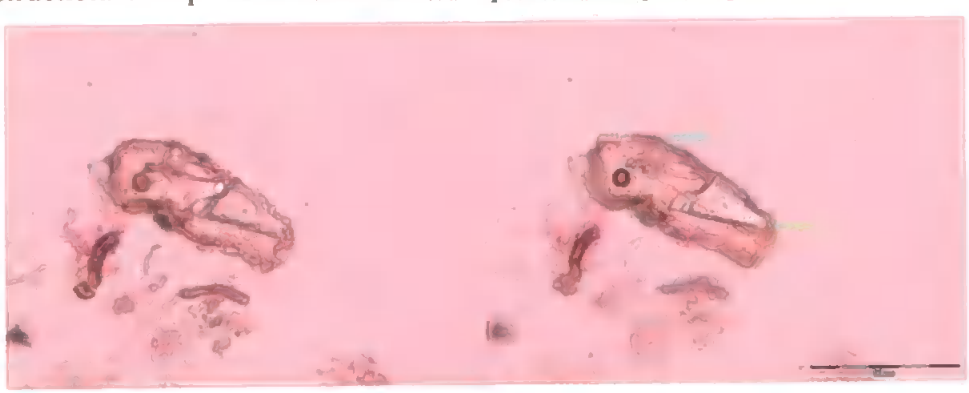

Plate A1.63 Difflugia oblonga test incorporating a tephra shard (K2 12-13 cm).

APPENDIX TWO – KOPOUATAI CORE STRATIGRAPHIES

A2.1 Z0106

Core Z0106 Description										
Depth (m)	Nig	Strf	Elas	Sicc	Lim	Humicity	Munsell colour	Fibrosity	Components	Other
2.70 to 2.72	LOST									
2.79 to 2.81	TEPHRA						10YR 8/3 very pale brown 10YR 5/8 yellowish brown			Large pumiceous Taupo?
2.81 to 2.87	3	0	3	1	1	2	7.5YR 2.5/3 very dark brown	3	Dh2 Th1 Tl1	
2.87 to 2.98	3	0	3	1	0	2	7.5YR 2.5/3 very dark brown	2	Dh1 Th2 Tl1	
2.98 to 3.00	2	0	2	2	1	2	7.5YR 4/4 brown	2	Dl2 Tl1 Dh1	Wood chunk
3.00 to 3.03	2	0	2	2	0	2	7.5YR 3/2 dark brown	3	Tl2 Th1 Dh1	
3.03 to 3.11	2	0	3	2	1	2	7.5YR 3/2 dark brown	2	Dh2 Tl1 Th1	
3.11 to 3.17	2	0	2	2	0	2	7.5YR 3/2 dark brown	3	Tl2 Th1 Dh1	Some cream tephra grains <1/2mm smeared down edge of core
3.17 to 3.30	LOST									
3.30 to 3.39	3	0	2	2	1	2	7.5YR 3/2 dark brown	3	Th2 Dl1 Th1	
3.39 to 3.41	3	0	2	2	0	2	7.5YR 3/1 very dark grey	4	Tl1 Th2 Dh1	
3.41 to 3.43	3	0	2	2	0	3	7.5YR 3/1 very dark grey	3	Th2 Dl1 Th1	
3.43 to 3.67	2	0	1	3	1	1	5YR 4/4 reddish brown	4	Th3 Dl1 Dh+	Cream tephra grains, washed down? 3.45-3.47
3.67 to 3.73	3	0	2	2	0	2	7.5YR 3/2 dark brown	3	Th2 Dl1 Dh1	
3.73 to 3.79	3	0	3	2	0	3	7.5YR 3/1 very dark grey	2	Dh1 Dg1 Th2 Tl+	
3.79 to 4.00	3	0	2	2	1	2	7.5YR 3/1 very dark grey	3	Tl2 Dh1 Dg1	Gleichenia roots
3.90 to 3.98	LOST									
4.00 to 4.08	3	0	2	2	0	2	7.5YR 3/2 dark brown	3	Tl2 Dl1 Dh1	Woody stems
4.08 to 4.23	3	0	3	2	0	3	7.5YR 3/2 dark brown	2	Dh2 Tl1 Dg1	
4.20 to 4.23	LOST									
4.23 to 4.33	3	0	2	2	1	2	7.5YR 4/1 dark grey	3	Th2 Tl1 Dh1	
4.33 to 4.47	3	0	3	3	1	3	7.5YR 3/2 dark brown	2	Th1 Tl1 Dh2	
4.47 to 4.51	3	0	2	2	1	2	7.5YR 3/2 dark brown	3	Tl2 Th1 Dh1	
4.51 to 4.65	3	0	3	2	0	3	7.5YR 3/2 dark brown	2	Th2 Tl1 Dh1	
4.65 to 4.72	3	0	2	3	0	2	5YR 3/3 dark reddish brown	3	Dl2 Th1 Dg1	
4.72 to 4.80	3	0	3	2	0	2	7.5YR 3/1 very dark grey	3	Dl1 Th1 Dh1 Dg1	
4.75 to 4.80	LOST									
4.80 to 4.82	LOST									
4.82 to 4.91	3	0	3	2	0	3	5YR 3/1 very dark grey	2	Dh2 Th1 Dg1 Tl+	
4.91 to 5.02	3	0	2	3	1	3	2.5YR 2.5/1 black	2	Tl1 Dh2 Dg1	
5.02 to 5.10	3	0	3	3	0	3	2.5YR 2.5/1 black	3	Dg2 Dh1 Th1	
5.10 to 5.12	LOST									
5.12 to 5.30	3	0	1	2	1	3	5YR 3/1 very dark grey	2	Tl1 Dh1 Th1 Dg1	
5.30 to 5.35	3	0	2	3	0	3/4	5YR 3/2 dark reddish brown	1	Dg3 Dh1 Th+	
5.35 to 5.42	3	0	1	2	0	3	5YR 3/2 dark reddish brown	2	Tl2 Th1 Dg1	Gleichenia roots
5.42 to 5.50	3	0	1	2	0	3	5YR 3/2 dark reddish brown	2	Tl1 Dh1 Th2	
5.50 to 5.58	3	0	2	3	0	4	5YR 2.5/1 black	1	Dh2 Dg1 Dl1	

5.58 to 5.67	3	0	2	2	0	3	5YR 2.5/1 black	2	Dh1 Dg1 Tl2	
5.67 to 5.73	LOST									
5.73 to 5.77	3	0	0	3	1	2	5YR 2.5/1 black	3	Dl2 Dg1 Tl1	Wood
5.77 to 5.90	3	0	2	1	0	3/4	5YR 3/1 dark reddish brown	1	Dg2 Dh1 Tl1	
5.90 to 5.95	3	0	2	2	0	3	2.5YR 2.5/1 reddish black	2	Tl2 Dg1 Th1	
5.95 to 6.00	LOST									
6.00 to 6.05	2	0	1	3	1	2	7.5YR 4/2 brown	2	Dl2 Dg1 Tl1	Wood chunks
6.05 to 6.14	3	0	2	2	0	2	7.5YR 4/2 brown	2	Dl1 Dg1 Tl1 Th1	Wood fragments
6.14 to 6.22	3	0	1	2	0	3	5YR 2.5/1 black	2	Tl2 Dh1 Dg1	Gleichenia roots
6.22 to 6.27	4	0	2	2	1	3/4	10YR 2/1 black	1	Dg2 Dh1 Tl1	
6.27 to 6.37	3	0	1	3	0	3	5YR 2.5/1 black	2	Tl2 Dh1 Dg1	Gleichenia roots
6.30 to 6.33	LOST									
6.37 to 6.49	4	0	1	2	0	4	10YR 2/1 black	0	Sh3 Tl1 Th+	
6.49 to 6.61	3	0	1	2	1	3	5YR 2.5/2 dark reddish brown	3	Tl2 Dh1 Sh1	Gleichenia roots
6.61 to 6.65	3	0	2	2	0	3/4	10YR 2/1 black	1	Sh3 Tl1	
6.65 to 6.70	3	0	1	3	0	3	5YR 2.5/2 dark reddish brown	3	Tl2 Dl2	
6.70 to 6.77	4	0	1	2	1	4	10YR 2/1 black	2	Sh2 Tl1 Dl1	
6.77 to 7.00	3	0	2	2	0	3	5YR 2.5/2 dark reddish brown	3	Tl3 Sh1	Gleichenia roots
6.87 to 6.90	LOST									
7.00 to 7.10	3	0	1	3	0	3	10YR 4/3 brown	2	Ag1 Dl1 Tl1 Dh1	
7.10 to 7.20	2	1	0	2	1	3	2.5Y 4/2 dark greyish brown	1	Ag3 Dh1	
7.14 to 7.34	LOST									
7.20 to 7.22	LOST									
7.34 to 7.40	2	1	1	3	0	3	2.5Y 3/1 very dark grey	2	Ag2 Dh1 Tl1	
7.40 to 7.50	4	0	2	2	0	3	2.5Y 2.5/1 black	3	Ag+ Tl2 Dh1 Dl1	
7.50 to 7.52	LOST									
7.52 to 7.58	3	0	1	3	0	3	5YR 4/2 dark reddish grey	2	Dh1 Tl2 Th1	
7.58 to 7.64	3	0	2	2	0	3/4	7.5YR 3/1 very dark grey	1	Dh2 Tl1 Th1	
7.64 to 7.73	2	0	0	2	1	2	7.5YR 3/1 very dark grey	2	Dl3 Tl1 Dh+	Wood chunk 5YR 4/8 yellowish red
7.73 to 7.84	TEPHRA						10YR 4/3 brown			
							10YR 6/4 light yellowish brown			Fine pumice 1/2mm diameter
7.84 to 7.90	TEPHRA						7.5YR 4/4 brown			Very fine sand layer
7.90 to 8.10	3	0	3	3	0	2	7.5YR 3/3 dark brown	2		Dh1 Tl2 Th1
8.0925 to 8.095	TEPHRA						2.5Y 8/1 white			Very thin tephra layer

Table A2.1 Z0106 Detailed core stratigraphy

A2.2 Z0108

Core Z0108 Description										
Depth (m)	Nig	Strf	Elas	Sicc	Lim	Humicity	Munsell colour	Fibrosity	Components	Other
3.30 to 3.35	3	0	3	1		1	5YR 4/2 dark reddish grey	4	Tl2 Th1 Dh1	
3.35 to 3.36	TEPHRA						10YR 5/4 yellowish brown			Pumiceous, 1/2 to 1mm diameter Taupo?
							10YR 7/4 very pale brown			
3.36 to 3.42	3	0	3	1	1	1	5YR 4/2 dark reddish grey	4	Tl1 Th1 Dh2	
3.42 to 3.48	3	0	2	1	0	2	5YR 4/2 dark reddish grey	2	Th1 Dh1 Tl1	
3.48 to 3.50	2	0	1	2	0	2	7.5YR 5/4 brown	2	Dl3 Dh1	Wood chunk

3.50 to 3.71	4	0	2	2	0	3	5YR 3/1 very dark grey	1	Th2 Dh1 Dg1			
3.54 to 3.60	LOST											
3.60 to 3.63	LOST											
3.71 to 3.87	3	0	3	2	0	3	5YR 3/2 dark reddish brown	2	Dh1 Th2 Tl1			
3.87 to 3.92	3	0	2	2	1	1	2.5YR 2.5/1 reddish black	1	Tl2 Dh1 Dl1			Gleichenia roots
3.92 to 3.96	4	0	2	2	0	3	5YR 2.5/1 black	1	Dh2 Dl1 Dg1 Tl+			
3.96 to 4.04	3	0	1	2	0	2	5YR 3/2 dark reddish brown	3	Dh2 Tl2 Th+			Gleichenia roots
4.04 to 4.12	3	0	1	2	0	2	5YR 3/2 dark reddish brown	2	Dh2 Tl1 Th1			
4.12 to 4.20	4	0	2	2	0	3	5YR 3/1 very dark grey	1	Dh2 Th1 Dg1 Tl+			
4.20 to 4.28	3	0	1	2	0	2	5YR 3/1 very dark grey	2	Tl2 Dl1 Dh1			Gleichenia roots
4.28 to 4.33	4	0	2	2	0	3	5YR 2.5/1 black	1	Dh2 Dg1 Th1			
4.33 to 4.42	4	0	1	1	0	2	5YR 3/3 dark reddish brown	1	Dh2 Tl1 Th1			Manuka seed pod 4.33 to 4.34
4.42 to 4.49	2	0	1	0/1	1	0	5YR 4/4 reddish brown	4	Tl3 Th1 Dh+			
4.49 to 4.50	LOST											
4.50 to 4.60	LOST											
4.60 to 4.66	3	0	1	2	0	1	7.5YR 4/2 brown	3	Dl1 Tl2 Dh1			Wood chunk
4.66 to 4.70	3	0	2	2	0	2	5YR 3/2 dark reddish brown	2	Th1 Tl1 Dh1 Dg1			
4.70 to 4.80	4	0	2	2	0	3	5YR 2.5/2 dark reddish brown	1	Dg2 Dh1 Th1			
4.80 to 4.92	LOST											
4.92 to 4.96	3	0	1	1	0	3	5YR 4/3 reddish brown	2	Dl2 Th1 Dg1			Woody chunks
4.96 to 5.03	4	0	2	2	1	3	5YR 2.5/1 black	1	Dg2 Dh1 Th1			
5.03 to 5.10	4	0	2	2	0	3/4	5YR 2.5/1 black	1	Dg2 Dh2 Th+			
5.10 to 5.12	LOST											
5.12 to 5.20	3	0	2	2	0	3	7.5YR 3/2 dark brown	1	Tl1 Dh2 Dg1			
5.20 to 5.37	3	0	1	2	0	2	7.5YR 3/1 very dark grey	2	Tl1 Th1 Dh2			
5.37 to 5.40	4	0	1	2	0	2	5YR 2.5/1 black	3	Tl2 Dg2 Th+			Gleichenia roots
5.40 to 5.49	4	0	2	2	0	4	5YR 3/1 very dark grey	2	Th1 Dh2 Dg1			
5.49 to 5.58	3	0	1	3	1	3	5YR 3/3 dark reddish brown	3	Tl2 Dl1 Dh1			
5.58 to 5.77	4	0	2	2	0	3	5YR 2.5/1 black	2	Tl2 Dg1 Dh1			
5.69 to 5.70	LOST											
5.70 to 5.71	LOST											
5.77 to 5.83	3	0	1	2	0	3	5YR 3/2 dark reddish brown	3	Dl2 Dh1 Dg1			Big branch
5.83 to 5.95	4	0	2	3	1	4	5YR 2.5/1 black	1	Dg3 Th1			
5.95 to 6.04	4	0	1	2	1	3	5YR 3/1 very dark grey	2	Tl2 Dg1 Dh1			
6.00 to 6.01	LOST											
6.04 to 6.16	4	0	1	2	0	2	5YR 3/1 very dark grey	3	Dl3 Dg1			Woody stems
6.16 to 6.30	4	0	1	2	0	3	5YR 3/1 very dark grey	3	Dl2 Dg1 Tl1			Woody stems, Gleichenia roots
6.30 to 6.40	4	0	1	3	1	3	7.5YR 3/1 very dark grey	1	Dh2 Dg2 Th+			
6.40 to 6.48	3	0	1	2	0	2	5YR 3/2 dark reddish brown	2	Dl1 Dh1 Dg1 Th1			
6.48 to 6.60	4	0	0	3	1	2	7.5YR 2.5/1 black	3	Dl2 Dh1 Dg1			Woody stems
6.59 to 6.60	LOST											
6.60 to 6.69	4	0	2	2	0	3/4	5YR 2.5/1 black	0	Dh1 Dg2 Th1			
6.69 to 6.75	4	0	1	2	0	3	5YR 2.5/2 dark reddish brown	1	Dh1 Dg1 Tl1 Th1			
6.75 to 6.81	3	0	1	1	0	2	7.5YR 4/2 brown	2	Tl2 Dh1 Dg1			
6.81 to 6.92	4	0	2	2	0	3/4	7.5YR 3/1 very dark grey	0	Dh2 Dg2			
6.88 to 6.90	LOST											

6.92 to 7.03	3	0	2	2	0	2	5YR 3/2 dark reddish brown	2	Dl1 Dh2 Dg1	Woody stems
7.03 to 7.20	3	0	1	2	0	2	5YR 3/2 dark reddish brown	3	Dl2 Tl2 Dh+	Gleichenia roots
7.11 to 7.20	LOST									
7.20 to 7.31	4	0	1	3	0	3/4	5YR 2.5/1 black	0	Dg4	
7.31 to 7.36	3	0	2	2	0	3	5YR 3/3 dark reddish brown	1	Dh2 Dg2 Th+	Sparse tephra grains throughout (washed)
7.36 to 7.50	TEPHRA						10YR 4/6 dark yellowish brown			Very fine pumice 1/4 to 1/2mm diameter
							10YR 6/6 brownish yellow			
7.41 to 7.50	LOST									
7.50 to 7.53	TEPHRA						7.5YR 4/3 brown			Fine sand
7.53 to 7.60	3	0	2	2	1	2	5YR 3/2 dark reddish brown	2	Th1 Dg2 Dh1	
7.60 to 7.76	3	0	1	3	0	1	5YR 3/2 dark reddish brown	3	Dl2 Dh1 Dg1	Woody stems
7.76 to 7.82	4	0	2	2	0	3	7.5YR 2.5/1 black	1	Dg2 Dh1 Th1	
7.82 to 7.89	4	0	1	2	1	2	5YR 3/1 very dark grey	3	Dl1 Tl1 Dg1 Dh1	Woody stems
7.89 to 7.93	4	0	2	2	0	3	5YR 3/1 very dark grey	1	Dg3 Dh1	
7.93 to 8.17	4	0	1	2	0	3	5YR 2.5/1 black	3	Tl1 Dl1 Dg2	Woody stems
8.17 to 8.22	4	0	1	2	0	3	5YR 2.5/1 black	3	Tl2 Dl1 Dg1	Woody stems
8.22 to 8.29	4	0	2	2	0	3/4	5YR 2.5/1 black	1	Dg2 Th1 Dh1	
8.29 to 8.40	4	0	1	1	1	2	5YR 3/1 very dark grey	3	Dl3 Tl1	Large wood chunk 6cm long
										Woody stems
8.40 to 8.45	3	0	0	2	0	1	5YR 4/3 reddish brown	4	Dl4 Dg+	Woody chunks
8.45 to 8.55	4	0	2	2	0	3/4	5YR 3/1 very dark grey	1	Dh1 Dg3	
8.55 to 8.62	3	0	1	1	0	2	5YR 3/2 dark reddish brown	3	Dl2 Dh1 Dg1	
8.62 to 8.70	4	0	1	2	0	3	5YR 3/1 very dark grey	1	Dh2 Dg2	
8.70 to 8.85	3	0	2	2	0	2	5YR 3/3 dark reddish brown	2	Dl1 Dh1 Dg2	
8.85 to 8.88	TEPHRA						10YR 7/6 yellow			Sandy
							10YR 4/6 dark yellowish brown			Sandy - same tephra or not?
8.88 to 8.92	3	0	2	2	0	2	5YR 3/3 dark reddish brown	2	Dl1 Dh1 Dg2	

Table A2.2 Z0108 Detailed core stratigraphy

A2.3 Z0204

Core Z0204 Description										
Depth (m)	Nig	Strf	Elas	Sicc	Lim	Humicity	Munsell colour	Fibrosity	Components	Other
0.75 to 0.90	2	0	3	0		0	7.5YR 4/3 Brown	4	Tl2 Th1 Dg1	Very fibrous, well preserved
1.50 to 1.80	2	0	3	1		1	5YR 3/4 Dark reddish brown	4	Tl1 Th1 Dh1 Dg1	Very fibrous
1.80 to 2.35	2	0	3	1	0	2	5YR 3/4 Dark reddish brown	4	Tl3 Th1 Dg+	Very fibrous
	TEPHRA									Grains washed down throughout core
										Concentrated at 2.30-2.35m. Kaharoa
2.35 to 2.75	2	0	2	1	0	2	5YR 3/4 Dark reddish brown	3	Tl2 Th1 Dh1	Very fibrous
2.75 to 3.02	3	0	1	2	0	3	5YR 3/1 Very dark grey	3	Tl1 Th1 Dh1 Dg1	Very fibrous
3.02 to 3.42	3	0	2	2	0	2/3	5YR 3/3 Dark reddish brown	3	Th2 Tl1 Dh1	Very fibrous
3.42 to 3.69	4	0	1	1	0	3	5YR 2.5/1 Black	2	Th2 Dh1 Dg1 Tl+	More decayed
3.69 to 3.73	TEPHRA				1		7.5YR 4/4 Brown			
3.73 to 3.94	4	0	1	2	1	3/4	5YR 2.5/1 Black	1	Th2 Dg1 Sh1 Tl+	Well decayed
3.94 to 4.40	4	0	1	2	0	4	5YR 2.5/1 Black	1	Dh1 Dg1 Th2	Well decayed
4.40 to 4.54	4	0	2	2	0	3/4	5YR 2.5/1 Black	2	Tl1 Th2 Dg1	Well decayed
4.54 to 4.80	4	0	1	2	0	3/4	5YR 2.5/1 Black	1	Th2 Dg1 Sh2	Well decayed

4.80 to 4.98	4	0	2	3	0	2	5YR 3/2 Dark reddish brown	3	Tt2 Th1 Dg1	Well decayed
4.98 to 5.12	4	0	1	2	0	3/4	5YR 2.5/1 Black	1	Th2 Dh1 Dg1	Well decayed
5.12 to 5.24	4	0	2	3	1	3	5YR 2.5/2 Dark reddish brown	2	Tt2 Th1 Dg1	Well decayed
5.24 to 5.43	4	0	1	2	0	4	5YR 2.5/1 Black	1	Dg2 Th1 Sh1	Well decayed
5.43 to 5.48	4	0	2	2	0	3	5YR 2.5/1 Black	2	Tt2 Th1 Dg1	Well decayed
5.48 to 5.83	4	0	1	2	1	4	5YR 2.5/1 Black	1	Th1 Dh1 Dg1 Sh1	Well decayed
5.83 to 6.10	4	0	1	2	0	3/4	5YR 2.5/1 Black	1	Sh2 Th1 Dg1	
6.10 to 6.20	4	0	1	2	0	3	5YR 3/2 Dark reddish brown	1	Tt2 Th1 Sh1	
6.20 to 6.47	4	0	2	2	0	3/4	5YR 2.5/1 Black	1	Th1 Dh1 Sh2	
6.47 to 6.64	4	0	1	2	0	3	5YR 2.5/1 Black	2	Th1 Dh2 Sh1	Wood lump 6.55m
6.64 to 6.79	4	0	1	1	0	4	5YR 2.5/1 Black	2	Dg2 Th1 Sh1	
6.79 to 7.20	4	0	1	1	1	3	5YR 2.5/2 Dark reddish brown	3	Tt2 Th1 Dg1	Gleicheria roots
7.20 to 7.52	4	0	1	1	0	4	5YR 2.5/2 Dark reddish brown	1	Th2 Tl1 Sh1	
7.52 to 7.78	4	0	1	1	0	2/3	5YR 2.5/2 Dark reddish brown	1	Tt2 Th1 Sh1	
7.78 to 8.25	1	0	0	1	1		2.5Y 6/2 Light brownish grey	1	As4 Sh+	Grey clay
										Wood chunk 7.80-7.90m
8.25 to 8.44	2	0	1	2	0	3	10YR 3/3 Dark brown	1	As2 Th+ Th1 Dh1	
	TEPHRA									Very fine white layer 8.43-8.45m
8.44 to 8.75	4	0	1	2	0	4	5YR 2.5/2 Dark reddish brown	1	Tl1 Th1 Dh1 Sh1	
	TEPHRA									Grains from 8.66 downwards (top of Tuhua?)
8.75 to 8.79	3	0	0	3	1		2.5Y 5/2 Greyish brown		Ga4	Coarse Tuhua layer
	TEPHRA									
8.79 to 8.82	2	0	0	3	1		2.5Y 6/2 Light brownish grey		Ag4	Fine Tuhua layer
	TEPHRA									
8.82 to 9.05	4	0	1	2	0	3	5YR 2.5/1 Black	2	Th2 Dh1 Dg1	
9.05 to 9.30	4	0	1	3	0	2	5YR 2.5/1 Black	3	Tt2 Dh1 Dg1	

Table A2.3 Z0204 Detailed core stratigraphy

APPENDIX THREE – MOANATUATUA CORE STRATIGRAPHIES

A3.1 Z0102

Core Z0102 Description									
Depth (m)	Nig	Strf	Elas	Sicc	Lim	Humicity	Munsell colour	Components	Other
0.2 to 0.42	4	0	4	3			7.5YR 2.5/1 black		Crumbly topsoil
0.42 to 0.485	3	0	3	2	0	3	2.5YR 3/3 dark reddish brown	Dg2 Dh2	
0.485 to 0.50	TEPHRA						7.5YR 6/3 light brown		Tephra layer
							pumiceous, up to 3mm diameter		
0.50 to 0.73	3	0	2	2	0	2	5YR 4/3 reddish brown	Dl1 Dh1 Dg1 Th1	
0.73 to 1.01	3	0	2	3	0	2	5YR 3/2 dark reddish brown	Dl2 Dh1 Tl1	
1.02 to 1.04	TEPHRA								Very fine creamy,white ash
1.01 to 1.33	3	0	3	3	0	3	7.5YR 2.5/1 black	Dl1 Dh1 Dg2	
1.33 to 1.67	3	0	3	3	0	2	5YR 4/4 reddish brown	Dl2 Dh1 Dg2	
1.67 to 1.82	3	0	3	3	1	2	5YR 4/4 reddish brown	Dh2 Dg2	
1.82 to 1.91	3	0	3	3	0	2	7.5YR 2.5/1 black	Dl2 Dh1 Dg1	
1.91 to 2.34	3	0	2	2	0	2	5YR 3/4 dark reddish brown	Dg3 Th1	
2.34 to 2.38	3	0	2	2	1	2	5YR 3/4 dark reddish brown	Dl1 Th1 Dg2	Woody
2.38 to 2.46	3	0	2	2	1	2	7.5YR 3/4 dark brown	Th2 Dg2	
2.46 to 2.50	3	0	1	3	2	3	5YR 3/4 dark reddish brown	Dl1 Th1 Dh2	Woody, twigs
2.50 to 2.57	3	0	2	2	1	3	5YR 3/4 dark reddish brown	Dh2 Th1 Dl1	
2.57 to 2.62	3	0	1	3	0	1	5YR 3/2 dark reddish brwon	Th2 Dg1 Th1 Dl+	Gleichenia
2.62 to 2.83	3	0	2	2	1	2	5YR 3/2 dark reddish brown	Th2 Dg2	
2.83 to 2.89	3	0	2	1	1	2	5YR 3/2 dark reddish brown	Th1 Dg2 Dl1	
2.89 to 2.96	2	0	3	2	1	2	5YR 2.5/2 dark reddish brown	Dl1 Dh2 Th1	
2.96 to 2.99	3	0	2	2	0	3	5YR 2.5/1 black	Dl2 Dh1 Th1	
2.99 to 3.08	2	0	2	2	0	3	5YR 3/2 dark reddish brown	Dh2 Dg2 Ga+	Tephra grains
3.07 to 3.08	TEPHRA						10YR 8/2 very pale brown		Fine tephra
							10YR 6/4 light yellowish brown		Concentrated layer/pod
3.08 to 3.14	3	0	2	3	0	3	5YR 3/2 dark reddish brown	Dh1 Dg2 Th1	
3.14 to 3.27	3	0	3	3	1	3	5YR 2.5/1 black	Dh2 Dg2	
3.27 to 3.42	3	0	1	3	1	3	5YR 3/1 very dark grey	Dl1 Dh2 Dg1 Ga+	
3.27 to ???	TEPHRA						7.5 YR 5/6 strong brown		Fine sandy grains
									Concentrated 3.36 to 3.375
3.42 to 3.70	2	0	2	2	0	3	5YR 3/2 dark reddish brown	Dl1 Dg2 Dh1	
3.70 to 3.74	3	0	2	3	1	3	5YR 2.5/1 black	Dl1 Dg2 Dh1	
3.74 to 3.83	3	0	1	2	1	3	5YR 3/2 dark reddish brown	Dl1 Dh1 Dg2	
3.83 to 3.95	4	0	2	3	0	3	5YR 2.5/1 black	Dh2 Dg2	

3.95 to 4.10	4	0	1	3	0	3	5YR 2.5/1 black	Dg1 Dh2 Th1 Dl+	
4.10 to 4.12	3	0	2	2	1	3	5YR 2.5/1 black	Dh2 Dl1 Th1	
4.12 to 4.43	4	0	3	2	0	3	5YR 2.5/1 black	Th1 Dh1 Dg2	
4.43 to 4.49	3	0	2	2	1	3	5YR 2.5/1 black	Dl1 Dh2 Dg1 Th+	
4.49 to 4.51	3	0	1	2	0	3	5YR 2.5/1 black	Dl2 Dh1 Dg1 Th+	Woody
4.51 to 4.67	3	0	2	2	1	3	5YR 2.5/1 black	Dl1 Dh2 Dg1 Th+	
4.67 to 4.88	3	0	3	2	0	3	5YR 2.5/1 black	Dh2 Dg2 Dl+ Th+	
4.98 to 5.12	3	0	2	1	0	3	5YR 2.5/2 dark reddish brown	Dl1 Dh2 Dg1 Th+	
5.12 to 5.30	3	0	2	2	1	3	5YR 2.5/1 black	Dh2 Dg2 Th+	
5.30 to 5.42	3	0	1	2	1	2	5YR 2.5/2 dark reddish brown	Dh1 Dg2 Dl1	
5.42 to 5.60	3	0	2	1	0	3	5YR 2.5/2 dark reddish brown	Dh2 Dg2 Th+	
5.60 to 5.75	3	0	2	1	0	3	5YR 2.5/2 dark reddish brown	Dh2 Dg1 Ag1	Start of Hinuera Formation
5.75 to 5.82	3	0	1	2	0	3	7.5YR 2.5/2 very dark brown	Dl1 Dh1 Ag2	
5.82 to 5.95	2	0	0	3/4	0	-	10YR 3/2 very dark greyish brown	Ag4 Tl+ Ga+	
5.95 to ???	1	0	0	3/4	0	-	10YR 5/4 yellowish brown	Ag4 Tl+ Ga+	
??? to 6.08	1/0	0	0	3/4	0	-	2.5Y 6/3 light yellowish brown	Ag4 Tl+ Ga+	

Table A3.1 Z0102 Detailed core stratigraphy

A3.2 Z0103

Core Z0103									
Description									
Depth (m)	Nig	Strf	Elas	Sicc	Lim	Humicity	Munsell colour	Components	Other
1.50 to 1.54	LOST								
1.54 to 1.615	2	0	2	1		2	5YR 3/2 Dark reddish brown	Dh2 Tl1 Th1	1.58 to 1.615 Gleichenia roots
									Some fine white ash (washed down?)
1.615 to 162.5	TEPHRA						10YR 5/3 brown		Pumiceous tephra (Taupo)
							10YR 6/4 Light reddish brown		
1.625 to 1.90	3	0	2	1	3	1	7.5YR 3/2 Dark brown	Dh3 Tl1	
1.80 to 1.85	LOST								
1.90 to 1.93	3	0	3	2	2	2	7.5YR 3/1 Very dark grey	Th2 Dh1 Dl1	Woody
1.93 to 1.99	3	0	2	1	2	2	7.5YR 2.5/2 Very dark brown	Tl1 Th1 Dh2 Dl+	
1.99 to 2.12	3	0	2	2	1	3	5 YR 3/1 Very dark grey	Th1 Tl1 Dh2	
2.12 to 2.195	3	0	2	2	1	3	5YR 3/2 Dark reddish brown	Tl2 Th1 Dh1	
2.195 to 2.29	3	0	2	2	0	3	7.5YR 3/1 Very dark grey	Dh2 Dl1 Th1	
2.29 to 2.48	3	0	2	2	1	3	7.5YR 3/1 Very dark grey	Dh1 Th1 Tl2	
2.35 to 2.40	LOST								
2.48 to 2.50	2	0	1	3	0	2	5YR 4/3 Reddish brown	Dl2 Tl1 Dl1	Wood chunks
2.50 to 2.76	3	0	2	2	0	3	5YR 3/2 Dark reddish brown	Tl2 Dh1 Dl1	
2.615 to 2.7	LOST								
2.76 to 2.86	3	0	1	3	2	2	5YR 3/2 Dark reddish brown	Dl1 Tl1 Dh1 Dg1	
2.86 to 2.975	3	0	1	3	0	2	5YR 3/2 Dark reddish brown	Dl2 Tl1 Dg1	Very woody branches
2.975 to 3.00	LOST								
2.975 to 3.15	3	0	2	2	1	2	7.5YR 2.5/1 Black	Dl1 Dg2 Tl1	
3.15 to 3.41	3	0	2	2	0	3	7.5YR 2.5/1 Black	Dh1 Dg2 Tl1	3.37 to 3.40 very fine white ash throughout

3.29 to 3.30	LOST									
3.30 to 3.345	LOST									
3.41 to 3.485	3	0	2	3	0	3	5YR 3/2 Dark reddish brown	Tl2 Dh1 Th1 Dg+	Gleichenia roots
3.485 to 3.53	3	0	2	3	0	3	5YR 3/2 Dark reddish brown	Tl2 Dh1 Th1 Dg+	Solid wood
3.53 to 3.61	3	0	2	3	0	3	5YR 3/2 Dark reddish brown	Dl2 Dh1 Th1	
3.60 to 3.65	LOST								
3.61 to 3.71	3	0	1	2	1	2	5YR 3/1 Very dark grey	Tl2 Dl1 Dh1	Gleichenia roots
3.71 to 4.00	3	0	2	2	1	3	5YR 3/1 Very dark grey	Th2 Dg1 Tl1	
3.9 to 3.935	LOST								
4.00 to 4.04	3	0	1	3	0	2	5YR 3/2 Dark reddish brown	Tl2 Th1 Dg1	Gleichenia roots
4.04 to 4.13	3	0	2	2	0	3	5YR 3/1 Very dark grey	Dg1 Dh1 Tl1 Th1	
4.13 to 4.31	3	0	2	2	1	3/4	5YR 3/1 Very dark grey	Dg2 Dh1 Tl1	
4.31 to 4.58	3	0	1	2	0	2	5YR 3/1 Very dark grey	Tl2 Dh1 Dg1	
4.58 to 4.70	3	0	1	3	0	3	5YR 3/1 Very dark grey	Dg2 Dh1 Tl1	
4.70 to 4.73	2	0	1	3	0	3	5YR 3/1 Very dark grey	Dh1 Dg2 Ag1	Tephra grains 7.5YR 5/4 Brown
4.73 to 4.75	TEPHRA						7.5YR 5/4 Brown		Very fine sandy grains
4.75 to 4.835	3	0	2	2	0	2	5YR 4/1 Dark grey	Dh1 Th1 Dg1 Ag1	Woody
4.75 to 4.8	LOST								
4.835 to 4.87	TEPHRA						7.5YR 4/4 Brown		Very fine sand
4.87 to 4.96	3	0	2	3	0	3	5YR 3/2 Dark reddish brown	Dh1 Dg2 Tl1	
4.96 to 5.04	3	0	1	2	1	2	5YR 2.5/2 Dark reddish brown	Tl1 Dl1 Dg2	Woody stems
5.04 to 5.10	LOST								

Table A3.2 Z0103 Detailed core stratigraphy

A3.3 Z0206

Core Z0206										
Description										
Depth (m)	Nig	Strf	Elas	Sicc	Lim	Humicity	Munsell colour	Fibrosity	Components	Other
0.30 to 0.35	2	0	3	2		1	2.5YR 3/1 Dark reddish grey	4	Dh2 Th2	Roots
0.35 to 0.60	2	0	3	2	0	2	2.5YR 3/3 Dark reddish brown	3	Th3 Dh1	Roots
0.60 to 0.75	2	0	2	3	1	2	2.5YR 2.5/2 Very dusky red	4	Th4 Dh+	Roots
0.75 to 0.87	3	0	2	3	0	3	2.5YR 2.5/1 Reddish black	3	Th3 Dh1 Dg+	
0.87 to 0.91	3	0	2	2	0	3	2.5YR 2.5/1 Reddish black	2	Th2 Dh1 Dg1	
0.91 to 0.95	2	0	3	3	1	2	2.5YR 3/4 Dark reddish brown	3	Th3 Dh1	
0.95 to 1.02	3	0	2	2	0	3	2.5YR 3/1 Dark reddish grey	2	Dh2 Dg2	
1.02 to 1.15	3	0	2	2	0	2	2.5YR 2.5/1 Reddish black	3	Th2 Dh2	
1.15 to 1.22	4	0	2	2	0	3	2.5YR 2.5/1 Reddish black	2	Th1 Dh2 Dg1	
1.22 to 1.33	4	0	1	2	1	4	5YR 3/2 Dark reddish brown	3	Tl2 Dh1 Th1	Gleichenia roots
1.33 to 1.54	4	0	1	2	1	4	5YR 3/1 Very dark grey	1	Dg1 Th3	
	TEPHRA									Pumice starts 1.52-1.62
1.54 to 1.66	4	0	1	2	1	4	5YR 3/3 Dark reddish brown	1	Dg1 Th2 Dh1	Taupo. No clear layer - spread out.
	TEPHRA									Highest concentration 1.54-1.61m
										Large pieces (>1cm).
1.66 to 1.80	4	0	2	2	0	3	5YR 3/1 Very dark grey	2	Th2 Dh1 Dg1	
EXTRA										
1.35 to 1.52	4	0	3	2		3	5YR 3/2 Dark reddish brown	1	Th2 Dh1 Dg1	
1.52 to 1.65	3	0	2	3	0	2	5YR 3/3 Dark reddish brown	2	Dh1 Th3	
	TEPHRA									Taupo 1.56-1.59 (at an angle)
1.80 to 2.03	3	0	1	2	1	2	5YR 3/2 Dark reddish brown	3	Dh2 Th2	Wood chunk 1.90-1.91

2.03 to 2.18	4	0	1	2	0	3/4	5YR 2.5/1 Black	1	Dh1 Th1 Dg2	
2.18 to 2.23	4	0	2	3	0	2	5YR 3/1 Very dark grey	3	Tl2 Dh1 Th1	Woody stems, roots
2.23 to 2.40	4	0	1	2	0	4	5YR 2.5/1 Black	1	Dg2 Th2	Very decomposed
2.40 to 2.54	4	0	1	3	0	3	5YR 3/2 Dark reddish brown	2	Tl2 Th1 Dh1	
2.54 to 2.70	4	0	1	3	0	4	5YR 2.5/1 Black	1	Dh2 Dg1 Th1	
2.70 to 2.79	4	0	1	3	0	3	5YR 3/1 Very dark grey	3	Th1 Tl1 Dh2	
2.79 to 2.88	4	0	2	2	0	4	5YR 2.5/1 Black	1	Dh2 Dg1 Th1	
2.88 to 3.00	4	0	1	3	0	3	5YR 3/1 Very dark grey	3	Th1 Tl1 Dh2	
3.00 to 3.15	4	0	1	2	0	4	5YR 2.5/1 Black	1	Dh2 Dg1 Th1	Woody stem at 3.09m
3.15 to 3.34	4	0	2	2	0	3	5YR 3/1 Very dark grey	2	Dh1 Th2 Tl1	
3.28 to 3.30	LOST									
3.34 to 3.50	3	0	1	2	0	3	5YR 3/2 Dark reddish brown	3	Tl1 Dl1 Dh2	Wood at 3.41m
3.50 to 3.60	4	0	2	2	1	4	5YR 2.5/1 Black	2	Dh1 Dg1 Th2	
3.60 to 3.63	3	0	2	2	1	3	5YR 3/1 Very dark grey	3	Tl2 Th1 Dh1	
3.63 to 3.79	4	0	2	2	0	4	5YR 4/2 Reddish brown	1	Th2 Dh1 Dg1	
3.79 to 3.99	4	0	2	2	1	3	5YR 3/1 Very dark grey	2	Tl2 Th1 Dh1	
3.99 to 4.15	4	0	1	2	1	4	5YR 3/1 Very dark grey	3	Th3 Dh1 Dg+	
4.15 to 4.20	4	0	2	2	0	3	5YR 4/2 Reddish brown	1	Tl2 Th1 Dh1	
4.20 to 4.35	4	0	2	3	0	3	5YR 3/1 Very dark grey	4	Tl2 Th1 Dh1	
4.35 to 4.52	4	0	2	2	0	4	5YR 3/3 Dark reddish brown	2	Th2 Dh1 Dg1	
4.52 to 4.60	4	0	1	3	1	3	5YR 3/3 Dark reddish brown	3	Tl2 Th1 Dh1	Large woody stems
4.60 to 4.80	4	0	2	2	0	4	5YR 3/2 Dark reddish brown	2	Th3 Dh1 Dg+	
4.80 to 4.94	4	0	2	3	0	3	2.5YR 3/3 Dark reddish brown	3	Tl2 Th1 Dh1	
4.94 to 5.10	4	0	2	2	1	4	2.5YR 2.5/1 Reddish black	1	Th2 Dh1 Dg1	
5.10 to 5.14	4	0	2	2	0	3	2.5YR 2.5/1 Reddish black	2	Tl2 Th1 Dh1	
5.14 to 5.33	4	0	2	2	1	4	2.5YR 2.5/2 Very dusky red	1	Th2 Dg1 Sh1	
5.33 to 5.54	3	0	1	3	0	4	7.5YR 3/2 Dark brown	1	Ga3 Sh1	
	TEPHRA									Tephra densest 5.33-5.40m
A										
5.54 to 5.60	4	0	2	2	0	3	5YR 3/2 Dark reddish brown	2	Tl2 Th1 Dg1	(David-tephra 5.30-5.43m)
5.60 to 5.70	4	0	2	2	0	4	5YR 2.5/1 Black	1	Th2 Dh1 Dg1	
(5.40 to 5.64	4	0	2	2	0	4	5YR 2.5/1 Black	1	Th2 Dh1 Dg1	
5.64 to 5.70)	4	0	2	3	0	3	5YR 2.5/1 Black	2	Tl2 Th1 Dg1	
5.70 to 5.90	4	0	2	3	0	4	5YR 2.5/1 Black	1	Dg2 Dh2	
5.90 to 6.26	4	0	2	3	1	3	5YR 2.5/1 Black	3	Tl2 Th1 Dg1	
6.26 to 6.30	4	0	2	2	1	4	5YR 2.5/1 Black	1	Th2 Dh1 Dg1	
6.30 to 6.82	4	0	1	3	0	3	5YR 2.5/1 Black	2	Tl2 Th1 Dh1	
6.82 to 6.90	4	0	2	2	0	4	5YR 2.5/1 Black	1	Th2 Dh1 Dg1	

Table A3.3 Z0206 Detailed core stratigraphy

APPENDIX FOUR - PALYNOLOGY

This appendix describes the results of the palynological investigation of the five samples of each of the clay layers in cores Z0106 and Z0204 from Kopouatai, according to Newnham (2004, pers. comm.).

Pollen concentrations varied strongly between samples but were generally lower than in peat samples analysed previously at this site (Newnham *et al.*, 1995). Pollen composition, likewise, is distinctly different from that in the peats, there being a rise in halophytic taxa, notably *Leptocarpus* and Chenopodiaceae, characteristic of estuarine and coastal environments in New Zealand. It is interesting to note that the only appearance of these two taxa (apart from single grains noted in scanning) in the 10 m+ pollen profile from Kopouatai Bog (Newnham *et al.*, 1995) is also seen in sediments deposited shortly after the Tuhua Tephra, although at this core site, a clay layer was not recorded.

Two other changes are notable in the clay layers of Z0106 and Z0204: a marked decline in taxa characteristic of the Kopouatai peat flora (Restionaceae and *Gleichenia*); and the presence in some samples of raphiated pinnate diatoms.

Taken together, this is unequivocal evidence that the clay layers reflect a marked change in the hydrological status of the bog at core sites Z0106 and Z0204, brought about by a marine incursion which is reported to have affected the northern-central parts of Kopouatai Bog around the time of, or shortly after, deposition of the Tuhua Tephra (Newnham *et al.*, 1995). It cannot be determined from this analysis whether the marine incursion extended as far as the core sites or, alternatively, sufficiently close to them as to have significantly altered hydrological characteristics and proximal vegetation, although this distinction might be possible with further analysis of the diatom flora. Either way, it can be concluded that these clay layers should be excluded from any investigation that relies upon the ombrogenous origin of sediments to elucidate palaeoclimatic signals.

REFERENCES

Aaby, B. 1976. Cyclic climatic variations in climate over the past 5,500 years reflected in raised bogs. *Nature* 263, 281-284.

Agnew, A., Rapson, G., Sykes, M. and Bastow Wilson, J. 1993. The functional ecology of *Empodisma minus* (Hook. f.) Johnson and Cutler in New Zealand ombrotrophic mires. *New Phytologist* 124, 703-710.

Anderson, A. 1991. The chronology of the settlement of New Zealand. *Antiquity* 65, 767-795.

Baker, M. 1997. Cloud microphysics and climate. *Science* 276, 1072-1078.

Ballinger, M. 2003. *Developing methods for identifying cryptic tephra in peat cores from the Waikato region, North Island, New Zealand.* Unpublished M.Res. dissertation, University of Plymouth.

Barber, K. 1981. *Peat stratigraphy and climatic change: a palaeoecological test of the theory of cyclic peat bog regeneration.* Balkema, Rotterdam 219pp.

Barber, K. 1982. Peat-bog stratigraphy as a proxy climate record, in Harding, A. (ed.) *Climatic change in later prehistory.* Edinburgh University Press, Edinburgh 103-113, 210pp.

Barber, K., Chambers, F., Maddy, D., Stoneman, R. and Brew, J. 1994. A sensitive high-resolution record of late Holocene climatic change from a raised bog in northern England. *The Holocene* 4(2), 198-205.

Barber, K., Dumayne-Peaty, L., Hughes, P., Mauquoy, D. and Scaife, R. 1998. Replicability and variability of the recent macrofossil and proxy-climate record from raised bogs: field stratigraphy and macrofossil data from Bolton Fell Moss and Walton Moss, Cumbria, England. *Journal of Quaternary Science* 13(6), 515-528.

Barber, K., Battarbee, R., Brooks, S., Eglington, G., Haworth, E., Oldfield, F., Stevenson, A., Thompson, R., Appleby, P., Austin, W., Cameron, N., Ficken, K., Golding, P., Harkness, D., Holmes, J., Hutchinson, R., Lishman, J., Maddy, D., Pinder, L., Rose, N. and Stoneman, R. 1999. Proxy records of climate change in the UK over the last two millennia: documented change and sedimentary records from lakes and bogs. *Journal of the Geological Society* 156, 369-380.

Barber, K., Maddy, D., Rose, N., Stevenson, A., Stoneman, R. and Thompson, R. 2000. Replicated proxy-climate signals over the last 2000 yr from two distant UK peat bogs: new evidence for regional palaeoclimate teleconnections. *Quaternary Science Reviews* 19, 481-487.

Barber, K., Chambers, F. and Maddy, D. 2003. Holocene palaeoclimates from peat stratigraphy: macrofossil proxy climate records from three oceanic bogs in England and Ireland. *Quaternary Science Reviews* 22, 521-539.

Barber, K. and Charman, D. 2003. Holocene palaeoclimate records from peatlands, in Mackay, A., Battarbee, R., Birks, J. and Oldfield, F. (ed.s) *Global change in the Holocene.* Hodder Arnold, London, 210-226, 480pp.

Bates, P. 1973. Peat bogs in the south Auckland area, New Zealand. *New Zealand Soil News* 21(6), 177-179.

Beerling, D. and Chaloner, W. 1993. Evolutionary responses of stomatal density to global carbon dioxide change. *Biological Journal of the Linnaean Society* 48, 343-353.

Berger, A. and Loutre, M. 1991. Insolation values for the climate of the last 10 million years. *Quaternary Sciences Reviews* 10(4), 297-317.

Berger, A. 1992. *Orbital Variations and Insolation Database.* IGBP PAGES/World DataCenter-A for Paleoclimatology Data Contribution Series #92-007 NOAA/NGDC Paleoclimatology Program, Boulder CO, USA. ftp://ftp.ngdc.noaa.gov/paleo/insolation/

Birks, H.J. and Heegaard, E. 2003. Developments in age-depth modelling of Holocene stratigraphical sequences. *PAGES News* 11(2&3), 7-8.

Blaauw, M., Heuvelink, G., Mauquoy, D., van der Plicht, J. and van Geel, B. 2003. A numerical approach to ^{14}C wiggle-match dating of organic deposits: best fits and confidence intervals. *Quaternary Science Reviews* 22, 1485-1500.

Blackford, J. 1993. Peat bogs as sources of proxy climatic data: past approaches and future research, in Chambers, F. (ed.) *Climate Change and Human Impact on the Landscape: studies in palaeoecology and environmental archaeology.* Chapman and Hall, London, 47-56, 304pp.

Blackford, J. and Chambers, F. 1993. Determining the degree of peat decomposition for peat-based palaeoclimate studies. *International Peat Journal* 5, 7-24.

Blackford, J. and Chambers, F. 1995. Proxy climate record for the last 1000 years from Irish blanket peat and a possible link to solar variability. *Earth and Planetary Science Letters* 133, 145-150.

Blaauw, M., van der Plicht, J. and van Geel, B. 2004. Radiocarbon dating of bulk peat samples from raised bogs: non-existence of a previously reported 'reservoir effect'?. *Quaternary Science Reviews* 23, 1537-1542.

Bond, G., Showers, W., Cheseby, M., Lotti, R., Almasi, P., deMendocal, P., Priore, P., Cullen, H., Hajdas, I. and Bonani, G. 1997. A pervasive millennial-scale cycle in North Atlantic Holocene and glacial climates. *Science* 278, 1257-1266.

Booth, R. and Jackson, S. 2003. A high-resolution record of late-Holocene moisture variability from a Michigan raised bog, USA. *The Holocene* 13(6), 863-876.

Brenstrum, E. 1998. *The New Zealand weather book.* Craig Cotton Publishing, Nelson 128pp.

Buck, C., Higham, T. and Lowe, D. 2003. Bayesian tools for tephrochronology. *The Holocene* 13(5), 639-647.

Burns, B. and Smale, M. 2002. Lowland forests, in Clarkson, B., Merrett, M. and Downs, T. (ed.s) *Botany of the Waikato.* Waikato Botanical Society, New Zealand, 73-81, 136pp.

Campbell, D. and Williamson, J. 1997. Evaporation from a raised bog. *Journal of Hydrology* 193, 142-160.

Campbell, E. 1964. The Restiad Peat Bogs at Motumaoho and Moanatuatua. *Transactions of the Royal Society of New Zealand* 2(16), 219-227.

Campbell, E. 1971. The vegetation of the Waikato peat-bogs. *New Zealand Soil News* 19,133-135.

Campbell, E. 1975. Peat deposits of northern New Zealand as based on identification of plant fragments in the peat. *Proceedings of the New Zealand Ecological Society* 22, 57-60.

Campbell, E., Heine, J. and Pullar, W. 1973. Identification of plant fragments and pollen from peat deposits in Rangitaiki Plains and Maketu Basins. *New Zealand Journal of Botany* 11, 317-330.

Carleton, A. 2003. Atmospheric teleconnections involving the Southern Ocean. *Journal of Geophysical Research* 108 8080 doi:10.1029/2000JC000379.

Carslaw, K., Harrison, R. and Kirkby, J. 2002. Cosmic rays, clouds and climate. *Science* 298, 1732-1737.

Carter, L., Nelson, C., Neil, H. and Froggatt, P. 1995. Correlation, dispersal and preservation of the Kawakawa tephra and other late Quaternary tephra layers in the southwest Pacific Ocean. *New Zealand Journal of Geology and Geophysics* 38, 29-46.

Cas, R. and Wright, J. 1987. *Volcanic successions.* Allen and Unwin, London 528pp.

Caseldine, C., Baker, A., Charman, D. and Hendon, D. 2000. A comparative study of optical properties of NaOH extracts: implications for humification studies. *The Holocene* 10(5), 649-658.

Cash, J. 1891. The freshwater Rhizopoda of the Manchester district. *Transactions of the Manchester Microscopic Society* 1891, 47-55.

Chambers, F. 1984. Studies on the initiation, growth-rate and humification of blanket peats in south Wales. *Department of Geography Occasional Paper 9* University of Keele.

Chambers, F., Barber, K., Maddy, D. and Brew, J. 1997. A 5500-year proxy-climate and vegetation record from blanket mire at Talla Moss, Borders, Scotland. *The Holocene* 7(4), 391-399.

Chambers, F., Ogle, M. and Blackford, J. 1999. Palaeoenvironmental evidence for solar forcing of Holocene climate: linkages to solar science. *Progress in Physical Geography* 23(2), 181-204.

Chambers, F. and Blackford, J. 2001. Mid- and late-Holocene climatic changes: a test of periodicity and solar forcing in proxy-climate data from blanket peat bogs. *Journal of Quaternary Science* 16(4), 329-338.

Charman, D. 1997. Modelling hydrological relationships of testate amoebae (Protozoa: Rhizopoda) on New Zealand peatlands. *Journal of the Royal Society of New Zealand* 27(4), 465-483.

Charman, D. 2001. Biostratigraphic and palaeoenvironmental applications of testate amoebae. *Quaternary Science Reviews* 20(16/17), 1753-1764.

Charman, D. and Warner, B. 1992. Relationships between testate amoebae (Protozoa: Rhizopoda) and micro-environmental parameters on a forested peatland in northeastern Ontario. *Canadian Journal of Zoology* 70, 2474-2482.

Charman, D. and Warner, B. 1997. The ecology of testate amoebae (Protozoa: Rhizopoda) in oceanic peatlands in Newfoundland, Canada: Modelling hydrological relationships for palaeoenvironmental reconstruction. *Ecoscience* 4(4), 555-562.

Charman, D., Hendon, D. and Packman, S. 1999. Multiproxy surface records from replicate cores on an ombrotrophic mire: implications for Holocene palaeoclimate records. *Journal of Quaternary Science* 14(5), 451-463.

Charman, D. and Hendon, D. 2000. Long-term changes in soil water tables over the past 4500 years: Relationships with climate and North Atlantic atmospheric circulation. *Climatic Change* 47, 45-49.

Charman, D., Hendon, D. and Woodland, W. 2000. *The identification of testate amoebae (Protozoa: Rhizopoda) in peats.* Technical Guide No. 9, Quaternary Research Association 147pp.

Charman, D., Caseldine, C., Baker, A., Gearey, B., Hatton, J. and Proctor, C. 2001. Palaeohydrological records from peat profiles and speleothems in Sutherland, northwest Scotland. *Quaternary Research* 55, 223-234.

Charman, D., Brown, A., Hendon, D., and Karofeld, E. 2004 Testing the relationship between Holocene peatland palaeoclimate reconstructions and instrumental data at two European sites. *Quaternary Science Reviews* 23, 137-143.

Clark, J. 1988. Particle motion and the theory of charcoal analysis: source area, transport, deposition, and sampling. *Quaternary Research* 30, 67-80.

Clarkson, B. 1990. A review of vegetation development following recent (<450 years) volcanic disturbance in North Island, New Zealand. *New Zealand Journal of Ecology* 14, 59-71.

Clarkson, B., McGlone, M., Lowe, D. and Clarkson, B. 1995. Macrofossils and pollen representing forests of the pre-Taupo volcanic eruption (*c.* 1850 years BP) era at Pureora and Benneydale, central North Island, New Zealand. *Journal of the Royal Society of New Zealand* 25(2), 263-281.

Clarkson, B.R., Thompson, K., Schipper, L. and McLeod, M. 1999. Moanatuatua Bog – proposed restoration of a New Zealand peat bog ecosystem, in Streever, W. (ed.) *An international perspective on wetland rehabilitation.* Dordrecht, Kluwer Academic, 127-137, 338pp.

Clarkson, B. 2002. Swamps, fens and bogs, in Clarkson, B., Merrett, M. and Downs, T. (ed.s) *Botany of the Waikato.* Waikato Botanical Society, New Zealand, 49-58, 136pp.

Clarkson, B., Schipper, L. and Lehmann, A. 2004. Vegetation and peat characteristics in the development of lowland restiad peat bogs, North Island, New Zealand. *Wetlands* 24(1), 133-151.

Clement, A., Seager, R. and Cane, M. 2000. Suppression of El Niño during the mid-Holocene by changes in the Earth's orbit. *Palaeoceanography* 15, 731-737.

Clement, A., Cane, M. and Seager, R. 2001. An orbitally driven tropical source for abrupt climate change. *Journal of Climatology* 14, 2369-2375.

Connor, H. and Edgar, E. 1987. Name changes in the indigenous New Zealand flora, 1960-1986 and Nomina Nova IV, 1983-1986. *New Zealand Journal of Botany* 25, 115-170.

Cook, J., Mark, A. and Shore, B. 1980. Responses of *Leptospermum scoparium* and *L. ericoides* (Myrtaceae) to waterlogging. *New Zealand Journal of Botany* 18, 233-246.

Cook, E. 1992. Using tree rings to study past El Niño/Southern Oscillation influences on climate, in Markgraf, V. and Diaz, H. (ed.s) *El Niño: historical and palaeoclimatic aspects of the Southern Oscillation.* Cambridge University Press, 203-214, 490pp.

Cook, E., D'Arrigo, R., Cole, J., Stahle, D. and Villalba, R. 2000. Tree-ring records of past ENSO variability and forcing, in Diaz, H. and Markgraf, V. (ed.s) *El Niño and the Southern Oscillation: Multiscale variability and global and regional impacts.* Cambridge University Press, 297-323, 512pp.

Corbet, S. 1973. An illustrated introduction to the testate rhizopods in *Sphagnum*, with special reference to the area around Malham Tarn, Yorkshire. *Field Studies* 3, 801-838.

Cranwell, L. 1953. An outline of New Zealand peat deposits. *7th Pacific Science Congress* 186-208.

Davidson, J. 1984. *The prehistory of New Zealand.* Longman Paul, Auckland 270pp.

Davoren, A. 1978. *A survey of New Zealand peat resources.* Water and Soil Technical Publication No. 14 155pp.

de Lange, P. 1989. *Late Quaternary development of the Kopouatai peat bog, Hauraki lowlands, and some palaeoenvironmental inferences.* Unpublished M.Sc. dissertation, University of Waikato, Hamilton.

de Lange, P. and Lowe, D. 1990. History of the vertical displacement of Kerepehi Fault at Kopouatai Bog, Hauraki Lowlands, New Zealand, since *c.* 10,700 years ago. *New Zealand Journal of Geology and Geophysics* 33, 277-283.

de Lange, P., Heenan, P., Clarkson B.D., and Clarkson, B.R. 1999. Taxonomy, ecology, and conservation of *Sporadanthus* (Restionaceae) in New Zealand. *New Zealand Journal of Botany* 37, 413-431.

de Vries, H. 1958. Variation in concentration of radiocarbon with time and location on Earth. *Proceedings Koninkijk Nederlandse Akademie van Wetenschappen, Amsterdam* B61 94-102.

Deflandre, G. 1936 Etude monographique sur le genre *Nebela* Leidy (Rhizopoda, Testacea). *Annales für Protistenkunde* 5, 201-322.

Dodson, J. 1998. Timing and response of vegetation change to Milankovitch forcing in temperate Australia and New Zealand. *Global and Planetary Change* 18, 161-174.

Dodson, J. 2001. Holocene vegetation change in the Mediterranean-type climate regions of Australia. *The Holocene* 11(6), 673-680.

Dodson, J. and Lu, J. 2000. A late Holocene vegetation and environment record from Byenup Lagoon, south western Australia. *Australian Geographer* 31(1), 41-54.

Dujardin, F. 1841. *Histoire naturelle des Zoophytes* Infusoires: comprenant la physiologie et la classification de ces animaux, et la manière de les étudier à l'aide du microscope. De Roret, collection 'Nouvelles suite à buBuffon, formant avec les oeuvres de cet auteir, un cours complet d'Histoire naturelle. Text volume pI-XII and 1-684. Plates volume p.1-14, pls 1-16, 16 bis, 17-22. Paris.

Dupont, L. 1986. Temperature and rainfall variation in the Holocene based on comparative palaeoecology and isotope geology of a hummock and hollow (Bourtangerveen, The Netherlands). *Review of Palaeobotany and Palynology* 48, 71-159.

Ehrenberg, C. 1830. *Organisation, Systematik und geographisches Verhältnis der Infusionsthierchen.* Druckerei der Königlichen Akademie der Wissenschaften, Berlin.

Elliott, M. 1998. Late Quaternary pollen records of vegetation and climate change from Kaitaia Bog, far northern New Zealand. *Review of Palaeobotany and Palynology* 99, 189-202.

Ellison, R. and Ogden, C. 1987. A guide to the study and identification of fossil testate amoebae in Quaternary lake sediments. *International Review of Hydrobiology* 72, 639-652.

Fisher, R. and Schmincke, H.-U. 1984. *Pyroclastic rocks.* Springer-Verlag, Berlin 472pp.

Fitzharris, B., Hay, J. and Jones, P. 1992. Behaviour of New Zealand glaciers and atmospheric circulation changes over the past 130 years. *The Holocene* 2, 97-106.

Fowler, A., Palmer, J., Salinger, J. and Ogden, J. 2000. Dendroclimatic interpretation of tree-rings in *Agathis australis* (kauri): 2. Evidence of a significant relationship with ENSO. *Journal of the Royal Society of New Zealand* 30(3), 277-292.

Froggatt, P. 1981. Review of Holocene eruptions from Taupo, in Howarth, R., Froggatt, P., Vucetich, C. and Collen, J. (ed.s) *Proceedings of the tephra workshop; number 20.* June 30th to July 1st 1980 Victoria University, Wellington 142pp.

Froggatt, P. and Lowe, D. 1990. A review of late Quaternary silicic and some other tephra formations from New Zealand: their stratigraphy, nomenclature, distribution, volume and age. *New Zealand Journal of Geology and Geophysics* 33, 89-109.

Froggat, P. and Rogers, G. 1990. Tephrostratigraphy of high-altitude peat bogs along the axial ranges, North Island, New Zealand. *New Zealand Journal of Geology and Geophysics* 33, 111-124.

Gellatly, A., Chinn, T. and Röthlisberger, F. 1988. Holocene glacier variations in New Zealand: a review. *Quaternary Science Reviews* 7, 227-242.

Giles, T. 1999. *Volcanic emissions and distal palaeoenvironmental impacts in New Zealand.* Unpublished PhD thesis, University of Plymouth.

Given, P. and Dickinson, C. 1975. Biochemistry and microbiology of peats, in Paul, E. and McLaren, A. (ed.s) *Soil Biochemistry: Volume 3.* 123-212 Marcel Dekker, New York 334pp.

GNS, 2004. http://www.gns.cri.nz/what/earthact/volcanoes/nzvolcanoes/taupoprint.htm *New Zealand volcanoes: the Taupo volcanic centre – volcanic hazards at Taupo Volcanic Centre.* 14/07/04.

Godwin, H. 1962. Half-life of radiocarbon. *Nature* 195, 944.

Gordon, N. 1985. The Southern Oscillation: a New Zealand perspective. *Journal of the Royal Society of New Zealand* 15(2), 137-155.

Greeff, R. 1888. Studien über Protozoan. *Sitzungsberichte der Gesellschaft zur Beförderung der gesammten Naturwissenschaften zu Marburg* 3, 90-158.

Green, J. and Lowe, D. 1985. Stratigraphy and development of *c.*17,000 year old Lake Maratoto, North Island, New Zealand, with some inferences about postglacial climatic change. *New Zealand Journal of Geology and Geophysics* 28, 675-699.

Griffiths, G. and McSaveney, M. 1983. Distribution of mean annual precipitation across some steepland regions of New Zealand. *New Zealand Journal of Science* 26, 197-209.

Grimm, E. 1993. Tilia and Tilia Graph (versions 2.0.b.4). Illinois State Museum.

Grimm, E. 2004. TGView (version 1.6.1). Illinois State Museum.

Grospietsch, T. 1954. Studien über die Rhizopodenfauna von Schwedisch-Lappland. *Archiv für Hydrobiologie* 49(4), 546-580.

Hall, V. and Pilcher, J. 2002. Late-Quaternary Icelandic tephras in Ireland and Great Britain: detection, characterization and usefulness. *The Holocene* 12(2), 223-230.

Harrison, S. and Dodson, J. 1993. Climates of Australia and New Guinea since 18,000 years BP, in Wright, H., Kutzbach, J., Webb, T., Ruddiman, W., Street-Perrott, F. and Bartlein, P. (ed.s) *Global climates since the last glacial maximum.* 265-293 University of Minnesota Press 544pp.

Hay, J., Salinger, J., Fitzharris, B. and Basher, R. 1993. Climatological seesaws in the southwest Pacific. *Weather and Climate* 13, 9-21.

Hays, J. 1977. The late Quaternary history of Antarctic seas *Abstracts of the 10th INQUA Congress, Birmingham.* Geoabstracts, Norwich 200.

Heal, O. 1962. The abundance and microdistribution of testate amoebae (Protozoa: Rhizopoda) in *Sphagnum. Oikos* 13(1), 35-47.

Heath, R. 1985. A review of the physical oceanography of the seas around New Zealand – 1982 *New Zealand Journal of Marine and Freshwater Research.* 19, 79-124.

Hellstrom, J., McCulloch, M. and Stone, J. 1998. A detailed 31,000-year record of climate and vegetation change, from the isotope geochemistry of two New Zealand speleothems. *Quaternary Research* 50, 167-178.

Hendon, D. and Charman, D. 1997. The preparation of testate amoebae (Protozoa: Rhizopoda) samples from peat. *The Holocene* 7(2), 199-205.

Hendon, D., Charman, D. and Kent, M. 2001. Palaeohydrological records derived from testate amoebae analysis from peatlands in northern England: within-site comparability and palaeoclimatic implications. *The Holocene* 11(2), 127-148.

Hendy, C. and Denton, G. 1994. Younger Dryas age advance of Franz Josef Glacier in the Southern Alps of New Zealand. *Science* 264, 1434-1437.

Hodder, A., de Lange, P. and Lowe, D. 1991. Dissolution and depletion of ferromagnesian minerals from Holocene tephra layers in an acid bog, New Zealand, and implications for tephra correlation. *Journal of Quaternary Science* 6(3), 195-208.

Hodell, D., Kanfoush, S., Shemesh, A., Crosta, X., Charles, C. and Guilderson, T. 2001. Abrupt cooling of Antarctic surface waters and sea ice expansion in the South Atlantic sector of the Southern Ocean at 5,000 cal yr B.P. *Quaternary Research* 56, 191-198.

Hogg, A., Higham, T., Lowe, D., Palmer, J., Reimer, P. and Newnham, R. 2003. A wiggle-match date for Polynesian settlement of New Zealand. *Antiquity* 77, 116-125.

Hoogenraad, H. 1935. Studien über die sphagnicolen Rhizopoden der niederländischen Fauna. *Archiv für Protistenkunde* 84, 1-100.

Hoogenraad, H. and de Groot, A. 1948. Thecamoebous moss-rhizopods from New Zealand. *Hydrobiologia* 1, 28-44.

Hotes, S., Poschlod, P., Takahashi, A., Grootjans, A. and Adema, E. 2004. Effects of tephra deposition on mire vegetation: a field experiment in Hokkaido, Japan. *Journal of Ecology* 92, 624-634.

Houghton, B., Wilson, C., McWilliams, M., Lanphere, M., Weaver, S., Briggs, R. and Pringle, M. 1995. Chronology and dynamics of a large silicic magmatic system: Central Taupo Volcanic Zone, New Zealand. *Geology* 23, 13-16.

Hughes, P., Mauquoy, D., Barber, K. and Langdon, P. 2000. Mire-development pathways and palaeoclimatic records from a full Holocene peat archive at Walton Moss, Cumbria, England. *The Holocene* 10(4), 465-479.

IPCC, 2001. http://www.grida.no/climate/ipcc_tar/wg1/087.htm 2.6.6 The Southern Hemisphere, in *Climate change 2001: Working group I: The scientific basis Chapter 2 Observed climate variability and change.* 10/05/2004.

Irving, R., Skinner, M. and Thompson, K. 1984. *Kopouatai Peat Dome: a vegetation survey.* Crown Land Series No.12, University of Waikato and Department of Lands and Survey, Hamilton, New Zealand.

Ivy-Ochs, S., Schlüchter, C., Kubik, P. and Denton, G. 1999. Moraine exposure dates imply synchronous Younger Dryas glacier advances in the European Alps and in the Southern Alps of New Zealand. *Geografiska Annaler* 81A, 313-323.

Janecek, T. and Rea, D. 1984. Pleistocene fluctuations in Northern Hemisphere tradewinds and westerlies, in Berger, A., Imbrie, J., Hays, J., Kukla, G. and Saltzman, B. (ed.s) *Milankovitch and Climate: part 1.* D.Reidel, Dordrecht, 331-347, 544pp.

Jenny, B., Valero-Garcés, B., Villa-Martínez, R., Urrutia, R., Geyh, M. and Veit, H. 2002. Early to mid-Holocene aridity in central Chile and the southern westerlies: the Laguna Aculeo record (34°S). *Quaternary Research* 58, 160-170.

Johnson, L, Damman, A. and Malmer, N. 1990. *Sphagnum* macrostructure as an indicator of decay and compaction in peat cores from an ombrotrophic south Swedish peat-bog. *Journal of Ecology* 78, 633-647.

Johnson, P. and Brooke, P. 1998. *Wetland Plants in New Zealand.* Manaaki Whenua Press, Lincoln 226pp.

Jones, R. and Maggs, G. 1990. *Piako/Waitoa surface water preliminary assessment.* Waikato Regional Council Technical Report no.1990/8, Waikato Regional Council, Hamilton.

Kamp, P. 1992. Tectonic architecture of New Zealand, in Soons, J. and Selby, M. (ed.s) *Landforms of New Zealand.* Longman Paul Ltd, 1-30, 392pp.

Kershaw, A. 1988. Australasia, in Huntley, B. and Webb, T. (ed.s) *Vegetation History: Handbook of Vegetation Science Volume 7* Kluwer Academic Publishers, 237-306, 803pp.

Kershaw, A. 1995. Environmental change in greater Australia. *Antiquity* 69, 656-675.

Kidson, J. 1988. Interannual variations in the Southern Hemisphere circulation. *Journal of Climate* 1; 1177-1198.

Kilian, M., van der Plicht, J. and van Geel, B. 1995. Dating raised bogs: new aspects of AMS ^{14}C wiggle-matching, a reservoir effect and climatic change. *Quaternary Science Reviews* 14, 959-966.

Kuder, T., Kruge, M., Shearer, J. and Miller, S. 1998. Environmental and botanical controls on peatification – a comparative study of two New Zealand restiad bogs using Py-Gc/Ms, petrography and fungal analysis. *International Journal of Coal Geology* 37, 3-27.

Lamb, H. 1965. The early Medieval warm epoch and its sequel. *Palaeogeography, Palaeoclimatology, Palaeoecology* 1, 13-37.

Lamb, H. 1977. *Climate: Present, past and future. Volume 2: Climatic history and the future.* Methuen 837pp.

Langdon, P., Barber, K. and Hughes, P. 2003. A 7500 year peat-based palaeoclimatic reconstruction and evidence for an 1100 year cyclicity of surface wetness from Temple Hill Moss, Pentland Hills, Southeast Scotland. *Quaternary Science Reviews* 22, 259-274.

Libby, W. 1955. *Radiocarbon dating.* 2nd edition, University of Chicago Press, Chicago 175pp.

Loubere, P., Richaud, M., Liu, Z. and Mekik, F. 2003. Oceanic conditions in the eastern equatorial Pacific during the onset of ENSO in the Holocene. *Quaternary Research* 60, 142-148.

Lowe, D. 1981. Late Quaternary tephras in the Hamilton Basin, North Island, New Zealand, in Howarth, R., Froggatt, P., Vucetich, C., Collen, J. (ed.s) *Proceedings of Tephra Workshop. 30th June-1st July 1980 Victoria University, Wellington* 80-86.

Lowe, D. 1988a. Late Quaternary volcanism in New Zealand: towards and integrated record using distal airfall tephras in lakes and bogs. *Journal of Quaternary Science* 3(2), 111-120.

Lowe, D. 1988b. Stratigraphy, age, composition and correlation of late Quaternary tephras interbedded with organic sediments in Waikato lakes, North Island, New Zealand. *New Zealand Journal of Geology and Geophysics* 31, 125-165.

Lowe, D., McFadgen, B., Higham, T., Hogg, A., Froggatt, P. and Nairn, I. 1998. Radiocarbon age of the Kaharoa Tephra, a key marker for late-Holocene stratigraphy and archaeology in New Zealand. *The Holocene* 8(4), 487-495.

Lowe, D. and Newnham, R. 1999. Advances in tephrostratigraphy and tephrochronology in New Zealand. *Quaternary Australasia* 17, 12-19.

Lowe, D., Newnham, R. and Ward, C. 1999. Stratigraphy and chronology of a 15ka sequence of multi-sourced silicic tephras in a montane peat bog, eastern North island, New Zealand. *New Zealand Journal of Geology and Geophysics* 42, 565-579.

Lowe, D. and Hunt, J. 2001. A summary of terminology used in tephra-related studies, in Juvigné, E. & Raynal, J.-P. (ed.s) Tephras: Chronology, Archaeology *Les Dossiers de l'Archeo-Logis.* 1, 17-22.

Lowe, J. and Walker, M. 1997. *Reconstructing Quaternary environments.* Addison Wesley Longman Ltd, Essex 446pp.

Maggs, G. 1997. Hydrology of the Kopouatai Peat Dome. *New Zealand Journal of Hydrology* 36(2), 147-172.

Magny, M. 1993. Solar influences on Holocene climate changes, illustrated by correlation between past lake level and fluctuations and the atmospheric ^{14}C record. *Quaternary Research* 40, 1-9.

Magny, M. 1995. Successive oceanic and solar forcing indicated by Younger Dryas and early Holocene climatic oscillations in the Jura. *Quaternary Research* 43, 279-285.

Magny, M. 2004. Holocene climate variability as reflected by mid-European lake-level fluctuations and its probable impact on prehistoric human settlement. *Quaternary International* 113, 65-79.

Maher, L. 1981. Statistics for microfossil concentration measurements employing samples spiked with marker grains. *Review of Palaeobotany and Palynology* 32, 153-191.

Mantua, N., Hare, S., Zhang, Y., Wallace, J. and Francis, R. 1997. A Pacific interdecadal climate oscillation with impacts on salmon production. *Bulletin of the American Meteorological Society* 78, 1069-1079.

Markgraf, V., Dodson, J., Kershaw, A., McGlone, M. and Nichols, N. 1992. Evolution of the Late Pleistocene and Holocene climates in the circum-South Pacific land areas. *Climate Dynamics* 6, 193-211.

Markgraf, V. 1993. Climate history of Central and South America since 18,000 years BP: comparison of pollen records and model simulations, in Wright, H., Kutzbach, J., Webb, T., Ruddiman, W., Street-Perrott, F. and Bartlein, P. (ed.s) *Global climates since the Last Glacial Maximum.* University of Minnesota Press, 357-385, 544pp.

McCarthy, F., Collins, E., McAndrews, J., Kerr, H., Scott, D. and Medioli, F. 1995. A comparison of postglacial arcellacean ("thecamoebian") and pollen succession in Atlantic Canada, illustrating the potential of arcellaceans for palaeoclimatic reconstruction. *Journal of Paleontology* 69(5), 980-993.

McCormac, F., Hogg, A., Higham, T., Baillie, M., Palmer, J., Xiong, L. and Brown, D. 1997. Spatial and temporal variation of radiocarbon in tree rings: preliminary results for 1725 to 1945AD *Abstracts from the 16th International Radiocarbon Conference, Groningen, The Netherlands.* 122.

McCormac, F., Hogg, A., Higham, T., Lynch-Stieglitz, J., Broecker, W., Baillie, M., Palmer, J., Xiong, L., Pilcher, J., Brown, D. and Hopper, S. 1998. Temporal variation in the interhemispheric ^{14}C offset. *Geophysical Research Letters* 25, 1321-1324.

McCormac, F., Reimer, P., Hogg, A., Higham, T., Baillie, M., Palmer, J. and Stuiver, M. 2002. Calibration of the radiocarbon timescale for the Southern Hemisphere: AD1850-950. *Radiocarbon* 44(3), 641-651.

McCraw, J. 1967. The surface features and soil pattern of the Hamilton Basin. *Earth Science Journal* 1, 59-74.

McCraw, J. 2002. Physical environment, in Clarkson, B., Merrett, M. and Downs, T. (ed.s) *Botany of the Waikato.* Waikato Botanical Society, New Zealand, 13-22, 136pp.

McGlone, M. 1981. Forest fire following Holocene tephra fall, in Howarth, R., Froggatt, P., Vucetich, C. and Collen, J. (ed.s) *Proceedings of Tephra Workshop 30th June-1st July 1980 Victoria University, Wellington.* 80-86.

McGlone, M. 1983. Holocene pollen diagrams, Lake Rotorua, North Island, New Zealand. *Journal of the Royal Society of New Zealand* 13(1/2), 53-65.

McGlone, M. 1988. New Zealand, in Huntley, B. and Webb, T. (ed.s) *Vegetation History: Handbook of Vegetation Science Volume 7.* Kluwer Academic Publishers, 557-599, 803pp.

McGlone, M. 1995. Lateglacial landscape and vegetation change in the Younger Dryas climatic oscillation in New Zealand. *Quaternary Science Reviews* 14, 867-881.

McGlone, M. and Moar, N. 1977. The *Ascarina* decline and post-glacial climatic change in New Zealand. *New Zealand Journal of Botany* 15, 485-489.

McGlone, M. and Topping, W. 1977. Aranuian (post-glacial) pollen diagrams from the Tongariro region, North Island, New Zealand. *New Zealand Journal of Botany* 15, 749-760.

McGlone, M., Kershaw, A. and Markgraf, V. 1992. El Niño/Southern Oscillation climatic variability in Australasian and South American paleoenvironmental records, in Diaz, H. and Markgraf, V. (ed.s) *El Niño: historical and paleoclimatic aspects of the Southern Oscillation.* University of Arizona Press, 435-462, 490pp.

McGlone, M., Salinger, M. and Moar, N. 1993. Palaeovegetation studies of New Zealand's climate since the Last Glacial Maximum, in Wright, H., Kutzbach, J., Webb, T., Ruddiman, W., Street-Perrott, F. and Bartlein, P. (ed.s) *Global Climates since the Last Glacial Maximum.* University of Minnesota Press, 294-317, 544pp.

McGlone, M. and Wilmshurst, J. 1999a. Dating initial Maori impact in New Zealand. *Quaternary International* 59(1), 5-16.

McGlone, M. and Wilmshurst, J. 1999b. A Holocene record of climate, vegetation change and peat bog development, east Otago, South Island, New Zealand. *Journal of Quaternary Science* 14(3), 239-254.

Meney, A. and Pate, J. 1999. *Australian rushes. Biology, identification and conservation of Restionaceae and allied families.* Australian Biological Resources Study. University of Western Australia Press 486pp.

Ménot, G. and Burns, S. 2001. Carbon isotopes in ombrogenic peat bog plants as climatic indicators: calibration from an altitudinal transect in Switzerland. *Organic Geochemistry* 32, 233-245.

MetService, 2001. http://www.metservice.co.nz/learning/weather_climate_of_nz.asp *The climate of New Zealand* (based on the Meteorological Service of New Zealand Information Publication No. 15) 13/02/01.

Mook, W. 1986. Recommendations/resolutions adopted by the 12th International Radiocarbon Conference. *Radiocarbon* 28(2A), 799.

Moore, P. and Webb, J. 1978. *An illustrated guide to pollen analysis.* Hodder and Stoughton 133pp.

New Zealand Meteorological Service 1973. *Summaries of climatological observations to 1970.* New Zealand Meteorological Service Miscellaneous Publication 143.

New Zealand tectonics. http://members.tripod.com/NZPhoto/volcano/atectonic.htm 14/07/04 (from Cox, 1999)

New Zealand tectonics (part 2a.)
http://members.tripod.com/NZPhoto/volcano/atectonic2a.htm 14/07/04

Newnham, R. 1999. Environmental change in Northland, New Zealand during the last glacial and Holocene. *Quaternary International* 57/58, 61-70.

Newnham, R., Lowe, D. and Green, J. 1989. Palynology, vegetation and climate of the Waikato lowlands, North Island, since *c.* 18,000 years ago. *Journal of the Royal Society of New Zealand* 19, 127-150.

Newnham, R. and Lowe, D. 1991. Holocene vegetation and volcanic activity, Auckland Isthmus, New Zealand. *Journal of Quaternary Science* 6(3), 177-193.

Newnham, R., de Lange, P. and Lowe, D. 1995. Holocene vegetation, climate and history of a raised bog complex, northern New Zealand based on palynology, plant macrofossils and tephrochronology. *The Holocene* 5(3), 267-282.

Newnham, R., Lowe, D., McGlone, M., Wilmshurst, J. and Higham, T. 1998a. The Kaharoa Tephra as a Critical Datum for Earliest Human Impact in Northern New Zealand. *Journal of Archaeological Science* 25, 533-544.

Newnham, R., Lowe, D. and Matthews, B. 1998b. A late-Holocene and prehistoric record of environmental change from Lake Waikaremoana, New Zealand. *The Holocene* 8(4), 443-454.

Newnham, R. and Lowe, D. 1999. Testing the synchroneity of pollen signals using tephrostratigraphy. *Global and Planetary Change* 21, 113-128.

Newnham, R., Lowe, D. and Williams, P. 1999. Quaternary environmental change in New Zealand: a review. *Progress in Physical Geography* 23(4), 567-610.

Newnham, R. and Lowe, D. 2000. Fine-resolution pollen record of late-glacial climate reversal from New Zealand. *Geology* 28(8), 759-762.

Newnham, R., Eden, D., Lowe, D. and Hendy, C. 2003. Rerewhakaaitu Tephra, a land-sea marker for the last termination in New Zealand, with implications for global climate change. *Quaternary Science Reviews* 22, 289-308.

Nilsson, M., Klarqvist, M., Bohlin, E. and Possnert, G. 2001. Variation in ^{14}C age of macrofossils and different fractions of minute peat samples dated by AMS. *The Holocene* 11(5), 579-586.

NIWA, 2004. *El Niño and La Niña.* http://www.niwa.cri.nz/edu/students/faq/enln 12/10/04.

Norton, D., McGlone, M. and Wigley, T. 1986. Quantitative analyses of modern pollen-climate relationships in New Zealand indigenous forests. *New Zealand Journal of Botany* 24 331-342

Ogden, J. and Ahmed, M. 1989. Climate response function analysis of kauri (*Agathis australis*) tree ring chronologies in northern New Zealand. *Journal of the Royal Society of New Zealand* 19, 205-221.

Ogden, J., Basher, L. and McGlone, M. 1998. Fire, forest regeneration and links with early human habitation: evidence from New Zealand. *Annals of Botany* 81, 687-696.

Pancost, R., Baas, M., van Geel, B. and Damsté, J. 2003. Response of an ombrotrophic bog to a regional climate event revealed by macrofossil, molecular and carbon isotopic data. *The Holocene* 13(6), 921-932.

Penard, E. 1890. Etude sur les Rhizopodes d'eau douce. *Mémoires de la Société de Physique et d'Histoire Naturelle de Genève* 31(65), 1-64.

Penard, E. 1902. *Faune Rhizopodique du Bassin du Léman.* Henry Kündig, Genève 714pp.

Pilcher, J. 1991. Radiocarbon dating, in Smart, P. and Frances, P. (ed.s) *Quaternary dating methods – a user's guide.* Technical Guide 4. Quaternary Research Association, 16-36, 233pp.

Pilcher, J. 2003. Radiocarbon dating and environmental radiocarbon studies, in Mackay, A., Battarbee, R., Birks, J. and Oldfield, F. (ed.s) *Global change in the Holocene.* Arnold, London, 63-74, 480pp.

Pillans, B., Pullar, W., Selby, M. and Soons, J. 1992. The age and development of the New Zealand landscape, in Soons, J. and Selby, M. (ed.s) *Landforms of New Zealand.* Longman Paul Ltd, 31-62, 392pp.

Poole, A, and Adams, N. 1994. *Trees and shrubs of New Zealand.* Manaaki Whenua Press, Lincoln 256pp.

Power, S., Tseitkin, F., Torok, S., Lavery, B., Dahni, R. and McAvaney, B. 1998. Australian temperature, Australian rainfall and the Southern Oscillation, 1910-1992: coherent variability and recent changes. *Australian Meteorological Magazine* 47, 85-101.

Pullar, W., Kohn, B. and Cox, J. 1977. Air-fall Kaharoa ash and Taupo pumice, and sea-rafted Loisels pumice, Taupo pumice and Leigh pumice in northern and eastern parts of the North Island, New Zealand. *New Zealand Journal of Geology and Geophysics* 20(4), 697-717.

Rasmusson, E., Wang, X. And Ropelewski, C. 1990. The biennial component of ENSO variability. *Journal of Marine Systems* 1, 71-96.

Riddolls, P. 1987. *New Zealand Geology: containing geological map of New Zealand 1:2,000,000.* DSIR Science Information Publishing Centre, Wellington 72pp.

Rind, D. 2002. The Sun's role in climate variations. *Science* 296, 673-677.

Rittenour, T., Brigham-Grette, J. and Mann, M. 2000. ENSO-like climate teleconnections in New England during the late Pleistocene. *Science* 288, 1039-1042.

Robertson, N. 1959. The climate of New Zealand, in McLintock, A. (ed.) *A descriptive Atlas of New Zealand.* Government Printer, Wellington, New Zealand, 19-22, 150pp.

Rogers, G. and McGlone, M. 1989. A postglacial vegetation history of the southern-central uplands of North Island, New Zealand. *Journal of the Royal Society of New Zealand* 19, 229-248.

Rycroft, D., Williams, D. and Ingram, H. 1975. The transmission of water through peat: I. review. *Journal of Ecology* 63(2), 535-556.

Salinger, M. 1984. New Zealand climate: the last 5 million years, in Vogel, J. (ed.) *Late Cainozoic Palaeoclimates of the Southern Hemisphere.* Proceedings of an international symposium held by the South African Society for Quaternary Research, Swaziland AA Balkema, 131-150, 520pp.

Salinger, M. and McGlone, M. 1990. New Zealand climate: the past 2 million years. *New Zealand Climate Report 1990, The Royal Society of New Zealand, Wellington* 13-18.

Sandweiss, D., Richardson, J., Reitz, E., Rollins, H. and Maasch, K. 1996. Geoarchaeological evidence from Peru for a 5,000 years BP onset of El Niño. *Science* 273, 1531-1533.

Shearer, J. 1997. Natural and anthropogenic influences on peat development in Waikato/Hauraki Plains restiad bogs. *Journal of the Royal Society of New Zealand* 27(3), 295-313.

Shore, J., Bartley, D. and Harkness, D. 1995. Problems encountered with the ^{14}C dating of peat. *Quaternary Science Reviews* 14, 373-383.

Shulmeister, J. and Lees, B. 1995. Pollen evidence from tropical Australia for the onset of an ENSO-dominated climate at *c.*4000 BP. *The Holocene* 5(1), 10-18.

Shulmeister, J. 1999. Australasian evidence for mid-Holocene climate change implies precessional control of Walker Circulation in the Pacific. *Quaternary International* 57/58, 81-91.

Shulmeister, J., Goodwin, I., Renwick, J., Harle, K., Armand, L., McGlone, M., Cook, E., Dodson, J., Hesse, P., Mayewski, P. and Curran, M. 2004. The Southern Hemisphere westerlies in the Australasian sector over the last glacial cycle: a synthesis. *Quaternary International* 118/119, 23-53.

Singer, C., Shulmeister, J. and McLea, B. 1998. Evidence against a significant Younger Dryas cooling event in New Zealand. *Science* 281, 812-814.

Sleigh, M. 1973. *The biology of the Protozoa.* Edward Arnold, London 315pp.

Smilauer, P. 1999-2003. *Canodraw for Windows version 4.1.*

Steig, E., Brook, E., White, J., Sucher, C., Bender, M., Lehman, S., Morse, D., Waddington, E. and Clow, G. 1998. Synchronous climate changes in Antarctica and the North Atlantic. *Science* 282, 92-95.

Stephenson, G. 1986. *Wetlands: Discovering New Zealand's shy places.* Government Printing Office Publishing 117pp.

Stevens, G. 1985. *Lands in collision: discovering New Zealand's past geography.* Science Information Publishing Centre, Department of Scientific and Industrial Research 128pp.

Stocker, T. 2002. North-south connections. *Science* 297, 1814-1815.

Stockmarr, J. 1971. Tablets with spores used in absolute pollen analysis. *Pollen et spores* 8, 615-621.

Stokes, S., Lowe, D. and Froggatt, P. 1992. Discriminant function analysis and correlation of Late Quaternary rhyolitic tephra deposits from Taupo and Okataina volcanoes, New Zealand, using glass shard major element composition. *Quaternary International* 13/14, 103-117.

Stuiver, M. and Reimer, P. 1993. Version 4.4 Extended ^{14}C database and revised CALIB radiocarbon calibration programme. *Radiocarbon* 35 215-230
http://radiocarbon.pa.qub.ac.uk/calib

Sturman, A., McGowan, H. and Spronken-Smith, R. 1999. Mesoscale and local climates in New Zealand. *Progress in Physical Geography* 23(4), 611-635.

Suggate, R. and Moar, N. 1970. Revision of the chronology of the late Otira glacial. *New Zealand Journal of Geology and Geophysics* 13, 742-746.

Sutton, D. 1987. A paradigmatic shift in Polynesian prehistory: implications for New Zealand. *New Zealand Journal of Archaeology* 9, 135-155.

Svensmark, H. and Friis-Christensen, E. 1997. Variation of cosmic ray flux and global cloud coverage: a missing link in solar-climate relationships. *Journal of Atmospheric and Terrestrial Physics* 59, 1225-1232.

Taránek, K. 1881. Beitrage zur Kenntniss der Süsswasser – Rhizopoden Böhmens. *Sitzungsbericht Böhmischer Gesellschaften Wissenschaften* 1881, 220-235.

Telford, R., Heegaard, E. and Birks, H. 2004a. All age-depth models are wrong: but how badly?. *Quaternary Science Reviews* 23, 1-5.

Telford, R., Heegaard, E. and Birks, H. 2004b. The intercept is a poor estimate of a calibrated radiocarbon age. *The Holocene* 14(2), 296-298.

ter Braak, C. 1986. CCA: A new eigenvector technique for multivariate direct gradient analysis. *Ecology* 67(5), 1167-1179.

ter Braak, C. and Smilauer, P. 1997-2003. *CANOCO for Windows version 4.54: A programme for canonical community ordination by [partial] [detrended] [canonical] correspondence analysis.* Biometris – Plant Research International, Wageningen.

Thompson, D. and Wallace, J. 2000. Annual modes in the extratropical circulation Part I: month-to-month variability. *Journal of Climate* 13, 1000-1016.

Thompson, M., Campbell, D. and Spronken-Smith, R. 1999. Evaporation from natural and modified raised peat bogs in New Zealand. *Agricultural and Forest Meteorology* 95, 85-98.

Tolonen, K. 1966. Stratigraphic and rhizopod analyses on an old raised bog, Varrassuo, in Hollola, South Finland. *Annales Botanici Fennici* 3, 147-166.

Tolonen, K. 1986. Rhizopod analysis, in Berglund, B. (ed.) *Handbook of Holocene Palaeoecology and Palaeohydrology.* John Wiley and Sons Ltd, 645-666, 869pp.

Tolonen, K., Warner, B. and Vasander, H. 1992. Ecology of testate amoebae (Protozoa: Rhizopoda) in mires in southern Finland: I Autecology. *Archiv für Protistenkunde* 142, 119-138.

Tolonen, K., Warner, B. and Vasander, H. 1994. Ecology of testaceans (Protozoa: Rhizopoda) in mires in southern Finland: II Multivariate analysis. *Archiv fur Protistenkunde* 144, 97-112.

Trenberth, K. and Shea, D. 1997. On the evolution of the Southern Oscillation. *Monthly Weather Review* 115, 3078-3096.

Troels-Smith 1955. Characterisation of unconsolidated sediments. *Danmarks Geologiske Undersogelse, Series IV* 3, 38-73.

Tudhope, A., Chilcott, C., McCulloch, M., Cook, E., Chappell, J., Ellam, J., Lea, D., Lough, J. and Shimmield, G. 2001. Variability in the El Niño-Southern Oscillation through a glacial-interglacial cycle. *Science* 291, 1511-1517.

Turney, C., Hunt, J. and Burrows, C. 2002. Deriving a consistent $\delta^{13}C$ signature from tree canopy leaf material for palaeoclimatic reconstruction. *New Phytologist* 155(2), 301-311.

Turney, C., McGlone, M. and Wilmshurst, J. 2003. Asynchronous climate change between New Zealand and the North Atlantic during the last deglaciation. *Geology* 31(3), 223-226.

Turney, C., Kershaw, A., Clemens, S., Branch, N., Moss, P. and Fifield, L. 2004. Millennial and orbital variations of El Niño/Southern Oscillation and high-latitude climate in the last glacial period. *Nature* 428, 306-310.

van Geel, B., Buurman, J. and Waterbolk, H. 1996. Archaeological and palaeoecological indications of an abrupt climate change in The Netherlands, and evidence for climatological teleconnections around 2650 BP. *Journal of Quaternary Science* 11(6), 451-460.

van Geel, B. and Renssen, H. 1998. Abrupt climate change around 2,650 BP in north-west Europe: evidence for climatic teleconnections and a tentative explanation, in Issar, A. and Brown, N. (ed.s) *Water, environment and society in time of climatic change.* Kluwer, Dordrecht, 21-41, 355pp.

van Geel, B., van der Plicht, J., Kilian, M., Klaver, E., Kouwenberg, J., Renssen, H., Reynaud-Farrera, I. and Waterbolk, H. 1998. The sharp rise of $\Delta^{14}C$ *ca.*800 cal. BC: possible causes, related climatic teleconnections and the impact on human environments. *Radiocarbon* 40(1), 535-550.

van Geel, B., Raspopov, O., Renssen, H., van der Plicht, J., Dergachev, V. and Meijer, H. 1999. The role of solar forcing upon climate change. *Quaternary Science Reviews* 18, 331-338.

van Geel, B., Heusser, C., Renssen, H. and Schuurmans, C. 2000. Climatic change in Chile at around 2700BP and global evidence for solar forcing: a hypothesis. *The Holocene* 10(5), 659-664.

van Oye, P. 1956. On the Thecamoeban fauna of New Zealand with description of four new species and biogeografical discussion. *Hydrobiologia: Acta Hydrobiologica, Hydrografica et Protistologia* 8(1-2), 16-37.

Veit, H. 1996. Southern westerlies during the Holocene deduced from geomorphological and pedological studies in Norte Chico, northern Chile (27-33°S). *Palaeogeography, Palaeoclimatology and Palaeoecology* 123, 107-119.

Verhoeven, J., Koerselman, W. and Meuleman, A. 1996. Nitrogen or phosphorus-limited growth in herbaceous, wet vegetation: relations with atmospheric inputs and management regimes. *Trends in Ecology and Evolution* 11(12), 494-497.

Villa-Martínez, R., Villagrán, C. and Jenny, B. 2003. The last 7,500 cal. years BP record of westerly rainfall in Central Chile inferred from a high-resolution pollen record from Laguna Aculeo (34°S). *Quaternary Research* 60, 284-293.

Wailes, G. and Penard, E. 1911. Clare Island Survey: Rhizopoda. *Proceedings of the Royal Irish Academy* 31(65), 1-64.

Walker, G. 1980. The Taupo pumice: product of the most powerful known (ultraplinian) eruption. *Journal of Volcanology and Geothermal Research* 8, 69-94.

Walker, G. 1981. The Waimihia and Hatepe plinian deposits from the rhyolitic Taupo Volcanic Centre. *New Zealand Journal of Geology and Geophysics* 24, 305-324.

Wardle, P. 1991. *Vegetation of New Zealand.* Cambridge University Press 672pp.

Warner, B. 1991. Fossil testate amoebae (Protozoa) and hydrological history of an ombrotrophic bog in northwestern Ontario, Canada. *Proceedings of the International Symposium on peat/peatland characteristics and uses* 5-14.

Warner, B. and Charman, D. 1994. Holocene changes on a peatland in northwestern Ontario interpreted from testate amoebae. *Boreas* 23, 270-279.

Wetlands International. *A Directory of Wetlands of International Importance*; NZ 5NZ004 http://www.wetlands.org/RDB/Ramsar_Dir/NewZealand/NZ004D02.htm 24/02/05

White, J., Ciais, P., Figge, R., Kenny, R. and Markgraf, V. 1994. A high-resolution record of atmospheric CO_2 content from carbon isotopes in peat. *Nature* 367, 153-156.

Williams, P., Marshall, A., Ford, D. and Jenkinson, A. 1999. Palaeoclimatic interpretation of stable isotope data from Holocene speleothems of the Waitomo district, North Island, New Zealand. *The Holocene* 9(6), 649-657.

Williams, P., King, D., Zhao, J.-X. and Collerson, K. 2003. Speleothem master chronologies: combined Holocene ^{18}O and ^{13}C records from the North Island of New Zealand and their palaeoenvironmental interpretation. *The Holocene* 13(6), 945-959.

Wilmshurst, J., Wiser, S. and Charman, D. 2003. Reconstructing Holocene water tables in New Zealand using testate amoebae: differential preservation of tests and implications for the use of transfer functions. *The Holocene* 13(1), 61-72.

Wohlfarth, B., Skog, G., Possnert, G. and Holmquist, B. 1998. Pitfalls in the AMS radiocarbon-dating of terrestrial macrofossils. *Journal of Quaternary Science* 13(2), 137-145.

Woodland, W. 1996. *Holocene palaeohydrology from testate amoebae analysis: developing a model for British peatlands.* Unpublished PhD thesis, University of Plymouth.

Woodland, W., Charman, D. and Sims, P. 1998. Quantitative estimates of water tables and soil moisture in Holocene peatlands from testate amoebae. *The Holocene* 8(3), 261-273.